

KU Leuven
Biomedical Sciences Group
Faculty of Medicine
Department of Microbiology, Immunology and Transplantation
Rega Institute for Medical Research
Laboratory of Virology and Chemotherapy



CLOSING THE GATES: THE INTERACTION BETWEEN ENVELOPED VIRUSES AND CELLULAR MEMBRANES AS ANTIVIRAL STRATEGY

Merel OEYEN

Jury:

Supervisor:	Prof. Dr. Dominique Schols
Co-supervisor:	Prof. Dr. Kurt Vermeire
Chair examining committee:	Prof. Dr. Tassos Economou
Chair public defense:	Prof. Dr. Philippe Van den Steen

Jury members:	Prof. Dr. Libor Grubhoffer <i>Biology Centre CAS</i>
	Prof. Dr. Laurent Gillet <i>University of Liège</i>
	Em. Prof. Dr. Erik De Clercq <i>KU Leuven</i>
	Prof. Dr. Kristel Van Laethem <i>KU Leuven</i>
	Prof. Dr. Mathy Froeyen <i>KU Leuven</i>

Dissertation presented in partial fulfilment of the requirements for the degree of
Doctor in Biomedical Sciences
October, 2020

Dankwoord

Voor vokka en opa, die misschien vonden dat dokter beter bij mij zou passen dan doctor, maar nu toch enorm blij zouden zijn.

Dankbaarheid. Dat is het belangrijkste wat ik onthoud van deze vijf jaar die dit doctoraat geduurd heeft. Dankbaarheid voor alle kansen en mogelijkheden die ik heb gekregen, voor alle fantastische mensen die ik heb mogen leren kennen, en voor alle helpende handen die dit doctoraat beter hebben gemaakt, en die ik hier verder wil toelichten.

Dominique, bedankt om mijn promotor te zijn. Ik ben jou dankbaar dat je onze zelfstandigheid en verantwoordelijkheid stimuleert en open staat voor onze ideeën. Ondanks dat je het enorm druk hebt met al je taken als afdelingshoofd, maakte je wel tijd om samen projecten te bespreken en om advies te geven. Bedankt om mijn schrijfsels na te kijken, en om de vele sappige verhalen over o.a. tenofovir en de gevangen vissen.

Ook veel dank aan mijn co-promotor Kurt. Bedankt voor de hulp bij het schrijven van PhD mijlpalen onderweg en de thesis op het einde. Jouw kritische blik kon de structuur die soms wat te vast zat in mijn hoofd weer een frisse wending geven. Ook enorm bedankt om als een deus ex machina te verschijnen met het fluovirus waardoor mijn paper vlot door de revisie geraakte.

Many thanks to the members of my thesis advisory and examining committee Prof. Philippe Van den Steen, Prof. Tassos Economou, Prof. Kristel Van Laethem, Prof. Mathy Froeyen, Prof. Libor Grubhoffer, Prof. Laurent Gillet, and Em. Prof. Erik De Clercq. Thank you for your time to critically evaluate my thesis manuscript and to attend my doctoral defense.

Ik zou heel graag mijn maatjes Anneleen, Thomas en Jordi bedanken waar ik veel zalige herinneringen mee heb. Dankzij jullie, en onze mini “labmeetings” kon ik altijd de knoop doorhakken om naar een volgende stap in mijn experimenten te gaan. Lienie, echt enorm bedankt voor de afgelopen jaren, alle hulp met resultaten bespreken, kritisch zijn, experimenten plannen, en thesis nalezen zelfs nadat je al een nieuwe job had. Dankzij jou staan de puntjes op de i! Ondanks dat je mijn collega niet meer bent hoop ik dat je nog heel lang mijn vriendin bent.

Thomie, super hard bedankt voor de hele fijne jaren samen en het vele lachen, de hulp bij de cloneringsexperimenten en het betere knip- en plakwerk, en het uitwisselen van Otto- en Mauroverhalen, en last but not least de state-of-the-art diy airco.

Jorre, heel hard bedankt voor alle input tijdens het schrijven, en voor alle inspirerende babbels over vanalles en nog wat. Jouw enthousiasme heeft mij meermaals gepusht om de technologie achter bepaalde toestellen uit te pluizen of nieuwe software uit te proberen.

Ik wens jullie enorm veel succes en plezier in jullie verdere carrière en leven, jullie waren niet alleen de coolste bureau maar ook de meest onvervangbare!

Eef, ik durf zeggen dat mijn doctoraat zoals het nu is geworden gewoonweg niet gelukt zou zijn zonder jou. Bedankt om mij uit de nood te helpen toen ik tijdens mijn zwangerschap en borstvoedingsperiode verbannen was uit het viruslabo, bedankt om mij met praktisch werk te helpen toen ik begon met schrijven tijdens de lockdown. En bedankt voor de vele deugddoende gesprekken, de sportieve avonturen door weer en wind, en de super fijne collega avonden en feestjes. Jouw flexibiliteit en inzet maken van jou een top lab technician.

Daisy en Evelyne, mijn mede "oude Rega chicks", bedankt om mij meteen op mijn gemak te laten voelen vanaf het begin dat ik in het labo rondliep, met de leuke babbels in de P3, en om mij wegwijs te maken in de HIV experimenten. Dankzij jullie (ver)bouwenenthousiasme neem ik nu ook (heel af en toe) eens een boormachine vast!

Ook alle andere mensen van de DS groep: een dikke dikke merci!

Eric, bedankt om de monocytentiptop te prepareren. Sam, heel hard bedankt voor alle Biacore experimenten en optimalisaties, liposomen hebben nu (bijna) geen geheimen meer voor jou! Peter, danku om mij wegwijs te maken in de flavivirus wereld toen ik er in het begin nogal mee aan het sukkelen was. Sandra, bedankt voor de mooie bioplexen. Geert, merci voor de cellsorts te doen zolang ons Melody het niet begaf, en mijn flow cytometrie vragen altijd perfect te beantwoorden. Tom, bedankt om mijn cover letter beter te maken. Ook bedankt aan de "nieuwe" mensen, Arnaud, Katrijn, Robin en Nathan, super leuk dat jullie onze groep zijn komen versterken en de collega avonden nog wat leuker hebben gemaakt, heel veel succes met jullie doctoraat! Lauranne, je werkte niet zo lang in onze groep maar ik ben blij dat ik je heb leren kennen. Antonis, keep up the nice zika work bro!

KV groep! Merci! Merci Becky en Anita, om mijn eerste jaar vele keren gezelliger te maken in ons tot bureau omgebouwde labje. Eva en Marijke, zowel op het werk als ernaast amuseer ik mij altijd super hard met jullie, bedankt om er te zijn. Eva, nog extra bedankt om mee de kar van de collega avonden (in pre-covidtijden) te trekken, ik ben ervan overtuigd dat deze onze groepen hechter maken. Ik apprecieer jou en onze koffie- en karmelietmomenten zowel in als buiten het Rega enorm hard. Marijke, ik ben blij dat jij verder werkt op de flavivirussen! Emiel, bedankt om mijn paper te vervolledigen met de vsv experimenten.

Ook bedankt aan alle andere mensen van het negende die mee voor de chille sfeer op ons verdiep zorgden. Annelies, ik vond het zalig om jou te leren kennen via Daan en Mauro, en om onze mama-avonturen te kunnen bespreken. (En bedankt voor de thesis lay-out tips!) Ook een groot hoedje-met-pluim op voor alle ecoteam mensen in het algemeen en Thy in het bijzonder, voor het engagement!

Lies, ik ga jouw aanstekelijke lach vanuit twee bureaus verder nooit vergeten, maar voor altijd missen.

Natuurlijk gaat er ook enorm veel dank uit naar de mensen van het secretariaat, die voor alles klaar stonden met hun praktische oplossingen, zelfs als je ziek bent en je op zoek bent naar een zetel om even uit te rusten tussen twee experimenten door (vroeger mochten we nog ziek komen werken!).

Ik zou ook graag verschillende mensen buiten het Rega willen bedanken voor hun positieve bijdragen aan dit doctoraat.

Eerst en vooral mama en papa, jullie zijn de reden dat ik dit doctoraat heb kunnen doen, door jullie onvoorwaardelijke steun en motivatie van de afgelopen dertig (!) jaar. En ook wel door het voorzien van lekker eten en goeie muziek op het perfecte moment. Door jullie weet ik hoe belangrijk het is om iets te doen wat je graag doet.

Maud, bedankt om nog altijd een voorbeeld voor mij te zijn. Ik kan enorm genieten van de familiemomenten met mapa en Rik, Milla en Nova.

Familie Frederickx, aka Superfreddies, ook aan jullie heel hard bedankt. Marleen en Luc, door de goeie zorgen voor Mauro kon ik onbezorgd verder werken. De uitstapjes en bourgondische festijnen samen met Ine en Toon zorgden ook altijd voor een welgekomen ontspanning.

Bedankt ook aan mijn vrienden, die er altijd waren voor afleiding en ontspanning. De fantastische biologen – en aanhangsels – groep: Boris, Bram, Caro, Charlotte, Dries, Ella, Gaëlle, Jochen, Karlijn, Lander, Laurens, Lin, Marlies, Mathieu, Sara, Steven, Ties en Tine, door de zalige tradities als kerstfeestjes, weekends en Koppenbergcrossen waren de afgelopen jaren niet enkel all work maar ook heel veel play (en hoofdpijn). Rover, Alice en Felix: Mauro kijkt er al heel hard naar uit om een kaartclub te beginnen met jullie. Maar er is nog veel plaats voor extra vriendjes hint hint.

Katrien en Heleen, mijn liefste pari-meisjes, onze jaaaarenlange vriendschap gaat hopelijk nog lang mee, met af en toe een zalige brunch.

Sara, jij nog eens extra bedankt voor alle doctoraatsventilaties die over en weer gevlogen zijn de voorbije vijf jaar, je bent op alle vlak een super goeie steun voor mij. Ella, bedankt om mij erop te wijzen dat 'important' 20 keer voorkwam in mijn introductie, zodat ik het kon vervangen door wat originelere alternatieven. (En bedankt voor de mega gezellige zwangerschapsverlofuitstapjes.)

Bedankt liefste Wout, met wie ik samen al zoveel geweldigs heb (mee)gemaakt, om er altijd voor mij te zijn. Ik ben nog steeds niet 100% zeker (en Dominique vermoedelijk ook niet) of mijn doctoraat de ideale periode was om drie keer te verhuizen, een huis te kopen, een (MEGA awesome) trouw te organiseren, de halve wereld rond te reizen, een baby te maken en verbouwingen te starten, maar deze fantastische avonturen hebben het er wel vele keren beter op gemaakt en gaan voor altijd mee.

Lieve kleine Mauro, je hebt de laatste (en middelste) loodjes van dit doctoraat er misschien niet lichter op gemaakt, maar het concept geluk wel naar het allerhoogste niveau getild.

Bedankt iedereen!

Merel, September 2020

Table of contents

List of abbreviations	vii
Summary	xi
Samenvatting	xiii
Chapter 1 General introduction	1
1.1 Entry of enveloped viruses	1
1.1.1 The heavy burden of viral infections	1
1.1.2 Biology of enveloped viruses	3
1.1.2.1 Retroviruses.....	4
1.1.2.1.1 HIV structure.....	4
1.1.2.1.2 HIV entry and replication	5
1.1.2.1.3 HIV inhibitors targeting the different steps of the viral life cycle	7
1.1.2.2 Flaviviruses.....	10
1.1.2.2.1 Flavivirus structure	10
1.1.2.2.2 Flavivirus entry and replication	11
1.1.2.2.3 Flavivirus tropism.....	13
1.1.2.2.4 Flavivirus entry receptors.....	14
1.1.2.2.5 Flavivirus entry inhibitors	16
1.2 Virus entry as antiviral target	17
1.2.1 Broad-spectrum antivirals	17
1.2.2 Inhibition of virus entry as broad antiviral strategy	18
1.3 Phosphatidylserine receptors as an interesting target to inhibit virus entry	19
1.3.1 The involvement of phosphatidylserine receptors in virus entry	19
1.3.2 TIM-1	21
1.3.2.1 The TIM gene family	21
1.3.2.2 TIM-1: expression and ligands.....	23
1.3.2.3 Physiological functions of TIM-1	23
1.3.2.4 The role of TIM-1 in diseases	25
1.3.2.5 Potential of TIM-1 as therapeutic target.....	26
1.3.3 CD300a	27
1.3.3.1 The CD300 gene family	27
1.3.3.2 CD300a: expression and ligands.....	28
1.3.3.3 Physiological functions of CD300a	28
1.3.3.4 The role of CD300a in diseases.....	28

1.3.3.5 Potential of CD300a as therapeutic target	29
Chapter 2 Research objectives	31
Chapter 3 Materials and methods	33
3.1 Cell lines, primary cells and viruses.....	33
3.1.1 Cell lines	33
3.1.2 Primary cells	34
3.1.3 Virus strains.....	35
3.2 Test compounds and chemicals	37
3.3 CPE reduction and cytotoxicity screening assays.....	38
3.4 HIV and HSV assays	39
3.4.1 Additional HIV screening assays	39
3.4.2 Time-of-drug addition assay	40
3.4.3 HIV-1 gp120 cellular binding assay	40
3.4.4 HSV-2 gD antibody cellular binding assay	40
3.4.5 HIV giant cell co-culture assay.....	41
3.4.6 DC-SIGN HIV-capture/transmission assay	41
3.4.7 Antiviral assays with several resistant HIV strains	42
3.4.8 Antiviral assay with VSVG-HIV-1 pseudovirus.....	42
3.5 Flavivirus assays	43
3.5.1 Antiviral assays.....	43
3.5.2 Viral plaque reduction assay.....	43
3.5.3 Immunofluorescence staining	44
3.5.4 Time-of-drug addition assay	44
3.5.5 Ultrafiltration assay	44
3.5.6 Virucidal assay.....	45
3.5.7 RNA isolation and quantitative RT-PCR	45
3.6 Flow cytometry assays	45
3.6.1 Surface receptor staining.....	45
3.6.2 Intracellular antigen staining	47
3.6.3 Phagocytosis assay	48
3.7 Surface plasmon resonance studies.....	49
3.7.1 Interaction between HIV glycoproteins and lignosulfonates.....	49
3.7.2 Interaction between DENV-2 envelope and Laby A1	49
3.7.3 Interaction between liposomes and Laby A1	50
3.7.3.1 Liposome preparation	50

3.7.3.2 SPR experiments with liposomes	50
3.8 Cellular electric impedance spectroscopy assay	51
3.9 Molecular cloning and entry receptor transfection	51
3.10 Statistical analysis	52
Chapter 4 A unique class of lignin derivatives displays broad anti-HIV activity by interacting with the viral envelope.....	55
4.1 Introduction.....	57
4.2 Results and discussion	59
4.2.1 Lignosulfonates with broad anti-HIV and anti-HSV activity	59
4.2.2 Lignosulfonates interfere with viral entry.....	67
4.2.3 Lignosulfonates interact with HIV glycoproteins	69
4.2.4 Lignosulfonates inhibit transmission and subsequent infection by cell- associated HIV	70
4.2.5 Cross-resistance of lignosulfonates against HIV entry inhibitor resistant strains.....	72
4.3 Conclusion.....	77
4.4 Supplementary figures.....	79
Chapter 5 Labyrinthopeptin A1 inhibits dengue and Zika virus infection by interfering with the viral phospholipid membrane.....	83
5.1 Introduction.....	85
5.2 Results and discussion	87
5.2.1 Broad-spectrum antiviral activity of Labyrinthopeptin A1 against ZIKV and DENV.....	87
5.2.1.1 Screening assay demonstrates anti-ZIKV and anti-DENV activity of labyrinthopeptins.....	87
5.2.1.2 Laby A1 exerts broad antiviral activity against other enveloped viruses	90
5.2.1.3 Laby A1 prevents the production of viral progeny.....	91
5.2.1.4 Laby A1 inhibits DENV and ZIKV in biologically relevant target cell lines	92
5.2.1.5 Laby A1 inhibits various DENV serotypes and ZIKV strains in primary human dendritic cells.....	94
5.2.2 Analysis of ZIKV-induced cytokines and chemokines in the absence or presence of Laby A1.....	95
5.2.3 Mechanism of action of Laby A1.....	97
5.2.3.1 Laby A1 interferes with DENV and ZIKV entry in target cells	97
5.2.3.2 Laby A1 is not active anymore when a washing step is included prior to infection	98

5.2.3.3 Laby A1 binds selectively to the viral particle and exerts virucidal activity	99
5.2.3.4 Laby A1 binds to viral envelope phospholipids	100
5.3 Conclusion	103
Chapter 6 Interaction of TIM-1 with Laby A1 and its role in ZIKV entry	105
6.1 Introduction	107
6.2 Results and discussion	107
6.2.1 TIM-1 expression in cell lines	107
6.2.2 Importance of the cell surface receptor TIM-1 in ZIKV infection	109
6.2.2.1 TIM-1 expression enhances ZIKV infection	109
6.2.2.2 TIM-1 surface expression is altered after ZIKV and DENV infection..	112
6.2.3 Evaluation of TIM-1 – Laby A1 interaction	115
6.2.3.1 Antibody binding assay suggests interaction of Laby A1 with viral entry receptor TIM-1	115
6.2.3.2 Optimization of a phagocytosis assay to study TIM-1 function and Laby A1 interaction.....	118
6.3 Conclusion.....	122
Chapter 7 CD300a: an entry receptor for ZIKV?	123
7.1 Introduction.....	125
7.2 Results and discussion	125
7.2.1 CD300a expression in cell lines.....	125
7.2.2 CD300a increases production of infectious ZIKV	126
7.2.3 CD300a expression increases ZIKV-induced CPE	128
7.2.4 CD300a expression increases ZIKV replication.....	130
7.2.5 aCD300a Ab inhibits ZIKV and DENV infection.....	131
7.2.5 Anti-CD300a decreases ZIKV infection in MDDC	132
7.3 Conclusion.....	133
Chapter 8 General discussion	135
8.1 Evaluation of entry inhibitors against enveloped viruses	135
8.1.1 Lignosulfonates display broad anti-HIV activity by interacting with the viral envelope	135
8.1.2 Labyrinthopeptin A1 inhibits DENV and ZIKV infection by interfering with the viral phospholipid membrane	137
8.2 Involvement of phosphatidylserine receptors in ZIKV entry	140
8.2.1 TIM-1 enhances entry of ZIKV and possibly interacts with Labyrinthopeptin A1	140
8.2.2 CD300a enhances entry of ZIKV	142

8.3 Considerations and limitations related to...	143
8.3.1 ... broad-spectrum antivirals	143
8.3.2 ... entry inhibitors	144
List of references	147
Acknowledgements, personal contribution and conflict of interest	171

List of abbreviations

AA	amino acid
Ab	antibody
ADE	antibody-dependent enhancement
AF	Alexa Fluor
AIDS	acquired immune deficiency syndrome
Akt	protein kinase B
APC	antigen-presenting cell
APC	allophycocyanin
Arbovirus	arthropod-borne virus
ART	antiretroviral therapy
Asn	asparagine
BAI	brain-specific angiogenesis inhibitor
BSA	broad-spectrum antiviral
C	capsid protein
CAM	cell adhesion molecule
CC	cell control
CC ₅₀	50% cytotoxic concentration
CCID ₅₀	50% cell culture infectious dose
CCR	CC chemokine receptor
CD	cluster of differentiation
CEI	cellular electrical impedance
CHIKV	chikungunya virus
CME	clathrin-mediated endocytosis
CPE	cytopathic effect
CXCR	CXC chemokine receptor
CYD-TDV	chimeric yellow fever-dengue tetravalent dengue vaccine
DaR	Donkey anti-Rabbit
DC	dendritic cell
DC-SIGN	dendritic cell – specific intercellular adhesion molecular 3-grabbing non-integrin
DENV	dengue virus

DMSO	dimethyl sulfoxide
DS	dextran sulfate
E	envelope protein
EBOV	Ebola virus
ER	endoplasmic reticulum
ERK	extracellular signal-regulated kinase
FBS	fetal bovine serum
FDA	the Food and Drug Administration
FITC	fluorescein isothiocyanate
GAG	glycosaminoglycan
GaM	Goat anti-Mouse
GaR	Goat anti-Rabbit
GM-CSF	granulocyte-macrophage colony-stimulating factor
gp	glycoprotein
HAVC(R)	hepatitis A virus cellular (receptor)
HCV	hepatitis C virus
HIV	human immunodeficiency virus
HRIG	human rabies immune globulin
HSP	heat shock protein
HSV	Herpes simplex virus
IC ₅₀	50% inhibitory concentration
Ig	immunoglobulin
Il	interleukin
IN	integrase
IRB	Institutional Review Board
ITIM	immunoreceptor tyrosine-based inhibitory motif
JEV	Japanese encephalitis virus
kb	kilobase
KIM	kidney injury molecule
KO	knockout
LAT	linker of activated T cells
LPS	lipopolysaccharides

L-SIGN	liver/lymph node – specific intercellular adhesion molecular 3-grabbing non-integrin
mAb	monoclonal antibody
MDDC	monocyte-derived dendritic cell
MERS-CoV	Middle East respiratory syndrome coronavirus
MOI	moiety of infection
MTS	3-(4,5-dimethylthiazol-2-yl)-5-(3-carboxymethoxyphenyl)-2-(4-sulfophenyl)-2H-tetrazolium)
NPC-1	Niemann–Pick C1
NFAT	nuclear factor of activated T cells
NK	natural killer cell
NS	nonstructural protein
PBMC	peripheral blood mononuclear cells
PBS	phosphate buffered saline
PE	phosphatidylethanolamine
PE	phycoerythrin
PerCP-Cy5.5	peridinin-chlorophyll-protein complex - cyanine 5.5
PES	phenazine ethosulfate
PFA	paraformaldehyde
PFU	plaque forming units
PHA	phytohemagglutinin
PI3K	phosphoinositide 3-kinase
PIC	pre-integration complex
PR	protease
PrEP	pre-exposure prophylaxis
(pr)M	(pre)membrane protein
PS	phosphatidylserine
PSR	phosphatidylserine receptor
RAGE	receptor for advanced glycation end products
RNA	ribonucleic acid
RSV	respiratory syncytial virus
RT	reverse transcriptase
RT	room temperature

SARS-CoV(2)	severe acute respiratory syndrome coronavirus type 2
SEM	standard error of the mean
SHP	Src homology region 2 domain-containing phosphatase
SI	selectivity index
SPR	surface plasmon resonance
TAM	Tyro3, Axl, Mer
TCR	T cell receptor
TFS	Thermo Fisher Scientific
Th	T helper cell
TIM	T cell immunoglobulin and mucin domain
UNAIDS	the Joint United Nations Programme on HIV/AIDS
VC	virus control
VZV	varicella-zoster virus
WHO	World Health Organization
WNV	West Nile virus
WT	wild type
YFV	yellow fever virus
ZIKV	Zika virus

Summary

Viral infections and epidemics cause severe physical, emotional and economic damage worldwide, as unfortunately illustrated by the current SARS-CoV 2 pandemic. Against many of these viral infections, there is still no effective treatment available. Furthermore, the development of preventive vaccines or specific antiviral drugs is a time-consuming and expensive process. Therefore, broad-spectrum antivirals would be useful during epidemics of (re)emerging viruses.

Many viruses wrap their genetic material in a host-derived lipid bilayer associated with viral glycoproteins: the envelope. Enveloped viruses engage with target cells through interactions between their envelope and cellular entry receptors that allow entry of viral particles into the cell, and subsequent replication and dissemination. Virus entry is an attractive target for the development of antiviral drugs with broad-spectrum activity, by either targeting the viral envelope or the cellular entry receptors.

In this doctoral thesis, we focused on the pathogenic enveloped viruses human immunodeficiency virus (HIV), Zika virus (ZIKV), and dengue virus (DENV). We concentrated on the development of antiviral molecules that inhibit entry of these viruses, and on the role of cellular phosphatidylserine (PS) receptors in ZIKV entry.

A first class of antiviral molecules that was studied in this thesis were the lignosulfonates. These anionic sulfonated polymers are byproducts formed during the production of wood pulp using sulfite processing. It was previously shown that a commercially available lignosulfonate inhibits entry of HIV and Herpes simplex virus (HSV). We have now determined the antiviral activity and mechanism of action of 24 structurally different lignosulfonates. Here, we demonstrate that this activity is correlated to the molecular weight of the compounds and that they inhibit HIV entry by interacting with viral envelope glycoproteins. Together with the low costs and apparent absence of cytotoxicity, these findings make lignosulfonates interesting molecules with a possible application as topical microbicides to prevent HIV transmission.

The second class of molecules examined in this PhD project were the labyrinthopeptins. These are a group of bacterial peptides of which one member, Labyrinthopeptin A1 (Laby A1) demonstrates broad anti-HIV and anti-HSV activity. We described the broad antiviral activity of Laby A1 against DENV and ZIKV by inhibiting viral entry through binding with the envelope phospholipids PS and

phosphatidylethanolamine, which compromises the integrity of the viral particle. Therefore, Laby A1 has potential for further development as a broad-acting entry inhibitor of enveloped viruses.

A second topic in this thesis was the study of an interesting class of viral entry receptors: the phosphatidylserine receptors (PSR). They bind to the phospholipids present in the viral envelope, leading to viral endocytosis and further replication, a process called apoptotic mimicry. To date, the role of these receptors in virus entry remains underexplored and there are no antivirals targeting them.

T cell immunoglobulin and mucin domain 1 (TIM-1) was the first PSR that was studied in this project. This receptor is generally expressed on cells of the immune system and has an important function in T cell activation and clearance of apoptotic cells. Although many receptors are involved in DENV and ZIKV entry, TIM-1 is the only one for which DENV internalization has actually been demonstrated. First, we confirmed that this receptor indeed enhances ZIKV and DENV infection. Secondly, we determined if Laby A1 exerts an additional mechanism of action by interacting with TIM-1. To this end, we also optimized a functional assay to determine the inhibition of TIM-1-mediated phagocytosis by Laby A1. Laby A1 inhibited TIM-1 receptor expression and function to some extent, but further research is needed to unravel this observation.

The second PSR we examined was CD300a. This receptor is involved in immune system regulation and inhibition of phagocytosis. It was previously shown that CD300a enhances DENV entry, but its role in ZIKV infection is still unknown. Here, we demonstrated that CD300a promotes ZIKV entry and replication. However, the exact role of this receptor in DENV and ZIKV entry will have to be further explored.

Altogether, this thesis contributes to the search for novel entry inhibitors with broad antiviral activity and distinct mechanisms of action by either interacting with the viral envelope or a cellular entry receptor.

Samenvatting

Virale infecties en epidemieën veroorzaken wereldwijd erge lichamelijke, emotionele en economische schade, zoals geïllustreerd door de huidige SARS-CoV 2 pandemie. Tegen de meeste van deze virale infecties bestaat er nog geen afdoende behandeling. Het ontwikkelen van preventieve vaccins of specifieke antivirale middelen is een tijdrovend en erg duur proces. Daarom zouden breedspectrum virusremmers heel nuttig zijn tijdens epidemieën van opkomende virussen.

Veel virussen verpakken hun genetisch materiaal in een dubbele fosfolipidenlaag die is afgeleid van de gastheer, en bezet is met virale glycoproteïnen: de virale envelop. Geënveloppeerde virussen interageren met hun doelwitcellen via associaties tussen hun envelop en cellulaire toegangsreceptoren. Deze interacties leiden tot het binnendringen van de virale partikels in de cel, gevolgd door virusrepletie en verdere verspreiding. Het binnendringen van een virus in de cel is een aantrekkelijk doelwit voor de ontwikkeling van breedspectrum antivirale middelen. Deze kunnen enerzijds de virale envelop of anderzijds de cellulaire toegangsreceptoren als doelwit hebben. In deze doctoraats thesis hebben we gefocust op de volgende pathogene virussen: humaan immunodeficiëntievirus (HIV), Zika virus (ZIKV), en dengue virus (DENV). We hebben ons enerzijds toegespitst op de ontwikkeling van antivirale moleculen die de toegang van deze virussen verhinderen, en anderzijds op de rol van de cellulaire fosfatidylserine (PS) receptoren in ZIKV toegang.

Een eerste klasse antivirale moleculen die we onderzochten waren de lignosulfonaten. Deze anionische gesulfoneerde polymeren zijn bijproducten die ontstaan tijdens de productie van houtpulp met behulp van het zogenaamde sulfiet proces. Eerder hebben we al aangetoond dat een commercieel verkrijgbaar lignosulfonaat de toegang van HIV en Herpes simplex virus (HSV) tot de cel verhindert. In dit onderzoek hebben we de antivirale activiteit en het werkingsmechanisme van 24 structureel verschillende lignosulfonaten bepaald. We tonen aan dat deze activiteit gecorreleerd is met de moleculaire massa van de producten, en dat deze het binnendringen van HIV in de cel verhinderen door te interageren met de glycoproteïnen in de virale envelop. Samen met hun lage kost en de afwezigheid van toxiciteit maken deze bevindingen van lignosulfonaten interessante moleculen met een mogelijke toepassing in microbiciden die de seksuele transmissie van HIV kunnen helpen voorkomen.

De tweede groep moleculen onderzocht tijdens dit doctoraatsproject waren de

labyrinthopeptiden. Dit is een groep bacteriële peptiden waarvan een van zijn leden, Labyrinthopeptin A1 (Laby A1), anti-HIV en anti-HSV activiteit vertoont. Hier beschrijven we de brede antivirale activiteit van Laby A1 tegen DENV en ZIKV. Dit gebeurt door binding met de fosfolipiden PS en fosfatidylethanolamine, wat leidt tot het verstoren van de integriteit van het viruspartikel. Hierdoor heeft Laby A1 potentieel om het verder te ontwikkelen als breedspectrum virusremmer die de toegang van geënveloppeerde virussen tot de cel verhindert.

Een tweede deelproject in deze thesis was de studie van een interessante klasse toegangsreceptoren: de fosfatidylserine receptoren (PSR). Deze binden aan de fosfolipiden in de virale envelop, wat leidt tot opname van het virus in de cel, en verdere replicatie. Dit proces wordt apoptose mimicry genoemd. Tot nu toe is de rol van deze receptoren in virustoegang echter nog onderbelicht, en er zijn nog geen antivirale middelen die de receptoren als doelwit hebben.

T cell immunoglobulin and mucin domain 1 (TIM-1) was de eerste PSR die we in dit project hebben bestudeerd. Deze receptor wordt over het algemeen tot expressie gebracht op immuuncellen en heeft een belangrijke functie in T cel activatie en het verwijderen van apoptotische cellen. Hoewel er veel receptoren betrokken zijn bij DENV en ZIKV toegang tot de cel, is TIM-1 de enige waarvan is aangetoond dat hij verantwoordelijk is voor effectieve internalisatie van DENV in de cel. In dit onderzoek toonden we eerst aan dat TIM-1 ZIKV en DENV infectie daadwerkelijk promoot. Ten tweede bepaalden we of Laby A1 een bijkomend werkingsmechanisme heeft, namelijk een interactie met TIM-1. Hiervoor trachtten we een functioneel assay te optimaliseren om te kunnen bepalen of Laby A1 fagocytose door TIM-1 afremt. Laby A1 verhinderde deels de expressie en functie van TIM-1, maar verder onderzoek is nodig om deze bevindingen verder op te helderen.

De tweede PSR die we onderzochten was CD300a. Deze receptor is mede verantwoordelijk voor de regulering van het immuunsysteem en het afremmen van fagocytose. Voorheen is aangetoond dat CD300a DENV toegang tot de cel promoot, maar zijn rol in ZIKV infectie was nog onbekend. Hier hebben we voor het eerst aangetoond dat CD300a ook ZIKV replicatie promoot. De exacte rol van de receptor in DENV en ZIKV toegang moet ook nog verder worden uitgeklaard.

We besluiten dat deze thesis bijdraagt aan de zoektocht naar nieuwe breedspectrum antivirale middelen die de toegang van virussen tot de cel verhinderen.

Chapter 1

General introduction

1.1 Entry of enveloped viruses

1.1.1 The heavy burden of viral infections

Viruses and the diseases they cause have had a major impact on human health throughout history, and will continue to affect human well-being in the future. They have caused deadly epidemics for many centuries, such as hemorrhagic fever (a group of illnesses characterized by fever and bleeding disorders). It was until 1901 that the first cause of hemorrhagic fever was recognized: the yellow fever virus (YFV). This arthropod-borne (arbo)virus was able to conquer the world in the 17th century when it was transported – along with its mosquito vector – to the Western Hemisphere by slave trade ships.¹

Another infamous example of an epidemic that has shaped human history is the 1918 flu pandemic (or “Spanish flu”), caused by the H1N1 influenza virus. Estimates suggest that this unprecedented pandemic has caused the death of at least 50 million people.² Fortunately, safe and effective YFV and influenza vaccines have been developed.^{3,4} However, **for many other viral infections there is no treatment available.**

The following **recent epidemics** also illustrate the major impact of viral infections on human health. Zika virus (ZIKV) has transformed from an obscure virus circulating for many decades without causing major threats, to a “Public Health Emergency of International Concern” in 2015, leaving behind more than 3700 newborns with microcephaly.⁵ This is a good example of how a low-risk virus can cause severe epidemics in a short time frame.

Another example is the Ebola virus (EBOV), which causes an often fatal hemorrhagic fever. The EBOV epidemics of 2013-2016 and 2018-2020 have killed thousands of people in respectively Western Africa and the Democratic Republic of the Congo.⁶

In the past 5 years, 15 dengue virus (DENV) outbreaks have been reported.⁷ Estimates suggest that more than half of the world’s population is at risk of DENV

infection, with 390 million symptomatic infections and 21,000 deaths every year.⁸ To illustrate this **high burden of virus infections**, Figure 1.1 gives an overview of all virus outbreaks reported by WHO during the first half of 2020.⁷

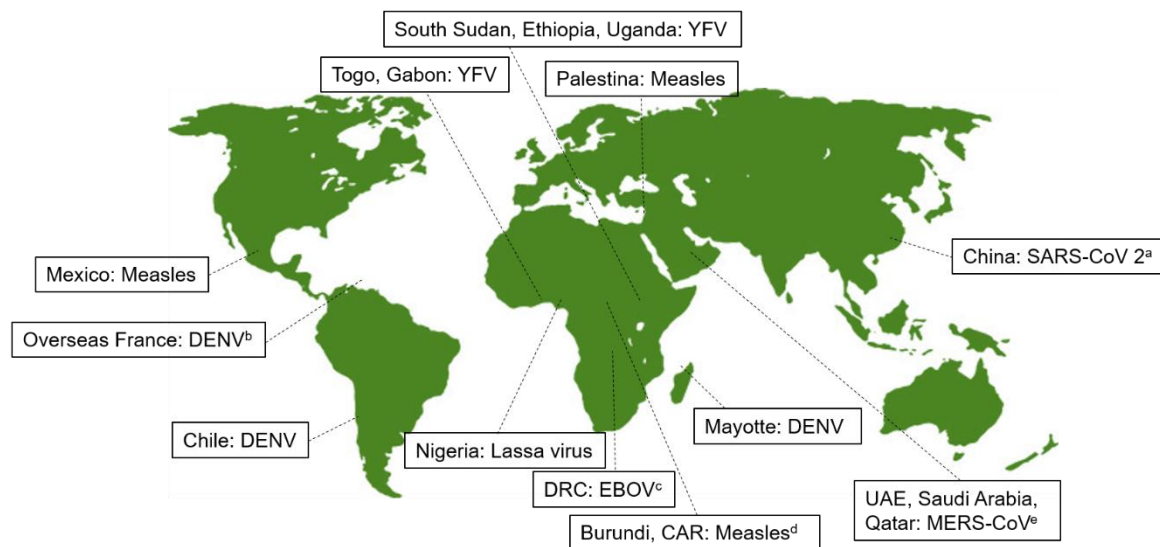


Figure 1.1 Virus outbreaks during the first 6 months of 2020. Overview of virus outbreaks as reported by WHO Disease Outbreak News from January to June 2020. According to WHO, an outbreak is defined as an exceptional event which requires extra human and financial resources and may also rely on additional partners, agencies and other sectors. ^aThis outbreak has grown to one of pandemic proportions. ^bFrench Guiana, Guadeloupe, Martinique, Saint-Martin, and Saint-Barthélemy. ^cDRC: Democratic Republic of the Congo. ^dCAR: Central African Republic. ^eUAE: United Arab Emirates.

Besides imposing **severe physical, emotional and financial costs** on people and health services, viral infections also involve **major socioeconomic disruptions**. This is illustrated by the ongoing outbreak of the severe acute respiratory syndrome coronavirus 2 (SARS-CoV-2) and subsequent worldwide 'lockdown', which is estimated to cause a decrease of the Belgian economic activity with 9% in 2020.⁹

The global spread of viruses is increasing dramatically because of several factors, including **globalization, urbanization, improper vector control, and lack of sufficient health care**.¹⁰ **Climate change** also has a major impact, since it increases the distribution of arthropod vectors such as *Aedes aegypti* and the viruses they carry (e.g. DENV, ZIKV, YFV, chikungunya virus (CHIKV)), prolonging transmission season and elevating transmission efficiency.¹¹ The current **overpopulation and severe perturbation of ecologic balance** due to augmented land use by humans also increases the risk of spreading of viruses that

jump from animals to humans (*i.e.* zoonotic viruses).¹² These factors will not only lead to epidemics caused by well-described viruses such as DENV, but also to the (re)emergence of viruses that were not previously encountered, like the coronaviruses SARS-CoV(2) and Middle East respiratory syndrome (MERS)-CoV.^{13–15}

On the other hand, 'controlled' viral epidemics also require attention. The emergence of human immunodeficiency virus (HIV) has caused the most considerable pandemic of the last decades. This virus has infected 75 million people (and killed more than 32 million) worldwide since the start of the epidemic in 1981.¹⁶ Although accurate **prevention and treatment strategies have seriously decreased HIV** incidence, mortality and morbidity, **eradication has not been obtained and resistance** to existing antiretroviral drugs is a major concern.¹⁷

These examples highlight the **urgent need for novel antivirals** to treat viral infections for which no treatment exists yet, and to supplement the currently limited arsenal of antiviral drugs and vaccines.

1.1.2 Biology of enveloped viruses

Viruses distinguish themselves from other biological entities because they depend on the infection of cells of other organisms to ensure the replication of their genetic material and thus their survival. Many RNA and DNA viruses wrap their nucleocapsid in an **envelope: a host-derived lipid bilayer associated with specific virally encoded proteins that are often glycosylated**.¹⁸ Although this envelope makes them more sensitive to heat, desiccation and detergents, it also provides crucial benefits. The envelope shields the virus against immune recognition and neutralizing antibodies, it provides anchor sites for other viral proteins, and it facilitates attachment to and entry in target cells.

The entry of enveloped viruses can occur through divergent mechanisms, such as direct fusion with the plasma membrane or by endocytosis. In the following sections, these entry mechanisms are illustrated by the viruses studied in this project (*i.e.* HIV, ZIKV and DENV). More specifically, the viruses' structure, their replication and entry process, together with the possible strategies to inhibit viral entry, are discussed.

1.1.2.1 Retroviruses

The human retrovirus **HIV** (family: *retroviridae*, genus: *Lentivirus*) mainly infects CD4⁺ T cells, key players of the human adaptive immune system, and – when untreated – leads to their destruction and progressive depletion. This eventually causes acquired immune deficiency syndrome (AIDS). The virus weakens the immune system, making AIDS patients vulnerable to various opportunistic infections, virus-induced cancers and other diseases (reviewed in ref 17).

1.1.2.1.1 HIV structure

Two HIV species exist, *i.e.* HIV-1 and HIV-2, further divided into groups and subtypes. The **general structure** of HIV-1 is described in the following section, because it is the more dominant and pathogenic strain.

HIV is a retrovirus containing two copies of single-stranded positive-sense RNA (< 10 kb) comprising **9 genes that encode 15 proteins**.¹⁹ The structural proteins are encoded by the *gag*, *pol* and *env* genes (Figure 1.2A). The RNA is closely associated with nucleocapsid proteins (NC, p7) and viral enzymes such as reverse transcriptase (RT, p51), integrase (IN, p31), and protease (PR). They are enclosed by a capsid (CA) of the p24 protein, which is further protected by the matrix (MA) protein p17, ensuring the viral integrity (Figure 1.2B). This structure is further surrounded by the viral envelope, containing the host-derived lipid bilayer spiked with the surface glycoprotein gp120 and the transmembrane glycoprotein gp41, which are encoded by *env*.

These spikes are organized as trimers of **non-covalently linked gp120 and gp41 heterodimers**.²⁰ Gp120 is a heavily glycosylated protein containing 5 conserved domains (C1-5) and 5 variable loops (V1-5) (Figure 1.2C and Figure 4.8A).²¹ It is involved in (co)receptor tropism and interaction, and immune evasion. Gp41 consists of an ectodomain containing a fusion peptide and 2 heptad repeats, a transmembrane domain, and a long intracellular tail (the ectodomain is shown in Figure 1.2C and Figure 4.8B).²²

The remaining HIV proteins, *i.e.* the regulatory proteins Tat and Rev and the accessory proteins Vif, Nef, Vpu and Vpr are involved in HIV infectivity, replication, and pathology (reviewed in ref 23).

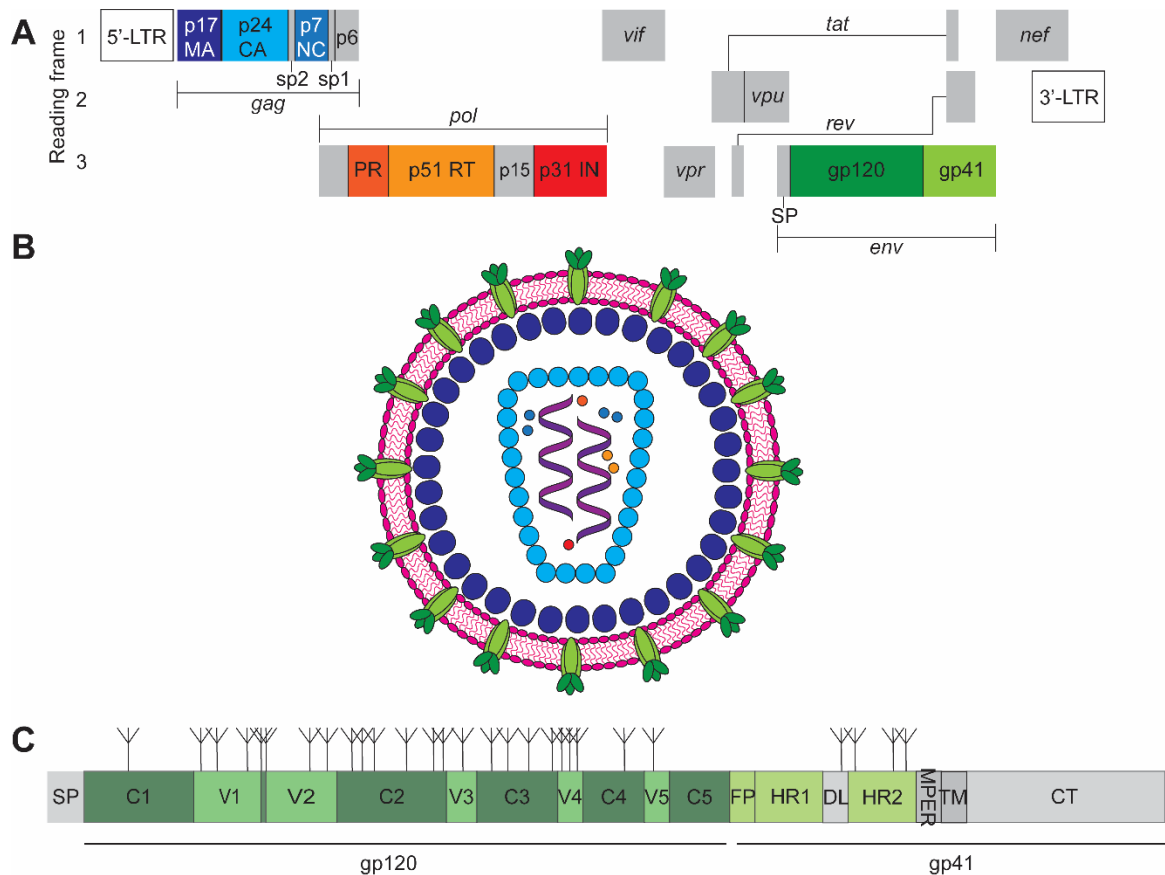


Figure 1.2 HIV-1 structure. (A) Organization of the HIV-1 RNA genome. Boxes represent regulatory and structural protein coding regions, black vertical lines show polyprotein-domain junctions. Gene names are written in *italic*. The colors are corresponding to the structural proteins in the schematic structure of a mature HIV particle (B). LTR: long terminal repeat; MA: matrix; CA: capsid; sp: spacer peptide; NC: nucleocapsid; PR: protease; RT: reverse transcriptase; IN: integrase; SP: signal peptide. (C) Primary structures of the envelope glycoproteins gp120 and gp41. Forked structures represent glycosylation sites. C1-5: conserved domains; V1-5: variable domains; FP: fusion peptide; HR: heptad repeat; MPER: membrane-proximal external region; TM: transmembrane region; CT: cytoplasmic tail.

1.1.2.1.2 HIV entry and replication

HIV enters the human body by transmission in body fluids like blood, semen or breast milk from an infected individual. A first but non-essential step in the viral life cycle is **attachment** of the viral gp120 envelope protein to various host cell membrane proteins, such as glycosaminoglycans (GAGs) or dendritic cell – specific intercellular adhesion molecular 3-grabbing non-integrin (DC-SIGN).^{24,25} This attachment brings the virus in close proximity to the **cluster of differentiation 4 (CD4) entry receptor**. CD4 is expressed on a wide variety of cells, such as lymphocytes, monocytes and dendritic cells and normally functions by enhancing T-cell receptor mediated signaling.²⁶ First, CD4 binds to the CD4 binding site in

gp120 (Figure 1.3 step 1).²⁷ This interaction leads to the formation of a bridging sheet and exposes the V3 loop binding site in gp120 for the **coreceptor**. These are either the CC chemokine receptor 5 (CCR5) or the CXC chemokine receptor 4 (CXCR4) (Step 2). CCR5 is highly expressed on memory T lymphocytes, macrophages and dendritic cells, while CXCR4 is expressed on both memory and activated T lymphocytes. HIV viruses can either use CCR5 (R5 strains), CXCR4 (X4 strains), or both (R5X4 strains). Of note, other chemokine receptors such as CXCR7 have been reported to facilitate HIV entry *in vitro*.²⁸ The coreceptor's engagement leads to insertion of the gp41 **fusion peptide** into the host cell membrane, which brings both membranes in close proximity, followed by the rearrangement of the heptad repeats in gp41 (Step 3). This induces the formation of a six-helix bundle which tethers the membranes even closer, and finally the formation of a fusion pore and **fusion** of the viral and host cell membranes (Step 4).²⁹

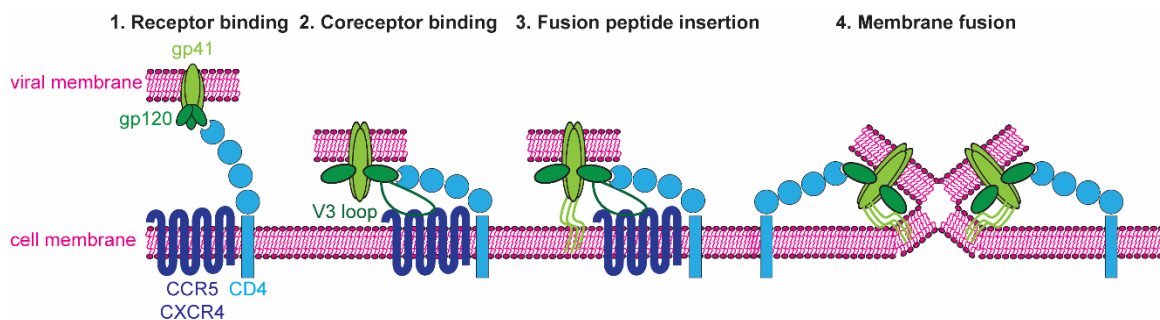


Figure 1.3 Schematic overview of HIV entry in host cells. HIV binds to the CD4 receptor of CD4⁺ T cells (1) followed by binding to the coreceptor (2). The subsequent conformation changes lead to fusion peptide insertion (3) and membrane fusion (4). Based on ref 29.

After membrane fusion, the viral content is delivered into the host cell cytoplasm. Briefly, the **remaining steps of the HIV life cycle** are as follows (Figure 1.4, upper part). The uncoating of the capsid protein releases the different viral enzymes and RNA (Step 2). HIV RT converts the RNA genome into linear double stranded DNA (Step 3). This DNA is bound to viral IN and forms the pre-integration complex (PIC) together with other viral and cellular factors. The PIC is imported into the cellular nucleus after which HIV IN catalyzes DNA integration into the host's genome (Step 4). The transcription machinery of the host cell transcribes viral genes and the resulting mRNA is transferred to the cytosol for translation (Step 5). Finally, two

RNA copies and viral proteins are assembled and budding occurs at the cell membrane (Step 6). Viral PR cleaves the GagPol polyprotein leading to the formation of the capsid and a mature HIV particle (Step 7).^{30,31}

1.1.2.1.3 HIV inhibitors targeting the different steps of the viral life cycle

Unfortunately, there is **no HIV vaccine or cure** available yet. The virus is highly polymorphic due to its error-prone RT and high replication rate. This complicates the development of an appropriate immune response or neutralizing vaccine³². Furthermore, HIV has developed escape strategies to secure its survival. The virus resides in multiple latent reservoirs, which are not accessible for immune cells or therapeutics.³³

However, various drugs have been developed that decrease the viral load to near-undetectable levels and significantly improve the patient's life quality and duration. This renders HIV infection into a chronic condition rather than a disease. Table 1.1 provides an overview of all FDA-approved HIV antivirals that are used in the clinic today. They target various steps in the HIV life cycle, *i.e.* the HIV proteins gp41, RT, IN and PR, or the human HIV entry (co)receptors CD4 and CCR5. The different classes are also indicated in Figure 1.4.

Treatment with HIV antivirals consists of lifelong combination therapy, called **antiretroviral therapy** (ART). In general, a treatment regimen includes three antivirals from at least two different classes.³⁴ This combination treatment reduces the likelihood of resistance development and strongly suppresses viral replication. Despite the significant improvement in outcome, ART is also associated with side effects, and resistance against drugs used in the treatment regimen always remains a threat. Another pitfall of ART therapy is that it is not accessible to everyone. Therefore, HIV disease management may not only focus on treatment. **Prevention of virus transmission** remains also crucial to limit HIV-related morbidity and mortality. Preventive measures include male condom use, the intake of antiretrovirals (called pre-exposure prophylaxis or PrEP) and the development of so-called microbicides. This is further discussed in Chapter 4.

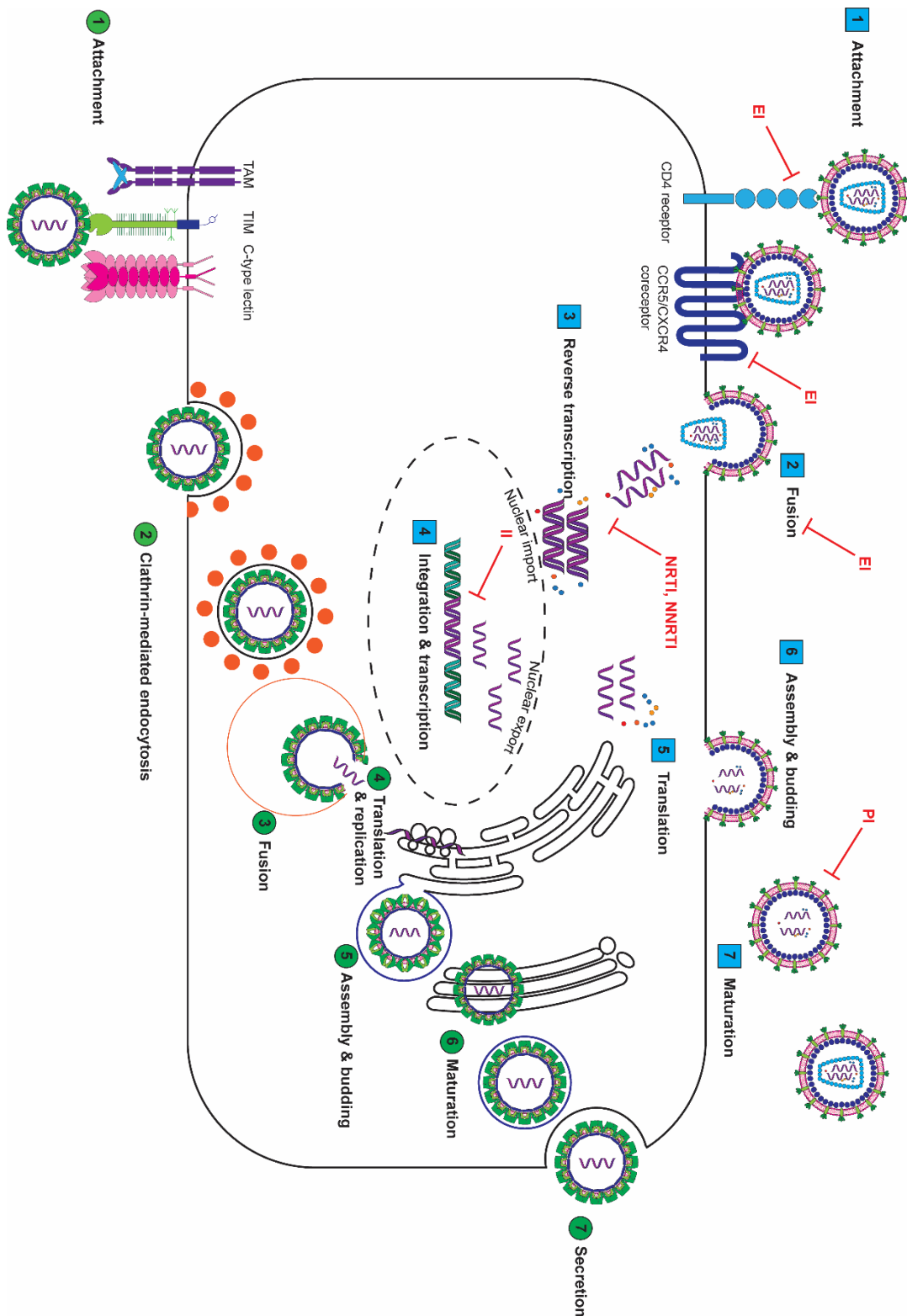


Figure 1.4 Schematic overview and comparison of the life cycles of HIV (blue squares) and flaviviruses such as ZIKV and DENV (green circles). HIV enters the cell through plasma membrane fusion, while flaviviruses use clathrin-mediated endocytosis for entry in target cells. The different steps in the viral life cycles are illustrated in Sections 1.1.2.1.2 (HIV) and 1.1.2.2.2. (flaviviruses). The different classes of antiretroviral therapy used in clinic and their site of action are indicated in red.

Table 1.1 Overview of FDA-approved HIV medicines used in the clinic

Class	Target	Approval year
Entry inhibitors (EI)		
Enfuvirtide	gp41	2003
Maraviroc	Human CCR5	2007
Ibalizumab	Human CD4	2018
Nucleoside or Nucleotide Reverse Transcriptase inhibitors (NRTI)		
Zidovudine	Deoxythymidine triphosphate	1987
Lamivudine	Deoxycytidine triphosphate	1995
Abacavir	Deoxyguanosine triphosphate	1998
Tenofovir disoproxil fumarate	Deoxyadenosine triphosphate	2001
Emtricitabine	Deoxycytidine triphosphate	2003
Non-nucleoside Reverse Transcriptase inhibitors (NNRTI)		
Nevirapine	HIV RT	1996
Efavirenz	HIV RT	1998
Etravirine	HIV RT	2008
Rilpivirine	HIV RT	2011
Doravirine	HIV RT	2018
Integration inhibitors (II)		
Raltegravir	HIV integrase	2007
Elvitegravir	HIV integrase	2012
Dolutegravir	HIV integrase	2013
Bictegravir	HIV integrase	2018
Protease inhibitors (PI)		
Saquinavir	HIV protease active site	1995
Ritonavir	HIV protease active site Cytochrome P450 3A4	1996
Lopinavir	HIV protease active site	2000
Atazanavir	HIV protease active site	2003
Tipranavir	HIV protease active site	2005

Darunavir	HIV protease active site	2006
Pharmacokinetic enhancers		
Cobicistat ^a	Cytochrome P450 3A4	2014

The antiretrovirals amprenavir, didanosine, delavirdine, indinavir, nelfinavir, stavudine, zalcitabine are not included in the table since they are no longer used or recommended in clinic due to unwanted side effects, resistance development or marketing issues. ^aCobicistat has no antiviral activity, but increases adsorption of PI in combination treatments.

1.1.2.2 Flaviviruses

DENV and ZIKV belong, together with other pathogenic arboviruses (such as YFV, Japanese encephalitis virus (JEV) and West Nile virus (WNV)), to the flaviviruses (family: *flaviviridae*, genus: *Flavivirus*). While most DENV and ZIKV infections are self-limiting causing no or only mild symptoms (e.g. fever, rash, joint pain), they can also be associated with dangerous hemorrhagic (DENV) or neurological (ZIKV) complications. A severe DENV infection can overstimulate the immune system, inducing endothelial dysfunction and plasma leakage (dengue hemorrhagic fever) and even life-threatening low blood pressure and organ failure (dengue shock syndrome).^{8,35} ZIKV on the other hand can cause the autoimmune disorder Guillain-Barre syndrome or severe developmental brain defects such as microcephaly.^{36–38}

1.1.2.2.1 Flavivirus structure

DENV and ZIKV are closely related and consist of a positive-sense single-stranded RNA (~11 kb) genome that **encodes 10 proteins** in 1 open reading frame (Figure 1.5A).³⁹ The RNA is protected by capsid proteins (C) and the envelope, consisting of the host-derived lipid bilayer anchored with viral envelope (E) and membrane ((pr)M) glycoproteins (Figure 1.5B). The 7 nonstructural proteins (NS1-NS5) are involved in viral replication, assembly and immune evasion.⁴⁰

The **E protein** consists of an extracellular part with 3 distinct domains (I-III) and a transmembrane part that anchors the protein into the viral envelope. Domain I stabilizes the E protein and is involved in its conformational rearrangements, domain II is critical for membrane fusion, and domain III is involved in receptor interaction (Figure 1.5C).⁴¹ In its immature noninfectious state, the envelope is organized as 60 trimers of prM-E heterodimers. Maturation induces conformational

changes which rearrange the E proteins to 90 homodimers tightly covering the viral membrane.^{41–43}

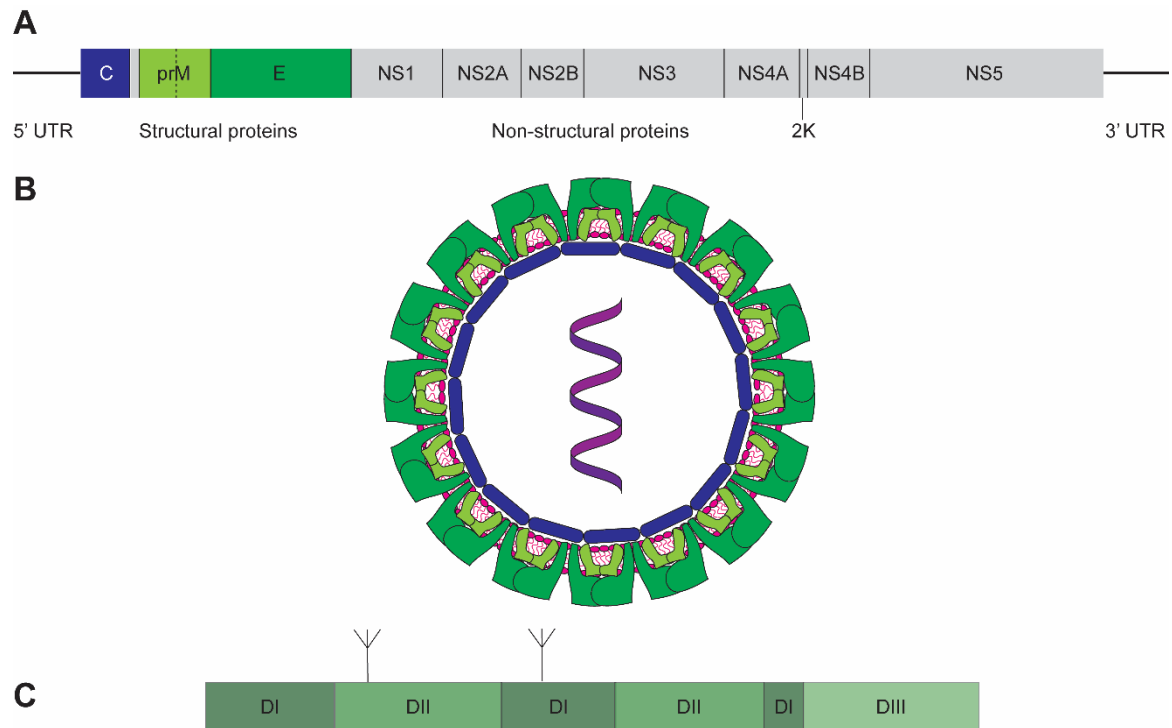


Figure 1.5 Overview of Flavivirus structure. (A) Organization of the Flavivirus RNA genome. Proteins are indicated with boxes, cleavage sites with black vertical lines. Structural proteins are indicated in color; non-structural proteins and 2K signal peptide in grey. (B) Schematic representation of a mature Flavivirus. Colors are corresponding to the proteins depicted in (A). (C) Primary structure of ectodomain of the E protein. D: domain. Forked structures represent N-linked glycosylation sites. DENV has two glycans at asparagine (Asn) 67 (in DII) and Asn 153 (in DI), whereas ZIKV has only one glycan at Asn 154 (in DI).

1.1.2.2.2 Flavivirus entry and replication

DENV and ZIKV are transmitted by infected *Aedes* mosquitoes, although sexual transmission of ZIKV (and extremely rarely of DENV) have also been reported.^{44,45} In the skin, the virus infects a variety of cells and disseminates to the lymph nodes in order to infect other cells through E protein interaction with various receptors (Section 1.1.2.2.4). These receptors can either function as **attachment factors**, thereby retaining viral particles on the cell membrane, or as **entry factors**, leading to viral uptake into the cell (Figure 1.6 step 1).^{46–48} This entry process occurs predominantly by **clathrin-mediated endocytosis** (CME), but other entry mechanisms have also been observed, which are reported elsewhere.^{49,50} During CME, the virus-receptor complex is first co-internalized by pre-existing clathrin-

coated pits through invagination and scission of the plasma membrane by dynamin, forming vesicles (Step 2). This vesicle is then delivered to an early endosome, where acidification due to endosome maturation rearranges the viral E protein (Step 3). This exposes its fusion peptide, which is inserted into the endosome membrane. This leads to further conformational changes in the E protein forming a six-helix bundle and the emergence of a **fusion pore** (Step 4).⁵¹⁻⁵⁴

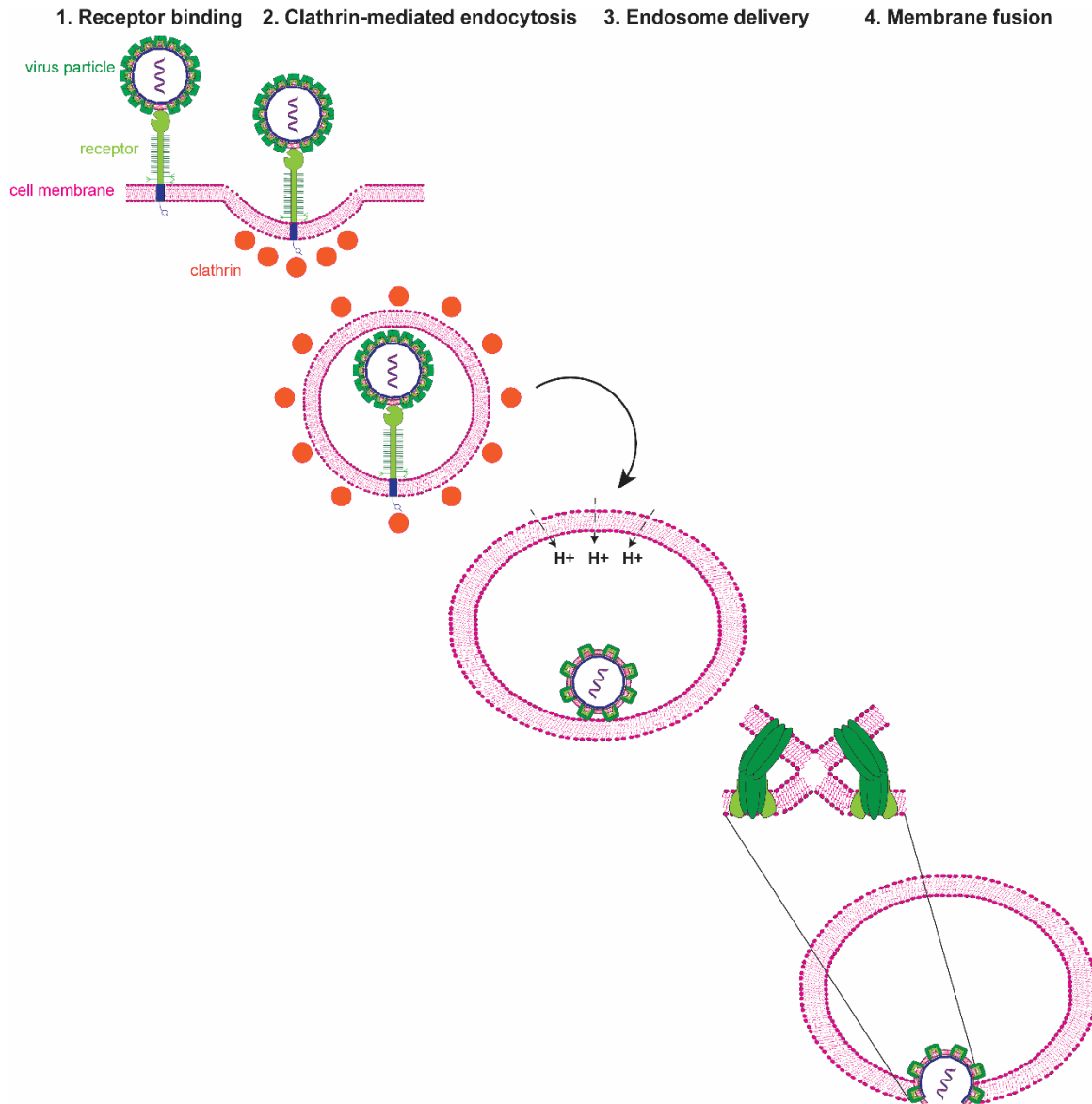


Figure 1.6 Schematic overview of Flavivirus entry through CME. The viral particle binds to an entry receptor (in the figure TIM-1 is depicted) (1). The virus and receptor are co-internalized through endocytosis mediated by the formation of clathrin-coated vesicles (2), followed by delivery to the endosome, indicated with an arrow (3). Acidification of the endosome, indicated with dashed arrows, leads

to rearrangement of the Flavivirus E protein and fusion of the viral and endosome membranes (4). Figure adapted from refs 51 and 53.

The fusion between the viral particle and late endosome results in the release of viral RNA into the cytosol and subsequent **viral replication** (Figure 1.4 lower part). In short, RNA is translated into a single polyprotein by ribosomes of the rough endoplasmic reticulum (ER) (Step 4). The cleavage into functional proteins is catalyzed by viral and cellular proteases, and RNA is amplified by viral RNA-dependent RNA polymerase (encoded by NS5) through a double-stranded RNA intermediate. RNA is encapsidated and buds into the ER lumen (Step 5). The immature viral particle is transported to the Golgi apparatus through the secretory pathway. Here, the low pH triggers another E protein conformational change, which results in the exposure of prM (Step 6). Next, cellular furin cleaves the prM protein to obtain a mature infectious virus that is finally released from the cell via secretory vesicles (Step 7).^{40,55}

1.1.2.2.3 Flavivirus tropism

DENV and ZIKV have a wide cellular tropism. In general, DENV mainly infects cells of the dendritic cell/macrophage/monocyte lineage in the skin and various lymphoid and non-lymphoid tissues.⁴⁷ For example, DENV replication has been observed in Langerhans cells⁵⁶, splenic macrophages⁵⁷ and blood monocytes⁵⁸, and in epithelial and endothelial cells.^{59,60} Furthermore, liver cells are an important DENV target, resulting in DENV-induced liver pathology.^{61,62} In patients, DENV has been detected in blood and tissues such as spleen, lymph nodes, lungs and liver.^{63,64}

In vitro infection studies demonstrate that **ZIKV also infects a broad range of human cells.**⁶⁵ Viral persistence and replication has been observed in dendritic cells⁶⁶, skin cells⁶⁷, neural cells^{68–70}, placental cells^{71–73} and cells of the male reproductive tract.^{74,75} In studies with nonhuman primates, ZIKV RNA has been isolated from nervous, lymphoid, muscle, joint, male/female reproductive tract tissues and from fetal brain tissue.^{76,77} ZIKV has also been detected in human body fluids such as blood, saliva, semen and urine.^{33,78} The persistence of ZIKV in reproductive tract tissues probably contributes to the vertical and sexual transmission of the virus, which is only rarely observed for DENV.

Although DENV and ZIKV **use the same receptors, they have different tropisms** and pathophysiology. For example, ZIKV productively replicates in prostate and Schwann cells, while they are unsusceptible for DENV. However, these cells express receptors that are involved in entry of both viruses.^{74,79} In general, ZIKV has a somewhat broader tropism than DENV.⁸⁰ More research has to determine if there are other cellular factors that stimulate ZIKV or, on the other hand, restrict DENV replication.⁸¹ It is also possible that the slight structural differences between ZIKV and DENV contribute to these species-specific characteristics.⁴³ This might explain differences in transmission ways between ZIKV and DENV. For example, ZIKV is more thermally stable than DENV, probably contributing to its survival in semen and saliva.^{82,83}

1.1.2.2.4 Flavivirus entry receptors

One of the factors controlling tropism is receptor expression. **Many cellular receptors are involved** in Flavivirus attachment and/or entry (Table 1.2).^{46,50,54} However, their precise functions in this entry process are not completely understood. Many receptors such as GAGs, glycosphingolipids and heat shock proteins (HSP) probably limit their role to attachment of the virus and its concentration on the cell membrane to facilitate subsequent interaction with entry receptors. An important role in Flavivirus entry is played by the C-type lectins such as DC-SIGN, L-SIGN and mannose receptor. They are involved in immune system activation by recognizing invading pathogens.⁸⁴ C-type lectins bind carbohydrate residues on the viral envelope glycoproteins. For example, DC-SIGN interacts with the asparagine 67 residue of the DENV E protein.⁸⁵ These C-type lectins are known to be internalized through CME, indicating their potential role as entry receptors.⁸⁶ Finally, also phosphatidylserine (PS) receptors (PSR) are involved in Flavivirus entry. They are further discussed in Section 1.3.

Table 1.2 Overview of mammalian cell receptors involved in Flavivirus entry

Receptor	Presumed role in entry	DENV (ref)	ZIKV (ref)
Carbohydrates			
GAGs	Attachment	87,88	Yes? ⁸⁹ No? ⁹⁰

Glycosphingolipids	Attachment	91,92	TBD
C-type lectins			
DC-SIGN	Presentation to other target cells ⁹³ + internalization? ⁸⁶	94,95	67
L-SIGN	Attachment ⁹³	94	96,97
Mannose receptor	Attachment	98	TBD
CLEC5A	Attachment leads to proinflammatory cytokine production	99	TBD ¹⁰⁰
Phosphatidylserine receptors			
TIM-1	Attachment (ZIKV, DENV) + internalization (DENV)	53,101	67
TIM-3	Attachment	Yes? ¹⁰¹	TBD
TIM-4	Attachment	101	No? ⁶⁷
Tyro3 ^a	Attachment	101	67
Axl ^a	Attachment	101	67
CD300a	Attachment	102	This thesis
Other Flavivirus receptors			
Integrin $\alpha_v\beta_5$ ^b	TBD	No? ¹⁰³	104
37/67-kDa high-affinity laminin receptor	Attachment	105,106 No? ¹⁰⁷	TBD
HSP90 and HSP70	Unclear, E protein interaction	108	109
Claudin-1	Attachment of prM	110	TBD
Scavenger receptor B 1	Apolipoprotein bridging/NS1 interaction?	111	112
NKp44	NK activation	113	TBD
CD14	Part of receptor-virus complex to enhance entry	114	TBD
Fc	Antibody-dependent enhancement	115,116	No? ¹¹⁷

^aIndirect PS interaction: TAM receptors are bridged with PS through Gas6 or Pros1. ^bProbably indirect PS interaction: integrins are bridged with PS through milk fat globule-EGF factor 8.¹¹⁸ This still has to be demonstrated for flaviviruses. TBD: to be determined. Question marks indicate that these findings still have to be confirmed.

1.1.2.2.5 Flavivirus entry inhibitors

The **current treatment** of DENV and ZIKV infection relies on supportive care to relieve symptoms such as bed rest and fluid administration. An important preventive measure is vector control by e.g. managing and/or eliminating vector habitats. Furthermore, DENV infection can be prevented by administration of the CYD-TDV (Dengvaxia) vaccine.¹¹⁹ This live recombinant tetravalent vaccine is the only one licensed until now. However, the vaccine increased hospitalization risk in young children and seronegative individuals, therefore it is only recommended for people aged 9-45 living in endemic areas¹²⁰.

Apart from these preventive measures, the **search for Flavivirus antivirals remains crucial**. Currently, no approved ant Flavivirus drug is available. However, many BSA targeting different steps in the Flavivirus life cycle are being investigated today.¹⁰ The entry of flaviviruses is an attractive target for BSA development. These can either inhibit viral or cellular factors. The high similarity of the Flavivirus envelope and its involvement in attachment, internalization and fusion makes it an ideal target.¹²¹ Since the wide array of cell receptors shown to interact with flaviviruses, much effort has been attributed to the development of inhibitors of these cellular factors as well. A serious drawback of the latter strategy could be viral escape by using other cellular receptors.

To demonstrate the wide array of antiviral strategies that is being investigated, **examples of BSA** targeting various steps in Flavivirus entry are represented in Table 1.3.

Table 1.3 Examples of broad-acting Flavivirus entry inhibitors in preclinical development

Compound	Target	<i>In vitro</i> activity against for example
Virus-targeting inhibitors		
Curcumin ¹²²	Viral membrane fluidity?	DENV, ZIKV, CHIKV
EGCG ¹²³	E protein	ZIKV, DENV, WNV
Carbohydrate-binding agents ¹²⁴	E protein glycans	DENV, JEV, HIV

Labyrinthopeptin A1 ^{125–127} , this thesis	Envelope PS/PE	DENV, ZIKV, HIV, RSV
Pyrimidine derivatives ¹²⁸	E protein β OG pocket ^a	DENV, ZIKV, WNV
Host-targeting inhibitor		
JG40, JG345 ^{129,130}	HSP70 ^b	DENV, ZIKV, WNV
Carrageenans ¹³¹	GAG	DENV, EBOV, HIV
Cabozantinib ¹³²	Axl receptor	ZIKV
Nanchangmycin ¹³²	CME?	ZIKV, DENV, WNV
Obatoclox ¹³³ , Ev37 ¹³⁴ , Niclosamide ¹³⁵	Endosomal pH regulation	ZIKV, DENV, CHIKV

^a β OG: *n*-octyl- β -D-glucoside. ^bThese compounds have possibly multiple mechanisms of action as HSP are involved in different steps of the virus' life cycle.

1.2 Virus entry as antiviral target

1.2.1 Broad-spectrum antivirals

Today, there are hundreds of viruses known to infect humans. However, the FDA-approved antiviral drugs (~100) target only a few of them (~10).¹³⁶ These drugs are mostly compounds that inhibit only one species ('one bug, one drug' concept). Another strategy to tackle viral infections is to target a wider range of viruses ('multiple bugs, one drug'). This type of drugs is called **broad-spectrum antivirals** (BSA). The first synthetic BSA described was ribavirin, approved as a nucleoside analog to treat hepatitis C virus (HCV). This compound also proved active against other RNA and DNA viruses such as respiratory syncytial virus (RSV) and adenovirus.¹³⁷

Another BSA approved in several countries (e.g. Russia, Ukraine, Belarus) is tilorone, which is used for the treatment of influenza, acute respiratory viral infections and viral hepatitis and encephalitis. This drug targets a cellular factor: it induces the production of interferon, the immune system's antiviral defense molecule¹³⁸. Several other BSA are currently in different stages of (pre)clinical development.¹³⁹

An important benefit of BSAs is that they are active against different species or classes of viruses, enabling their **instant use during an epidemic** of (re)emerging viruses, when specific vaccines or antivirals are not yet available. They can be

administered before accurate diagnosis has occurred, **quickly controlling viral load**.¹⁴⁰ This broad antiviral activity is obtained by targeting evolutionarily conserved viral structures (**direct-acting antiviral**) or cellular receptors/pathways hijacked by different virus groups (**host-targeting antiviral**). For example, the nucleotide analog remdesivir was initially developed to inhibit EBOV replication but failed in clinical trials. However, because *in vitro* studies had previously demonstrated activity against pneumo-, paramyxo-, and coronaviruses, the compound was repurposed in several clinical trials during the 2019-2020 SARS-CoV-2 outbreak, resulting in promising therapeutic effects.^{141,142} The use of BSA could also **save time and money** normally spent during drug development, which on average costs more than 2 billion dollars and lasts more than 10 years.¹⁴³ This slow drug development process is a major hazard when a novel epidemic occurs.

1.2.2 Inhibition of virus entry as broad antiviral strategy

Antiviral drugs can target various stages in the viral life cycle. **Entry inhibitors** target the first step in this cycle: the engagement of the viral particle with the host cell and its subsequent uptake (Section 1.1.2). Drugs targeting this step have several benefits. First, **some entry mechanisms are widely conserved** between viral groups. CME for example is used by e.g. alpha-, flavi-, and orthomyxoviruses, and is therefore an interesting target, as well as macropinocytosis, employed by filo-and poxviruses.¹⁴⁴ Secondly, entry inhibitors do not need to enter the cell because they interact with either a viral or a cell surface factor. This is beneficial for structural and chemical drug characteristics and thus **improves target accessibility** for drug candidates such as peptides and antibodies.¹⁴⁵ Thirdly, severe damage caused by the virus during a later stage in its life cycle is prevented. For example, some viral infections such as DENV or EBOV can lead to over activation of the immune system. This could be decreased by an entry inhibitor, which might **improve disease outcome**.¹²¹ Finally, entry inhibitors might be used as **both therapeutic and prophylactic** drugs. The latter is especially interesting for people traveling to endemic countries or to prevent infection with sexually transmitted viruses such as HIV.

Until now, there are **9 FDA-approved antiviral entry inhibitors**, which demonstrates that this is a useful and validated strategy to combat viral infections. These drugs target HIV (maraviroc, enfuvirtide and ibalizumab, Section 1.1.2.1.3),

Herpes simplex virus (HSV; docosanol), varicella-zoster virus (VariZIG and VZIG), respiratory syncytial virus (RSV; palivizumab and RSV-IGIV) and rabies virus (HRIG).

A BSA targeting entry of several viruses is an interesting therapeutic strategy. Various broad-acting entry inhibitors have been developed and studied, targeting different entry stages or a cellular factor.¹⁴⁴ The search for inhibitors targeting the viral particle has yielded many candidates over the years but these are also more prone to rapid resistance development, while targeting a host cellular factor might be more associated with side effects development due to the blocking of critical pathways or to off-target effects.¹²¹ Unfortunately, **no entry inhibitor with broad antiviral activity has made it to the market yet.**

1.3 Phosphatidylserine receptors as an interesting target to inhibit virus entry

1.3.1 The involvement of phosphatidylserine receptors in virus entry

In healthy cells, the negatively charged phospholipid **PS** is located on the inner leaflet of the plasma membrane. During apoptosis, PS is externalized to the outer leaflet, a hallmark of programmed cell death.¹⁴⁶ PSR on phagocytes recognize and interact with the exposed PS, followed by endocytic engulfment, trafficking, and degradation of this apoptotic debris. Furthermore, the clearance of apoptotic cells also suppresses an inflammatory response that could otherwise provoke tissue damage and inflammation.¹⁴⁷ Many viruses, including DENV and ZIKV, hijack the apoptotic clearance machinery of the host by exposing PS on their envelope. This process is called **apoptotic mimicry** (Figure 1.7; reviewed in ref 148). It implies 2 benefits for the virus: infection of host cells is facilitated, and the host's inflammatory response is dampened.

PSR are a very important class of virus entry receptors.¹¹⁸ Significant members are the TIM (TIM-1, TIM-3, TIM-4) and TAM (Tyro3, Axl, Mer) receptor families (Figure 1.8). While TIM receptors directly interact with PS, TAM receptors are bridged to PS by their ligands Gas6 and Protein S. The PSR involved in Flavivirus entry are also included in Table 1.2.

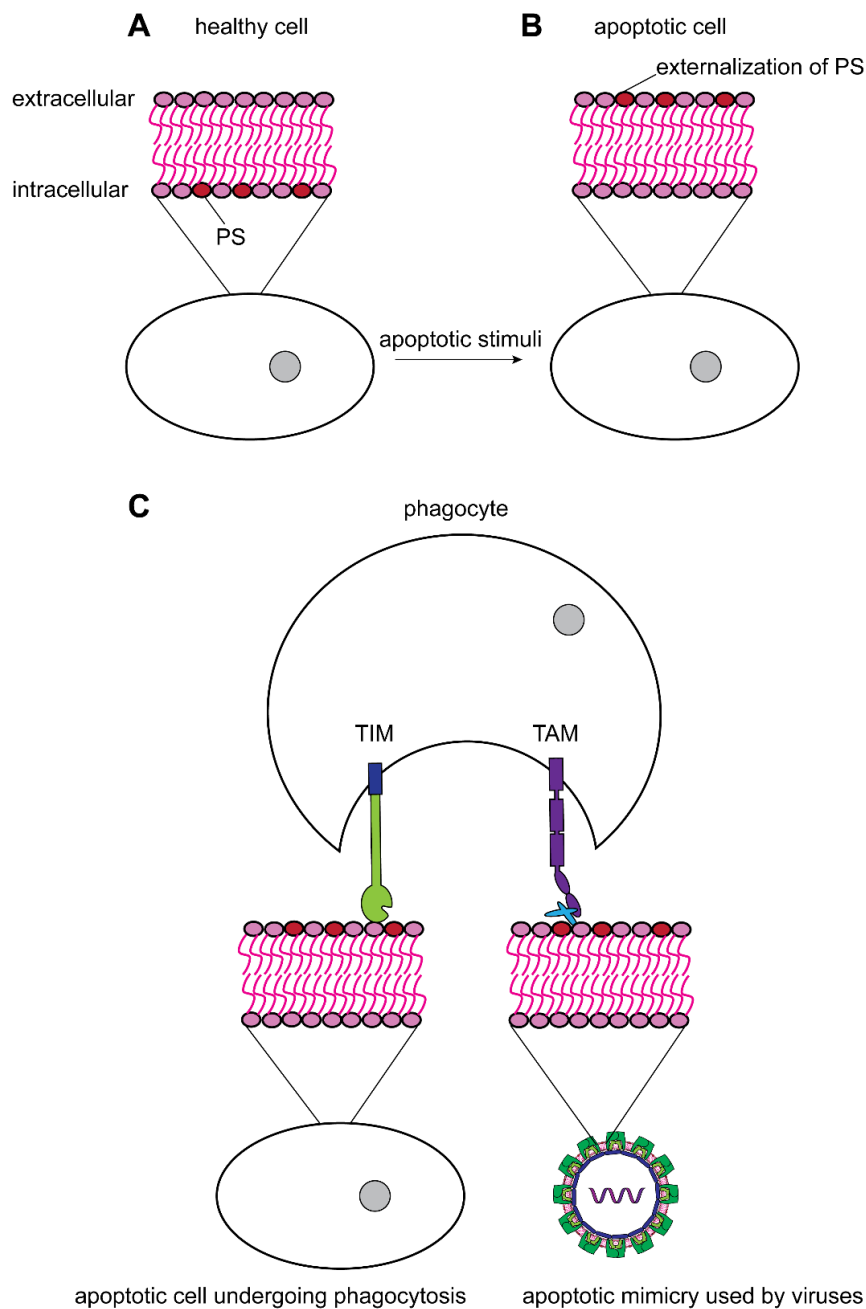


Figure 1.7 Schematic overview of apoptosis and apoptotic mimicry. (A) In healthy cells, PS is localized on the inner leaflet of the plasma membrane. (B) During apoptosis, which can be triggered by various stimuli, PS is externalized to the outer leaflet. (C) Exposed PS is recognized by PSR such as TIM and TAM receptor families expressed by phagocytes. During apoptosis, phagocytes engulf these apoptotic particles for further degradation. Some viruses hijack this process to enter target cells, which is called apoptotic mimicry. A general Flavivirus structure is depicted here as an example.

PSR are exploited by a **wide array of enveloped viruses** to promote cellular attachment, endocytosis and/or subsequent infection.¹¹⁸ The various mechanisms

of PSR-virus interaction are complex and depend on the involved receptor, cell type, and virus.^{81,118,148,149}

The complex role of the PSR is illustrated by the Axl receptor tyrosine kinase (Axl). Several research groups have demonstrated the role of this PSR as ZIKV entry factor in various cell types, e.g. skin fibroblasts⁶⁷, endothelial cells^{150,151}, and neural cells.^{69,152,153} However, others showed that it was not required for ZIKV replication in neural progenitor cells¹⁵⁴ or in ZIKV-infected mice.^{155,156} This suggests that receptor use is cell type/tissue-dependent or that cells can express a diverse set of entry receptors, playing a redundant role during viral entry.

Note, however, that **not every enveloped virus** (e.g. H7N1 influenza virus, HSV-1 or SARS CoV) **utilizes PSR** although they expose PS on their membranes. This might be explained by the presence of other high-affinity entry receptors or by other specific viral entry proteins that prevent interaction of envelope PS with PSR by steric hinderance.¹⁵⁷ Also, **not every PSR enhances infection**.¹¹⁸ For example, the PSR BAI1, RAGE and Stabilin-1/2 are probably not involved in virus entry.^{101,149,158} Even between flaviviruses, there are differences in receptor use. The $\alpha\beta 3-5$ integrin probably only enhances entry of WNV, JEV and ZIKV, and not of DENV.^{103,104}

In this study, we focus on the interaction between the flaviviruses ZIKV and DENV and the PSR TIM-1 (Section 1.3.2 and Chapter 6) and CD300a (Section 1.3.3 and Chapter 7).

1.3.2 TIM-1

1.3.2.1 The TIM gene family

The role of **T cell immunoglobulin and mucin domain-1** (TIM-1) as viral entry receptor has gained a lot of attention in the last years. However, its role in other biological processes has been studied for almost 30 years.

Genome-wide linkage studies indicated that chromosome 5q23-35 was found to be associated with asthma and allergy.^{159,160} Using congenic mice, the TIM gene family containing TIM-1 was discovered.¹⁶¹ This protein could be linked to hepatitis A virus (HAV) cellular receptor (**HAVCR**), a receptor which was identified and isolated a few years earlier.^{162,163} HAVCR expressing cells are susceptible to HAV infection and antibody treatment blocked the receptor and subsequently protected

cells against HAV (see below). In addition, TIM-1 was also known as kidney injury molecule 1 (**KIM-1**), which is upregulated on epithelial cells after renal ischemic injury.¹⁶⁴

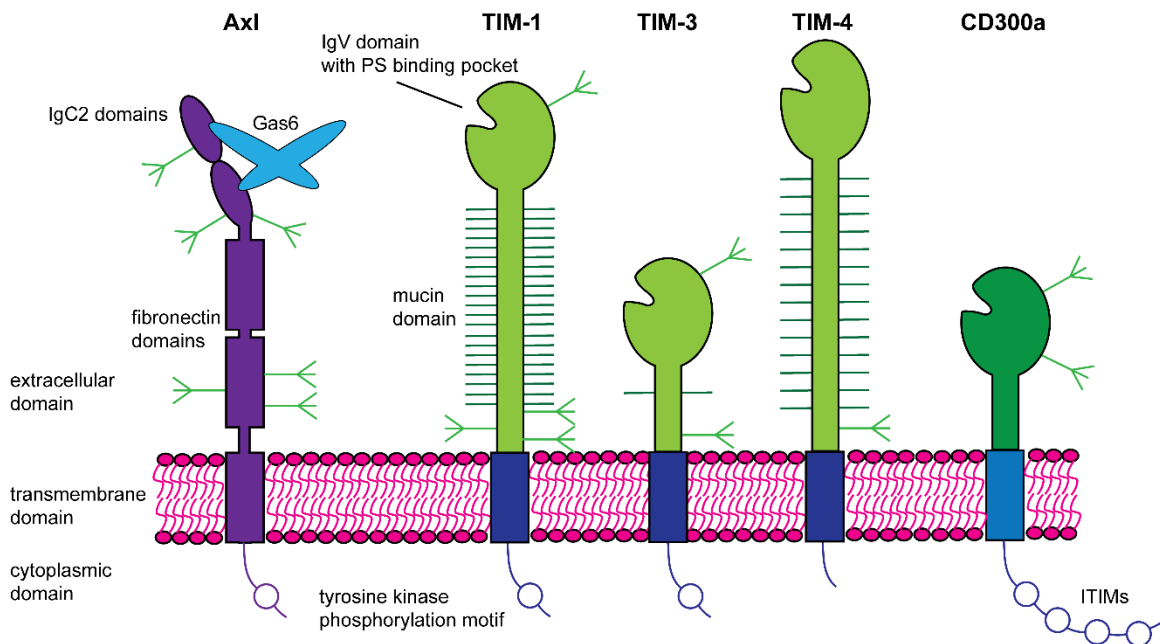


Figure 1.8 Overview of the PSR Axl, TIM-1, TIM-3, TIM-4 and CD300a. Axl is depicted, being representative of the TAM receptor family, together with all members of the human TIM receptor family and one member of the CD300 receptor family, *i.e.* CD300a. Axl is bridged to PS by Gas6. Ligand binding induces dimerization but for simplicity reasons only one Axl receptor is drawn. TIM receptors and CD300a directly interact with PS. Light green forked structures mark N-linked glycosylation sites while dark green horizontal lines depict O-linked glycosylation sites. Adapted from refs 118 and 165^{118,165}.

The human **TIM gene family** consists of three members: TIM-1, TIM-3, and TIM-4. They are type I cell-surface glycoproteins with an immunoglobulin variable (IgV) domain containing 6 cysteine residues and the PS binding pocket, a mucin-like domain of variable length, a transmembrane domain, a cytoplasmic domain, and a variable number of O-linked glycosylation sites (Figure 1.8).^{166,167} TIM-1 and TIM-3 also have a tyrosine-kinase phosphorylation motif in the cytoplasmic domain. They are all PSR, with different expression sites and functions. In general, TIM receptors determine whether apoptotic cell recognition leads to immune activation or tolerance, depending on the receptor and cell type.¹⁶⁶ TIM-1 is preferentially expressed on T-helper 2 (Th2) cells and has a costimulatory function, while TIM-3 plays an inhibitory role on T-helper 1 (Th1) and cytotoxic T cells and is involved in antigen presentation on dendritic cells. TIM-4, whose expression is confined to

antigen-presenting cells (APC) such as macrophages and mature dendritic cells, is important in maintaining tolerance.¹⁶⁸

1.3.2.2 TIM-1: expression and ligands

TIM-1 (359 amino acids (aa)) is mainly **expressed** on the cell surface of **several T and B cell subsets** such as Th2 cells and on tubular epithelial cells after kidney injury.¹⁶⁶ Besides cell surface expression, it is also found in large intracellular pools such as the Golgi apparatus, ER and lysosomes, and travels between intra- and extracellular pools by CME.^{169,170} TIM-1 ligands increase the amount of cell surface expression.¹⁷⁰ Its main **ligands** are PS¹⁶⁸ and phosphatidylethanolamine (PE)¹⁷¹, TIM-4¹⁷², and P-selectin¹⁷³, which will be further addressed below (Figure 1.9).

1.3.2.3 Physiological functions of TIM-1

TIM-1 is most studied for its costimulatory role in adequate immune responses. Interaction of TIM-1 expressing T cells with specific antibodies or with TIM-4, which is expressed on APC, can trigger **T cell activation**, thereby regulating their proliferation and cytokine production.^{172,174–177} More specifically, TIM-4 binding induces Src tyrosine kinase-mediated TIM-1 tyrosine phosphorylation in its cytoplasmic tail, and leads to promotion of T cell stimulation, expansion and survival. It is thought that TIM-1 ligation provides a third costimulatory signal to the T cell receptor (TCR)/CD3 and CD28 complex, which offer the respective first and second signal of T cell activation.^{174,176,178} However, it is still unclear whether this TCR stimulation is essential for TIM-1-induced T cell activation, as TCR-independent activation has also been observed.^{176,177} Furthermore, the effect of TIM-1 on T cell behavior depends on the properties of engaged TIM-1 antibodies: agonistic antibodies enhance T cell activation and a proinflammatory response, while antagonistic antibodies prohibit autoimmunity development.^{179,180} This suggests that TIM-1 has both activating and inhibiting effects on immune responses.

The **intracellular signal transduction** of TIM-1 upon this tyrosine phosphorylation is not completely understood, but various downstream changes are observed such as phosphoinositide 3-kinase (PI3K) recruitment and phosphorylation of linker of activated T cells (LAT), protein kinase B (Akt), and extracellular signal-regulated kinase (ERK) 1/2.^{176,181} TIM-1 ligation induces a rise in intracellular calcium and

calcineurin-dependent nuclear translocation of nuclear factor of activated T cells (NFAT/AP-1), and subsequent transcription and up-regulation of surface activation markers (CD25, CD69) and cytokines (e.g. IL-2, IL-4) that are important in Th2 cell activation and function.¹⁷⁵⁻¹⁷⁷

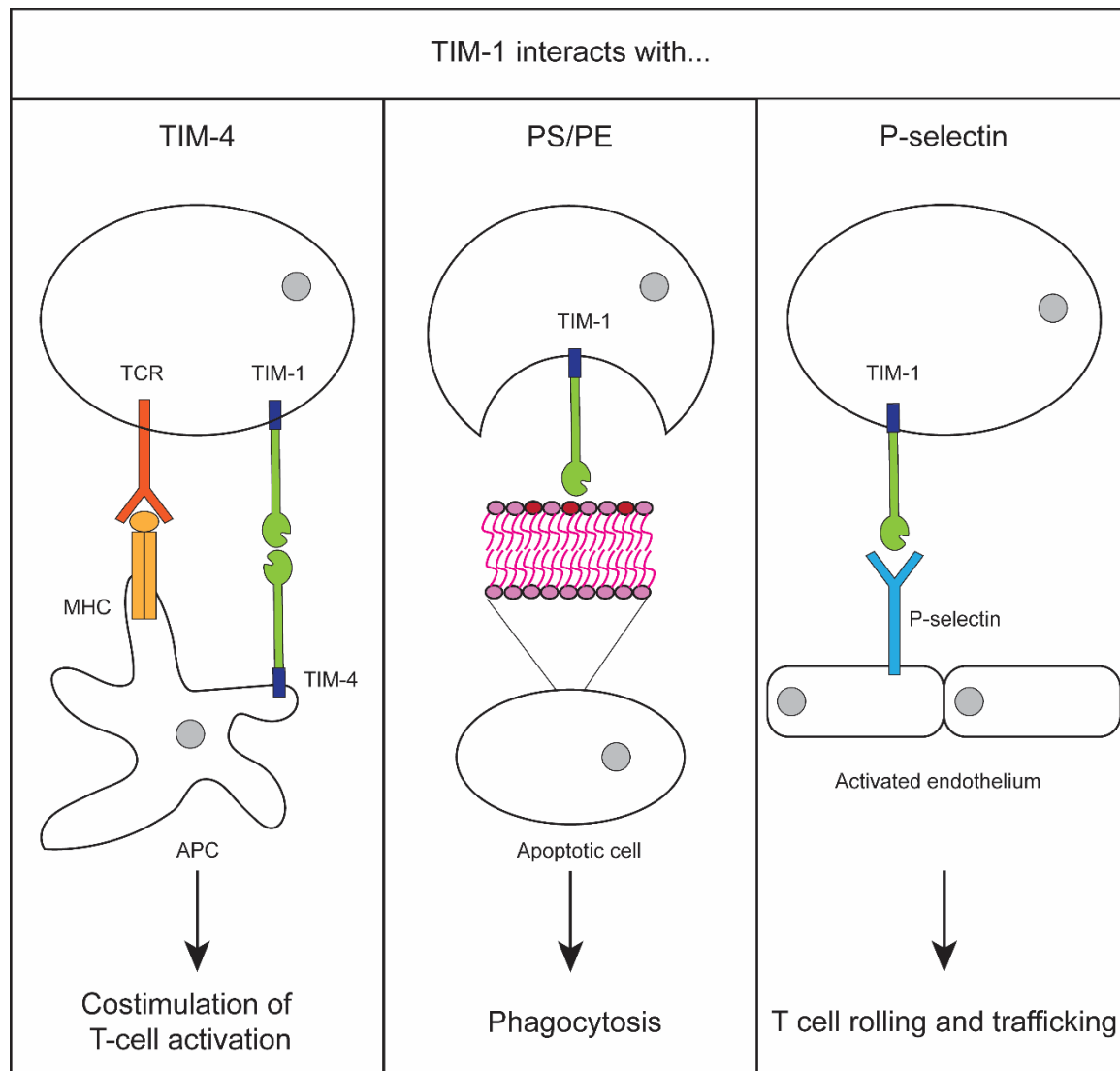


Figure 1.9 Schematic overview of physiological TIM-1 functions. TIM-1 interaction with TIM-4 is a costimulatory signal for T cell activation, induced by TCR interaction with MHC presented on APC. TIM-1 interacts with PS/PE exposed on apoptotic cells, inducing phagocytosis. TIM-1 interacts with P-selectin on activated endothelial cells or platelets to regulate T cell trafficking. TCR: T cell receptor; MHC: major histocompatibility complex; APC: antigen-presenting cell.

Next to its importance in the development of proper immune responses, TIM-1 is also responsible for **phagocytosis of apoptotic cells**. Phagocytosis occurs through the binding of TIM-1 to exposed PS on apoptotic cells (Section 1.3.1). Rapid and effective clearance of these cells is crucial to maintain tissue

homeostasis and avoid the development of inflammation and autoimmunity against antigens which are released by these dying cells.¹⁶⁸ For example, expression of TIM-1 following kidney epithelial injury converts epithelial cells into phagocytes.¹⁸² These cells then assist endogenous phagocytes such as macrophages in tissue remodeling.

Finally, TIM-1 is also involved in **leukocyte recruitment** during inflammation by interacting with P-selectin.^{173,183} This cell adhesion molecule (CAM) is expressed on activated platelets and vascular endothelial cells. By interacting with TIM-1 on activated T cells, it controls T cell rolling and trafficking to sites of inflammation.

1.3.2.4 The role of TIM-1 in diseases

TIM-1 is a **susceptibility gene for asthma and allergy**.^{184,185} Polymorphisms in TIM-1 are primarily found in the mucin-like domain. Certain insertions and deletions are correlated with decreased risk of atopy development, and this effect is strongest in people who have been previously exposed to HAV.^{161,186} In other words, HAV infection protects against atopy development.

Furthermore, TIM-1 polymorphisms have been associated with **autoimmune diseases** such as rheumatoid arthritis and systemic lupus erythematosus.^{187,188} TIM-1 is also a **biomarker** of renal injury, where it plays a role in the phagocytosis of apoptotic and necrotic cells.¹⁸⁹ It is also upregulated in renal and ovarian carcinomas.¹⁹⁰

Besides HAV, TIM-1 also **promotes the entry of many other enveloped viruses** such as the flaviviruses DENV¹⁰¹, ZIKV⁶⁷, WNV^{101,171}, JEV¹⁹¹ and HCV¹⁹², the filoviruses EBOV^{171,193} and Marburg virus¹⁹³, and the alphaviruses CHIKV and Ross River virus.^{157,158} This interaction is mediated by viral PS or PE binding to the IgV domain PS binding pocket of TIM-1.^{158,171} Viral entry through TIM-1 requires a functional PS binding pocket in the IgV domain and a mucin-like domain of sufficient length. The cytoplasmic tail and transmembrane domain are not essential for its role as viral entry receptor.^{101,194} Overexpression/ablation of TIM-1 increased/decreased cell susceptibility to viral infection.^{67,101,191–193,195} Moreover, TIM-1-specific antibodies could block virus binding and entry *in vitro*.^{101,193,195}

However, it was still unclear if TIM-1 merely acts as an attachment factor which binds the virus or as an authentic entry receptor that leads to viral internalization.

Recently, it has been determined that **TIM-1 and DENV are co-internalized** through CME and TIM-1 is therefore a DENV entry receptor rather than just an attachment factor.⁵³ For the other viruses engaging with TIM-1, the exact role of the receptor remains to be elucidated. For example, it has been shown that TIM-1 is involved in EBOV attachment and entry, but the entry factor NPC-1 is still necessary for effective fusion with the endosome.¹⁵⁷ The *in vivo* importance of TIM-1 has also been demonstrated, since TIM-1 KO mice survive EBOV infection, compared to WT mice.^{196,197}

Next to the role of TIM-1 as a receptor for viral infection, it might also be directly **involved in virus-related pathology**. The engagement of the virus with TIM-1 on CD4⁺ T cells can induce T cell activation and an inflammatory response, which is for example involved in EBOV and DENV diseases (the so-called cytokine storm).¹⁹⁶ We note, however, that not every virus (*e.g.* ZIKV) that engages with TIM-1 is related to a cytokine storm pathology. Further research is needed to explain this discrepancy between viruses and virus-related pathology.

The **complex role** of TIM-1 during viral infection is also illustrated during HIV infection. Interaction of HIV envelope PS with TIM-1 during the entry process can enhance uptake of the virus by increasing cell attachment and virus concentration on CD4⁺ target cells, while TIM-1 interaction during the budding process can inhibit HIV release by trapping viral PS on the cell surface. This can in turn be counteracted by the HIV Nef protein, that induces internalization of TIM-1.^{198–200}

1.3.2.5 Potential of TIM-1 as therapeutic target

Developing compounds **targeting TIM-1 implies many therapeutic options** because of the importance of the receptor in a wide variety of physiological and pathological processes, ranging from adequate immune responses, atopy and autoimmunity development, to kidney injury and viral infections. **To date, no TIM-1-targeting small molecule or other therapeutic drug is available.**

Inhibiting TIM-1 signaling might decrease Th2 responses in allergic reactions, a **potential therapy for atopic diseases**.¹⁷⁴ Several *in vivo* mouse studies have shown that blocking TIM-1 with specific antagonistic antibodies reduces airway hyperresponsiveness in asthma models or decreases disease progression in an atherosclerosis model.^{180,201–203} TIM-1 targeting could also promote repair after

acute kidney injury. It has also been hypothesized that targeting TIM-1 might have antitumoral properties, because of its essential immune regulatory role.²⁰⁴ In this regard, a TIM-1 monoclonal antibody-drug conjugate (CDX-014), developed to treat renal, ovarian and lung cell carcinomas, has been tested in a phase I clinical trial.^{190,205}

It is crucial that an **appropriate targeting** of TIM-1 happens: for example in acute kidney disease, the presence of dysfunctional TIM-1 decreases phagocytosis of apoptotic cells, leading to inflammatory responses and subsequent poor prognosis.²⁰⁶ Also, depending on the TIM-1 epitope that is targeted, a decreased or exacerbated (and undesired) immune response occurs in a mouse airway inflammation model.²⁰¹ This indicates that it is essential to understand the role of TIM-1 in a specific pathological condition in order to improve prognosis with agonists or antagonists of TIM-1-mediated signaling.

TIM-1 is specifically **attractive for the development of BSA**, regarding the many enveloped viruses that engage with this receptor to facilitate viral entry. Various research groups have demonstrated the potential of TIM-1 antibodies in decreasing *in vitro* EBOV infection.^{193,195} Based on studies with TIM-1 KO mice, Brunton *et al.* have also suggested that inhibiting TIM-1 *in vivo* significantly reduces viral loads in EBOV-infected mice.¹⁹⁷ To our knowledge, TIM-1 inhibitors have not yet been evaluated in an *in vivo* viral infection model. Next to direct TIM-1 targeting, its ligands PS and PE are also an attractive target to interfere with TIM-1 related functions.¹⁷¹

1.3.3 CD300a

1.3.3.1 The CD300 gene family

The **human CD300 family** contains 8 members (CD300a-CD300h) which are broadly expressed on lymphoid and myeloid cell types. In general, they determine leukocyte responses in an activating or inhibitory way and are therefore crucial in immune regulation. By the divergent expression of various CD300 receptors, the host can shape the outcome of an immune response to invading pathogens or dead cells.^{207,208} CD300 receptors are type I transmembrane proteins with an IgV-like extracellular domain and a variable cytoplasmic tail, depending on their function. The receptors with an immune activating function (*i.e.* CD300b, CD300c,

CD300d, CD300e and CD300h) have a short tail and a charged transmembrane domain that associates with adaptor proteins, while the inhibitory receptors (*i.e.* CD300a and CD300f) have a long cytoplasmic tail with **immunoreceptor tyrosine-based inhibitory motifs** (ITIMs) (Figure 1.8). CD300g is an exception since it contains no stimulatory or inhibitory cytoplasmic motif, but an additional extracellular mucin-like domain. Although specific ligands are unknown, most human CD300 receptors recognize lipids (*e.g.* lipopolysaccharides (LPS)), but only 2 receptors are known to bind PS and PE, *i.e.* CD300a and CD300c.²⁰⁹

1.3.3.2 CD300a: expression and ligands

CD300a (299 aa) is expressed on **many leukocyte types** such as natural killer (NK) cells, subsets of B and T cells, neutrophils, mast cells, basophils, eosinophils, monocytes, and DC subsets.^{208,210} It resides in intracellular pools and cell surface expression can be up- or downregulated by various stimuli, *e.g.* on monocytes its expression is rapidly increased upon presence of LPS or granulocyte-macrophage colony-stimulating factor (GM-CSF).²¹¹ Being a PSR, CD300a binds PE, and to a lesser extent PS.²¹²

1.3.3.3 Physiological functions of CD300a

The important function of CD300a is indicated by the strong evidence of evolutionary conservation.²¹³ CD300a is thought to be an **inhibitory receptor in immune regulation**. For example, it decreases NK cytotoxic activity, it suppresses eosinophil survival and migration, and might reduce reactive oxygen species production in neutrophils.^{208,210,214} Furthermore, CD300a induces downregulation of phagocytosis and is therefore involved in regulating the clearance of dead cells, providing a 'don't eat me yet' signal.^{208,212}

Tyrosine phosphorylation of the ITIM by the Src tyrosine kinase Lck induces the **inhibitory signal** by recruiting a selection of phosphatases such as Src homology region 2 domain-containing phosphatase (SHP)-1.²¹⁰ SHP-1 in turn dephosphorylates downstream proteins, subsequently terminating activated signals or inducing other pathways.²¹⁵

1.3.3.4 The role of CD300a in diseases

Although the underlying mechanisms are not completely understood, CD300a is involved in **inflammatory responses, allergy, and autoimmune disorders**.²¹⁰ A

single nucleotide polymorphism in the CD300a gene has been associated with psoriasis susceptibility and its usefulness as biomarker for acute lymphoblastic leukemia and ulcerative colitis has also been reported.^{216–218}

Until now, CD300a is the only CD300 family receptor known to be involved in **viral entry**. However, the importance of CD300a in viral infections has been studied to a limited extent only. It has been shown that the receptor enhances binding, but not transduction of a pseudotyped lentiviral vector with Sindbis virus envelope, unlike TIM-1.¹⁴⁹

Recently it has been demonstrated that CD300a but not CD300c **promotes binding and infection of DENV, WNV, YFV, and CHIKV** by means of apoptotic mimicry.¹⁰² However, its cytoplasmic tail was dispensable for infection, indicating that CD300a mainly acts as DENV attachment receptor, and viral internalization is mediated by other host factors. Furthermore, not all cells endogenously expressing CD300a, such as monocytes and mast cells, were susceptible to infection. It is possible that the inhibitory properties of CD300a allow binding of viral particles, but do not promote their engulfment. The role of CD300a in ZIKV infection remains unresolved.

It has been shown that CD300a plays **other roles in viral infection** as well. For example, CD300a expression on B cells is downregulated in HIV-infected patients, which might contribute to B cell dysfunction.²¹⁹ On the other hand, CD300a expression increases susceptibility of CD4⁺ T cells to HIV infection, and it is overexpressed on this cell population in HIV patients.²²⁰ Furthermore, by engaging with CD300a and inducing the subsequent inhibitory immune response, viruses might also escape from effective clearance.²⁰⁹

1.3.3.5 Potential of CD300a as therapeutic target

The substantial role of CD300a in diseases such as allergy and viral infections marks the receptor as a potential therapeutic target. **No CD300a inhibitors are currently available.**

Since CD300a is expressed on mast cells, eosinophils and basophils – all involved in regulation of allergic responses – targeting this receptor might down regulate the responses of these cells.²⁰⁸ For example, a bispecific antibody fragment was

designed that links CD300a with IgE and subsequently decreases allergic airway inflammation in a mouse model.²²¹

In viral infections, the consequences of CD300a targeting has only been studied to a limited extent. Carnec *et al.* showed that incubating monocyte-derived macrophages with **CD300a antibodies inhibits DENV infection**.¹⁰² It is crucial that the potential of CD300a blocking is further examined, as the difficult search for antivirals requires the investigation of new targets.

Chapter 2

Research objectives

Viral infections are a major cause of morbidity and mortality. A lot of research is directed towards the discovery of novel antiviral agents to combat these infections. Whereas most approved antivirals target one virus species, the use of broad-spectrum antivirals (BSA) would be another interesting therapeutic approach. These agents can target either a conserved viral factor or a cellular component that is widely used by different viruses during specific steps of their replication cycle. BSA also have the benefit that they can be immediately employed when a new viral epidemic occurs. An interesting therapeutic target of BSA is viral entry, preventing the interaction of a virus with a cellular receptor.

The general aim of this PhD work is to further study viral entry inhibition (*i.e.* the triangle virus – cellular receptor – inhibitor), as a better understanding of this process can aid the discovery of novel BSA that prevent and/or treat viral infections. In this thesis, we first evaluate the activity of **entry inhibitors** that block the interaction of diverse viruses (*i.e.* HIV and flaviviruses) with their host cell receptor (**Chapters 4-5**). Secondly, we explore the involvement of the **phosphatidylserine receptors** in the entry of flaviviruses (**Chapters 6-7**).

In **part I** of the thesis, we first focus on HIV entry inhibitors. HIV continues to cause tremendous health-related and economic problems. Therefore, it still remains crucial to explore safe and accessible methods that prevent viral transmission. Our first aim is to study the **antiretroviral activity of a series of closely related compounds derived from lignosulfonic acid (Chapter 4)**. These compounds were synthesized by Borregaard LignoTech. Using various cellular assays (*i.e.* virus replication and receptor binding assays as well as protein interaction studies) we determine if these compounds inhibit HIV entry and replication and further unravel their mechanism of action. We also explore their use as potential microbicides, *i.e.* topical applicable gels or creams containing an antiretroviral drug, which are currently not yet available.

In the second chapter of part I, we focus on flaviviruses. Besides preventing viral transmission, entry inhibitors also have potential as antiviral agents in established infections. This is particularly interesting for emerging viruses, such as DENV and ZIKV, for which currently no treatment is available. Hence, our second aim is to **study the antiviral activity of labyrinthopeptins**, a unique class of bacterially-derived peptides, synthesized by Dr. Roderich Süssmuth (**Chapter 5**). We evaluate their broad-antiviral potency, specifically against ZIKV and DENV infections, using different virus replication assays with various readouts. We also study their mechanism of action with time-of-drug addition experiments and protein interaction studies.

In **part II** of this thesis, we focus on the involvement of a cellular component involved in viral entry, *i.e.* the phosphatidylserine receptors (PSR). First, we study the possible role of TIM-1 as an antiviral target. Targeting TIM-1 with small molecules or antibodies would be a promising strategy to interfere with viral entry, but no TIM-1-targeting inhibitors are currently available. In this chapter, we study the **potential interaction between TIM-1 and Labyrinthopeptin A1** using various cellular assays. In addition, we investigate the **potential of TIM-1 as antiviral target by further exploring its role in *in vitro* ZIKV infection (Chapter 6)**.

In the last chapter, we study CD300a, another PSR. Although it is known that this receptor might be involved in DENV attachment and subsequent entry, its role in ZIKV infection has not been studied. Hence, our final aim is to **study the role of CD300a cell surface expression in ZIKV infection**, and the antiviral potency of a receptor-specific antibody (**Chapter 7**).

Chapter 3

Materials and methods

3.1 Cell lines, primary cells and viruses

3.1.1 Cell lines

Table 3.1 gives an overview of all cell lines used throughout this thesis. All cell cultures were maintained at 37°C in a humidified environment with 5% CO₂ except for C6/36 cells, which were cultured at 28°C in the absence of CO₂. Cells were subcultivated every 3 to 4 days.

Table 3.1 Overview of used cell lines

Cell type	Origin	Medium ^b	Source
A549	Human lung carcinoma	MEM + 10% FBS 2 mM L-glutamine, 0.075% sodium bicarbonate	ATCC ^c
BHK-21	Hamster kidney fibroblast	MEM + 10% FBS 2 mM L-glutamine, 0.075% sodium bicarbonate	ATCC ^c
C6/36	Mosquito larva	Leibovitz's L-15 + 10% FBS 0.01 M HEPES, NEAA	ATCC ^c
C8166	Human T cell leukemia	RPMI-1640 + 10% FBS 2 mM L-glutamine	ATCC ^c
CHO.k1	Hamster ovary epithelium	Ham's F12 + 10% FBS	ATCC ^c
HEK293	Human embryonic kidney epithelium	DMEM + 10% heat-inactivated FBS 0.1 M HEPES, 0.075% sodium bicarbonate, penicillin/streptomycin glutamine	Dr. A. Inoue ^d
HEK293T	Human embryonic kidney epithelium	DMEM + 10% FBS 0.01 M HEPES	ATCC ^c
HEL	Human embryonic lung fibroblast	DMEM + 10% FBS 0.01 M HEPES	ATCC ^c
HeLa	Human cervical adenocarcinoma	DMEM + 10% FBS 0.01 M HEPES	ATCC ^c

HEp-2	Human laryngeal carcinoma	DMEM + 10% FBS 0.01 M HEPES	ATCC ^c
Huh-7	Human hepatoma	DMEM + 10% FBS 0.01 M HEPES	Dr. R. Barten-schlager ^e
HuT-78	Human T cell lymphoma	RPMI-1640 + 10% FBS 2 mM L-glutamine	ATCC ^c
Jeg-3	Human chorioblastoma	MEM + 10% FBS NEAA, 1 mM sodium pyruvate	ATCC ^c
MT-4	Human T cell lymphoma	RPMI-1640 + 10% FBS 2 mM L-glutamine	Dr. L. Montagnier ^f
Raji	Human B cell lymphoma	RPMI-1640 + 10% FBS 2 mM L-glutamine	Dr. L. Burleigh ^g
Raji L-SIGN	Raji transfected with L-SIGN	RPMI-1640 + 10% FBS 2 mM L-glutamine, 0.2 µg/ml geneticin	Derived from Raji ^h
Raji DC-SIGN	Raji transfected with DC-SIGN	RPMI-1640 + 10% FBS 2 mM L-glutamine	Dr. L. Burleigh ^{g,i}
SupT1	Human T cell lymphoma	RPMI-1640 + 10% FBS 2 mM L-glutamine	ATCC ^c
TZM-bl	Derived from HeLa ^a	DMEM + 10% FBS 0.01 M HEPES	Dr. G. Vanham ^j
U87	Human glioblastoma	DMEM + 10% FBS 0.01 M HEPES	ATCC ^c
Vero	African green monkey kidney epithelium	MEM + 10% FBS 2 mM L-glutamine, 0.075% sodium bicarbonate	ATCC ^c

^aExpresses CD4, CCR5 and CXCR4 and contains reporter genes for firefly luciferase. ^bAll media and supplements were purchased from TFS. ^cAmerican Type Culture Collection, Manassas, VA, USA. ^dTohoku University, Sendai, Japan. ^eHeidelberg University, Heidelberg, Germany. ^fFormerly at the Pasteur Institute, Paris, France. ^gInstitut Pasteur, Paris, France. ^hThe plasmid containing L-SIGN cDNA was a kind gift of Dr. S. Pöhlmann (Institute for Clinical and Molecular Virology, Erlangen, Germany). Raji L-SIGN cells were constructed using the Amaxa Nucleofection electroporation system (Lonza, Cologne, Germany). ⁱConstructed by Geijtenbeeck *et al.*²⁵ ^jInstitute for Tropical Medicine, Antwerp, Belgium.

3.1.2 Primary cells

Human peripheral blood mononuclear cells (PBMC) were isolated from buffy coats from healthy donors (after receiving informed consent, Red Cross; Mechelen, Belgium) by density gradient centrifugation over Lymphoprep (Stemcell Technologies, Vancouver, BC, Canada).

In order to obtain a significant population of activated T cells, PBMCs were cultured in RPMI-1640 medium supplemented with 10% FBS and 2 mM L-glutamine and stimulated with 2 µg/ml of the mitogenic phytohemagglutinin (PHA; Sigma-Aldrich, St. Louis, MO, USA) for 3 days at 37°C before their further use in antiviral assays (Section 3.4.1).

In order to obtain monocyte-derived dendritic cells (MDDC), PBMCs were gently rotated at 4°C to form aggregates of monocytes. After sedimentation, the pellet was grown in RPMI-1640 medium supplemented with 10% FBS and 2 mM L-glutamine. To stimulate differentiation into immature dendritic cells, 25 ng/ml IL-4 and 50 ng/ml GM-CSF (Peprotech, London, UK) were added. After 5 days, various cell markers of immature MDDC were analyzed by flow cytometry.²²² These cells were used in experiments in Chapters 5 and 7.

3.1.3 Virus strains

An overview of the used virus strains is provided in Table 3.2.

Table 3.2 Overview of used virus strains

Virus strain	Info	Source
HIV		
HIV-1 NL4.3	X4	NIAID ^a
HIV-1 IIIB	X4	NIAID
HIV-1 BaL	R5	NIAID
HIV-1 HE	R5/X4	University Hospital and Rega Institute ^b
HIV-2 ROD	R3/R5/X4	MRC ^c
HSV		
HSV-1 KOS	Reference laboratory strain	Dr. W. Rawls ^d
HSV-2 G	Reference laboratory strain	ATCC ^e VR-734
DENV		
DENV-1 Djibouti D1/H/IMTSSA/98/606	Low-passage clinical isolate	X. de Lamballerie ^f
DENV-2 New Guinea C (NGC)	Laboratory-adapted	Dr. V. Deubel ^g

DENV-3 H87 prototype	Laboratory-adapted	Dr. X. de Lamballerie ^f
DENV-4 Dak HD 34 460	Low-passage clinical isolate	Dr. X. de Lamballerie ^f
ZIKV		
MR766	prototype strain; sentinel Rhesus monkey, Uganda, 1947	ATCC ^e VR-84
IB H 30656	human blood, Nigeria, 1968	ATCC ^e VR-1839
PRVABC59	human serum, Puerto Rico, 2015	ATCC ^e VR-1843
FLR	human serum, Colombia, 2015	ATCC ^e VR-1844
Other viruses	Strain	
VSV	Indiana Lab	ATCC ^e VR-1238
Orthoreovirus 1	Lang	ATCC ^e VR-230
Coxsackievirus B4	J.V.B (Benschoten)	ATCC ^e VR-184
Sindbis virus	Ar-339	ATCC ^e VR-68
Parainfluenza virus 3	C 243	ATCC ^e VR-93
CoV	229E	ATCC ^e VR-740
SARS-CoV-2	BetaCov/Belgium/GHB- 03021/2020	University hospital ^b
Punta Toro virus	Balliet	ATCC ^e VR-559
RSV A	A2	ATCC ^e VR-1540
RSV B	18537	ATCC ^e VR-1580
YFV	17D-YFV Stamaril vaccine	Sanofi Pasteur ^h

^aNational Institute of Allergy and Infectious Diseases, North Bethesda, MD, USA. ^bIsolated from a patient, Leuven, Belgium. ^cMedical Research Council, London, UK. ^dBaylor University College of Medicine, Houston, TX, USA. ^eAmerican Type Culture Collection, Manassas, VA, USA. ^fUniversité de la Méditerranée, Marseille, France. ^gInstitut Pasteur, Paris, France. ^hLyon, France.

HIV and HSV stocks were obtained by propagating the virus in MT-4 cells for 5 days and collecting supernatant. Viral titers were determined by calculating the cell culture infectious dose (CCID₅₀) in MT-4 cells, according to the Reed and Muench method, as described in ref 223.

DENV and ZIKV strains were propagated in C6/36 cells, supernatant containing the virus was harvested 7-10 days after infection and stored at -80°C. For DENV-2 and all ZIKV strains, viral titers were determined by plaque assay in BHK-21 cells, as described below. DENV-1, DENV-3 and DENV-4 did not induce viral plaques in these cells so viral titers were determined through a flow cytometry assay, according to literature.²²⁴ In short, Vero cells were infected with 10-fold serial dilutions of DENV stock for the duration of one replication cycle and the number of FACS infectious particles (FIU) was calculated by viral antigen detection using the DENV complex antibody clone 2H2.

All viruses were obtained and used as approved according to the rules of Belgian equivalent of IRB (Departement Leefmilieu, Natuur en Energie, protocol SBB 219 2011/0011n and the Biosafety Committee at the KU Leuven).

3.2 Test compounds and chemicals

Table 3.3 represents all used compounds.

Table 3.3 Overview of used compounds and chemicals

Compound	MW (g/mol)	Source
Study compounds		
LA ^{low}	8000	Sigma-Aldrich ^a
LA ^{high}	52000	Sigma-Aldrich ^a
LA derivatives (LA01 – LA24)	See Table 4.1	Borregaard LignoTech ^b
Laby A1	2073.7	Dr. R. D. Süßmuth ^c
Laby A2	1922.7	Dr. R. D. Süßmuth ^c
Reference compounds used in HIV assays		
AMD3100	830.5	Dr. G. Bridger ^d
AZT	267.2	Tocris ^e
Dextran sulfate	5000, 10000	Sigma-Aldrich ^a
Enfuvirtide	4492	Dr. E. Van Wijngaerden ^f
Maraviroc	513.7	Dr. G. Bridger ^d
PRO 2000	5000	Dr. A.T. Profy ^g
Tenofovir	287.2	Gilead Sciences ^h
2G12	145000	Polymun Scientific ⁱ

Reference compound used in HSV assays		
Acyclovir	225.2	GlaxoSmithKline ^j
Reference compounds used in Flavivirus assays		
Duramycin	2013.3	Sigma-Aldrich ^a
Nisin	3354.1	Sigma-Aldrich ^a
Epigallocatechin gallate	458.4	Sigma-Aldrich ^a
NITD008	290.3	Sigma-Aldrich ^a
Other chemicals		
Camptothecin	348.4	Sigma-Aldrich ^a
Cytochalasin D	507.6	Sigma-Aldrich ^a

^aSt. Louis, MO, USA. ^bSarpsborg, Norway. ^cTechnische Universität Berlin, Germany. ^dFormerly at AnorMed, Langley, Canada. ^eBristol, UK. ^fUniversity hospitals, Leuven, Belgium. ^gFormerly at Indevus Pharmaceuticals Inc., Lexington, MA, USA. ^hFoster City, CA, USA. ⁱVienna, Austria. ^jBrentford, UK.

3.3 CPE reduction and cytotoxicity screening assays

All study compounds (*i.e.* lignosulfonate derivatives and labyrinthopeptins) were initially screened for their antiviral activity using a colorimetric antiviral assay which was originally described by Pauwels *et al.*²²⁵ We adapted the protocol as described in detail in Van Hout *et al.*²²⁶ Cells were seeded in cell culture medium ('growth medium') in a 96-well plate. Adherent cells such as Vero or HeLa were allowed to adhere overnight, obtaining confluent monolayers. Suspension cells (MT-4 cells) were seeded on the day of infection (5×10^4 cells/well). Antiviral assays were performed in the same medium except that FBS concentration was decreased to 2% ('assay medium'). Cells were pre-incubated with two-fold serial dilutions of test compound (100 μ l) at 37°C for 30 min. Flaviviruses were added at a multiplicity of infection (MOI) of 1 while HIV, HSV and other viruses were added according to their CCID₅₀. These were determined by titration of the viral stocks. Following 4-5 days of incubation, according to the used cell line, virus-induced cytopathic effect (CPE) was scored with light microscopy and IC₅₀ was calculated using the spectrophotometric MTS/PES viability staining assay (Cell-Titer 96 Aqueous One Solution Proliferation Assay kit; Promega, Leiden, The Netherlands). Absorbance was measured at 498 nm using the Versamax microplate reader and analyzed using SoftMax Pro software (Molecular Devices, Sunnyvale, Ca, USA). To

determine the compounds' potential cellular cytotoxicity the assays were performed without the addition of virus. The 50% inhibitory concentration (IC_{50}), which is defined as the compound concentration that is required to inhibit virus-induced CPE by 50%, and 50% cytotoxic concentration (CC_{50}), which is defined as the compound concentration that is required to reduce the cell viability by 50%, were determined. Each experiment was performed in duplicate or triplicate.

3.4 HIV and HSV assays

These assays are performed to determine the antiviral activity and mechanism of action of lignosulfonate derivatives, which is further discussed in Chapter 4.

3.4.1 Additional HIV screening assays

To further determine the anti-HIV activity of the lignosulfonate derivatives, a luminescence-based antiviral assay was carried out, as described in detail by others.²²⁷ $CD4^+$ $CXCR4^+$ $CCR5^+$ TZM-bl cells are HeLa cells that are transfected to contain the reporter gene for firefly luciferase under control of the HIV promoter. Cells (3.4×10^5 cells/ml) were pre-incubated with serial dilutions of test compound in duplicate. Cell culture medium was supplemented with 15 μ g/ml diethylaminoethyl-dextran (DEAE-Dextran; Sigma-Aldrich) to facilitate the infection. Next, virus (HIV-1 NL4.3 or BaL) was added according to the $CCID_{50}$ of the stock. After an incubation period of 2 days, viral replication was measured by luminescence. Steadylite Plus reagent (Perkin Elmer, Zaventem, Belgium) and lyophilized substrate were mixed according to the Manufacturer's guidelines. Supernatant was removed from the plates and 75 μ l of the mix solution was added. After 10 minutes incubation in the dark in a plate shaker, 100 μ l was transferred to white 96-well plates (Greiner Bio-One, Frickenhausen, Germany). To determine viral replication, relative luminescence units were measured using the SpectraMax L microplate reader (Molecular Devices) and SoftMax Pro software with an integration time of 0.6 s. and dark adaptation of 5 minutes.

We also performed a HIV-1 p24 Ag ELISA-based antiviral assay in PBMCs, as described previously.²²⁸ PHA-stimulated PBMCs (5×10^5 cells/ml; 200 μ l) were seeded in 48-well plates (Costar, Elscolab NC, Kruibeke, Belgium) and pre-incubated for 30 minutes with various concentrations of test-compound (250 μ l) in the presence of 2 ng/ml interleukin 2 (IL-2) (Roche Applied Science, Vilvoorde, Belgium). Next, virus (HIV-1 NL4.3 and BaL) was added and 2 ng/ml IL-2 was

supplemented again at day 3 and 6 after infection. After 10 days of infection, supernatant was collected and stored. Viral replication was determined by HIV-1 p24 Ag ELISA (Perkin Elmer), according to the Manufacturer's instructions.

3.4.2 Time-of-drug addition assay

To determine at what time point the test compounds intervene in the viral life cycle, we performed a time-of-drug addition assay as described previously.²²⁹ Briefly, MT-4 cells (5×10^5 cells/ml) were infected with HIV-1 NL4.3 (to reach an MOI of 0.5) and seeded in a 96-well culture plate and incubated at 37°C. Test compounds (LA02, LA13, LA14, LA20, LA^{low}, and the reference anti-HIV compounds with a specific mode of action *i.e.* PRO 2000, tenofovir and AZT) were diluted to 1000-fold their IC₅₀ in cell culture medium. At defined time points after infection, the compounds were added to the cell cultures. Thirty-one hours after infection, cell cultures were examined light-microscopically for CPE and supernatant was collected. We performed HIV-1 p24 Ag ELISA to determine the level of HIV-1 infection and replication.

3.4.3 HIV-1 gp120 cellular binding assay

This gp120 binding assay was described in detail by Gordts *et al.*²³⁰ CD4⁺ SupT1 cells (2×10^5) were seeded in a 48-well plate and incubated with dilutions of test compound and HIV-1 NL4.3 stock (2×10^5 pg of HIV-1 p24 Ag). After an incubation time of 2 hours at 37°C, cells were transferred to 15 ml conical polypropylene tubes (Falcon, BD Biosciences) and thoroughly washed 2 times with 12 ml PBS/FCS 2% solution. Then the cells were transferred to 5 ml polypropylene tubes and virus binding was detected using mouse monoclonal anti-gp120 Ab NEA-9205. After 30 minutes incubation time, cells were thoroughly washed and GaM-PE was added. After an additional incubation time of 30 minutes, cells were washed and fixed with a 1% paraformaldehyde (PFA) solution (Sigma-Aldrich). Aspecific binding on the T cells was determined using GaM-PE only. Inhibition of gp120 binding by the test compounds was analyzed by flow cytometry (Accuri C6, BD Biosciences) and FlowJo software (Tree Star, San Carlos, CA, USA).

3.4.4 HSV-2 gD antibody cellular binding assay

MT-4 cells, which express the HSV receptors nectin-1 and nectin-2, were infected with HSV-2 strain G. Four days after infection, cells (3×10^6) were transferred to 5 ml polypropylene tubes and incubated with dilutions of test compound for 1 hour at

37°C. Virus binding was detected using mouse monoclonal anti-HSV-1 + HSV-2 gD Ab. After 30 minutes incubation time, cells were thoroughly washed and GaM-AF488 was added. After an additional incubation time of 30 minutes, cells were washed and fixed with a 1% paraformaldehyde solution. Aspecific binding on the T cells was determined using GaM-AF488 only. Inhibition of HSV gD mAb binding by the test compounds was analyzed by flow cytometry and FlowJo software.

3.4.5 HIV giant cell co-culture assay

This assay was performed as described by Férir *et al.*²³¹ Briefly, CD4⁺ CD8⁺ SupT1 cells are very susceptible to virus-induced giant cell formation when co-cultured with persistently HIV-infected HuT-78 T cells. Test compounds (5-fold dilutions) were added to a 96-well culture plate and incubated with an equal mix of SupT1 (1x10⁵ cells) cells and persistently infected HLA-DR⁺ HuT-78 cells (HuT-78/IIIB or HuT-78/NL4.3) at 37°C for 24 hours. Afterwards, giant cell formation was scored light-microscopically and cells were stained with specific mAbs to accurately calculate IC₅₀ values. Samples were incubated with FITC-conjugated anti-CD8 and PerCP-Cy5.5-conjugated HLA-DR mouse monoclonal antibodies to distinguish between both cell populations (HLA-DR⁺ HuT-78 cells and CD8⁺ SupT-1 cells). After 30 minutes incubation, cells were washed with PBS and fixed with 1% PFA solution. Samples were analyzed by flow cytometry and IC₅₀ values were determined using FlowJo software.

3.4.6 DC-SIGN HIV-capture/transmission assay

Cells expressing DC-SIGN are described to capture and transmit HIV to CD4⁺ target cells. This can be experimentally simulated in capture/transmission assays, as published previously.²³² In the capture assay, test compound was diluted in cell culture medium in 15 ml conical polypropylene tubes and incubated with HIV-1 HE stock (100 000 pg) at 37°C for 30 minutes. Raji DC-SIGN cells (5x10⁵ cells) were added and incubated at 37°C for 1.5 hour. Afterwards, cells were washed thoroughly in cell culture medium and then resuspended in a triton X-100 solution and viral presence was quantified by HIV-1 p24 Ag ELISA.

In the transmission assay, Raji DC-SIGN cells (5x10⁵ cells) were incubated with HIV-1 HE stock (100 000 p of p24 HIV-1 Ag) at 37°C for 1.5 hour. Afterwards, cells were washed thoroughly and resuspended in cell culture medium (2x10⁶ cells/ml). Test compounds were diluted in a 96-well plate and incubated for 30 minutes with

CD4⁺ CXCR4⁺ CD25⁺ C8166 cells (2x10⁶ cells/ml). Then, the virus-exposed Raji DC-SIGN cells were added. After an incubation period of 48 hours, all wells were scored microscopically for syncytium formation and samples were washed and stained with PE-conjugated anti-CD25 and FITC-conjugated anti-DC-SIGN mAbs to distinguish the cell populations. Aspecific binding was determined using SimulTest control. After fixation in 1% paraformaldehyde solution, samples were analyzed by flow cytometry to determine the IC₅₀ values.

3.4.7 Antiviral assays with several resistant HIV strains

LA^{low} and LA^{high} resistant NL4.3 HIV-1 were obtained by passaging the virus in increasing concentrations of the respective compound in MT-4 cells. Every 5 days, virus-induced CPE was scored light-microscopically and when full CPE was observed, cell supernatant was used to infect the next passage of cells. After 85 and 100 passages respectively, the virus was able to replicate in the presence of 90 µg/ml LA^{high} (1.7 µM) and LA^{low} (11.3 µM). This virus was collected by centrifugation, RNA was extracted using the QIAamp Viral RNA Mini Kit (Qiagen, Hilden, Germany) and the *env* gene was sequenced using the BigDye Terminator v3.1 Cycle Sequencing Kit to determine relevant mutations compared to wild-type virus. Reactions were run on an ABI3100 Genetic Analyzer (Applied Biosystems, Foster City, CA, USA). The sequences were analyzed using Sequence Analysis version 3.7 and SeqScape version 2.0 (Applied Biosystems). Antiviral assays with resistant viruses were performed in MT-4 cells as described above. Additionally, we performed antiviral assays with HIV-1 strains that were resistant to several well-defined entry inhibitors such as AMD3100, PRO 2000, DS 5000, 2G12 mAb and T20. These resistant virus strains were characterized in earlier publications.^{233–235}

3.4.8 Antiviral assay with VSVG-HIV-1 pseudovirus

Pseudovirus was produced using plasmids encoding GFP (pQCXIP-AcGFP), VSV envelope (pCF-VSVG) and HIV vector (pCG-gagpol). They were kindly provided by Dr. L. Naesens. Plasmids were co-transfected into HEp-2 cells using FuGENE HD transfection reagent (Promega) according to the Manufacturer's protocol. After 24 hours incubation, medium was replaced by fresh transfection medium containing 1mM sodium butyrate (Sigma-Aldrich). 48 hours post-transfection, supernatant containing VSVG-HIV-1 pseudovirus was collected, centrifuged and used for transduction.

HeLa cells (1.5×10^4 cells/well) were seeded in a 96 well plate and after overnight incubation, cells were incubated for 15 minutes with various concentrations of lignosulfonates. Cells were then transduced with VSVG-HIV-1 pseudovirus. Viral infection was quantified microscopically, 48 hours after transduction. As a control, antiviral activity of lignosulfonates was also determined against replication-competent VSV.

3.5 Flavivirus assays

These assays were performed to determine the antiviral activity and mechanism of action of Laby A1 (Chapter 5) and to study the viral entry receptors TIM-1 (Chapter 6) and CD300a (Chapter 7).

3.5.1 Antiviral assays

Cells were seeded in growth medium in microwell plates of different formats according to the experiment. Vero, U87, A549, Huh-7, Jeg-3, HEK293(T), CHO.k1 cells were allowed to adhere overnight to obtain confluent monolayers. The suspension Raji cells and MDDC were seeded on the day of infection. Cells were incubated for 30 min with compound dilutions in assay medium. Then, virus was added at a MOI of 0.001, 0.1, 1, or 10. After 1 h incubation, unbound virus was removed by extensive washing and fresh assay medium was added. Cells were incubated for 2 days (MDDC), 3 days (HEK293(T)), 4 days (Vero, A549, Raji, Huh-7, Jeg-3, HEK293(T), CHO.k1), or 6 days (U87). Virus-induced CPE was scored microscopically, and supernatant containing virus was harvested and stored at -80°C for RT-qPCR quantification, viral plaque reduction, and cytokine/chemokine determination. Cells were used to detect viral antigen by flow cytometry and for RT-qPCR quantification. Experiments were performed in duplicate.

3.5.2 Viral plaque reduction assay

BHK-21 cells were seeded in 12-well plates in growth medium (4×10^5 cells/well). The next day, cells were incubated in triplicate with 10-fold viral stock dilutions or supernatant dilutions in assay medium. After 1 h, medium was replaced with a microcrystalline cellulose overlay (Avicel RC 581, IMCD Benelux, Mechelen, Belgium) and incubated for 4 days. Overlay was removed, the cells were fixed in 70% ethanol and stained with Crystal Violet solution (Merck, Darmstadt, Germany).

Plaques were counted and infectious viral titer was determined according to the following formula: number of plaques x dilution factor x (1/inoculation volume).

3.5.3 Immunofluorescence staining

Vero cells were seeded in clear bottom black well plates (Merck) and allowed to adhere overnight. Confluent monolayers were incubated for 30 min with Laby A1 serial dilutions and infected with DENV-2 or ZIKV MR766 at MOI 1. Thirty hours after infection, cells were fixed in 2% PFA for 10 minutes at RT and permeabilized with 0.1% Triton X-100 (TFS) for 5 min at RT. After washing, cells were blocked for 20 min in 1% BSA (Merck) at RT. Cells were stained overnight with DENV-2 envelope antibody and DENV-2 NS3 antibody, or Flavivirus 4G2 antibody. Cells were thoroughly washed and incubated for 1 h with secondary antibodies at RT (GaM-AF555; DaR-AF488; GaM-AFF488). After washing, cells were incubated for 20 min with 2 µg/ml Hoechst (TFS) to stain the cell nuclei. After final washing, plates were examined with an EVOS FL imaging system (TFS).

3.5.4 Time-of-drug addition assay

Vero cells (15×10^3 cells/well) were seeded in 96 well plates. After overnight incubation, cells were infected with DENV-2 NGC or ZIKV MR766 at MOI 1. Laby A1 (5 µM) and reference compounds were added 2 hours prior to, at the moment of, or 2, 4, 6, 8 or 12 hours after infection. One hour after infection, the virus inoculum was replaced by assay medium and plates were incubated for 24 hours. Next, the intracellular viral RNA was isolated and quantified through RT-qPCR using the CellsDirect One-Step qRT-PCR Kit (TFS) according to the Manufacturer's instructions. For every time point, viral RNA quantity of treated, infected cells was compared to that of untreated, infected cells.

3.5.5 Ultrafiltration assay

An undiluted ZIKV MR766 stock was incubated in the absence or presence of Laby A1 dilutions for 1h at 4°C. The samples were transferred to sterilized Vivaspin 500 tubes (100 000 MWCO, Sigma-Aldrich) and centrifuged 3 times for 10 min at 15 000 x g in a fixed angle rotor. Samples were recovered from the bottom of the concentrate insert and infectious viral titer was determined through plaque assay. EGCG was included as a positive control.¹²³

3.5.6 Virucidal assay

An undiluted stock of DENV-2 NGC or ZIKV MR766 was mixed with Laby A1 (10 or 1 μ M). After an incubation of 1h at 4°C, 10-fold dilutions of these mixtures were prepared in assay medium and used to infect BHK-21 cells, subsequently followed by plaque assay as described above. As a control, virus-Laby A1 mixtures that were immediately diluted (without pre-incubation) were included.

3.5.7 RNA isolation and quantitative RT-PCR

Virus lysis, RNA isolation and RT-qPCR was performed using the CellsDirect One-Step qRT-PCR Kit (TFS) according to the Manufacturer's instructions. During RT-qPCR, the ZIKV E protein encoding region (nucleotides 1193-1269) and DENV 3'UTR noncoding regions were amplified. Primers and probes were obtained from Integrated DNA Technologies (IDT, Leuven, Belgium) and are shown in Table 3.4. Viral copy numbers were quantified based on a standard curve produced using serial 10-fold dilutions from viral DNA templates with known concentrations.

Table 3.4 Primer and probe sequences used in RT-qPCR

Primer/probe	Sequence (5'-3')	Ref
DENV-1-4 forward	GGATAGACCAGAGATCCTGCTGT	236
DENV-1-3 reverse	CATTCCATTTTCTGGGGTTC	236
DENV-1-3 probe	FAM/CAGCATCATTCCAGGCACAG/MGB	236
DENV-4 reverse	CAATCCATCTTGCGGCGCTC	236
DENV-4 probe	FAM/CAACATCAATCCAGGCACAG/MGB	237
ZIKV forward	CCGCTGCCCAACACAAG	238
ZIKV reverse	CCACTAACGTTCTTTTGCAGACAT	238
ZIKV probe	FAM/AGCCTACCT/ZEN/TGACAAGCAATCA GACTACTCAA/IBFQ	239

3.6 Flow cytometry assays

3.6.1 Surface receptor staining

To stain surface antigens, cells of interest were washed in phosphate buffered saline (PBS) containing 2% FBS and incubated at RT in the dark for 30 min with

primary unlabeled or fluorescence-labeled antibodies directed against the receptor of interest, or with isotype control (Table 3.5). Cells were washed and incubated with labeled secondary antibody at RT in the dark for 30 min. After a final washing step, cells were fixed in 1% PFA and analyzed by flow cytometry using a BD Accuri C6 or BD FACSCelesta (BD Biosciences, San Jose, CA, USA). Data were analyzed using FlowJo software (Tree Star, San Carlos, CA, USA). In the antibody binding assays, cells were incubated with various compounds prior to antibody staining.

Table 3.5 Overview of antibodies used in flow cytometry assays

Antibody	Clone	Labeling	Source	Section
Isotype control Abs				
SimulTest	IgG1/IgG2a	FITC/PE	BD ^g	
Mouse IgG1	MOPC-21	FITC; PE	BD ^g	
Mouse IgG2a	G155-78	PerCP- Cy5.5	BD ^g	
Mouse IgG2b	27-35	APC; FITC; PE	BD ^g	
Virus Abs				
DENV-2 E ^a	3H5-1	/	Merck ^h	3.5.3; 3.6.2
DENV-2 NS3 ^b	polyclonal	/	TFS ⁱ	3.5.3
DENV prM ^c	D3-2H2-9-21	/	Merck ^h	3.6.2
Flavivirus ^c	D1-4G2-4-15	/	Merck ^h	3.5.3
HIV-1 gp120 ^a	NEA-9205	/	NEN ^j	3.4.3
HSV-1 + HSV-2 gD ^c	2C10	/	Abcam ^k	3.4.4
ZIKV E ^b	polyclonal	/	Protein Specialists ^l	3.6.2
Receptor Abs				
Axl ^b	polyclonal	/	Abcam ^k	3.6.1
CD8 ^a	SK1	FITC	BD ^g	3.4.5
CD25 ^a	2A3	PE	BD ^g	3.4.6
CD56 ^d	NCAM16.2	APC	BD ^g	3.6.1

CD300a ^a	E59.126	PE	Beckman Coulter ^m	3.6.1; 3.8
CD300a ^e	polyclonal	/	R&D Systems ⁿ	3.5.1
CXCR7 ^d	8F11-M16	APC	Biolegend ^o	3.6.1
DC-SIGN ^d	DCN46	FITC	BD ^g	3.4.6
DC-SIGN ^d	DCN46	PE	BD ^g	3.6.1
Heparan sulfate ^f	10E4	/	US Bio ^p	3.6.1
HLA-DR ^c	L243	PerCP- Cy5.5	BD ^g	3.4.5
Mannose receptor ^a	19.2	PE	BD ^g	3.6.1
PTK7 ^c	188B	PE	Miltenyi ^q	3.6.1
TIM-1 ^a	1D12	PE	Biolegend ^o	3.6.1; 3.8
TIM-1 ^e	polyclonal	/	R&D Systems ⁿ	3.5.1

Secondary Abs

Goat anti-Mouse		PE	Biolegend ^o	3.4.3; 3.6.2
Goat anti-Mouse		AF488	Abcam ^k	3.4.4
Goat anti-Mouse		AF555	TFS ⁱ	3.5.3
Goat anti-Mouse		AF488	TFS ⁱ	3.5.3
Donkey anti-Rabbit		AF488	TFS ⁱ	3.5.3
Goat anti-Rabbit		PE	TFS ⁱ	3.6.2

^aMouse IgG1, ^bRabbit IgG, ^cMouse IgG2a, ^dMouse IgG2b, ^eGoat IgG, ^fMouse IgM, ^gBD Biosciences, San Jose, CA, USA. ^hMerck, Darmstadt, Germany. ⁱThermo Fisher Scientific, Waltham, MA, USA. ^jNEN Life Science Products, Boston, MA, USA. ^kAbcam, Cambridge, UK. ^lProtein Specialists, Ness Ziona, Israel. ^mBeckman Coulter, Indianapolis, IN, USA. ⁿR&D Systems, Minneapolis, MN, USA. ^oBiolegend, San Diego, CA, USA. ^pUS Biological, Salem, MA, USA. ^qMiltenyi Biotec, Bergisch Gladbach, Germany.

3.6.2 Intracellular antigen staining

To stain intracellular antigens, we used a protocol based on the literature.²⁴⁰ Briefly, cells were fixed in 2% PFA, followed by permeabilization in ice cold 90% methanol. Cells were subsequently stained with antibodies as described above. We also used a slight variant of this protocol to evaluate internalization of TIM-1 after Laby A1 pre-incubation. Immediately prior to flow cytometry analysis, cells were transferred to either a PBS pH7 solution or a PBS pH2 solution. In the latter situation,

denaturation of externally expressed receptors occurs. By comparing the fluorescence of samples in pH7 and pH2, the amount of internalized TIM-1 can be determined.

In assays using virus, cells were intra- or extracellularly stained with primary antibody detecting the viral antigens. For DENV-2, monoclonal mouse anti-DENV-2 NGC antibody specific to the viral envelope glycoprotein was used. For the other DENV serotypes, monoclonal mouse antibody recognizing the DENV premembrane protein was used. ZIKV envelope was detected using polyclonal rabbit anti-ZIKV envelope antibody. Cells were subsequently stained with a secondary antibody conjugated to phycoerythrin (PE), *i.e.* goat anti-mouse (GaM-PE) or goat anti-rabbit (GaR-PE).

3.6.3 Phagocytosis assay

This protocol was adapted from Miksa *et al.*²⁴¹ Jurkat cells (1×10^6 cells/ml) were incubated with Camptothecin (50 μ M, Merck) for 24 h to induce apoptosis. TIM-1-positive or –negative cells were seeded in 24 well plates and allowed to adhere overnight until a confluent monolayer was obtained. Medium was replaced with compound dilutions in serum-free culture medium and incubated for 1 hour at 37°C. Apoptotic Jurkat cells were incubated with pHrodo Red succinimidyl ester (200 ng/ml and per 10^6 Jurkat cells; TFS) for 30 min at RT. This pH-dependent dye only emits a fluorescent signal when localized in the acidic environment of the phagolysosome, making it a useful tool to study phagocytosis. Stained non-apoptotic Jurkat cells served as a control. Then, compound dilutions were removed, Jurkat cells were washed and dissolved in serum-free medium and added to the 24 well plates (500 000 Jurkat cells per well). Plates were incubated at 37°C for various time points to allow phagocytosis of Jurkat cells. Medium was removed, cells were detached, washed, and fixed using 1% PFA. Samples were analyzed using flow cytometry performed on a FACSCelesta (BD Biosciences). As a control, the fluorescence of the samples that had been incubated at 4°C was also determined. The percentage of cells that engulfed stained apoptotic Jurkat cells was calculated.

3.7 Surface plasmon resonance studies

3.7.1 Interaction between HIV glycoproteins and lignosulfonates

SPR technology was used to determine the binding of gp120 and gp41 with lignosulfonates. Recombinant gp120 HIV-1 strain IIB (ImmunoDiagnostics Inc., Woburn, MA), recombinant gp41 HIV-1 strain HxB2 (Acris Antibodies GmbH, Herford, Germany) and human serum albumin (Sigma) were covalently immobilized on the carboxymethylated dextran matrix of a CM5 sensor chip in 10 mM sodium acetate, pH 4.5 (gp120) or pH 5 (gp41 and HSA), using standard amine coupling chemistry. A reference flow cell was used as a control for non-specific binding and refractive index changes. Interaction studies were performed at 25°C on a Biacore T200 instrument (GE Healthcare, Uppsala, Sweden) in HBS-P+ (10 mM HEPES, 150 mM NaCl, 0.05% surfactant P20; pH 7.4). Lignosulfonates were serially diluted, covering a concentration range between 10 000 and 1.5 nM by using 3-fold dilution steps. Samples were injected for 2 minutes at a flow rate of 30 μ l/min and the dissociation was followed for 4 minutes. The sensor chip surface was regenerated with 50 mM NaOH and stabilized for another 2 minutes. Several buffer blanks were used for double referencing. Binding affinities (K_D) were derived after fitting the experimental data to the 1:1 binding model in the Biacore T200 Evaluation Software 2.0. Because of a large deviation from the 1:1 binding model at higher LA concentrations, only the lower concentrations were used in the fitting procedure and the apparent K_D values are reported.

3.7.2 Interaction between DENV-2 envelope and Laby A1

Recombinant envelope protein from DENV-2 (GenWay Biotech, San Diego, CA) was covalently immobilized on a CM5 sensor chip in 10 mM sodium acetate, pH 4.0, using standard amine coupling chemistry. The chip density was 9515 resonance units (RU). A reference flow cell was used as a control for analyzing non-specific binding and changes in refractive index. All interaction studies were performed at 25°C on a Biacore T200 instrument (GE Healthcare, Uppsala, Sweden). Laby A1 was serially diluted in HBS-P+ (10 mM HEPES, 150 mM NaCl and 0.05% surfactant P20; pH 7.4) supplemented with 5% DMSO (Merck), and 10 mM CaCl_2 covering a concentration range of Laby A1 between 20 and 1.25 μ M by using two-fold dilution steps. Samples (in duplicate) were injected for 2 minutes at

a flow rate of 45 $\mu\text{l}/\text{min}$ and the dissociation was analyzed for 4 minutes. Several control buffers were used for double referencing as described previously.²⁴² The CM5 sensor chip surface was regenerated with a single injection of 50 mM NaOH to remove all bound peptides. A flow of dose-dependent DMSO was included to eliminate the contribution of DMSO to the measured response. The experimental data were fit using the 1:1 binding model Biacore T200 Evaluation software 1.0 to determine the binding kinetics in each condition.

3.7.3 Interaction between liposomes and Laby A1

3.7.3.1 Liposome preparation

Lipids were obtained from Avanti Polar Lipids (Merck) and dissolved in chloroform at the desired ratios (10 mg/ml). The solvent was removed using rotary evaporation and vacuum drying under a stream of argon gas for at least 3 hours. Samples were dissolved in buffer (140 mM NaCl, 20 mM Tris-HCl; pH 8.0) containing glass beads and vigorously vortexed to obtain multilamellar liposomes. They were converted to unilamellar liposomes by exposing them to 8 freeze-thaw cycles and sonication (30 min with 10 s on/off cycles) using a 750W Ultrasonic Processor (Cole-Parmer, Vernon Hills, IL, USA). After centrifugation the samples were incubated for 45 min at 40°C, and stored at 4°C until further use (within two weeks).

3.7.3.2 SPR experiments with liposomes

Samples were passed 19 times through a 100 nm polycarbonate filter of a Mini-Extruder (Avanti Polar Lipids). Unilamellarity was confirmed by dynamic light scattering. Interaction studies between liposomes and Laby A1 were performed at 25°C on a Biacore T200 instrument (GE Healthcare, Upsalla, Sweden) in HBS-N (10 mM HEPES, 150 mM NaCl; pH 7.4) supplemented with 1 mM CaCl_2 and 1% DMSO. Liposomes were first captured on a L1 sensor chip for 10 minutes at a low flow rate of 2 $\mu\text{l}/\text{min}$. Loosely bound liposomes were subsequently removed by treatment with 100 mM NaOH. Next, 1 mg/ml BSA was injected for 10 minutes at a flow rate of 30 $\mu\text{l}/\text{min}$ to block non-specific binding. After a 10 minute stabilization period, Laby A1 was injected for 2 minutes at a flow rate of 30 $\mu\text{l}/\text{min}$ and the dissociation was followed for 4 minutes. Finally, the L1 sensor chip was regenerated with isopropanol/50 mM NaOH (2:3, vv) and new liposomes were captured for the next analysis.

3.8 Cellular electric impedance spectroscopy assay

Changes in cell morphology after incubation with virus or compound were measured with the xCELLigence Real Time Cell Analysis instrument from ACEA Biosciences (San Diego, USA). This assay was performed according to Doijen *et al.*²⁴³ In short, a 16-well plate embedded with gold electrodes was coated with 10 µg/ml fibronectin (Sigma-Aldrich) in Milli-Q water at RT for 30 min. A549, HEK293 or HEK293 TIM-1 cells were seeded and placed in the device at 37°C to allow cell growth. After overnight incubation, compound or virus dilutions were prepared and added to the cells for further incubation. Cell index (CI) was continuously monitored. Data were processed using Matlab R2016b (Mathworks, Natick, MA, USA). CI values were normalized to the point just before compound or virus addition.

3.9 Molecular cloning and entry receptor transfection

The shuttle vectors containing human TIM-1 and CD300a cDNA ('inserts') were purchased from R&D Systems (Minneapolis, MN, USA). The pBABE-Puro retroviral expression vector was created by H. Land and J. Morgenstern and purchased from Addgene (Watertown, MA, USA).²⁴⁴ This vector contains a puromycin resistance marker. Using PCR with appropriately designed primers we amplified insert and expression vectors and introduced overlapping DNA ends. PCR was performed with Q5 Hot Start HF DNA Polymerase (New England Biolabs (NEB), Ipswich, MA, USA). The size of the PCR products was verified through gel electrophoresis on a 1.2 % FlashGel (Lonza, Basel, Switzerland). PCR products were cleaned up using the QIAquick PCR Purification Kit (Qiagen, Antwerp, Belgium). Insert cDNA was integrated in the expression vector using NEBuilder HiFi DNA Assembly Master Mix (NEB) according to the Manufacturer's instructions. The ligation product was added to NEB5α competent *E. coli* (NEB). Transformation was performed according to the Manufacturer's guidelines and bacteria were streaked on lysogeny broth (LB) agar plates containing 100 µg/ml ampicillin (Merck). After overnight incubation, single colonies were selected and grown overnight in liquid LB medium with ampicillin (100 µg/ml). Plasmid isolation was performed using the Wizard Plus SV Miniprep DNA Purification System

(Promega). Isolated plasmid DNA was sequenced to verify correct insert incorporation (performed by Macrogen, Amsterdam, The Netherlands).

Cells (3.5×10^5) were seeded in a 6 well plate and allowed to adhere overnight. Cells were transfected with TIM-1 or CD300a plasmid DNA vectors using the lipid-based transfection reagent FuGENE HD (Promega). A 3:1 lipid:DNA ratio mixture was prepared in Opti-MEM medium (TFS) and applied dropwise to the cells. After overnight incubation, cells were subjected to puromycin selection (2 – 20 $\mu\text{g/ml}$, depending on the cell type) and further cultured in selection medium. TIM-1 and CD300a receptor expression was verified with flow cytometry.

In order to increase receptor expression, cells were sorted. They were washed in PBS with 2% FCS, resuspended to 10×10^6 cells/ml and stained for 30 min using monoclonal mouse TIM-1 antibody conjugated to PE (clone 1D12; Biolegend) or mouse monoclonal CD300a antibody conjugated to PE (clone E59.126; Beckman Coulter, Indianapolis, IN, USA), respectively. Cell sorting was performed in the VIB-KU Leuven FACS Core using the BD FACSMelody™ (BD Biosciences). The sorted populations were cultured for at least one week in culture medium supplemented with P/S/G prior to checking the receptor expression and performing further experiments. Receptor expression was verified regularly.

3.10 Statistical analysis

The % inhibition of a compound concentration was obtained by subtracting the negative control response and normalizing to the positive control response according to the following formula:

$$\% \text{ inhibition} = \left(1 - \frac{(\text{response}_x - \text{response}_{nc})}{(\text{response}_{pc} - \text{response}_{nc})} \right) \cdot 100$$

Here, response_x belongs to the compound treated sample, response_{nc} to the negative control, and response_{pc} to the positive control.

IC_{50} values were used to represent the potency of the compounds. They were calculated by applying the following formula:

$$IC_{50} = \exp \left[\ln(C1) - \left(\ln \left(\frac{C1}{C2} \right) \cdot \frac{(\%inhib_{c1-50})}{(\%inhib_{c1} - \%inhib_{c2})} \right) \right]$$

Here, C1 is the compound concentration resulting in more than 50% inhibition, C2 is the compound concentration resulting in less than 50% inhibition, with their respective % inhibition (%inhib_{C1/C2}).

All data were represented using Graphpad Prism 8 (Graphpad software Inc, San Diego, CA, USA). Dose-response curves were obtained using the nonlinear regression fitting tool.

Statistical analyses were performed with Graphpad Prism 8. Variation between repeated experiments was depicted using the standard error of the mean (SEM), which is defined as the standard deviation of the averages of repeated experiments. In Section 4.2.1 correlations were calculated using the Spearman correlation test, except when data were normally distributed. In this case, the Pearson correlation test was used. These tests state that there is no correlation between variables, and are defined by the correlation coefficient r . P-values < 0.05 were considered as statistically significant. To compare the means of two groups in Figures 6.4, 7.2 and 7.4, the two-tailed one sample t-test was used. P-values < 0.05 were indicated with *.

Chapter 4

A unique class of lignin derivatives displays broad anti-HIV activity by interacting with the viral envelope

This chapter has been published in the following article:

A unique class of lignin derivatives displays broad anti-HIV activity by interacting with the viral envelope.

Oeyen, M., Noppen, S., Vanhulle, E., Claes, S., Myrvold, B. O., Vermeire, K., Schols, D. (2019) *Virus Res.* 274. DOI: 10.1016/j.virusres.2019.197760.

4.1 Introduction

More than 30 years after its discovery, HIV is still a major health problem. According to UNAIDS data, an estimated 37.9 million people (including 1.7 million children) were living with HIV in 2018.¹⁶ Although the incidence has decreased in the last decade, still 770 000 people died of AIDS-related illnesses in 2018. Moreover, for women of reproductive age, it is the main cause of death globally.²⁴⁵ The vast majority of people living with HIV are from low- and middle- income countries, 20.6 million people are living in eastern and southern Africa, where 800 000 new HIV infections occurred in 2018.¹⁶ Women in sub-Saharan Africa have a higher risk of becoming HIV-infected, because of biological, structural and social reasons.^{246,247} Examples are increased genital inflammation due to the more vulnerable female genital tract, intergenerational relationships, man-controlled communities, polygamy, and lack of schooling. Furthermore, current preventive measures like condom use and male circumcision are mainly under control of men. This underscores that efforts are needed to increase the number of measures that can be controlled by women. As long as an adequate HIV vaccine does not exist, research should still focus on the development of other preventive mechanisms. Microbicides are self-administered topical drugs that, when applied vaginally or in the rectum, prevent transmission of HIV and possibly other sexually transmitted infections (STI). Implemented in pre-exposure prophylaxis (PrEP) they have great potential to protect women. Microbicides have several requirements: next to efficacy on the long term they also have to be safe, affordable to at-risk populations, and easy to apply.²⁴⁸ Drugs that have been considered as microbicides cover a wide array of origins: surfactants, acid-buffering gels, polyanionic compounds, and antiretroviral drugs.²⁴⁶ Currently, microbicide research is also focused on compounds such as polyanionic dendrimers²⁴⁹ and on development of user-friendly application methods.^{250,251} Several anti-retroviral microbicides are under clinical investigation.^{252–254}

Naturally occurring compounds are an attractive source for the development of novel antivirals.^{255,256} They possess several advantages such as reduced side effects, increased cost-efficiency, higher bioavailability, and various modes of action. Furthermore, their high diversity and chemical variability could contribute to overcome problems with drug-resistant viral strains.²⁵⁷ Lignin is the second most

abundant natural polymer, after cellulose.²⁵⁸ It is a class of cross-linked phenolic polymers that confers structural integrity to plants. Until now, lignin is highly underutilized. Ninety-eight percent of the lignin isolated in the pulping industry is burned as a low-value fuel.²⁵⁹ Because of their abundance, low cost and sustainability, lignins are attractive sources of novel applications in times of environmental problems. Recent studies indicate this application potential, such as conversion into renewable chemicals as biofuel, carbon fiber and activated carbon^{259–261} and thermoplastics.²⁶²

Lignin derivatives are generated during the processing of lignocelluloses in the paper industry or bioethanol production. One of the employed methods is sulphite pulping. In the course of this process lignin is extracted from the wood using salts of sulfurous acid. This process leads to the formation of liginosulfonic acid (LA) – a liginosulfonate – as byproduct (Figure 4.1).²⁶³ Due to their dispersing, binding, complexing, and emulsifying properties, liginosulfonates have been utilized for several decades. At the end of the 19th century, it was used as a tanning agent.²⁶⁴ Furthermore, it has several other applications such as protection agent of protein degradation^{265,266}, pellet binder in animal food²⁶⁷, binding agent in phenolic resins²⁶⁸, plasticizer in cement²⁶⁹, and use in detergents, glues and surfactants.²⁶³

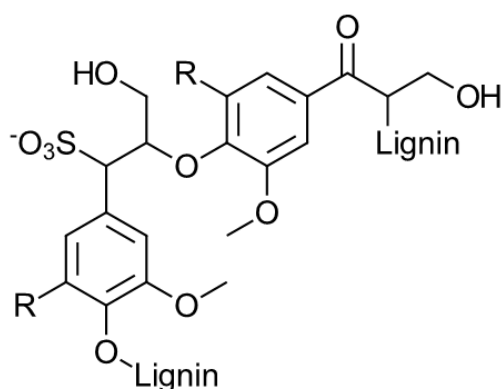


Figure 4.1 Schematic structure of a liginosulfonate dimer. For softwood R=H, for hardwood R=H or -OCH₃ in approximately 1:1 ratio.

In Gordts *et al.*, we have shown that a commercially available liginosulfonate (LA^{low}) possesses broad antiviral activity against HIV and Herpes simplex virus (HSV) by preventing viral entry into susceptible target cells.²³⁰ Because of these interesting properties, we determined the antiviral activity profile of a series of liginosulfonates in order to deduce which molecular features contribute to the

antiviral activity and to discover compounds with potential higher antiviral potency. Here, we evaluated 24 structurally different lignosulfonates and defined their capacity to inhibit viral (HIV and HSV) transmission and replication in several cell-based assays. These lignin derivatives differ in origin (hardwood or softwood), counter-ion used during sulphite processing (Na^+ , Ca^{2+} , or NH_4^+), sulphur content, carboxylic acid percentage, and molecular weight fraction, which allows to determine structure-activity relationships. We demonstrate that the antiviral activity of lignosulfonates is dependent on their molecular weight, and that their mechanism of action is based on interactions with viral envelope glycoproteins.

4.2 Results and discussion

4.2.1 Lignosulfonates with broad anti-HIV and anti-HSV activity

Twenty-four lignosulfonates with varying molecular properties were evaluated (Table 4.1). Inhibition of viral replication by these compounds was tested in two well-described cellular assay systems (MT-4 cells and TZM-bl cells) against two HIV-1 strains and one HSV-2 strain (Table 4.2). The antiviral activity between the compounds varied by 100- to even 1000-fold. Overall, compounds LA06, LA07, LA08, LA09, LA13, LA14, and LA20 showed the most prominent antiviral activity in these assays (IC_{50} : 10- 300 nM), while LA04 showed the weakest inhibitory effect (IC_{50} : 30.0 - 236.6 μM). The compounds had a more prominent activity towards HIV replication inhibition when compared to HSV, but the best-rated compounds still have anti-HSV IC_{50} values in the low nanomolar range (70 – 300 nM).

Figure 4.2 shows that the antiviral activity of the lignosulfonates in the different screening assays correlate with each other (Figure 4.2A, 4.2B), and with their molecular weight (Figure 4.2C). So the compounds with the highest antiviral activity in the screening assays in MT-4 and TZM-bl cells were associated with a higher molecular weight. This is in line with previous studies on sulfated polyanionic macromolecules and is attributed to multivalent interactions between larger molecules and multiple HIV gp120 molecules or attachment proteins of other enveloped viruses.²⁷⁰ The absence of activity of LA04 (900 g/mol) suggests that a certain 'threshold' molecular weight is necessary to obtain significant antiviral activity.

Table 4.1 Chemical characteristics of 26 lignin-derived compounds used in the study

Compound	MW (g/mol)^a	Counter ion^a	Raw material^a	Organic sulfur (%)^a	COOH (%)^a
LA01	6300	Sodium	Softwood	1.8	15.1
LA02	6300	Sodium	Softwood	1.8	0
LA03	8000	Sodium	Softwood	1.6	ND
LA04	900	Sodium	Softwood	2.0	ND
LA05	40000	Sodium	Softwood	5.7	9.0
LA06	58100	Sodium	Softwood	5.6	6.0
LA07	58100	Sodium	Softwood	5.6	0
LA08	60000	Sodium	Softwood	5.8	8.8
LA09	54900	Sodium	Softwood	7.1	6.9
LA10	6700	Sodium	Hardwood	4.6	10.0
LA11	6600	Calcium	Hardwood	4.3	13.9
LA12	41000	Calcium	Softwood	5.0	8.2
LA13	58000	Calcium	Softwood	5.4	6.5
LA14	82500	Calcium	Softwood	5.5	6.5
LA15	12500	Calcium	Hardwood	5.6	10.6
LA16	10400	Calcium	Hardwood	4.8	8.6
LA17	6500	Calcium	Hardwood	4.3	14.3
LA18	40000	Ammonium	Softwood	5.0	ND
LA19	28000	Ammonium	Softwood	5.0	ND
LA20	58000	Ammonium	Softwood	5.5	6.3
LA21	26000	Sodium	Softwood	9.4	9.6
LA22	16100	Sodium	Softwood	10.5	9.6
LA23	11000	Calcium	Hardwood	4.7	ND
LA24	16500	Calcium	Hardwood	3.3	ND
LA ^{high}	52000	Sodium	Softwood	6.3	6.2
LA ^{low}	8000	Sodium	Softwood	5.6	6.5

^aCharacterized by Borregaard LignoTech; ND: not determined

Table 4.2 Antiviral activity of the evaluated lignosulfonates

	IC_{50} (μM) ^a			
	MT-4		TZM-bl	
	HIV-1 NL4.3	HSV-2	HIV-1 NL4.3	HIV-1 BaL
LA01	0.2 ± 0.03	3.9 ± 0.7	0.4 ± 0.1	0.6 ± 0.02
LA02	0.8 ± 0.08	6.4 ± 1.2	0.5 ± 0.06	0.7 ± 0.06
LA03	0.1 ± 0.02	2.1 ± 0.3	0.2 ± 0.05	0.4 ± 0.04
LA04	30.0 ± 0.9	236.6 ± 26.2	73.2 ± 0.01	104.8 ± 0.01
LA05	0.05 ± 0.02	0.6 ± 0.04	0.09 ± 0.02	0.1 ± 0.03
LA06	0.02 ± 0.001	0.2 ± 0.06	0.05 ± 0.01	0.07 ± 0.02
LA07	0.02 ± 0.002	0.3 ± 0.02	0.04 ± 0.02	0.09 ± 0.02
LA08	0.02 ± 0.002	0.3 ± 0.03	0.06 ± 0.01	0.07 ± 0.01
LA09	0.02 ± 0.001	0.2 ± 0.07	0.06 ± 0.003	0.09 ± 0.001
LA10	0.7 ± 0.07	10.7 ± 1.7	1.7 ± 0.3	3.2 ± 0.3
LA11	0.9 ± 0.04	9.6 ± 3.8	0.8 ± 0.2	3.0 ± 0.4
LA12	0.05 ± 0.01	0.5 ± 0.02	0.1 ± 0.02	0.3 ± 0.08
LA13	0.02 ± 0.004	0.1 ± 0.02	0.05 ± 0.003	0.07 ± 0.004
LA14	0.01 ± 0.007	0.07 ± 0.004	0.04 ± 0.004	0.05 ± 0.002
LA15	0.5 ± 0.05	9.3 ± 0.8	0.8 ± 0.2	2.3 ± 0.2
LA16	0.6 ± 0.08	8.2 ± 0.8	1.1 ± 0.2	2.3 ± 0.08
LA17	0.7 ± 0.04	11.6 ± 4.6	1.2 ± 0.1	3.2 ± 0.2
LA18	0.04 ± 0.01	0.5 ± 0.01	0.1 ± 0.02	0.2 ± 0.01
LA19	0.08 ± 0.04	0.8 ± 0.03	0.2 ± 0.06	0.4 ± 0.1
LA20	0.02 ± 0.003	0.2 ± 0.04	0.05 ± 0.02	0.08 ± 0.005
LA21	0.02 ± 0.007	0.6 ± 0.02	0.2 ± 0.02	0.3 ± 0.04
LA22	0.07 ± 0.01	1.3 ± 0.2	0.9 ± 0.2	1.2 ± 0.2
LA23	0.2 ± 0.03	1.2 ± 0.5	0.2 ± 0.04	0.6 ± 0.01
LA24	0.09 ± 0.02	1.3 ± 0.06	0.4 ± 0.02	1.2 ± 0.1
LA ^{low}	0.1 ± 0.04	1.1 ± 0.5	0.4 ± 0.03	0.5 ± 0.09
LA ^{high}	0.03 ± 0.01	0.09 ± 0.02	0.06 ± 0.01	0.1 ± 0.02

^aCompound concentration required to inhibit viral replication by 50%. Antiviral activity was determined in MT-4 cells against HIV-1 NL4.3 (X4) and HSV-2 G and in TZM-bl cells against HIV-1 NL4.3 and HIV-1 BaL (R5) replication. Mean \pm SEM of three independent experiments is shown.

We also observed a weak but statistically significant correlation between the antiviral activity and organic sulfur content (Figure 4.2D). A significant correlation between carboxylic acid content and antiviral activity was not detected. Sulfur has been shown before to be an important determinant of antiviral activity and a higher sulfation degree is associated with better antiviral activity.^{271–273} LA21 (sulfur content 9.4%) is 4-fold more active than LA19 (sulfur content 5%) which has a comparable molecular weight. Another observation was that some hardwood lignosulfonates (e.g. LA10, LA11, LA15, LA16 and LA17) possess less antiviral activity compared to softwood lignosulfonates (LA01, LA02, LA22 and LA^{low}) of comparable molecular weight. Hardwood lignosulfonates possess extra $-\text{OCH}_3$ groups on the aromatic rings (Figure 4.1), which prevents this carbon position from further chemical reactions during both the lignification and pulping process. This makes them in general more linear and thus less branched polymers, which could be an explanation for the decreased antiviral activity.²⁷⁴ LA23 and LA24 are more active than expected from their known properties (low molecular weight and low sulfur content). This can be related to other chemical properties that are unknown. We did not find correlations between antiviral activity of lignosulfonates and other characteristics such as counter-ion or carboxylic acid content. In solution, the counter-ions are probably dissociated from the acidic lignosulfonate, preventing them to contribute to the antiviral properties. Taken together, our results suggest that the molecular weight of lignosulfonates has the most decisive influence on antiviral activity, but it would be interesting to study high molecular weight lignosulfonates with higher sulfur contents and from hardwood origin. This would allow us to more accurately determine the contribution of the chemical properties to their antiviral activity.

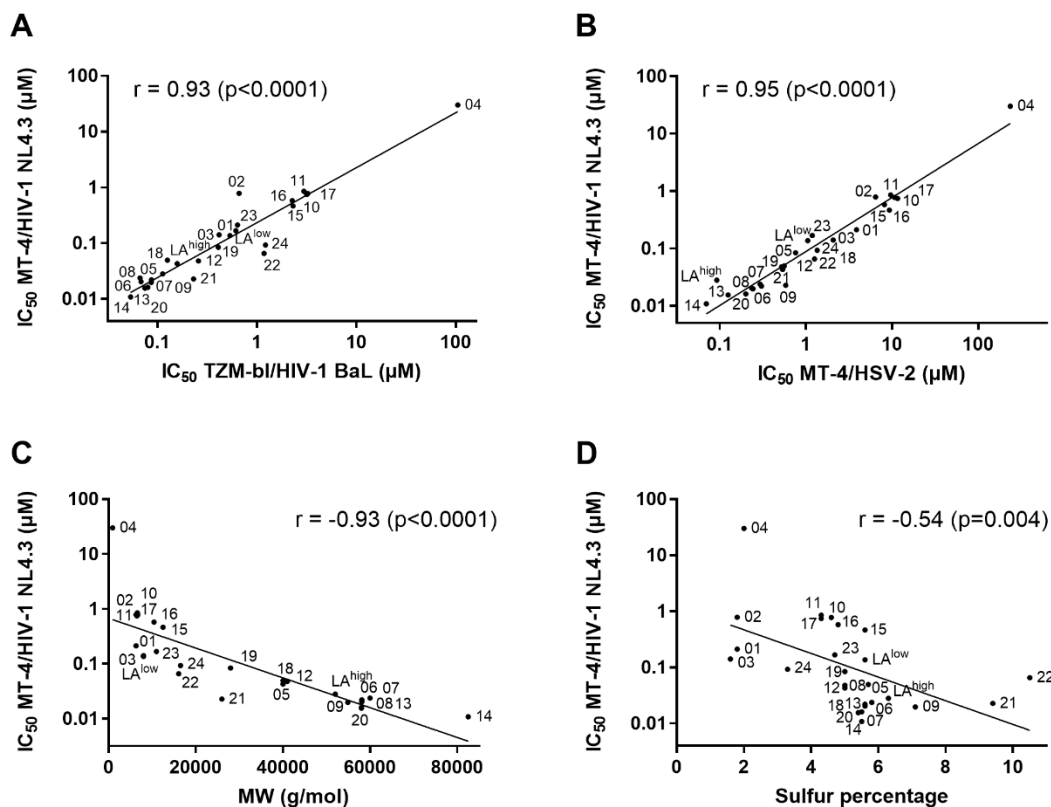


Figure 4.2 IC_{50} s of lignosulfonates correlate with each other and with molecular weight and sulfur content. Correlation of the IC_{50} value of the compounds for inhibition of HIV-1 NL4.3 replication in MT-4 cells with (A) their IC_{50} for inhibition of HIV-1 BaL in TZM-bl cells ($p < 0.0001$), (B) their IC_{50} for inhibition of HSV-2 in MT-4 cells ($p < 0.0001$), (C) their molecular weight ($p < 0.0001$), (D) their sulfur content ($p = 0.004$). Correlations were calculated in Graphpad using the Spearman correlation test, except for (D) where Pearson correlation test was used (p -values < 0.05 were considered as statistically significant).

The cellular cytotoxicity of the lignosulfonates was also evaluated in CD4⁺ MT-4 and TZM-bl cells. Most compounds did not show any cellular cytotoxicity, except for LA02 and LA03 (Table 4.3). However, their selectivity index in MT-4 cells against HIV-1 NL4.3 replication was 30 and 189, respectively.

Table 4.3 Cellular toxicity of the evaluated lignosulfonates

	CC_{50} (μM) ^a	
	MT-4	TZM-bl
LA01	> 40.0	> 40.0
LA02	24.0 \pm 1.2	25.0 \pm 2.4
LA03	26.5 \pm 2.6	> 31.0

LA04	> 278.0	> 278.0
LA05	> 6.0	> 6.0
LA06	> 4.5	> 4.5
LA07	> 4.5	> 4.5
LA08	> 4.0	> 4.0
LA09	> 4.5	> 4.5
LA10	> 38.0	> 38.0
LA11	> 38.0	> 38.0
LA12	> 6.0	> 6.0
LA13	> 4.5	> 4.5
LA14	> 3.0	> 3.0
LA15	> 20.0	> 20.0
LA16	> 24.0	> 24.0
LA17	> 38.5	> 38.5
LA18	> 6.0	> 6.0
LA19	> 9.0	> 9.0
LA20	> 4.5	> 4.5
LA21	> 9.5	> 9.5
LA22	> 15.5	> 15.5
LA23	> 22.5	> 22.5
LA24	> 15.0	> 15.0
LA ^{low}	> 31.3	> 31.3
LA ^{high}	> 4.8	> 4.8

^aCompound concentration required to decrease cell viability with 50%. Cellular toxicity was determined in MT-4 cells and in TZM-bl cells.

When we included a washing step after incubation of the cells with the compound, and thus removed the compound during the viral infection period, no antiviral activity whatsoever was observed. This is in contrast with data obtained with compounds that bind to the target cells, such as the CXCR4 antagonist AMD3100 (data not shown). Based on the results, we decided to perform most subsequent experiments with three lignosulfonates with high viral inhibiting properties (*i.e.* LA13, LA14, and LA20) and two derivatives with lower inhibiting properties (*i.e.* LA02 and LA04). We also observed that the antiviral activity of these

lignosulfonates was irrespective of viral tropism or co-receptor use, since they inhibited equally well CXCR4-using or X4 (NL4.3, IIIB), CCR5-using or R5 (BaL) or dual–using R5/X4 (HE) HIV-1 strains. They also inhibited with equal potency the multi-tropic (R3/R5/X4) HIV-2 (ROD) strain (Table 4.4). Furthermore, also in PBMCs expressing CD4 and various chemokine receptors (defined as PHA-blasts) comparable antiviral activity of the compounds was observed (Table 4.4). These PHA-blasts simulate the physiological target cells and can be seen as a model for the blood barrier that has to be crossed by the virus after vaginal/rectal intercourses.²⁷⁵

Table 4.4 Antiviral activity profile of selected lignosulfonates.

	IC ₅₀ (μM) ^a				
	MT-4			PHA-blasts	
	HIV-1 IIIB	HIV-1 HE	HIV-2 ROD	HIV-1 NL4.3	HIV-1 BaL
LA02	1.2 ± 0.3	1.2 ± 0.3	2.5 ± 0.09	0.8 ± 0.2	4.5 ± 1.5
LA04	58.8 ± 9.2	38.9 ± 5.6	28.1 ± 6.8	43.6 ± 24.1	46.0 ± 8.5
LA13	0.02 ± 0.007	0.03 ± 0.003	0.04 ± 0.004	0.02 ± 0.009	0.06 ± 0.02
LA14	0.02 ± 0.005	0.02 ± 0.004	0.03 ± 0.002	0.02 ± 0.004	0.05 ± 0.02
LA20	0.04 ± 0.009	0.04 ± 0.004	0.05 ± 0.005	0.01 ± 0.006	0.06 ± 0.02
LA ^{low}	0.2 ± 0.03	0.2 ± 0.002	0.3 ± 0.01	0.1 ± 0.05	0.4 ± 0.1
LA ^{high}	0.04 ± 0.004	0.03 ± 0.009	0.06 ± 0.002	ND	ND

^aCompound concentration required to inhibit viral replication by 50%. The antiviral activity of 7 selected lignosulfonates was determined in MT-4 cells against HIV-1 IIIB (X4), HIV-1 HE (R5/X4), HIV-2 ROD (R3/R5/X4). In PHA-blasts antiviral activity was determined against HIV-1 NL4.3 (X4) and HIV-1 BaL (R5) replication. Mean ± SEM of three to four independent experiments is shown.

Finally, the test compounds also inhibited HSV-1 and HSV-2 replication when evaluated in HEL cells and, importantly, dual HIV-1 and HSV-2 infections (when both viruses were added simultaneously at the start of the assay) in susceptible MT-4 cells (Table 4.5). This is not observed with the well-described compounds AMD3100 and acyclovir, which respectively inhibit HIV and HSV replication. These compounds have no activity in inhibiting virus-induced CPE when dual viral infections were performed in MT-4 cells (data not shown). The inhibition of HIV-1/HSV-2 co-infection by lignosulfonates is an important observation since it is described that an infection with HSV-2 increases the risk of acquiring HIV, and

conversely.²⁷⁶ Because HSV infections often remain unnoticed and both viruses seem to cooperate and facilitate their infections, it is perhaps essential that a microbicide has dual antiviral activity, which is associated with health benefits and decreased costs.²⁷⁷.

Finally, to determine if there was a broad antiviral activity against enveloped viruses, we also determined the activity of LA^{low} and LA^{high} against the flaviviruses ZIKV and DENV-2, but no activity was observed at the highest concentration tested (100 µg/ml) (Table 4.5).

Table 4.5 Antiviral activity of lignosulfonates against HSV, dual infection with HIV-1 and HSV-2, VSV, ZIKV and DENV-2

	IC ₅₀ (µM) ^a					
	HEL	MT-4		HEp-2	Vero	
	HSV-1	HSV-2	HIV-1 + HSV-2	VSV	ZIKV	DENV-2
LA02	5.8 ± 0.5	1.2 ± 0.03	4.6 ± 1.0	> 15.9	ND	ND
LA04	> 111.1	41.2 ± 2.8	101.9 ± 1.3	> 111.1	ND	ND
LA13	0.1 ± 0.01	0.02 ± 0.008	0.1 ± 0.04	0.7 ± 0.2	ND	ND
LA14	0.09 ± 0.009	0.02 ± 0.004	0.07 ± 0.03	0.4 ± 0.2	ND	ND
LA20	0.1 ± 0.002	0.09 ± 0.06	0.1 ± 0.06	0.9 ± 0.1	ND	ND
LA ^{low}	1.0 ± 0.006	0.2 ± 0.03	1.0 ± 0.5	4.5 ± 1.0	> 25.0	> 25.0
LA ^{high}	0.2 ± 0.02	0.09 ± 0.06	0.2 ± 0.09	0.8 ± 0.1	> 3.8	> 3.8

^aCompound concentration required to inhibit viral replication by 50%. The antiviral activity of selected lignosulfonates was determined in HEL cells against HSV-1 KOS and HSV-2 G, in MT-4 cells against dual virus infection with HIV-1 NL4.3 and HSV-2 G, in HEp-2 cells against VSV and in Vero cells against ZIKV strain MR766 and DENV-2. Mean ± SEM of three independent experiments is shown.

4.2.2 Lignosulfonates interfere with viral entry

In the time-of-drug addition experiments, antiviral activity of the lignosulfonates started to decline when they were added more than 30 minutes after infection. When added after 2 hours, no inhibition of viral replication was observed (Figure 4.3). This coincides with the HIV entry process, which is described to be completed in less than 1 hour in MT-4 cells.²²⁹ A comparable pattern was observed for the reference entry inhibitor PRO 2000. Two different reverse transcriptase inhibitors, tenofovir and AZT, still exerted their full antiviral activity when they were added up to 5 hours after infection, which concurs with the reverse transcription process (that starts 4-6 hours after infection).²²⁹ We thus conclude that lignosulfonates exert their antiviral activity at an early time point of infection by interfering with the viral entry process, which includes binding and adsorption to the surface of target cells, interaction with (co)receptors, and subsequent fusion. This was expected since lignosulfonates are polyanionic molecules.^{230,278} Entry inhibitors are still attractive microbicide candidates, because inhibiting this early step in the viral life cycle also prevents the establishment of a latent phase infection in the host cells.

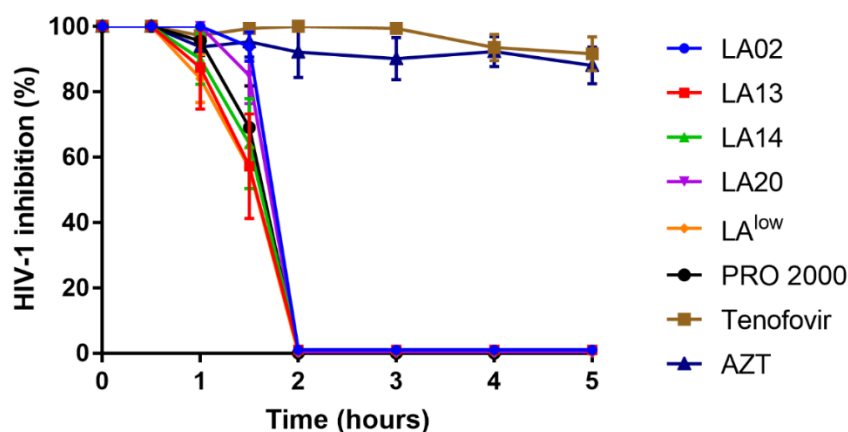


Figure 4.3 Lignosulfonates inhibit viral replication at an early time point in the viral life cycle. MT-4 cells were infected with HIV-1 NL4.3 and 100 $\mu\text{g/ml}$ lignosulfonates (16 μM LA02, 1.7 μM LA13, 1.2 μM LA14, 1.7 μM LA20, 13 μM LA^{low}), 20 μM PRO 2000, 1 μM AZT, and 100 μM tenofovir were added at different time points post-infection (0-5h). After 31 hours, viral replication was determined in the supernatant by specific HIV-1 p24 Ag ELISA. Data were plotted relative to the positive control to show the percentage inhibition of viral replication over time. Mean \pm SEM of three independent experiments is shown.

This interaction with cellular (co)receptors is a complex process that is mediated through interaction between the viral glycoprotein gp120 and the CD4 receptor

expressed on the target cell.²⁹ To determine if lignosulfonates exert their antiviral activity by interfering with this process, we evaluated HIV binding to the surface of CD4⁺ T cells with a specific anti-envelope gp120 antibody. As shown in Figure 4.4A, all lignosulfonates dose-dependently inhibited this binding. LA14 (IC₅₀: 0.15 ± 0.03 μM), LA13 (IC₅₀: 0.24 ± 0.03 μM) and LA20 (IC₅₀: 0.25 ± 0.01 μM) were the most potent inhibitors, followed by LA02 (IC₅₀: 2.6 ± 0.2 μM) and LA^{low} (IC₅₀: 5.2 ± 0.7 μM). LA04 was much less active in anti-HIV replication assays and in this assay the compound showed no inhibition (IC₅₀: >111 μM). The polyanionic virus-binding inhibitor PRO 2000 also inhibited this process (IC₅₀: 0.43 ± 0.1 μM). These results indicate that lignosulfonates perturb the interaction between the viral glycoprotein gp120 and the cellular receptor CD4. To determine if lignosulfonates also interact with HSV glycoproteins, we evaluated if they interfere with anti-gD envelope mAb binding to HSV-2-infected MT-4 cells. Fig 4B shows that they dose-dependently inhibit the gD mAb binding. Again, LA14 (IC₅₀: 0.94 ± 0.1 μM), LA13 (IC₅₀: 1.2 ± 0.1 μM), and LA20 (IC₅₀: 1.5 ± 0.1 μM) were the most potent inhibitors. LA^{low} (IC₅₀: 10.0 ± 0.7 μM) and LA02 (IC₅₀: 13.1 ± 2.3 μM) were less active, and LA04 showed no activity at all (IC₅₀: >111 μM). These IC₅₀ are higher than those of HIV binding inhibition (Figure 4.4A), which corresponds to the lower activity of lignosulfonates against HSV replication compared to HIV in MT-4 cells (Table 4.2). These results suggest that lignosulfonates interact with the HSV gD glycoprotein.

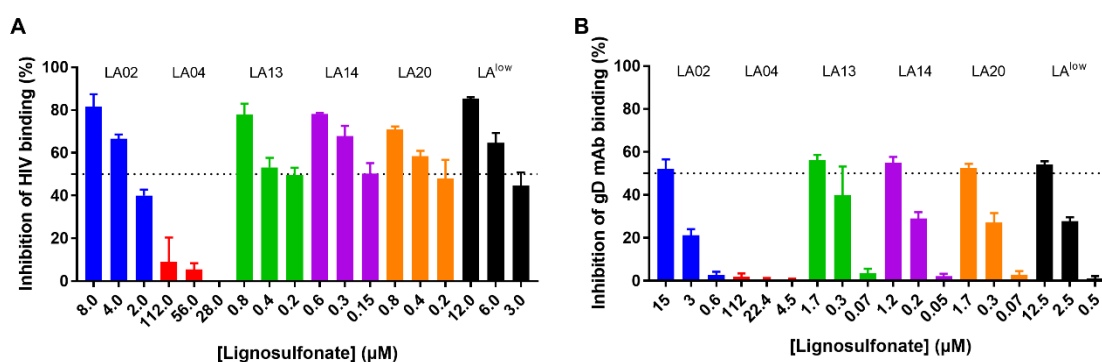


Figure 4.4 Lignosulfonates interfere with the viral glycoproteins that are involved in entry. (A) SupT1 cells were incubated with HIV-1 NL4.3 in the presence or absence of different concentrations lignosulfonates (8.0 – 4.0 – 2.0 μM LA02, 112.0 – 56.0 – 28.0 μM LA04, 0.8 – 0.4 – 0.2 μM LA13, 0.6 – 0.3 – 0.15 μM LA14, 0.8 – 0.4 – 0.2 μM LA20, 12.0 – 6.0 – 3.0 μM LA^{low}). After 2 hours, binding of HIV-1 gp120 to CD4 was measured using anti-gp120 NEA-9205 mAb. The graph demonstrates the percentage inhibition of HIV-1 gp120 binding to CD4⁺ SupT1 cells. Mean ± SEM of three independent experiments is shown. (B) MT-4

cells were infected with HSV-2 G. After four days, they were incubated with various concentrations of lignosulfonates (15.0 – 3 – 0.6 μ M LA02, 112.0 – 22.4 – 4.5 μ M LA04, 1.7 – 0.3 – 0.07 μ M LA13, 1.2 – 0.2 – 0.05 μ M LA14, 1.7 – 0.3 – 0.07 μ M LA20, 12.5 – 2.5 – 0.5 LA^{low}). After 1 hour, binding of HSV-2 gD envelope antibody to the infected cells was determined. The graph shows the percentage inhibition of gD mAb binding to HSV-2-infected MT-4 cells. Mean \pm SEM of three independent experiments is shown.

4.2.3 Lignosulfonates interact with HIV glycoproteins

SPR experiments further supported the hypothesis of the compounds interacting with HIV envelope proteins since we showed that they interacted with the gp120 glycoprotein. The affinity of the lignosulfonates for gp120 – as presented by their equilibrium dissociation constant k_D – reflected their antiviral potency. LA14 (k_D : 0.38 \pm 0.05 nM), LA20 (k_D : 0.58 \pm 0.29 nM), and LA13 (k_D : 0.79 \pm 0.26 nM) had the highest gp120 affinities, followed by LA^{high} (k_D : 0.98 \pm 0.25 nM), LA^{low} (k_D : 4.62 \pm 1.26 nM), and LA04 (k_D : 118.0 \pm 28.3 nM). The gp120 affinity k_D of the polyanionic control compound PRO 2000 was 2.6 \pm 0.70 nM, which also reflects its antiviral activity (HIV-1 NL4.3 EC₅₀: 0.2 \pm 0.07 μ M). Furthermore, these SPR experiments support the correlation between antiviral activity and molecular weight, as the lignosulfonates with higher MW bind with a higher affinity to gp120.

We also determined binding affinities between LA^{high} /LA^{low} and HIV gp41 and human serum albumin (HSA). Interestingly, there was also a potent interaction with gp41 (LA^{high} k_D : 1.65 \pm 0.81 nM, LA^{low} k_D : 3.59 \pm 0.14 nM). HSA was included to determine aspecific binding. For this interaction, the k_D s were very low varying from 0.36 \pm 2.97 μ M for LA^{high} and 0.31 \pm 0.17 μ M for LA^{low} (Figure 4.5).

Finally, we evaluated if these compounds also inhibit VSVG-HIV-1 pseudovirus production and we observed that this production was inhibited in the presence of these compounds (SFigure 4.1). This suggests a mechanism of action based on electrostatic interactions between positively charged envelope proteins and the polyanionic character of the compounds. Replication competent VSV was dose-dependently inhibited as well, albeit with lower potency than for HIV or HSV (Table 4.5).

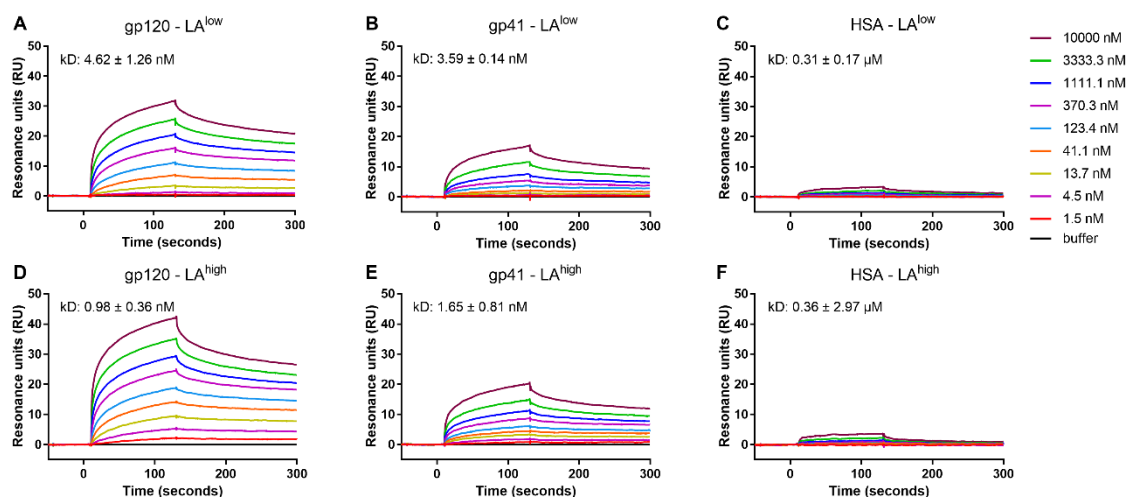


Figure 4.5 Lignosulfonates interfere with the interaction of viral gp120 and cellular CD4 by binding to gp120 and to a lesser extent to gp41. SPR sensorgrams of the interaction between gp120 (left panels A,D), gp41 (middle panels B,E), and HSA (right panels C,F) and various concentrations of LA^{low} (upper panels A-C) and LA^{high} (lower panels D-E). The binding curves of 0 to 120 s show the association, whereas those of 120 to 300 s show the dissociation phase. The equilibrium dissociation constant k_D is shown. One representative experiment out of three is shown.

4.2.4 Lignosulfonates inhibit transmission and subsequent infection by cell-associated HIV

HIV is capable of inducing syncytia ('giant cells') formation between HIV-infected and uninfected CD4⁺ T cells. We simulated this process in a co-cultivation assay by mixing persistently HIV-infected and uninfected CD4⁺ T cells. Three lignosulfonates (LA13, LA14, and LA20) strongly and dose-dependently inhibited giant cell formation by two HIV-1 strains (IC_{50} : 0.1-0.3 μ M) (Table 4.6, SFigure 4.2). They were approximately ten times more active than LA^{low} (IC_{50} : 1.4-2.5 μ M). LA04 was not able to inhibit this giant cell formation process (IC_{50} : > 111 μ M) and LA02 was weakly active (IC_{50} : 3.9-5.6 μ M). The observed IC_{50} s were somewhat higher against HIV-1 NL4.3 than against HIV-1 IIIB.

Table 4.6 Lignosulfonates inhibit the HIV-induced formation of giant cells

	IC ₅₀ (μM) ^a	
	HIV-1 NL4.3	HIV-1 IIB
LA02	5.6 ± 0.4	3.9 ± 1.1
LA04	> 111.1	> 111.1
LA13	0.3 ± 0.01	0.2 ± 0.02
LA14	0.2 ± 0.01	0.1 ± 0.01
LA20	0.3 ± 0.02	0.2 ± 0.02
LA ^{low}	2.5 ± 0.2	1.4 ± 0.1

^aCompound concentration needed to reduce virus-induced giant cell formation with 50%. Giant cell formation of HIV-1 NL4.3 and IIB was evaluated. Mean ± SEM of three independent experiments is shown.

Cells that express DC-SIGN, *e.g.* immature dendritic cells, bind pathogens and present them to T cells to evoke an appropriate immune response. Viruses like HIV exploit this receptor to facilitate access to and infection of target T cells. We simulated this capture by DC-SIGN⁺ cells and the subsequent transmission to CD4⁺ T cells in two separate assays. In the virus capture assay, only LA13 and LA14 inhibited DC-SIGN-mediated HIV capture, as indicated in Figure 4.6 This inhibition was dose-dependent although not that potent, since their respective IC₅₀ values were 2.0 and 2.4 μM. However, this observation is important, as LA^{low} is not able to inhibit this process (IC₅₀: > 31.0 μM). Table 4.7 and SFigure 4.3 show that all lignosulfonates inhibited the transmission of HIV-1 presented by DC-SIGN⁺ cells to CD4⁺ T cells. LA13, LA14, and LA20 had the highest inhibitory activity, which was ~10-fold more potent compared to LA^{low}. LA02 and LA04 had the lowest HIV-1 transmission inhibition potential, which is in agreement with the other results, as presented above. Taken together, the lignosulfonates also inhibit transmission of cell-associated virus. This is beneficial since it prevents further spread of infection in the case viral transmission has already occurred. To conclude, a topical application of these compounds lies in the prevention of viral transmission and of further spread to neighboring cells after an established infection.

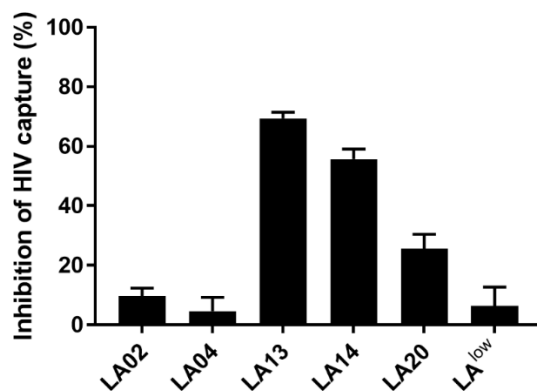


Figure 4.6 Lignosulfonates inhibit DC-SIGN-mediated capture of HIV-1 to CD4⁺ target cells. DC-SIGN⁺ Raji cells were infected with HIV-1 HE for 2 hours in the presence of lignosulfonates. All lignosulfonates were tested at 250 µg/ml (LA02: 39.7 µM, LA04: 277.8 µM, LA13: 4.3 µM, LA14: 3.0 µM, LA20: 4.3 µM, LA^{low}: 31.3 µM). Viral binding percentage was determined using HIV-1 p24 Ag ELISA. Mean ± SEM of two independent experiments is shown.

Table 4.7 Lignosulfonates inhibit DC-SIGN-mediated capture and transmission of HIV-1 to CD4⁺ target cells

	IC ₅₀ (µM) ^a	
	Capture	Transmission
LA02	> 40.0	1.6 ± 0.7
LA04	> 278.0	35.8 ± 18.1
LA13	2.01 ± 1.2	0.04 ± 0.006
LA14	2.4 ± 1.7	0.02 ± 0.002
LA20	> 4.3	0.03 ± 0.007
LA ^{low}	> 31.0	0.3 ± 0.06

^aCompound concentration needed to reduce DC-SIGN-mediated capture or transmission of HIV-1 by 50%. Mean ± SEM of two to three independent experiments is shown.

4.2.5 Cross-resistance of lignosulfonates against HIV entry inhibitor resistant strains

HIV-1 NL4.3 was cultured in MT-4 cells in the presence of increasing concentrations of lignosulfonates to obtain resistant strains. The commercially available LA^{low} (MW 8000 g/mol) and LA^{high} (MW 51900 g/mol) were used. The IC₅₀ of LA^{low} against LA^{low} resistant NL4.3 HIV-1 was 9.2 ± 0.7 µM, compared to 0.1 ± 0.04 µM against the wild type virus. The IC₅₀ of LA^{high} against LA^{high} resistant NL4.3 HIV-1 increased from 0.03 ± 0.01 µM to 1.7 ± 0.1 µM. This respective 90- and 60-

fold increase in IC_{50} is a clear indication of the presence of compound resistance. Subsequently, the activity of five selected lignosulfonates against these resistant viruses was evaluated. All compounds showed decreased antiviral activity, varying between 50- and 90-fold. LA02 and LA04 were completely inactive (Table 4.8, Figure 4.7A). The polyanionic entry inhibitor PRO 2000 also exerted a ~20-fold decreased antiviral activity against these resistant strains (from 0.2 ± 0.07 (wild type NL4.3 EC_{50}) to $3.7 \pm 0.3 \mu M$ (LA^{low} resistant NL4.3 EC_{50}) and $2.9 \pm 0.8 \mu M$ (LA^{high} resistant NL4.3 EC_{50})), indicating a comparable mechanism of action of this compound. The CXCR4 inhibitor AMD3100 showed no cross-resistance (< 4-fold increase in IC_{50}), which was expected since its mechanism of action is based upon an interaction with the CXCR4 receptor expressed on the cell surface instead of the virus itself.

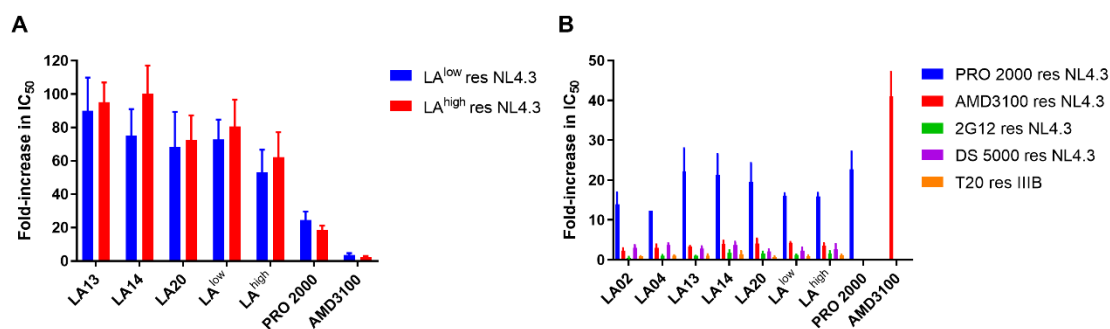


Figure 4.7 Lignosulfonates show cross resistance against HIV-1 strains that are resistant against the commercially available LA and PRO 2000. (A) Antiviral activity (IC_{50}) of lignosulfonates and control compounds PRO 2000 and AMD100 against LA-resistant HIV-1 strains was compared to their IC_{50} against the wild type HIV-1 strain. The ratio of LA02 and LA04 could not be determined as these compounds completely lost their antiviral activity. (B) Antiviral activity (IC_{50}) of lignosulfonates against HIV-1 strains resistant to various entry inhibitors was compared to IC_{50} against the wild type HIV-1 strain. The ratios of control compounds 2G12, DS 5000 and T20 is not shown since they completely lost antiviral activity against their respective resistant viral strains. Mean \pm SEM of three independent experiments is shown.

Table 4.8 Antiviral activity of lignosulfonates against LA-resistant HIV-1 NL4.3

	IC ₅₀ (μM) ^a	
	LA ^{low} res	LA ^{high} res
LA02	> 31.8	> 31.8
LA04	> 222.2	> 222.2
LA13	1.2 ± 0.2	1.3 ± 0.1
LA14	0.8 ± 0.2	0.9 ± 0.1
LA20	1.3 ± 0.2	1.2 ± 0.2
LA ^{low}	9.2 ± 0.7	9.0 ± 1.8
LA ^{high}	1.5 ± 0.1	1.7 ± 0.1
PRO 2000	3.7 ± 0.3	2.9 ± 0.8

^aCompound concentration required to inhibit HIV-1 replication by 50%. This assay was performed in MT-4 cells. Mean ± SEM of three independent experiments is shown.

The sequencing of these lignosulfonate-resistant strains shows eleven mutations that occurred in both LA^{low}- and LA^{high}-resistant NL4.3, of which seven mutations occurred in gp120 and four mutations in gp41 (Figure 4.8). Eight of these residues were also mutated in the PRO 2000-resistant HIV-1 NL4.3 which explains the observed cross-resistance. In gp120, two mutations (R116K, S160N) occurred in the V1V2 loop, three (V170N, R389T, F393I) in or adjacent to the CD4-induced epitopes, and two (N271E, Q280H) in the V3 loop (Figure 4.8A). These gp120 regions are involved in CD4 and coreceptor binding, so the mutations in these regions further support the presumed mechanism of action of lignosulfonates, *i.e.* inhibiting the binding of gp120 to the cellular HIV receptors. In gp41, all four mutations (N42D, K77Q, N126K, H132Y) occurred in or adjacent to the two heptad repeat regions (Figure 4.8B). These are involved in the formation of a hairpin structure that precedes fusion of viral and cellular membranes during the entry process. The occurrence of mutations in gp41 suggests perhaps an additional mode of action of the lignosulfonates, which was also suggested by the results obtained in the SPR experiments.

We evaluated the presence of cross-resistance against several other entry inhibitor resistant HIV-1 NL4.3 or HIV-1 IIIB strains that were obtained previously (Table 4.9, Figure 4.7B).^{233–235} When lignosulfonates were tested against 2G12 mAb- or

T20-resistant strains, the IC_{50} changed between 0.5-2.4 fold. However, the 2G12 mAb IC_{50} increased more than 100-fold, and the T20 IC_{50} more than 17-fold, against the respective resistant viruses. 2G12 mAb is a unique mAb that binds to several specific mannose residues on gp120, while T20 is a biomimetic gp41 peptide interfering with the HIV fusion process. These results indicate that lignosulfonates have an alternative mechanism of action. The lignosulfonates' IC_{50} increased between 2.1 and 5.8 fold when evaluated against the AMD3100-resistant strain. AMD3100 itself had an inhibitory activity that was more than 40-fold higher compared to the wild type virus (IC_{50} increased from 20.3 ± 3.1 nM to 911.0 ± 128.0 nM). Two HIV-1 strains that were resistant against the polyanionic entry inhibitors DS 5000 and PRO 2000 were also evaluated. The lignosulfonates' IC_{50} against DS 5000-resistant HIV-1 increased between 2.1 and 4.4-fold, while the DS 5000 IC_{50} increased 200-fold (from 0.05 ± 0.02 μ M to 10.0 ± 5.3 μ M). However, IC_{50} values increased between 11-and 24-fold when antiviral activity was tested against the PRO 2000-resistant strain. The PRO 2000 IC_{50} increased 20-fold (from 0.08 ± 0.01 μ M to 1.7 ± 0.1 μ M). Cross-resistance against PRO 2000-resistant HIV-1 could be attributed to a more comparable structure of PRO 2000 and lignosulfonates, both being sulfonated phenolic polymers, while DS 5000 is a sulfated polysaccharide.²⁷⁸

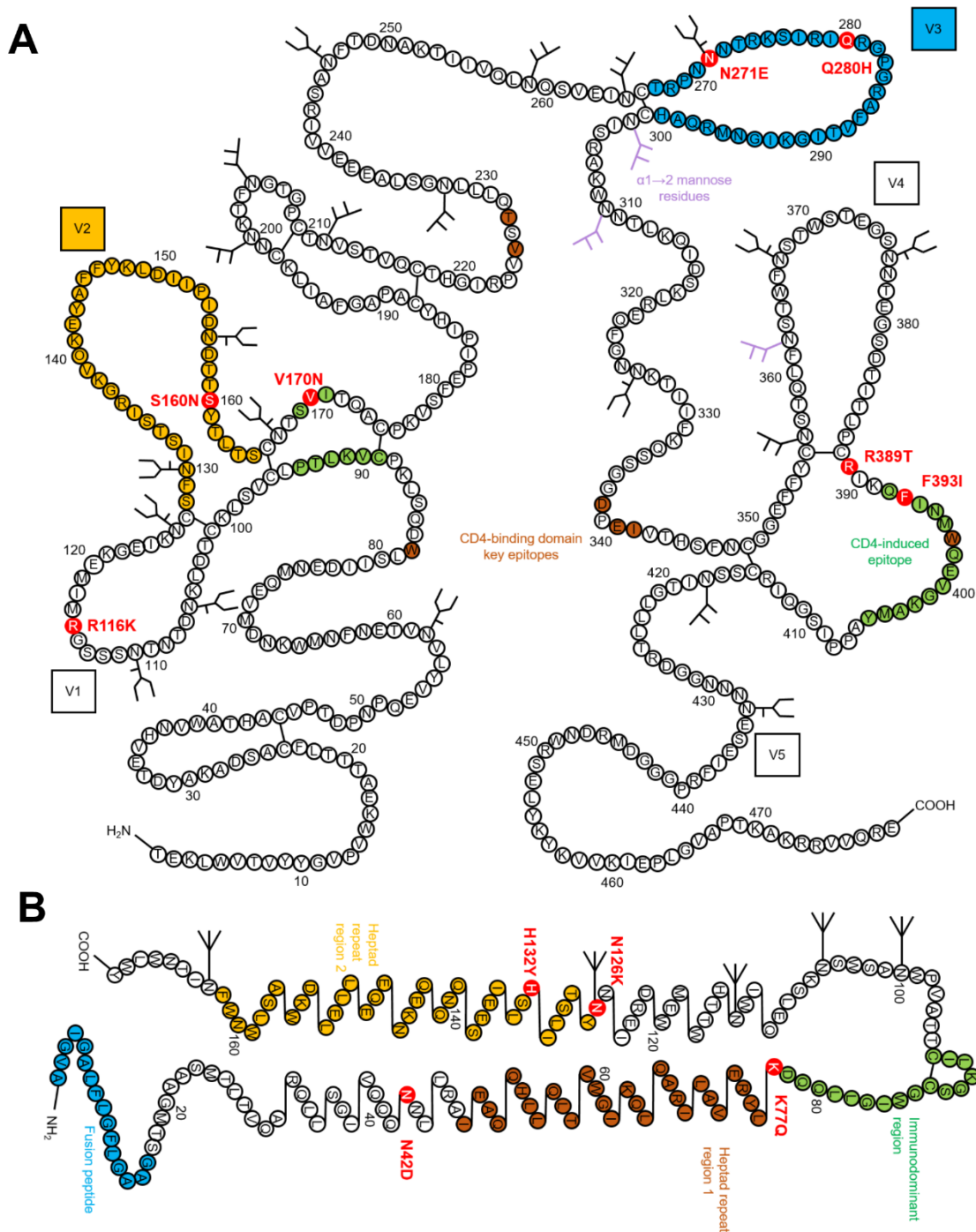


Figure 4.8 Schematics of HIV envelope glycoproteins gp120 and gp41, depicting the mutations observed in LA^{low} and LA^{high} resistant HIV-1 NL4.3. (A) HIV-1 gp120 molecule showing the mutations in the resistant strains in red. The glycosylation sites containing high mannose-type and/or hybrid-type oligosaccharide structures are indicated by the branched structures, and glycosylation sites containing complex-type oligosaccharide structures are indicated by the U-shaped branches. The variable regions (V1-V5) are marked in boxes. Epitopes that induce neutralizing antibodies are marked in color: the CD4-binding domain key epitopes (brown), the CD4-induced epitope (green), an epitope

composed of $\alpha 1 \rightarrow 2$ mannose residues (purple), the V2 loop (orange) and the V3 loop (blue). Figure 4.8A is adapted from refs 21 and 279. (B) HIV-1 gp41 molecule depicting the mutations in the resistant strains in red. Forked structures show the glycosylation positions. Important gp41 regions are marked in color: N-terminal heptad repeat region 1 (brown), C-terminal heptad repeat region 2 (orange), immunodominant region (green), fusion peptide (blue). Figure 4.8B is adapted from refs 280 and 281.

Table 4.9 Antiviral activity of selected lignosulfonates against various classes of viral entry inhibitor resistant HIV-1 strains

	IC ₅₀ (μ M) ^a				
	AMD3100-res	PRO 2000-res	2G12-res	DS 5000-res	T20-res
LA02	1.6 \pm 0.2	8.9 \pm 2.3	0.4 \pm 0.1	1.8 \pm 0.3	1.1 \pm 0.4
LA04	65.0 \pm 2.8	> 111.1	28.8 \pm 10.7	64.0 \pm 7.8	59.7 \pm 8.9
LA13	0.07 \pm 0.02	0.4 \pm 0.06	0.03 \pm 0.004	0.07 \pm 0.02	0.03 \pm 0.01
LA14	0.05 \pm 0.006	0.2 \pm 0.05	0.02 \pm 0.003	0.03 \pm 0.002	0.03 \pm 0.02
LA20	0.09 \pm 0.02	0.4 \pm 0.05	0.04 \pm 0.002	0.07 \pm 0.02	0.03 \pm 0.01
LA ^{low}	0.8 \pm 0.05	3.0 \pm 0.5	0.2 \pm 0.002	0.5 \pm 0.2	0.2 \pm 0.06
LA ^{high}	0.1 \pm 0.03	0.7 \pm 0.04	0.07 \pm 0.02	0.1 \pm 0.05	0.05 \pm 0.009

^aCompound concentration required to inhibit HIV-1 replication by 50%. All tests were performed in MT-4 cells. All resistant viruses were derived from culturing HIV-1 NL4.3 virus in MT-4 cells with increasing concentrations of the products AMD3100, PRO 2000, 2G12 mAb and DS 5000, except virus generated resistant to T20 was derived from the HIV-1 IIIB. Mean \pm SEM of three independent experiments is shown.

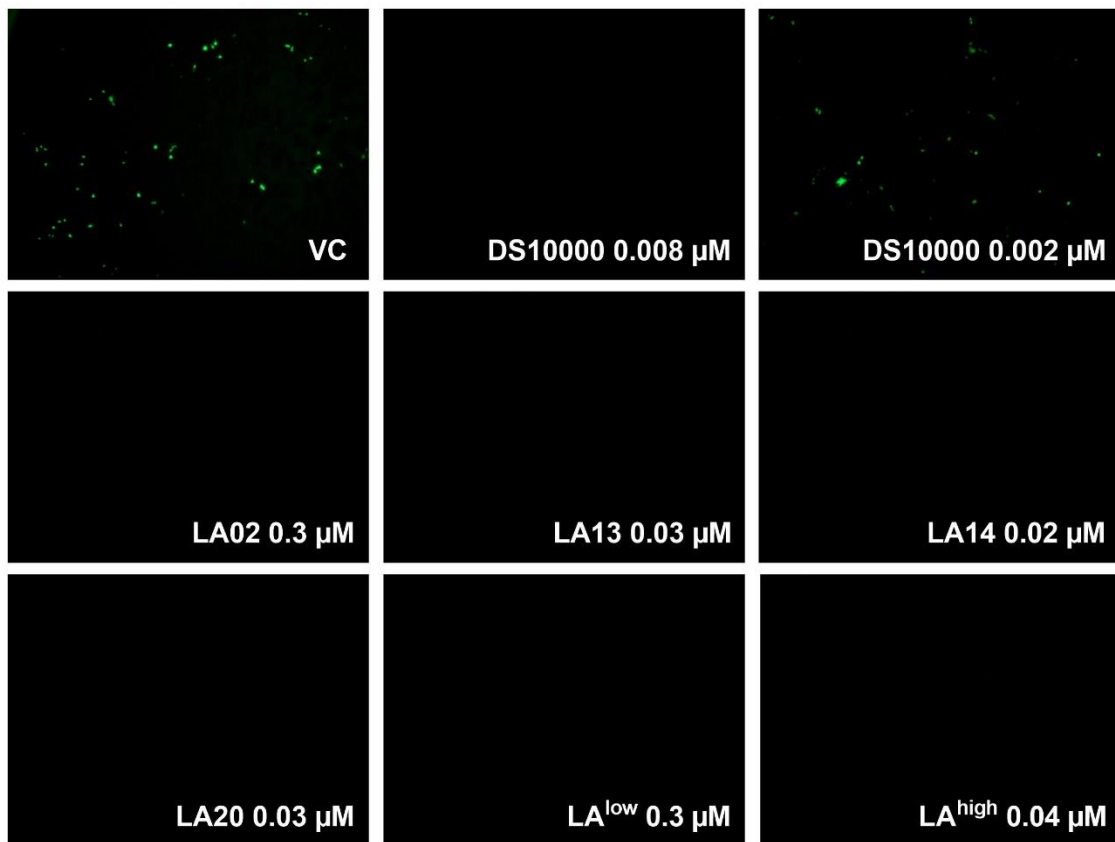
4.3 Conclusion

In this study, we identified the antiviral activity against HIV and HSV of 24 sulfonated lignin derivatives with varying properties (Table 4.1). All lignosulfonates inhibited replication of various strains of HIV-1, HIV-2, HSV-1, and HSV-2 (Table 4.2-4.5). The compounds also inhibit dual HIV-1/HSV-2 co-infection (Table 4.5). The mechanism of action of these polyanionic compounds is inhibition of glycoprotein adsorption to the susceptible target cells (Figure 4.4), through electrostatic interactions between this glycoprotein and negatively loaded lignosulfonates. This mechanism of action is supported by the finding that lignosulfonates show cross-resistance against the HIV virus strain resistant to PRO

2000, another polyanionic compound (Table 4.9 and Figure 4.7B). In SPR experiments, binding between HIV gp120 and the lignosulfonates was shown (Figure 4.5A and 4.5D), further supporting the proposed mechanism of action. The lignosulfonates with the highest antiviral activity (LA14, LA20 and LA13) have the highest MW and the highest affinity for gp120 binding. Importantly, SPR experiments and viral resistance experiments also suggest an important interaction between the lignosulfonates and the HIV glycoprotein gp41 (Figure 4.5B and 4.5E and Figure 4.8). Lignosulfonates are known to interact with proteins through hydrogen bonding, dipole-dipole, charge-charge, and hydrophobic interactions, further supporting the mechanism of action.^{265,282} Lignosulfonates also inhibit HIV-1 pseudovirus with a VSV envelope, which is positively charged as well, showing that these interactions are not limited to HIV glycoproteins alone.²⁸³ This decrease in VSVG HIV-1 pseudovirus production by sulfated polymers has been observed previously.^{284,285}

Together with its low cost, non-toxicity, and inhibition of dual HIV/HSV infection these are all good properties for the application of lignosulfonates as microbicide.

4.4 Supplementary figures



SFigure 4.1 Lignosulfonates inhibit the production of VSVG-HIV-1 pseudovirus. Adhered HeLa cells were incubated in the absence or presence of lignosulfonates or DS 10000 and subsequently transduced with VSVG-HIV-1 pseudovirus. Viral infection was quantified microscopically, 48 hours after transduction. Pictures show the GFP signal, which is proportional to pseudovirus production. Lignosulfonates still inhibited pseudovirus production at their lowest concentration tested (2 $\mu\text{g}/\text{ml}$), which is shown. Pictures were taken with an EVOS FL imaging system from TFS.

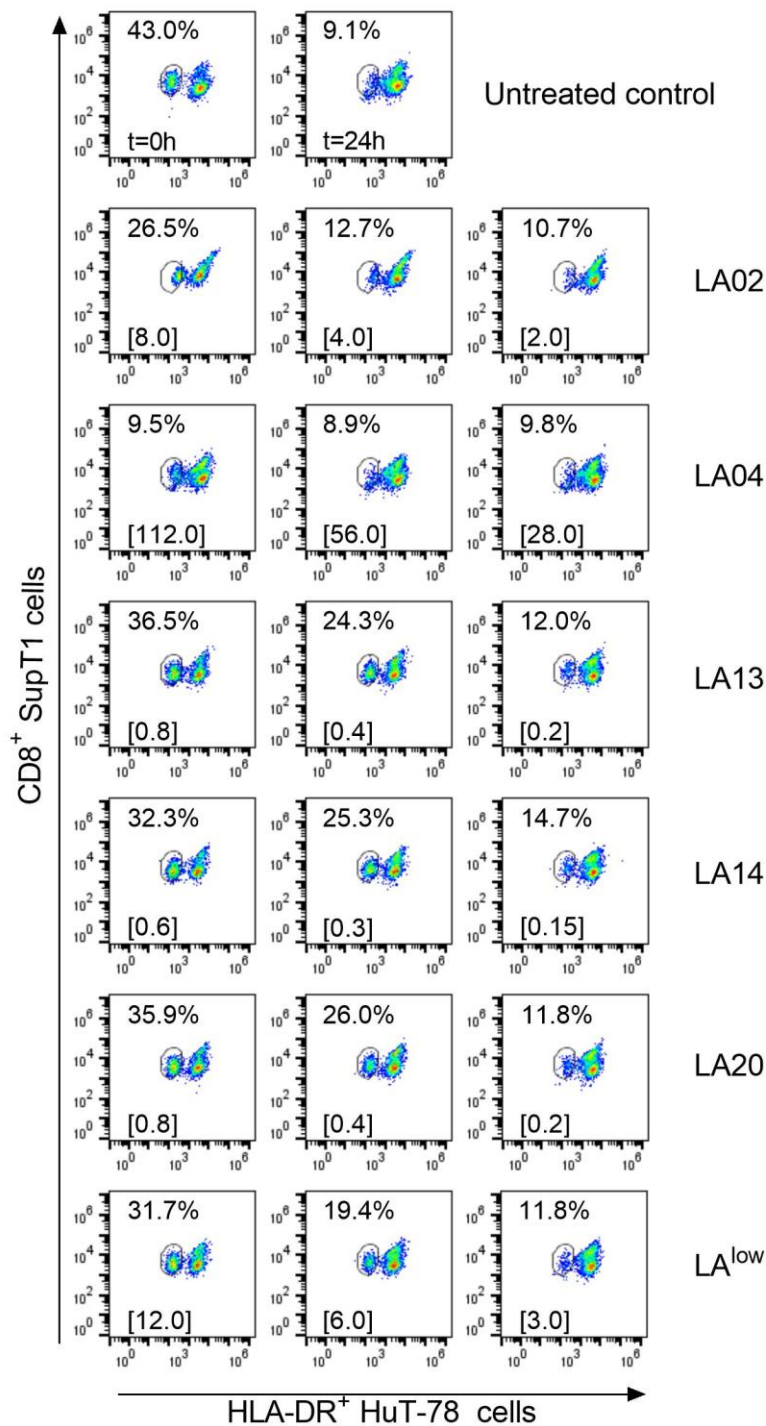


Figure 4.2 Lignosulfonates dose-dependently inhibit the HIV-induced formation of giant cells. Persistently HIV-1 NL4.3 infected Hut-78 cells were mixed with uninfected SupT1 cells in the presence of different concentrations of lignosulfonates. After 24 hours, formation of giant cells was scored first light-microscopically and then evaluated with flow cytometry by determining the percentage of remaining SupT1 cells. The plots show this flow cytometric analysis. The percentage of CD8⁺ SupT1 cells is given at 0 or 24 hours post infection, or after treatment with various concentrations of lignosulfonates, which are mentioned

between square brackets (μM). This percentage was used to determine the percentage of viral inhibition and subsequently the IC_{50} . One representative experiment out of three is shown, and the assay was also repeated with persistently HIV-1 IIB infected HuT-78 cells.

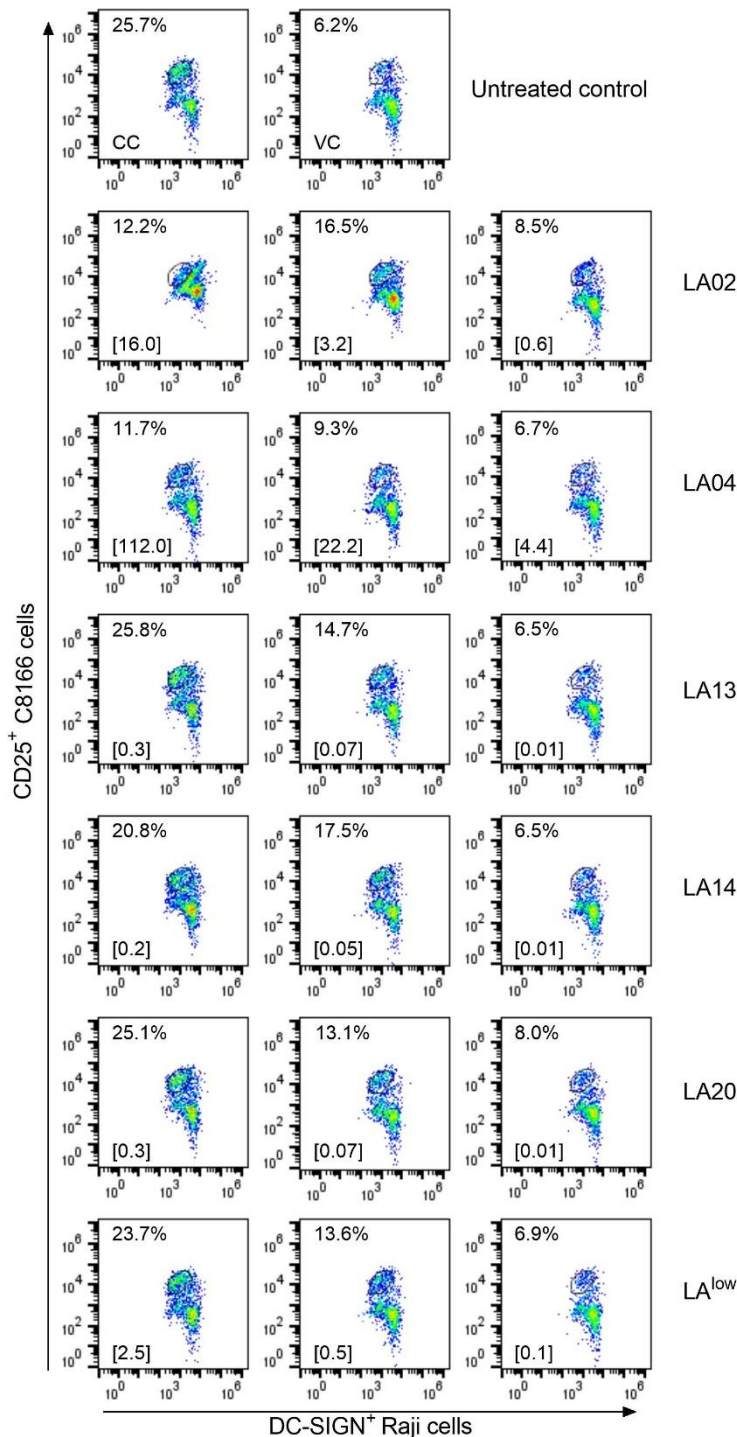


Figure 4.3 Lignosulfonates dose-dependently inhibit DC-SIGN-mediated transmission of HIV-1 to CD_4^+ target cells. Raji^{DC-SIGN} cells were infected with HIV-1 HE for 2 hours and mixed with CD_4^+ C8166 cells in the presence of various

concentrations of lignosulfonates. Inhibition of viral reproduction was determined visually and through flow cytometry. The plots show the flow cytometric analysis of the transmission assay. The percentage of CD25⁺ C8166 cells is given when they are mixed with uninfected (CC) or infected (VC) Raji^{DC-SIGN} cells, and after treatment with various concentrations of lignosulfonates. This percentage was used to determine the percentage of viral inhibition and subsequently the IC₅₀. One representative experiment out of four is shown.

Chapter 5

Labyrinthopeptin A1 inhibits dengue and Zika virus infection by interfering with the viral phospholipid membrane

This chapter is in preparation for publication.

Labyrinthopeptin A1 inhibits dengue and Zika virus infection by interfering with the viral phospholipid membrane.

Oeyen, M., Meyen, E., Noppen, S., Claes, S., Vermeire, K., Süßmuth, R.D., Schols, D. (2020)

5.1 Introduction

Lantibiotics, or lanthionine-containing antibiotics, are an interesting class of antimicrobial compounds. These small peptides (19-38 aa), produced by bacteria such as staphylococci, lactobacilli and actinomycetes, are ribosomally synthesized followed by posttranslational modification. Lantibiotics contain the noncanonical amino acid lanthionine, which allows the formation of covalent bridges and subsequent internal ring formation. This confers lantibiotics conformational stability, and their unique structure and function.^{286,287} Lantibiotics are subdivided in several classes, based on their biosynthetic pathways.²⁸⁸ For example, Class III lantibiotics are post-translationally modified by LabKC, a protein kinase-cyclase that catalyzes phosphorylations, dehydrations and cyclizations.^{289,290}

Lantibiotics were first known for their antimicrobial biological function against competing bacteria, either by inducing membrane pore formation, or by inhibiting enzymes. The producing bacteria have a specific immunity mechanism against their own lantibiotic.²⁸⁷ The most prominent lantibiotic is nisin, which has been exploited extensively over the last 50 years as an antimicrobial food preservative²⁹¹ (Figure 5.1A). Nisin binds to lipid II, a precursor molecule of bacterial cell walls, which induces pore formation and inhibits further peptidoglycan synthesis. Following the successful commercialization of nisin, research efforts have led to the discovery and development of other lantibiotics applications, such as probiotics, prophylactics, additives, and therapeutics²⁸⁸.

Labyrinthopeptins are class III lantibiotics produced by the actinomycete *Actinomadura namibiensis*.²⁹² They contain the unusual carbacyclic triamino acid labionin, a structural variation of lanthionine.^{289,290,293} Furthermore, they consist of two peptides connected by a disulfide bond. Each peptide contains two ring structures formed by a methylene group and thioether bridge between labionin residues. Three natural variants exist: Labyrinthopeptin A1, A2, and A3 (Figure 5.1B-C).²⁸⁹ Unlike the majority of lantibiotics, labyrinthopeptins do not exert antimicrobial activity. Instead, Labyrinthopeptin A2 (Laby A2, Figure 5.1B) possesses pain relieving activity in an *in vivo* model of spinal nerve injury.²⁸⁹

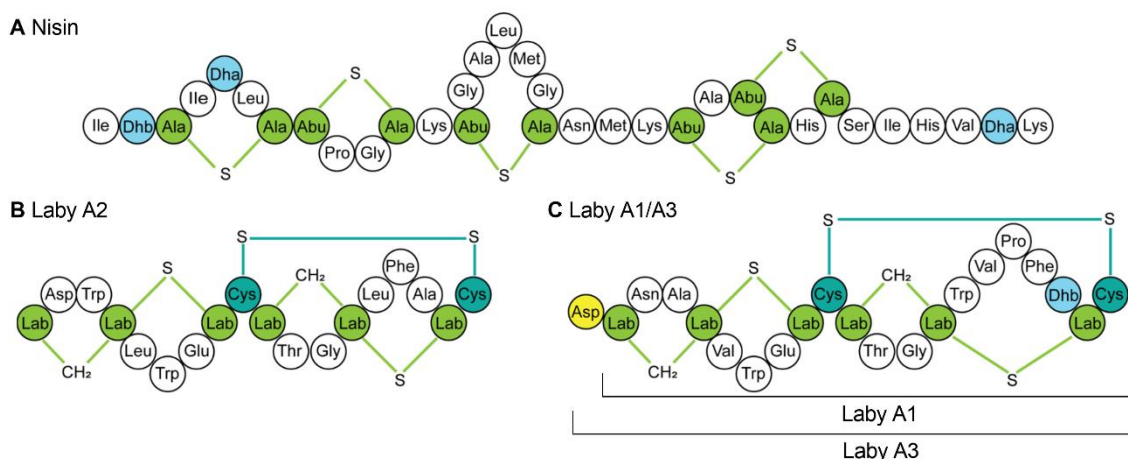


Figure 5.1 Schematic structures of various lantibiotics. (A) Nisin, (B) Laby A2, (C) Laby A1/A3. Abu: aminobutyric acid; DHA: dehydroalanine; DHB: dehydrobutyrine; Ala-S-Ala: lanthionine; Abu-S-Ala: β -methylanthionine; Lab: labionine. Adapted from ref 289.

Furthermore, our research group demonstrated the potential of labyrinthopeptins as a novel class of antiviral molecules. Labyrinthopeptin A1 (Laby A1, Figure 5.1C) showed broad and potent antiviral activity against HIV and HSV.¹²⁷ Using time-of-drug addition experiments we determined that Laby A1 interacts with an initial step in the viral life cycle, by inhibiting entry into target cells. SPR interaction studies showed that Laby A1 interacts with the HIV envelope protein gp120. Because of this interesting antiviral activity and the low cytotoxicity, we were interested in the potential of Laby A1 as a broad-spectrum antiviral agent against emerging viruses such as ZIKV. Recently, the broad anti-DENV and anti-ZIKV activity of Laby A1 (and to a lesser extent Laby A2) was demonstrated.¹²⁵ We also demonstrated binding of labyrinthopeptins to envelope phospholipids and the concomitant induction of pore formation in the viral membrane as their antiviral mechanism of action. Finally, it has also been recently demonstrated that Laby A1 and Laby A2 potently inhibit RSV entry by interacting with the envelope phospholipids (IC_{50} : 0.39 μ M and 4.97 μ M, respectively).¹²⁶

In this study, we aim to further decipher this antiviral activity against ZIKV and DENV. Resolving its precise mechanism of action in detail is also pivotal to decide whether Laby A1 has potential as a broad-acting antiviral entry inhibitor.

5.2 Results and discussion

5.2.1 Broad-spectrum antiviral activity of Labyrinthopeptin A1 against ZIKV and DENV

5.2.1.1 Screening assay demonstrates anti-ZIKV and anti-DENV activity of labyrinthopeptins

In an initial antiviral screening assay using Vero cells the antiviral activity of labyrinthopeptins was determined against DENV (DENV-2 NGC) and ZIKV (MR766, IBH 30656, PRV ABC59, and FLR) laboratory strains. These strains were selected because they cause severe CPE in this cellular screening assay. Antiviral activity was determined by quantification of cell viability after 4 days using MTS/PES. Laby A1 consistently inhibited all virus strains with IC_{50} s in the low micromolar range ($0.51 \pm 0.06 \mu\text{M}$ against ZIKV IBH 30656 to $0.99 \pm 0.1 \mu\text{M}$ against ZIKV MR766) (Figure 5.2A), while Laby A2 was almost ten times less active ($3.7 \pm 0.4 \mu\text{M}$ against IBH 30656 to $8.1 \pm 0.3 \mu\text{M}$ against ZIKV FLR) (Figure 5.2B). As a positive control, we used the well-described lantibiotic duramycin (IC_{50} : $0.02 \pm 0.009 \mu\text{M}$ against ZIKV IBH 30656 to $0.2 \pm 0.05 \mu\text{M}$ against DENV-2 NGC, Figure 5.2C).¹⁷¹ In contrast, nisin, a lantibiotic used as a food preservative, did not show any antiviral activity against DENV or ZIKV at the highest concentration tested (0.7 mM, data not shown). All compounds were tested at non-toxic concentrations, as explained below. We performed all follow-up experiments with the most potent inhibitor, Laby A1.

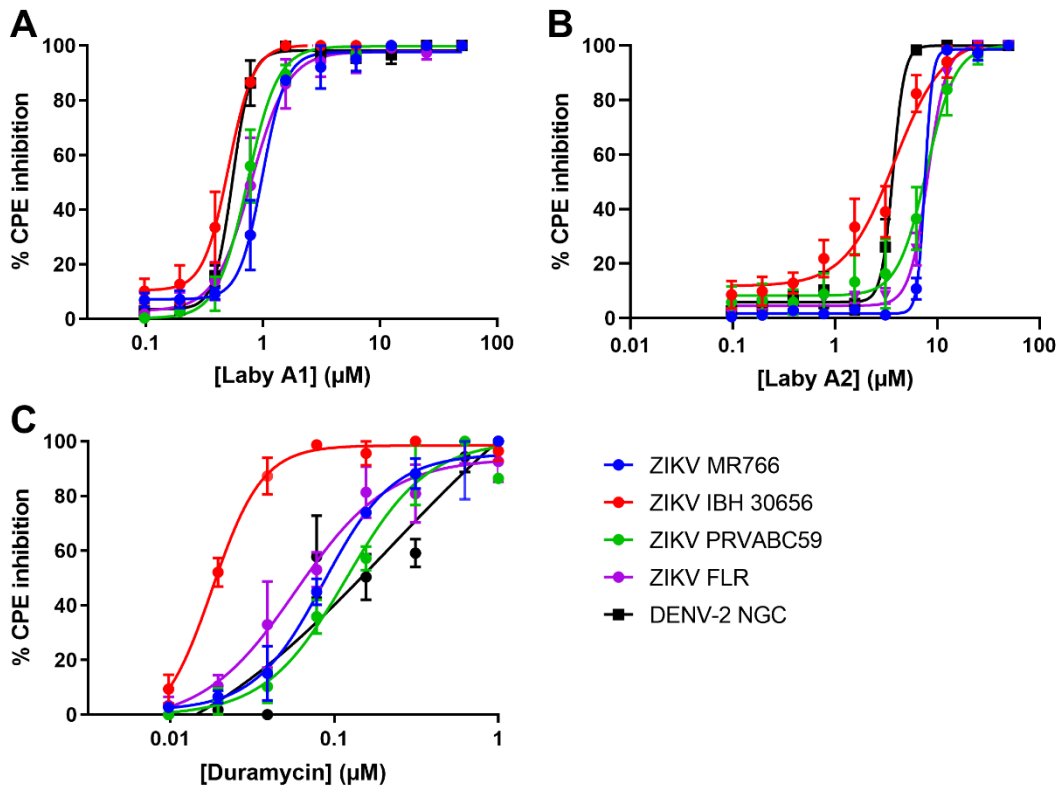


Figure 5.2 Antiviral activity profiles of lantibiotics against DENV-2 and various ZIKV strains. Vero cells were treated with various concentrations of (A) Laby A1, (B) Laby A2 or (C) duramycin and infected with DENV-2 or one of four ZIKV strains (MOI 1). After 4 days, inhibition of virus-induced CPE was quantified using the MTS/PES method. Every experiment was performed in triplicate. Mean \pm SEM of 3 independent experiments is shown.

The cellular toxicity of Laby A1 was determined in all cell lines that were used in our experiments. CC_{50} s ranged between $95.3 \pm 10 \mu\text{M}$ in U87 cells and $133.5 \pm 6.3 \mu\text{M}$ in A549 cells. Laby A1 was more toxic in the Raji L-SIGN and Raji DC-SIGN cell lines ($43.7 \pm 4.6 \mu\text{M}$ and $21.5 \pm 5.5 \mu\text{M}$, respectively) (Figure 5.3A). This higher cytotoxicity was also observed in the wild type Raji cell line (data not shown). To determine if Laby A1 exerted a more general toxicity towards B lymphocyte cell lines, we also tested its cytotoxicity in RPMI 1788 cells. However, in this cell line no cytotoxicity was observed at $100 \mu\text{M}$ (data not shown). To further assess the long-term *in vitro* cytotoxicity of Laby A1, we cultured A549 cells for several passages in the continuous presence of the peptide at $10 \mu\text{M}$, the concentration ~ 10 times higher than its IC_{50} value. Cell viability when being exposed to Laby A1 remains constant during 10 passages, in contrast to when being cultured in the presence of $1 \mu\text{M}$ duramycin (Figure 5.3B). Dose-dependent cytotoxicity was also

determined in Vero cells (Figure 5.3C). Duramycin (CC_{50} : $1.1 \pm 0.1 \mu\text{M}$) showed a >100-fold increased cytotoxicity compared to Laby A1 (CC_{50} : $124.6 \pm 3.1 \mu\text{M}$).

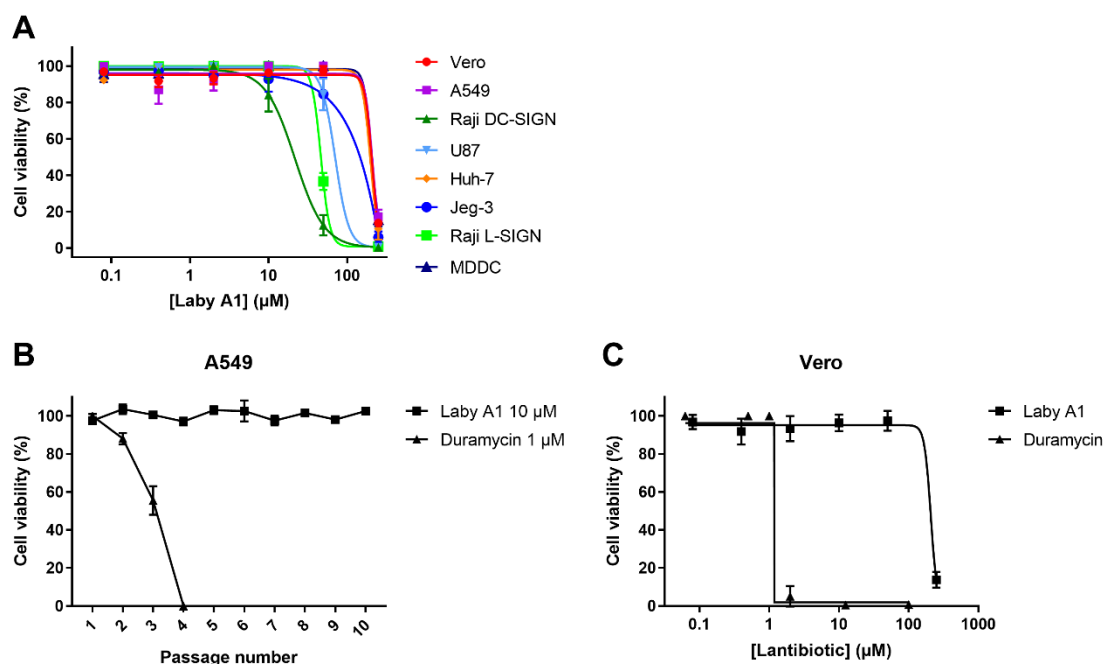


Figure 5.3 Cellular toxicity of Laby A1 and duramycin. (A) Cell viability after treatment with various concentrations of Laby A1 was examined in several cell lines and MDDC using the MTS/PES assay. Mean \pm SEM out of 3-4 independent experiments is shown. (B) Evaluation of long-term cytotoxicity pressure of Laby A1 and duramycin in A549 cells. A549 cells were passaged in the presence or absence of Laby A1 (10 μM) or duramycin (1 μM). Cell viability was determined using acridine orange staining and a Luna-FL cell counter (Logos Biosystems, Anyang, South Korea). The number of viable cells in lantibiotic-treated samples was quantified relative to the number of cells in vehicle-treated control cells. The experiment was performed once and every passage was performed in duplicate. (C) Dose-dependent cytotoxicity of Laby A1 and duramycin in Vero cells, determined using the MTS/PES assay. Mean \pm SEM of 3 independent experiments is shown.

Despite the more potent antiviral activity of duramycin compared to Laby A1, the latter has a more favorable selectivity index (SI) (Table 5.1). This means that Laby A1 is in theory more effective and safe than duramycin, displaying a larger therapeutic window between antiviral activity and cytotoxicity.

Table 5.1 Laby A1 has a more favorable selectivity index than duramycin

	Laby A1	Duramycin
CC_{50} (μM)^a	124.6 ± 3.1	1.1 ± 0.1

	IC ₅₀ ^b (μM)	SI ^c	IC ₅₀ ^b (μM)	SI ^c
ZIKV				
MR766	0.99 ± 0.1	126	0.09 ± 0.007	13
IBH 30656	0.51 ± 0.06	245	0.02 ± 0.003	61
PRVABC59	0.74 ± 0.12	169	0.12 ± 0.006	9
FLR	0.80 ± 0.18	156	0.06 ± 0.02	19
DENV-2	0.55 ± 0.02	227	0.22 ± 0.05	4.9

^aCompound concentration required to inhibit Vero cell viability by 50%. Values are obtained from the experiments performed in Figure 5.3. ^bCompound concentration required to inhibit viral replication by 50%. Values are obtained from the experiments performed in Figure 5.2. ^cSelectivity index (SI) was calculated by dividing CC₅₀ obtained in Vero cells by IC₅₀ obtained against each virus in Vero cells.

5.2.1.2 Laby A1 exerts broad antiviral activity against other enveloped viruses

To assess the broad antiviral activity of Laby A1, the peptide was tested against several other (un)related viruses (Table 5.2). Our results indicate that Laby A1 has a broad antiviral activity. However, the peptide is not active against the evaluated non-enveloped viruses, and lacks activity against certain enveloped viruses (*i.e.* parainfluenza virus, Sindbis virus, influenza and corona viruses).

Table 5.2 Antiviral activity of Laby A1 against a selection of enveloped and non-enveloped viruses

Viral strain	Virus family	Budding from	IC ₅₀ (μM) ^e
Non-enveloped viruses			
Orthoreovirus 1 ^a	<i>Reoviridae</i>	n/a	> 50
Coxsackievirus B4 ^a	<i>Picornaviridae</i>	n/a	> 50
Adenovirus 5 ^b	<i>Adenoviridae</i>	n/a	> 25
Enveloped viruses			
Influenza A virus ^c	<i>Orthomyxoviridae</i>	Plasma membrane	> 20
Influenza B virus ^c	<i>Orthomyxoviridae</i>	Plasma membrane	> 20
Parainfluenza virus 3 ^a	<i>Paramyxoviridae</i>	Plasma membrane	> 50
Punta Toro virus ^a	<i>Phenuiviridae</i>	Golgi complex	5.6 ± 1.1
HIV-1 ^c	<i>Retroviridae</i>	Plasma membrane	1.7

HIV-2 ^c	<i>Retroviridae</i>	Plasma membrane	1.9
HSV-1 ^c	<i>Herpesviridae</i>	Golgi complex	0.6
HSV-2 ^c	<i>Herpesviridae</i>	Golgi complex	0.3
HCMV ^b	<i>Herpesviridae</i>	Golgi complex	1.3
Coronavirus ^a	<i>Coronaviridae</i>	ER/Golgi complex	> 50
SARS-CoV-2 ^d	<i>Coronaviridae</i>	ER/Golgi complex	> 50
RSV A ^a	<i>Pneumoviridae</i>	Plasma membrane	0.5 ± 0.1
RSV B ^a	<i>Pneumoviridae</i>	Plasma membrane	0.4 ± 0.1
Sindbis virus ^a	<i>Togaviridae</i>	Plasma membrane	> 50
CHIKV ^b	<i>Togaviridae</i>	Plasma membrane	2.2
YFV ^a	<i>Flaviviridae</i>	ER	1.6 ± 0.3
TBEV ^b	<i>Flaviviridae</i>	ER	24.1
WNV ^b	<i>Flaviviridae</i>	ER	0.2
HCV ^b	<i>Flaviviridae</i>	ER	1.1

n/a: not applicable

^aAntiviral activity was evaluated by determining virus-induced CPE in the presence or absence of Laby A1 in Vero or HeLa cells. Mean ± SEM of 3-4 independent experiments is shown. ^bThese data are obtained from Prochnow *et al.*¹²⁵ ^cThese data are obtained from Féirir *et al.*¹²⁷ See these references for methods. ^dAntiviral activity was evaluated by determining emission of fluorescence by EGFP reporter Vero cells in the absence or presence of Laby A1. ^eCompound concentration required to inhibit viral replication by 50%.

5.2.1.3 Laby A1 prevents the production of viral progeny

We further investigated if Laby A1 decreases the infectivity of viral progeny. We used the supernatant of Laby A1-treated or untreated Vero cells to infect BHK-21 cells, followed by determination of viral titer using a plaque assay. Laby A1 inhibits the replication of infectious virus in a dose-dependent way, as shown in Figure 5.4. The IC₅₀ value of Laby A1 was 0.8 ± 0.2 μM for DENV-2 and 0.9 ± 0.01 μM for ZIKV MR766, which is in line with our other results (Figure 5.2A).

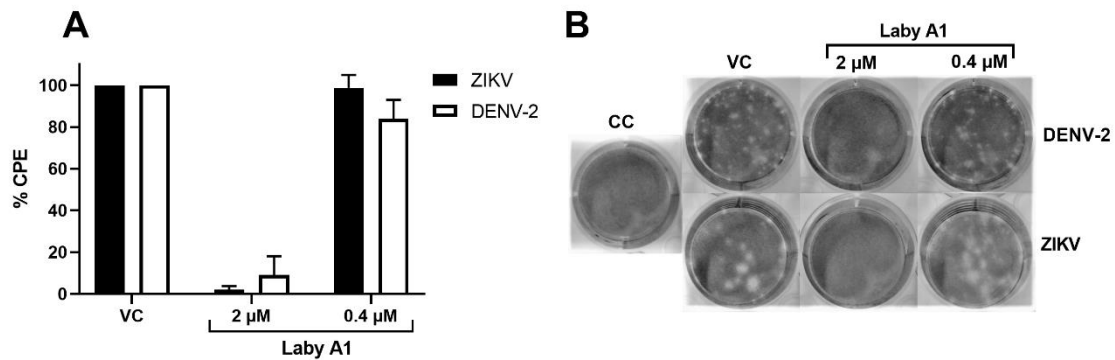


Figure 5.4 Laby A1 inhibits the production of infectious viral progeny. BHK-21 cells were incubated with supernatant from Vero cells, which were infected with DENV-2 or ZIKV MR766 (MOI 1) in the absence or presence of Laby A1 (0.4 or 2 μ M). The formation of viral plaques was quantified 4 days after infection. (A) The number of plaques was compared between treated and untreated infected cells. Each experiment was carried out in triplicate, and mean \pm SEM of 3 independent experiments is shown. (B) Plaque formation from one representative experiment is shown (only one well of each condition is shown).

5.2.1.4 Laby A1 inhibits DENV and ZIKV in biologically relevant target cell lines

Because of our specific interest in ZIKV and DENV, we performed some additional experiments to further determine whether the antiviral activity against these viruses is a cell type-dependent effect. First, we evaluated the production of viral envelope after treatment with Laby A1 in several cell lines (Figure 5.5A, B). We selected the cell lines Vero and A549 because they express the phosphatidylserine receptors TIM-1 and AXL, and chose Raji DC-SIGN cells because they express the DC-SIGN receptor. All these receptors are involved in DENV as well as ZIKV infection, and Flavivirus infection in these cell lines has been extensively studied by our and several other research groups.^{222,294,295} On top of these, we chose additional cell lines that are biologically relevant for either DENV or ZIKV infection. More specifically, liver cells are an important target during DENV infection, so antiviral activity of Laby A1 was evaluated in the hepatoma cell line Huh-7 and in Raji cells expressing L-SIGN.^{62,63} This DC-SIGN-related receptor is normally expressed on liver endothelial cells, and these cell lines have been used before to study DENV infection.^{93,296} The potency against ZIKV was further evaluated in U87 cells and Jeg-3 cells, cell lines in which ZIKV infection has been previously studied.^{297,298} They represent brain and placental tissue, respectively, which are described to be

relevant target tissues of ZIKV.^{68,71}

Cells were infected with DENV-2 or ZIKV MR766 in the absence or presence of Laby A1. After 4-6 days, intracellular viral envelope antigen was quantified by flow cytometry analysis using DENV or ZIKV-specific envelope antibodies. In all evaluated cell lines, Laby A1 exerted dose-dependent antiviral activity. Differences were rather small, but Laby A1 was most potent (IC_{50} : $0.8 \pm 0.1 \mu\text{M}$) in Vero cells and less potent (IC_{50} : $1.7 \pm 0.4 \mu\text{M}$) in Huh-7 cells when evaluated against DENV-2 replication (Figure 5.5A). When evaluated against ZIKV MR766, the IC_{50} ranged between $0.5 \pm 0.1 \mu\text{M}$ in U87 cells and $2.5 \pm 1.1 \mu\text{M}$ in Jeg-3 cells (Figure 5.5B).

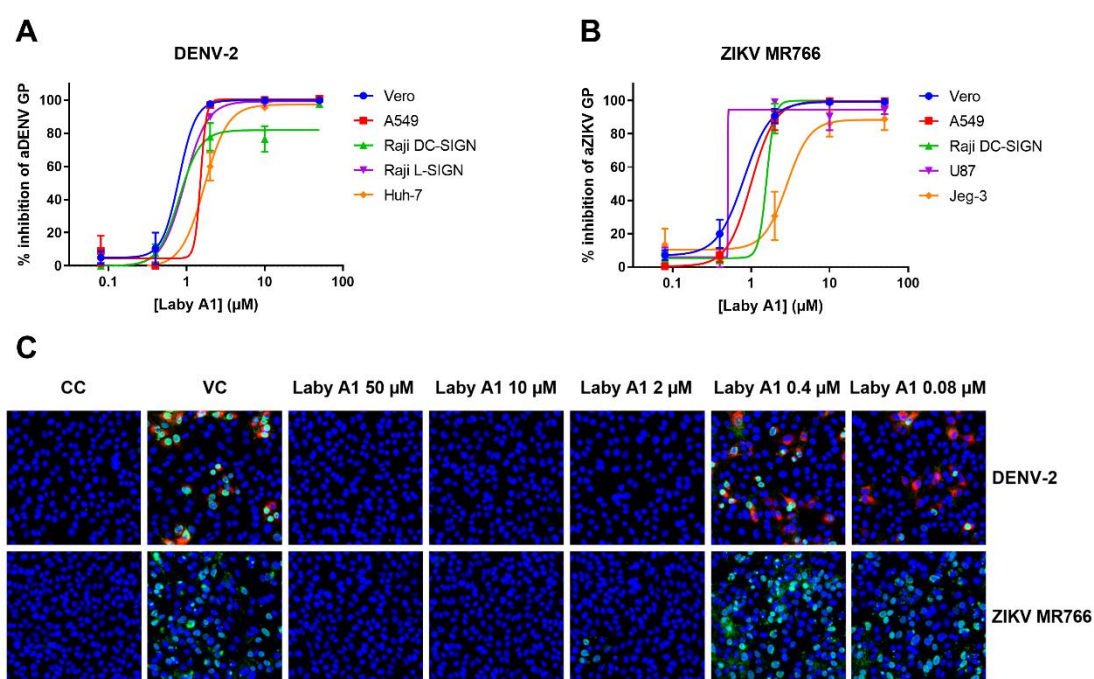


Figure 5.5 Laby A1 inhibits the production of viral antigens. (A,B) Different cell lines were treated with various concentrations of Laby A1 and infected with (A) DENV-2 or (B) ZIKV MR766. All cell lines were infected with MOI 1, except for U87 (MOI 10). Unbound virus was removed and after 4 (Vero, A549, Huh-7, Jeg-3), 5 (Raji) or 6 (U87) days an intracellular staining was performed to quantify the viral envelope antigen, using flow cytometry. DENV envelope antigen was detected using DENV envelope antibody (clone 3H5), while the ZIKV envelope was detected using ZIKV envelope antibody. Mean \pm SEM of 3 independent experiments is shown. (C) Vero cells were grown to confluency and treated with various concentrations of Laby A1 prior to infection with DENV-2 NGC or ZIKV MR766 at MOI 1. Cells were fixed and viral protein expression was visualized (DENV-2 E (red) and DENV-2 NS3 (green) and Flavivirus 4G2 (green)). Nuclei were stained with Hoechst (blue). Pictures were taken with an EVOS FL imaging system from TFS. Results from one representative experiment are shown.

This antiviral activity against DENV-2 NGC and ZIKV MR766 was also confirmed with immunofluorescence using antibodies directed against the viral envelope and/or nonstructural proteins (Figure 5.5C).

5.2.1.5 Laby A1 inhibits various DENV serotypes and ZIKV strains in primary human dendritic cells

Antigen-presenting cells in the skin represent an early target encountered by flaviviruses and other arboviruses in the human body. Hence, we evaluated the antiviral activity profile of Laby A1 in these cells using primary human MDDC, as these are a widely used model for dendritic cell studies.^{299,300} Previous studies have demonstrated that DENV and ZIKV replicate well in these cells.^{66,124} To determine if Laby A1 has serotype-dependent antiviral activity, cells were infected with one of four DENV serotypes for 48 hours and viral reproduction was quantified through RT-qPCR (Figure 5.6A). We also infected MDDC with two ancestral (MR766 and IBH 30656) and two contemporal (PRVABC59 and FLR) ZIKV strains (Figure 5.6B). Our data indicate that Laby A1 exerts a broad-spectrum dose-dependent antiviral activity against all four DENV serotypes and several ZIKV strains in MDDC.

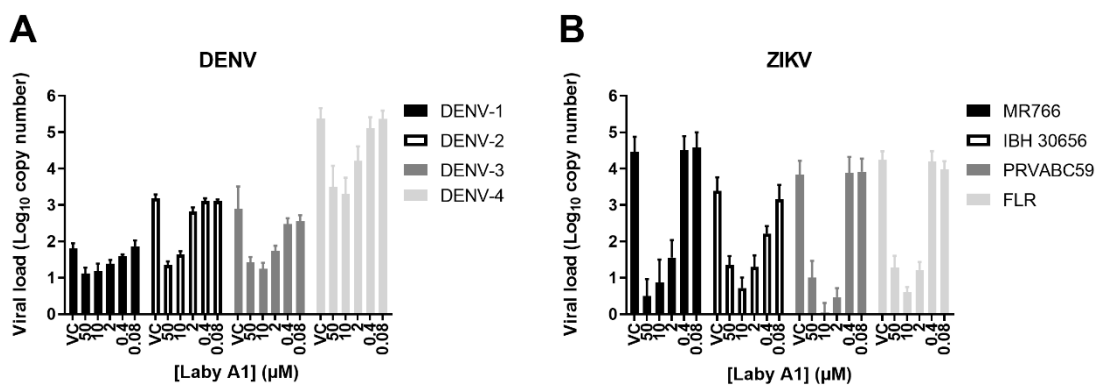


Figure 5.6 Laby A1 inhibits replication of 4 DENV serotypes and 4 ZIKV strains in MDDC. MDDC were treated with various concentrations of Laby A1 prior to infection with different DENV serotypes (A) or ZIKV strains (B). Unbound virus was removed and after 2 days the viral copy number was determined using RT-qPCR. Mean \pm SEM of 3 independent experiments performed on 6 different blood donors is shown.

5.2.2 Analysis of ZIKV-induced cytokines and chemokines in the absence or presence of Laby A1.

DENV infection has been associated with the release of pro-inflammatory mediators such as IFN- γ and TNF- α , which contribute to the pathophysiology of vascular leakage.³⁰¹ Our lab has previously demonstrated that Laby A1 decreases this DENV-induced cytokine/chemokine release in MDDC.³⁰² ZIKV-induced pathology is not associated with vascular leakage, but its effect on various cytokines/chemokines in dendritic cells, which are an important ZIKV replication site, has only been studied to a limited extent.⁶⁶ Therefore, we evaluated the consequences of MDDC infection with 4 different ZIKV strains on a panel of 27 cytokines and chemokines in the absence or presence of Laby A1 (Figure 5.7). In general, ZIKV did not strongly influence the secretion of most cytokines/chemokines, which is in line with the work of Bowen *et al.*⁶⁶ Also other studies examining immune responses following ZIKV infection did not report enhancement of cytokine/chemokine release *e.g.* IFN- β or TNF- α .³⁰⁰ The contemporary FLR strain induced most pronounced changes, followed by the ancestral reference strain MLR766. The most notable increase in secretion was observed for CXCL10 (IP-10). This ZIKV-induced CXCL10 increase in MDDC was also observed in other studies of Bowen and Österlund.^{66,303} Moreover, CXCL10 secretion has been associated with ZIKV infection in other tissues as well. This increase probably contributes to the ZIKV-associated neuronal damage.^{304,305} Importantly, Laby A1 decreased this ZIKV-induced CXCL10 secretion in all strains.

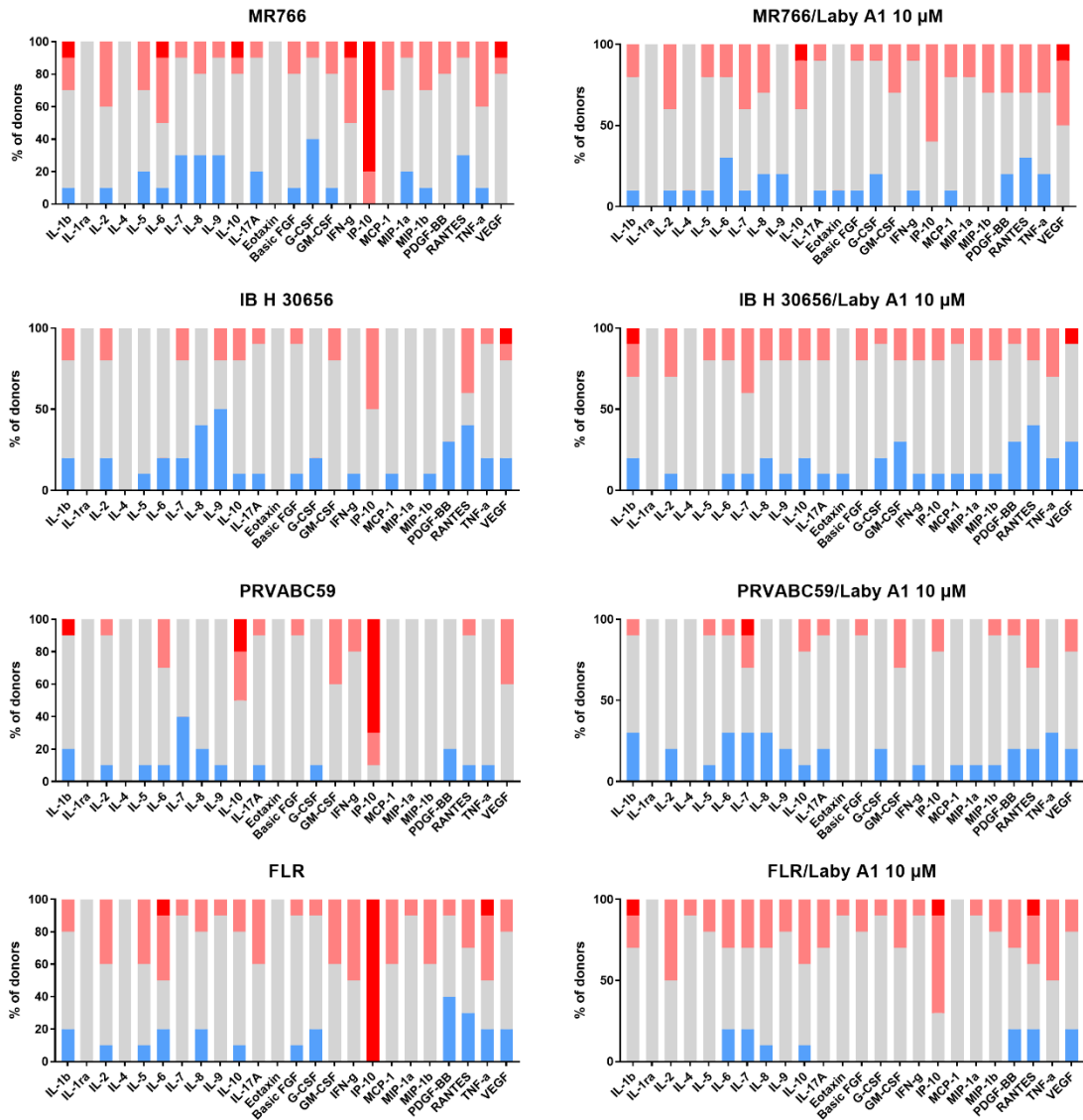


Figure 5.7 Analysis of ZIKV-induced cytokine and chemokine release in MDDC in the absence or presence of Laby A1. MDDC were infected with one of the four ZIKV strains in the absence (left graphs) or presence (right graphs) of 10 μ M Laby A1. 48 hours after infection, the profile of 27 cytokines/chemokines was determined in supernatant by means of a multiplex fluorescent microsphere immunoassay. The fold-increase values of the cytokine/chemokine concentrations in both Laby A1-treated and untreated infected MDDC compared to the concentrations in untreated uninfected MDDC are shown. The experiment was performed on MDDC isolated from buffy coats of 10 healthy blood donors, and two duplicates of every condition were included. The fold-increase values are divided into 4 subgroups which are indicated with different colors. The total fold-increase for each cytokine/chemokine is shown as percentage of the total number of donors.

5.2.3 Mechanism of action of Laby A1

5.2.3.1 Laby A1 interferes with DENV and ZIKV entry in target cells

To determine at which stage of the viral life cycle Laby A1 exerts its antiviral activity, we performed a time-of-drug addition assay. Vero cells were infected with DENV-2 or ZIKV MR766 and incubated with Laby A1 at several time points before, during, or after infection. After one replication cycle (ca. 24h), viral RNA was quantified. Results show that Laby A1 exerts antiviral activity when added prior to or at the same time of virus addition (time points -2 and 0), but was not efficacious anymore when added after DENV or ZIKV infection (time points 2-12 hpi) (Figure 5.8). These results suggest that Laby A1 interferes with viral entry processes.

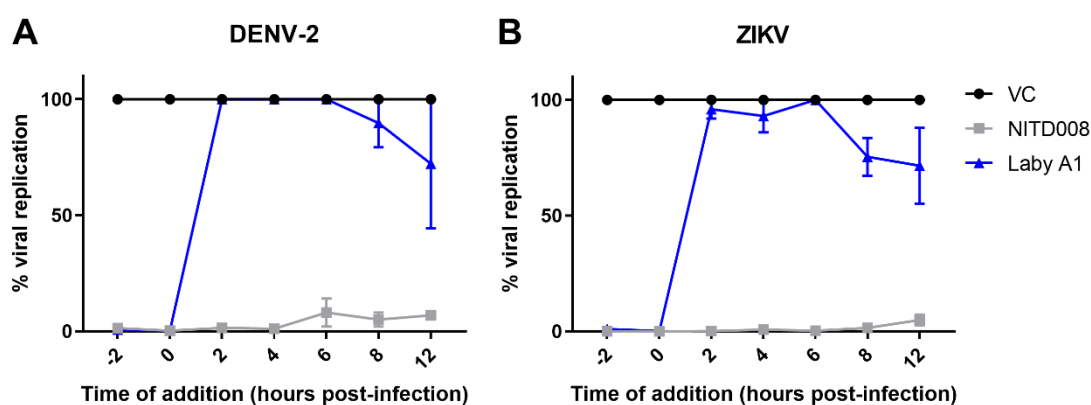


Figure 5.8 Laby A1 interferes with the early stages of the DENV-2 and ZIKV MR766 replication cycle. Vero cells were treated with Laby A1 (5 μ M) or NITD008 (10 μ M) at several time points before, at the same time of, or after infection with DENV-2 NGC (A) or ZIKV MR766 (B). The amount of intracellular viral RNA was determined through RT-qPCR and normalized to the viral load of VC. The mean \pm SEM of 2-3 independent experiments is shown.

Prochnow *et al.* also performed a time-of-drug addition assay with DENV-2, albeit in Huh-7 cells. Comparable results were obtained and they further demonstrated that the antiviral activity of Laby A1 and Laby A2 against DENV-2 already starts to decline when applied as early as 10 min after infection.¹²⁵ Time-of-drug addition experiments with Laby A1 were also included in the study of F  rir *et al.* and here the compound acted as entry inhibitor of HIV infection as well.¹²⁷

5.2.3.2 Laby A1 is not active anymore when a washing step is included prior to infection

Inhibitors exerting their activity in an early phase of infection can either target a host factor involved in viral entry, or the viral particle itself. To explore the first hypothesis, we pre-incubated several cell lines with Laby A1 for 1 hour, followed by thorough washing to remove unbound peptide. Cells were subsequently infected with ZIKV MR766. After 4-6 days (depending on the cell line), virus-induced CPE was compared to cells where Laby A1 was not removed before infection. Results clearly demonstrate that an additional washing step after pre-incubation leads to loss of its antiviral activity (Figure 5.9). This suggests that Laby A1 does not exert its antiviral activity by binding to a viral entry factor. However, it cannot be excluded that there is indeed an interaction between Laby A1 and a cellular receptor, but that the virus still manages to enter the cell through interaction with another redundant entry factor present on the membrane. For example, A549 cells express various Flavivirus entry receptors such as TIM-1, AXL and heparan sulfate.

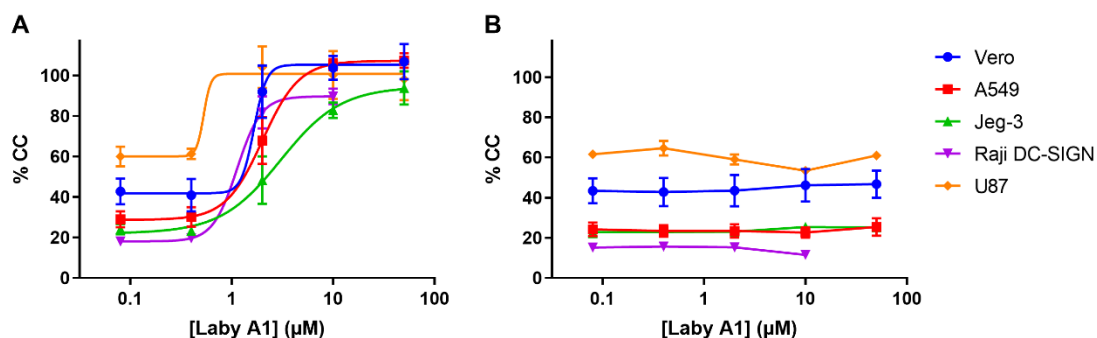


Figure 5.9 Loss of antiviral activity upon removal of Laby A1 prior to infection. Various cell lines were incubated with several concentrations of Laby A1. After 1 h, Laby A1 was (A) either kept present, or (B) replaced by assay medium. Afterwards, cells were infected with ZIKV MR766 (MOI 1) and 4 (Vero, A549, Jeg-3), 5 (Raji DC-SIGN) or 6 (U87) days later virus-induced CPE was quantified using MTS/PES. Cell viability of infected cells was compared to the uninfected cell control (% CC). Mean \pm SEM of 3 independent experiments is shown.

Comparable results were described by Prochnow *et al.*, when pre-incubation of Huh-7 with Laby A1 or Laby A2 did not protect the cells against DENV-2 infection when an additional washing step was included prior to infection.¹²⁵

5.2.3.3 Laby A1 binds selectively to the viral particle and exerts virucidal activity

To determine a possible interaction between Laby A1 and the viral particle, we pre-incubated ZIKV MR766 with Laby A1, followed by ultrafiltration centrifugation through a spin filter column with a 100 kDa size-exclusion membrane and subsequently performed a plaque assay with the concentrates to determine if this virus was still infectious. Pre-incubation with 2 μM to 50 μM Laby A1 inhibited the production of viral progeny completely, which suggests a direct interaction between the viral particle and the peptide (Figure 5.10A). This inhibition disappeared at 0.4 μM , a concentration whereby the compound is inactive in the antiviral assays as well. As a positive control, we included epigallocatechin gallate (EGCG), a ZIKV entry inhibitor demonstrated to bind to the viral envelope.¹²³ This compound also inhibited the production of viral progeny after pre-exposure to the virus followed by ultrafiltration.

A comparable assay was performed with DENV-2 by Prochnow *et al.* They obtained similar results and thus both studies demonstrate that Laby A1 interacts with a ZIKV as well as a DENV factor.

To determine if this interaction was virucidal, we pre-incubated DENV-2 or ZIKV MR766 with Laby A1 (10 μM or 1 μM) and diluted this mixture to sub-therapeutic peptide concentrations, followed by a plaque assay of these dilutions on BHK-21 cells to determine the viral titer. By diluting, any inhibition of viral plaque forming is due to a virucidal effect during pre-incubation instead of the presence of low amounts of compound in the medium. As an additional control, mixtures of virus and Laby A1 without pre-incubation were included.

When ZIKV or DENV virus was pre-incubated with 10 μM Laby A1, it was no longer able to produce infectious virus, demonstrating the virucidal capacity of Laby A1 (Figure 5.10B, C). This activity cannot be attributed to the remaining compound concentration in the medium (final concentration of 0.001 μM Laby A1 does not exert antiviral activity anymore). The virucidal activity was lost when virus was pre-incubated with only 1 μM Laby A1. As was expected, when no pre-incubation step was included, Laby A1 had no virucidal effect.

Prochnow *et al.* demonstrated the virucidal effect of labyrinthopeptins in another way.¹²⁵ They treated DENV particles with Laby followed by RNase digestion.

Treated virus led to a decrease in genome copies, which is indicative of viral lysis because an intact envelope would protect the viral genome from digestion.

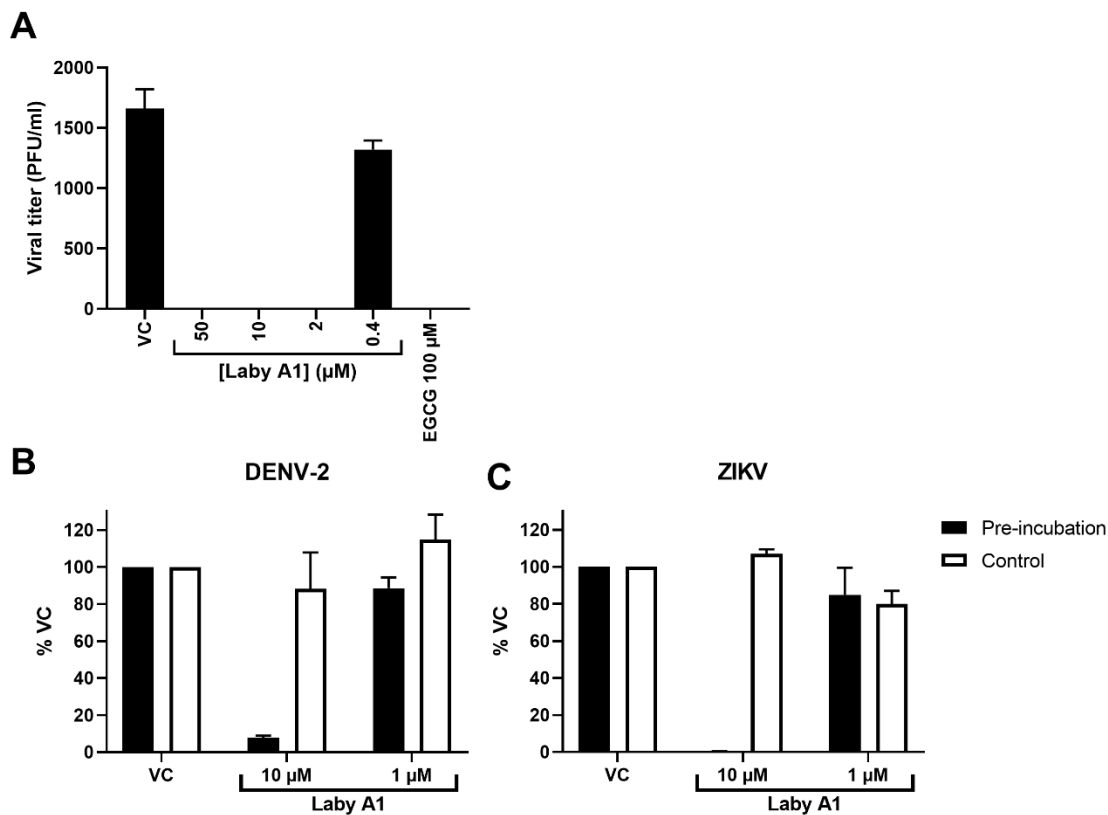


Figure 5.10 Laby A1 interacts with the viral particle and demonstrates virucidal activity. (A) Ultrafiltration assay. Laby A1 or EGCG were pre-incubated with ZIKV MR766 and passed through a 10 kDa filter membrane prior to viral titer determination in the plaque assay. Results are presented as % plaques compared to VC. Mean \pm SEM of 1 experiment performed in triplicate is shown. (B) Virucidal assay. DENV-2 NGC (B) or ZIKV MR766 (C) were pre-incubated with 10 or 1 μ M Laby A1 for 1h at 4°C followed by dilution and determination of viral titer in the plaque assay (black bars). As a control, no pre-incubation was performed and samples were immediately diluted and used in the plaque assay (white bars). Results are presented as % PFU/ml compared to VC. Mean \pm SEM of 3 independent experiments performed in triplicate is shown.

5.2.3.4 Laby A1 binds to viral envelope phospholipids

In Section 5.2.3.3 we have shown that Laby A1 interacts with the viral envelope. The viral envelope consists of virally encoded envelope proteins and host cell-derived phospholipids.¹⁸ We used SPR technology to investigate if Laby A1 interacts with one of these components.

To test the first hypothesis, recombinant DENV E protein domain III was immobilized on a chip and binding of Laby A1 was determined. However, no

significant interaction with Laby A1 concentrations up to 20 μM was observed (Figure 5.11A), in contrast to DENV 3H5 envelope mAb, which dose-dependently bound to the envelope protein (Figure 5.11B).

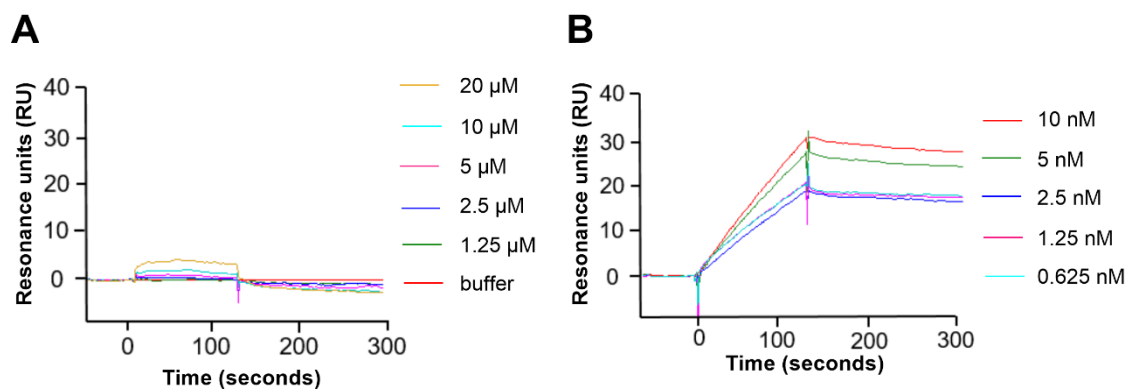


Figure 5.11 Laby A1 does not bind to DENV envelope protein. (A, B) DENV envelope domain III was coupled on a CM5 chip and interaction with Laby A1 (A) and a specific anti-DENV mAb (clone 3H5) (B) was determined.

Secondly, SPR was also used to determine an interaction between membrane phospholipids and Laby A1. Phosphatidylserine (PS), located on the inner side of the cell membrane in live cells, is flipped to the outer side during apoptosis, and is incorporated in the viral membrane during budding from the host cell (Section 1.2.3). To test this, we optimized a SPR assay with liposome immobilization and subsequently determined the interaction between these liposomes and several lantibiotics. A L1 sensor chip was chosen because lipophilic modifications are added, allowing binding to liposomes. Various liposomes (1,2-dioleoyl-sn-glycero-3-phosphoethanolamine (POPE), 1,2-dioleoyl-sn-glycero-3-phospho-L-serine (POPS) and 1,2-dioleoyl-sn-glycero-3-phosphocholine (POPC)) were prepared and captured at various concentrations on the L1 chip in the presence or absence of BSA. We selected the condition that uses 0.2 mg/ml in the presence of BSA for subsequent experiments because at that dose the highest response (resonance units) was observed.

Compounds were injected at 3-fold increasing concentrations and affinity constants (k_D) were calculated if a steady-state affinity could be obtained. Our results demonstrate that Laby A1 binds to liposomes containing POPE (k_D : $3.6 \pm 0.3 \mu\text{M}$) and POPS (k_D : $5.3 \pm 0.3 \mu\text{M}$). Duramycin only interacted with POPE (k_D :

$4.5 \pm 0.3 \mu\text{M}$). We could not calculate a steady state affinity between Laby A2 or nisin with these liposomes (Figure 5.12).

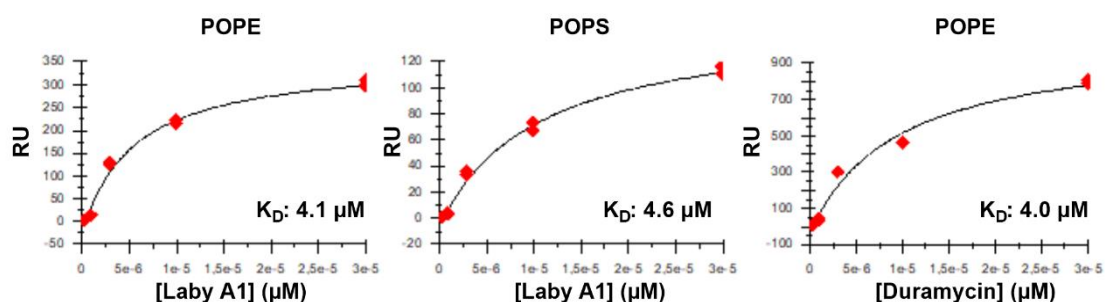


Figure 5.12 Laby A1 interacts with the phospholipids POPE and POPS. Various liposomes (0.2 mg/ml) were coupled on a L1 chip of a Biacore T200 instrument. Compounds were injected at different concentrations and binding to liposomes was detected. Results from one representative experiment are shown.

Duramycin was included in our study as a positive control because it has been demonstrated to interact with PE.³⁰⁶ In Prochnow *et al.*, interaction with phospholipids was determined by adsorbing various lipids to a surface and measuring subsequent binding with Laby A1, A2 and duramycin using a color reaction based on biotin-streptavidin binding. They observed a strong binding between Laby A1 and Laby A2 to PE-containing liposomes and a weak binding to liposomes containing PC and sphingomyelin with an ethanolamine head group. No binding with other lipids was observed (Figure 5.13). Altogether, we observe a stronger interaction between PS and Laby A1 with SPR than when the method of Prochnow *et al.* is used. Future experiments are needed to further unravel these distinct observations.

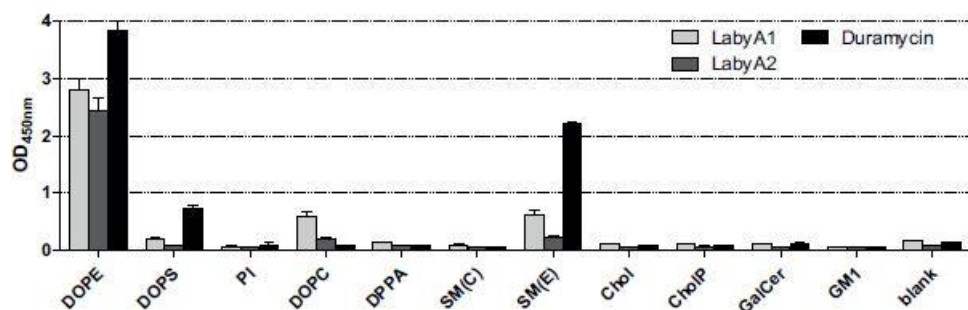


Figure 5.13 Binding of lantibiotics to lipids. Various lipids were adsorbed to a Polysorp surface and incubated with hexynoyl-labyrinthopeptins attached to biotin and duramycin-biotin. Bound compounds were detected by a streptavidin-HRP-catalyzed color reaction. Figure obtained from Prochnow *et al.*¹²⁵

5.3 Conclusion

In this chapter, we determined the broad antiviral activity of the lantibiotic Labyrinthopeptin A1. We showed that Laby A1 inhibits all DENV serotypes and various ZIKV strains with IC_{50} around 1 μ M. The structurally related Laby A2 has a ~tenfold lower activity (Figure 5.2). Furthermore, Laby A1 also inhibits other viruses from divergent families such as YFV, RSV and Punta Torovirus (Table 5.2). Previously it was already shown that it also broadly inhibits HIV and HSV.¹²⁷ It shows no activity against non-enveloped viruses. This antiviral activity is independent of the exploited cell line or the used evaluation method, and is also observed in MDDC, a physiologically relevant primary cell type (Figures 5.4-5.6). Laby A1 demonstrates low cellular toxicity and has a more favorable SI than duramycin, another lantibiotic with antiviral activity (Figure 5.3, Table 5.1).

Time-of-drug addition experiments demonstrate that Laby A1 inhibits entry of ZIKV and DENV (Figure 5.8). This activity early in the viral life cycle was also observed against HIV. We showed that Laby A1 performs its antiviral activity by interacting with a viral rather than a cellular factor, and has virucidal activity (Figures 5.9-5.10). SPR interaction studies demonstrated the mechanism of action of Laby A1: it interacts with phospholipids (*i.e.* PE and PS) present in the viral envelope.

Together with the other recent Labyrinthopeptin studies, this chapter demonstrates the activity of Laby A1 as broad antiviral entry inhibitor with a unique mechanism of action and its potential development as antiviral agent against emerging viruses.

Chapter 6

Interaction of TIM-1 with Laby A1 and its role in ZIKV entry

This chapter contains unpublished results.

6.1 Introduction

In the second part of this thesis, we focus on phosphatidylserine receptors (PSR) and their involvement in viral entry, with the scope of developing a novel class of entry inhibitors with broad antiviral activity.

TIM-1 is a meaningful entry receptor of flaviviruses and other enveloped viruses. Hamel *et al.* were the first to report its involvement in ZIKV infection.⁶⁷ In DENV infection, TIM-1 appears to be the only known receptor whose interaction with the virus not only leads to host cell attachment, but also to subsequent virus internalization.⁵³ Therefore, TIM-1 is an interesting target for the development of antiviral molecules that inhibit this process. Unfortunately, no TIM-1 inhibitors are currently available.

TIM-1 is mainly studied for its important role in T cell activation using immunological *in vitro* and *in vivo* assays.^{174–178} Another relevant physiological function of TIM-1 is phagocytosis of apoptotic cells. These functions can, however, be exploited to optimize functional assays, which are necessary to study potential TIM-1 inhibitors.

In this chapter, we first determine the consequences of TIM-1 expression on ZIKV infection. Secondly, we evaluate the effect of Laby A1 treatment on TIM-1 expression, and further determine if Laby A1 affects TIM-1 functioning. To this end, we optimize an assay that evaluates the effect of compounds on phagocytosis.

6.2 Results and discussion

6.2.1 TIM-1 expression in cell lines

We used flow cytometry to determine TIM-1 surface expression in all cell lines that have been routinely used throughout this thesis. As shown in Fig 6.1, TIM-1 receptor expression varies substantially between cell lines. A549 and Vero cells have the highest expression, followed by Jeg-3 cells and Huh-7 cells. CHO.k1, HEK293, HEK293T, U87, BHK-21, Jurkat, Raji and SupT1 cells have low TIM-1 expression. This high expression in A549 and Vero cells is according to the literature.^{67,198,307}

Of note, all evaluated cell lines showed high intracellular TIM-1 expression (results not shown). This is in agreement with the literature, which states that TIM-1 preferentially resides in large intracellular pools in the ER or Golgi apparatus.¹⁷⁰ This might also explain the small fluorescence shift in all cell lines when stained

extracellularly. Because A549 cells are human cells with high endogenous TIM-1 expression on the cell membrane, we chose this cell line for further experimentation. Because HEK293(T) and CHO.k1 cells have low endogenous TIM-1 expression and are good transfection hosts, we chose to transfect these cells with a TIM-1 construct.

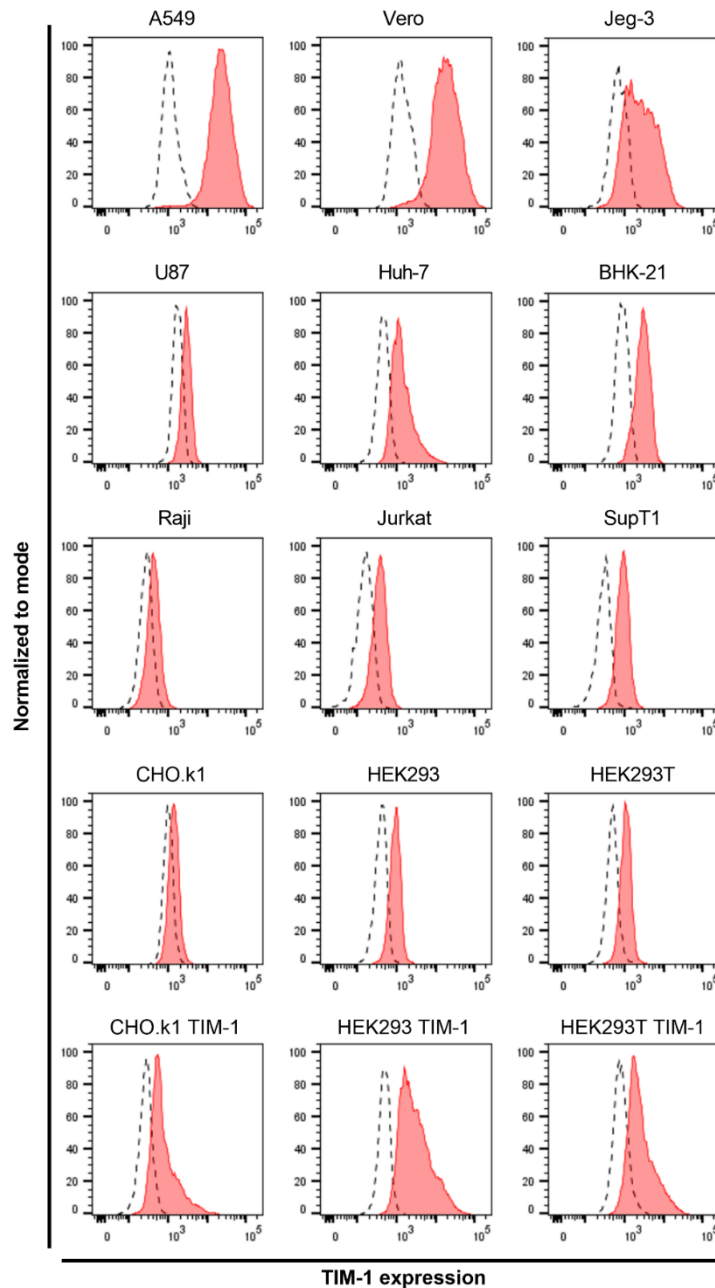


Figure 6.1 TIM-1 receptor surface expression in various cell lines. Cells were stained with IgG1-PE isotype control or TIM-1-PE. Dashed black and filled red histograms represent isotype control and TIM-1 staining, respectively. Data from one representative staining experiment are shown.

6.2.2 Importance of the cell surface receptor TIM-1 in ZIKV infection

6.2.2.1 TIM-1 expression enhances ZIKV infection

The observed interaction between Laby A1 and TIM-1 moved our interest to the potential role of this receptor in Flavivirus – and more specific in ZIKV – infection, and towards the assessment of TIM-1 as a potential antiviral target. First, we transfected human TIM-1 in HEK293 cells (*i.e.* HEK293 TIM-1) and infected them with the ZIKV reference strain MR766, to confirm the importance of TIM-1 in ZIKV entry. TIM-1 expression was confirmed by flow cytometry (Figure 6.1). As shown in Figure 6.2, although HEK293 cells are already susceptible to infection as the cell monolayer is disturbed at MOI 1, ZIKV clearly increases CPE in TIM-1-transfected cells (at MOI 0.1 and 1). Of interest, pretreatment of the cells with Laby A1 (10 μ M) inhibited this ZIKV-induced CPE.

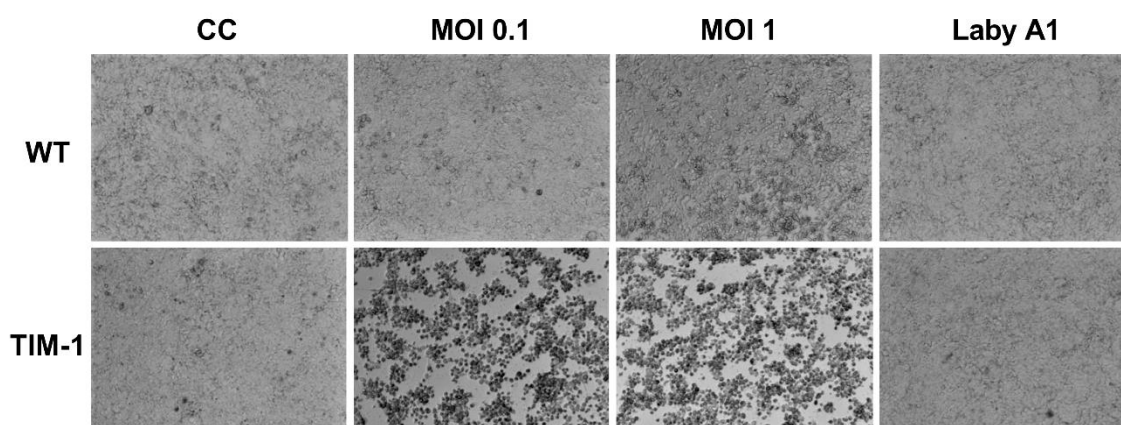


Figure 6.2 TIM-1 enhances ZIKV infection of transfected HEK293 cells. HEK293 cells with and without TIM-1 were uninfected (CC), infected with ZIKV MR766 at MOI 0.1 or MOI 1 or treated with Laby A1 (10 μ M) and infected with ZIKV MR766 at MOI 1. CPE was determined 3 days after infection. Results from one representative experiment are shown.

RT-qPCR results confirmed that transfection with TIM-1 increases viral replication and that Laby A1 completely inhibits infection (Figure 6.3A). HEK293 cells are susceptible to infection, but transfection with TIM-1 increases viral load with 4 log (MOI 0.1), 2.5 log (MOI 1) or 1.8 log (MOI 10). ZIKV replication in TIM-1-transfected cells does not increase significantly when MOI is increased, probably because cells are dying and no longer maintaining virus replication.

We also determined if Laby A1 and Laby A2 dose-dependently inhibit ZIKV

infection using MTS-PES, and obtained comparable IC_{50} values (Laby A1: 1.5 μ M; Laby A2: 10.2 μ M) as the ones reported for Vero cells in Figure 5.2 (*i.e.* 0.99 μ M and 7.6 μ M, respectively). Including an additional washing step after Laby A1 pre-incubation did not prevent infection (Figure 6.3B). This suggests that the antiviral activity of Laby A1 depends on its interaction with the viral envelope and not on its potential TIM-1 interaction. Interestingly, the MTS-PES method was not sensitive enough to determine inhibition of ZIKV by Laby A1 in WT HEK293 cells, although the virus causes some CPE in this cell line (results not shown).

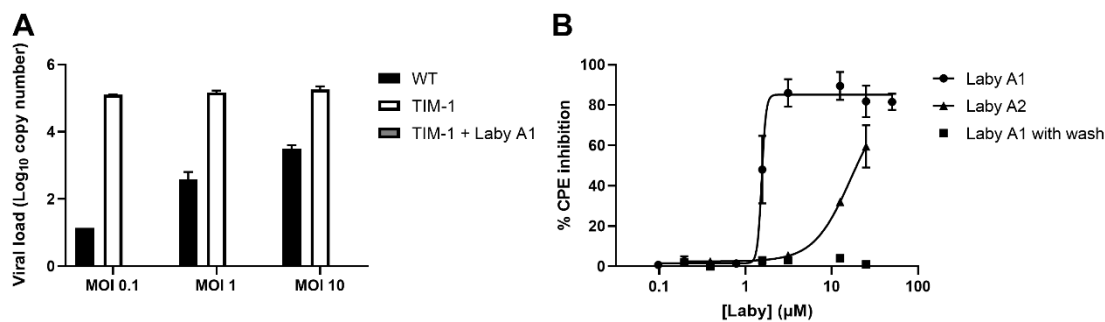


Figure 6.3 ZIKV replication is increased in TIM-1-transfected HEK293 cells and inhibited by Laby A1. HEK293 and HEK293 TIM-1 cells were seeded to confluency and infected with ZIKV MR766 (MOI 0.1, 1, and 10) for 3 days. (A) SN was lysed and viral copy number was determined using RT-qPCR. Results (Mean \pm SEM) from 2 technical replicates are shown. (B) Virus-induced CPE in HEK293 TIM-1 cells after treatment with Laby A1 or Laby A2 was determined using MTS-PES. Data are shown for infection at MOI 1. Results (Mean \pm SEM) from 3 independent experiments performed in duplicate are shown.

To facilitate comparisons with literature, we continued our experiments with HEK293T cells stably transfected with TIM-1 (*i.e.* HEK293T TIM-1). While WT cells were susceptible to infection as well, TIM-1 transfection increased replication with 3 log (MOI 0.1), 2.3 log (MOI 1) or 1.6 log (MOI 10) (Figure 6.4). Viral load did not vary substantially between different MOI in HEK293T TIM-1, as was observed in HEK293 cells as well. To validate the importance of TIM-1, we pre-incubated HEK293T TIM-1 cells with aTIM-1 Ab (10 μ g/ml). There was a decrease in viral load, albeit not significant. In the study of Meertens *et al.*, the same aTIM-1 Ab partly inhibited DENV infection in cell lines endogenously expressing TIM-1, *i.e.* Huh-7 and A549.¹⁰¹ However, in A549 cells we did not observe ZIKV infection inhibition by aTIM-1 Ab (results not shown).

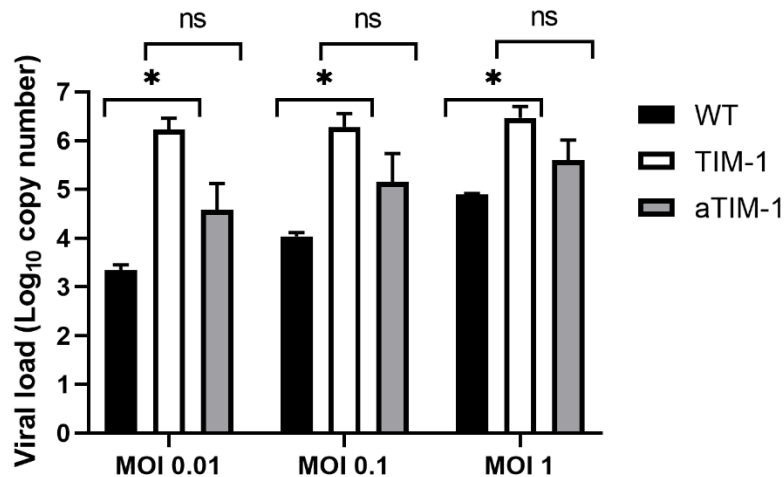


Figure 6.4 ZIKV replication is increased in TIM-1-transfected HEK293T cells and partly inhibited by aTIM-1 Ab. HEK293T and HEK293T TIM-1 cells were seeded to confluency and infected with ZIKV MR766 (MOI 0.1, 1, and 10) for 3 days. SN was lysed and viral copy number was determined using RT-qPCR. Results (mean \pm SEM) from 3 independent experiments are shown. Significance was calculated by comparing the means of two groups using a two-sample t-test; * $p < 0.05$, ns not significant.

Next, we evaluated the consequences of TIM-1 expression in a different way. We infected HEK293T or HEK293T TIM-1 cells with ZIKV MR766 (MOI 1). 24 hpi, the supernatant was used to infect BHK-21 cells in a plaque assay and viral titer was determined. Hence, we determined if TIM-1 increased the production of viral progeny, *i.e.* if there was more infectious virus after TIM-1 transfection. As shown in Figure 6.5A, TIM-1 expression increased viral titer by 17-fold, confirming that TIM-1 enhances ZIKV infection. This effect was completely inhibited when cells were pre-treated with aTIM-1 Ab, indicating the enhancing role of TIM-1.

We repeated the experiment with DENV-2, and here viral titer was increased by 9-fold after TIM-1 transfection (Figure 6.5B). This increase was inhibited with 57% when cells were pre-treated with aTIM-1 Ab.

Of note, ZIKV titer is higher than DENV-2 titer, although cells were infected at the same MOI.

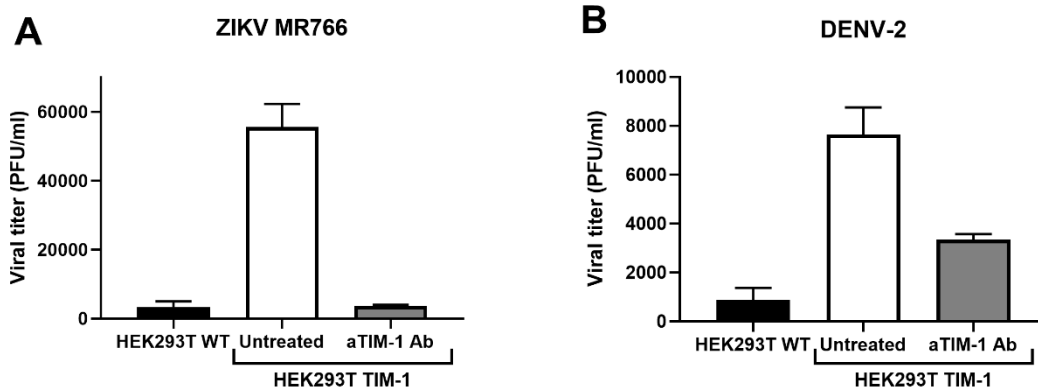


Figure 6.5 ZIKV and DENV-2 infection in HEK293T cells is enhanced by TIM-1 expression and inhibited by aTIM-1 Ab. HEK293T and HEK293T TIM-1 cells were infected after overnight growth with ZIKV MR766 (A) or DENV-2 (B) at MOI 1 for one hour. Unbound virus was then replaced by assay medium and 24 hpi viral titer in supernatant was determined using the plaque assay in BHK-21 cells. HEK293T TIM-1 cells were also pre-treated for 30 min with 10 μ g/ml aTIM-1 Ab (grey graphs). In (A), viral titer was calculated using the 10^{-3} dilution, while in (B) this was the 10^{-2} dilution. Data from 3 independent experiments performed in triplicate are shown (Mean \pm SEM).

6.2.2.2 TIM-1 surface expression is altered after ZIKV and DENV infection

As mentioned before, it has been shown that DENV and TIM-1 are co-internalized after viral binding to the receptor.⁵³ We were interested if this binding/internalization was also reflected in TIM-1 surface expression. To this end, we pre-incubated A549 cells endogenously expressing TIM-1 with ZIKV MR766 or DENV-2 for 2 or 4 hours, or for 24 hours with a washing step after 1 hour incubation at MOI 1. After extensive washing, cells were stained extracellularly with anti-TIM-1 Ab and analyzed using flow cytometry. After 2 or 4 hours incubation with either ZIKV or DENV, TIM-1 expression was decreased with \sim 30% (Figure 6.6A). This can probably be attributed to binding or internalization of the receptor. The remaining Ab binding could be explained by higher TIM-1:viral particle ratio, since cells were infected at MOI 1, *i.e.* on average one viral particle infected each cell. It would be interesting to evaluate the effect of infection with higher MOI on TIM-1 expression. Compared to short incubation, there was a remarkable difference between ZIKV and DENV 24 hpi. While TIM-1 surface expression only decreased with 22% after DENV-2 infection, it was almost completely inhibited by ZIKV (90%). Although CPE is not yet observed in A549 cells 24 hpi (Figure 6.6C), it is possible that the virus already causes structural rearrangements of the cytoskeleton and cell membrane,

changing receptor expression.

To test this, we determined the surface expression of other receptors normally present on A549 cells: the TAM receptor AXL, the chemokine receptor CXCR7, the adhesion molecule CD56, and the tyrosine kinase PTK7 (Figure 6.6B). The expression of AXL, another Flavivirus entry receptor, was inhibited with 66% after ZIKV infection, while only with 13% after DENV infection. For CD56 and PTK7, the difference between ZIKV and DENV was less clear. DENV infection had no effect on CD56 expression (5% inhibition) and inhibited PTK7 with only 24%, while ZIKV decreased CD56 expression with 35% and PTK7 with 51%. Surprisingly, the expression of CXCR7 is increased by 73% after ZIKV and by 34% after DENV infection.

We used electrical impedance to monitor changes in cell morphology after ZIKV or DENV infection in real-time. As shown in Figure 6.6D, the A549 cell index (CI) – a measure of cell number and morphology changes– starts to decrease around 24 hpi when cells are infected with ZIKV, while this only starts to decline more than 60 hpi when infected with DENV. This shows that impedance is more sensitive than morphological observation since disturbance of the monolayer could be observed as of this early time point.

We conclude that the inhibition of TIM-1 expression by ZIKV is mainly due to its higher CPE compared to DENV-2, since the expression of receptors unrelated to Flavivirus infection (CD56 and PTK7) is also altered. The more pronounced inhibition of the entry receptors TIM-1 and AXL might be due to an additional effect of receptor binding to the virus and subsequent internalization. Future experiments will have to unravel the surprising observation of CXCR7 expression.

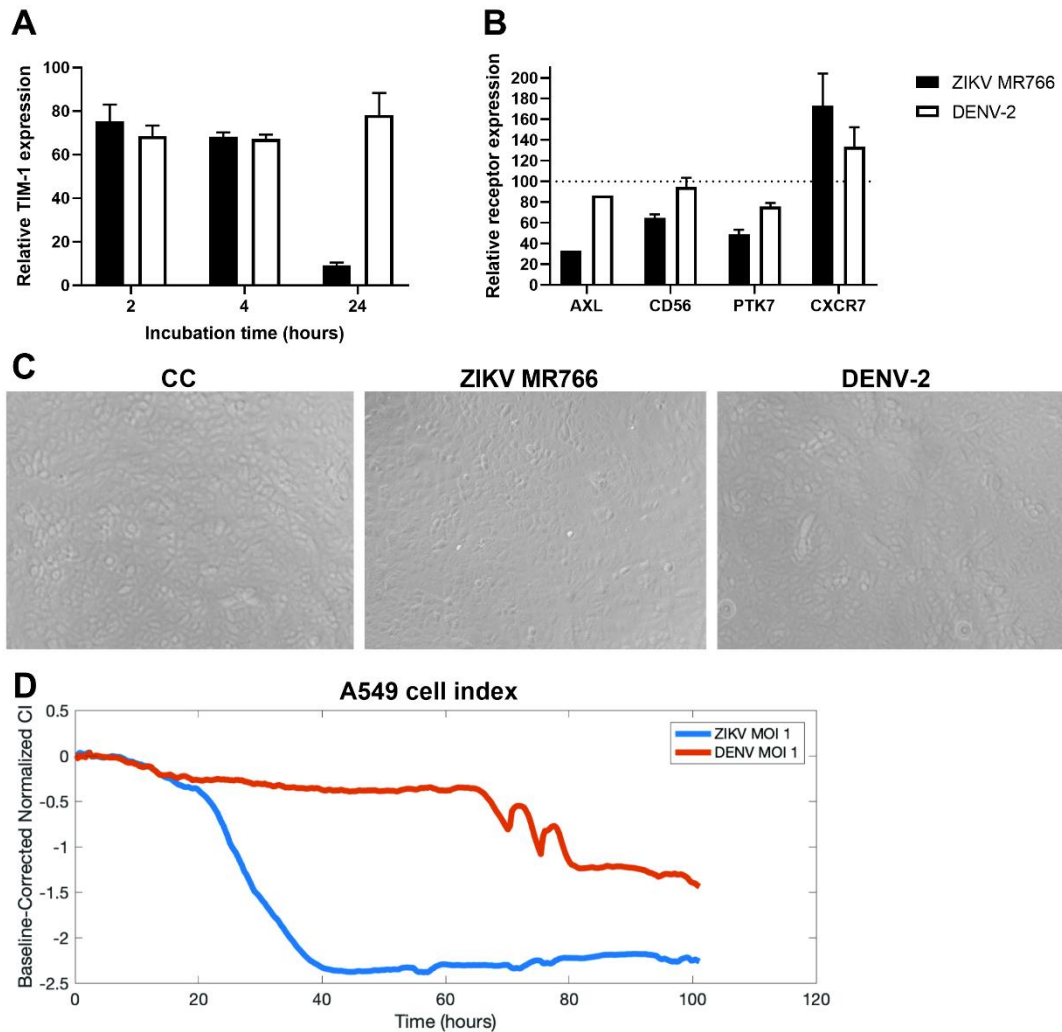


Figure 6.6 ZIKV alters surface expression of TIM-1 and various other receptors. (A, B) A549 cells were infected after overnight growth with ZIKV or DENV-2 (MOI) for 1 hour. Unbound virus was replaced by assay medium and 24 hpi cells were extracellularly stained with antibodies targeting TIM-1 (A) or various other receptors (B) and mean fluorescence intensity was determined using flow cytometry. Receptor expression level was normalized to expression in untreated cells. Mean \pm SEM of 3 independent experiments is shown. (C) CPE was determined in uninfected, ZIKV MR766-infected or DENV-2-infected A549 cells 24 hpi. (D) A549 cell number and morphology changes after ZIKV and DENV infection were observed over time using electrical impedance. The cell index was monitored using the xCELLigence system. Data are normalized compared to uninfected cell control. Data from one experiment are shown.

6.2.3 Evaluation of TIM-1 – Laby A1 interaction

6.2.3.1 Antibody binding assay suggests interaction of Laby A1 with viral entry receptor TIM-1

In the previous chapter we have studied the antiviral activity of Laby A1. To simply and quickly determine possible interactions between this peptide and potential Flavivirus entry factors, we performed an antibody binding assay by means of flow cytometry. Various cell lines expressing a variety of Flavivirus entry receptors were treated for 30 min with Laby A1 (10 μ M) and afterwards incubated with antibodies directed against these receptors. In this way, binding competition between Laby A1 and the receptor-specific antibody could be determined. We did not observe any significant decrease in antibody binding for heparan sulfate, DC-SIGN, L-SIGN, mannose receptor, AXL or CD300a when untreated and Laby A1-treated cells were compared. However, Laby A1 (10 μ M) decreased TIM-1 antibody binding with almost 50% (Figure 6.7A).

We performed some additional experiments to study this observation in more detail. A 30 min incubation of Laby A1 dose-dependently inhibited anti-TIM-1 Ab binding to cells expressing TIM-1 endogenously, *i.e.* Vero and A549 cells (Figure 6.7A and 6.7B). Furthermore, this was also observed in TIM-1-transfected HEK293 cells (Figure 6.7C). Ab binding inhibition was more pronounced when cells were treated with Laby A1 for 4 hours (Figure 6.7B-D, white bars). Longer incubation periods (8 or 24h) did not further improve the binding inhibition (evaluated in A549 and Vero cells, data not shown). Decreased antibody binding to TIM-1 was also observed for Laby A2, but not observed using duramycin, another lantibiotic with antiviral activity (data not shown).

These findings suggest that Laby A1 (and Laby A2) and the antibody compete for binding with the same TIM-1 epitope, or that TIM-1 expression decreases after Laby A1 incubation, due to internalization of the receptor. Note that when the antibody binding does not decrease, as seen for the other tested entry factors, it remains possible that Laby A1 interacts with other epitopes on the receptor that do not interfere with the binding of the tested antibody. Nevertheless, because of the clear effect of Laby A1 on TIM-1 antibody binding, we continue with TIM-1 as the receptor of interest.

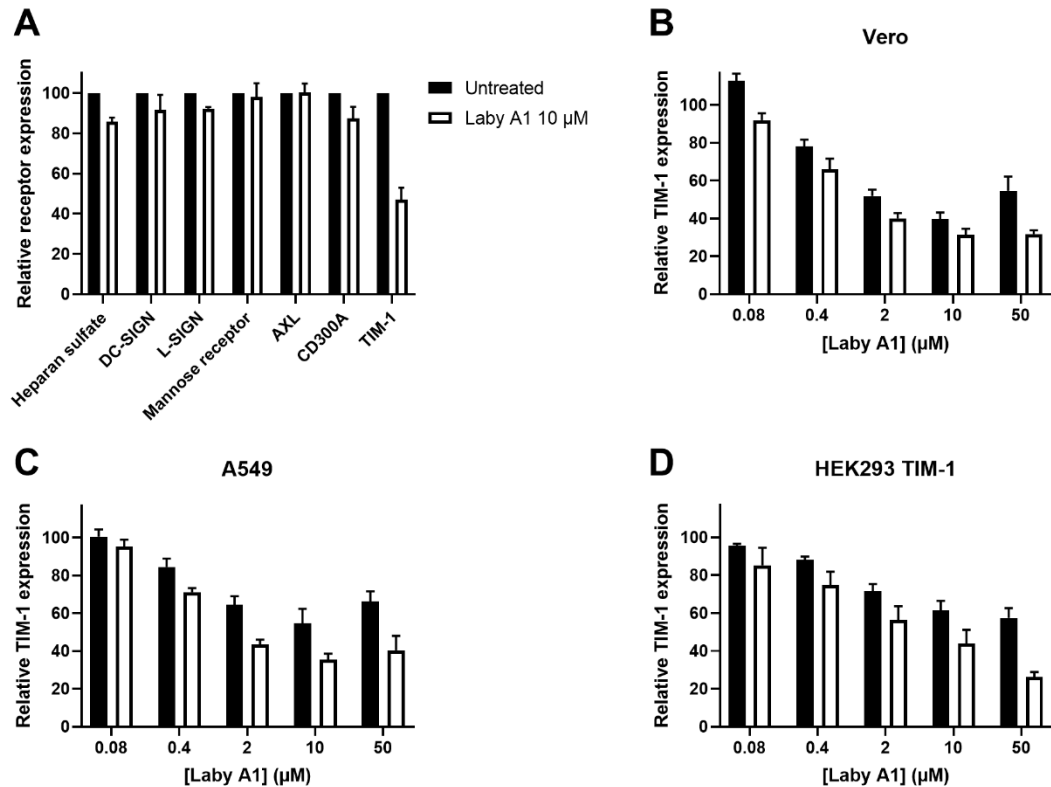


Figure 6.7 Interaction between Laby A1 and Flavivirus entry factors. (A) Selected cell lines expressing various Flavivirus entry receptors were incubated for 30 min with 10 μM Laby A1, after which receptor expression was determined with specific antibodies by flow cytometry. Relative receptor expression of untreated compared (black bars) to Laby A1-treated (white bars) cells is shown. Mean ± SEM of 3 independent experiments is shown. Vero cells were used for heparan sulfate, AXL and TIM-1 expression, Raji^{L-SIGN} cells for L-SIGN expression, and MDDC for DC-SIGN, mannose receptor and CD300a expression. (B-D) Vero (A), A549 (B) or HEK293 TIM-1 (D) cells were incubated for 30 min (black bars) or 4 hours (white bars) with various concentrations of Laby A1, after which TIM-1 Ab binding was determined by flow cytometry. Mean ± SEM of 3 independent experiments is shown.

We performed additional experiments in order to further elucidate the potential interaction between TIM-1 and Laby A1. First, we determined if Laby A1 competed for TIM-1 receptor binding with one of its ligands, TIM-4¹⁷². However, only weak inhibition of TIM-4 binding seemed to occur in the presence of Laby A1 (Figure 6.8A). This suggests that Laby A1 does not compete with TIM-4 for TIM-1 binding, but it does not exclude that Laby A1 interacts with another TIM-1 epitope. However, this still has to be determined. Secondly, to study putative internalization of TIM-1, we incubated Laby A1 with A549 cells for 30 min at different temperatures: RT (at which the 30 min experiment was initially performed), 37°C (at which the 4 hours

experiment was performed), and 4°C (at this temperature binding but minimal internalization occurs¹⁵⁸). As shown in Figure 6.8B, at all temperatures comparable results were obtained which suggests that internalization of TIM-1 by Laby A1 treatment does not explain the observed inhibition of TIM-1 Ab binding in Figure 6.8. To confirm this, we determined the amount of intracellular TIM-1 in the presence or absence of Laby A1 in A549 cells. After incubating the cells with Laby A1, extracellular TIM-1 was denatured by transferring the cells to acidic PBS (pH 2). Using this protocol, only intracellular receptor expression was detected.²²⁶ Surprisingly, Laby A1 slightly increased the amount of intracellular TIM-1 to some extent, which might partly explain the decreased extracellular TIM-1 Ab binding (Fig. 6.8C). The incongruent observations made in Figure 6.8A and B will have to be further examined in the future.

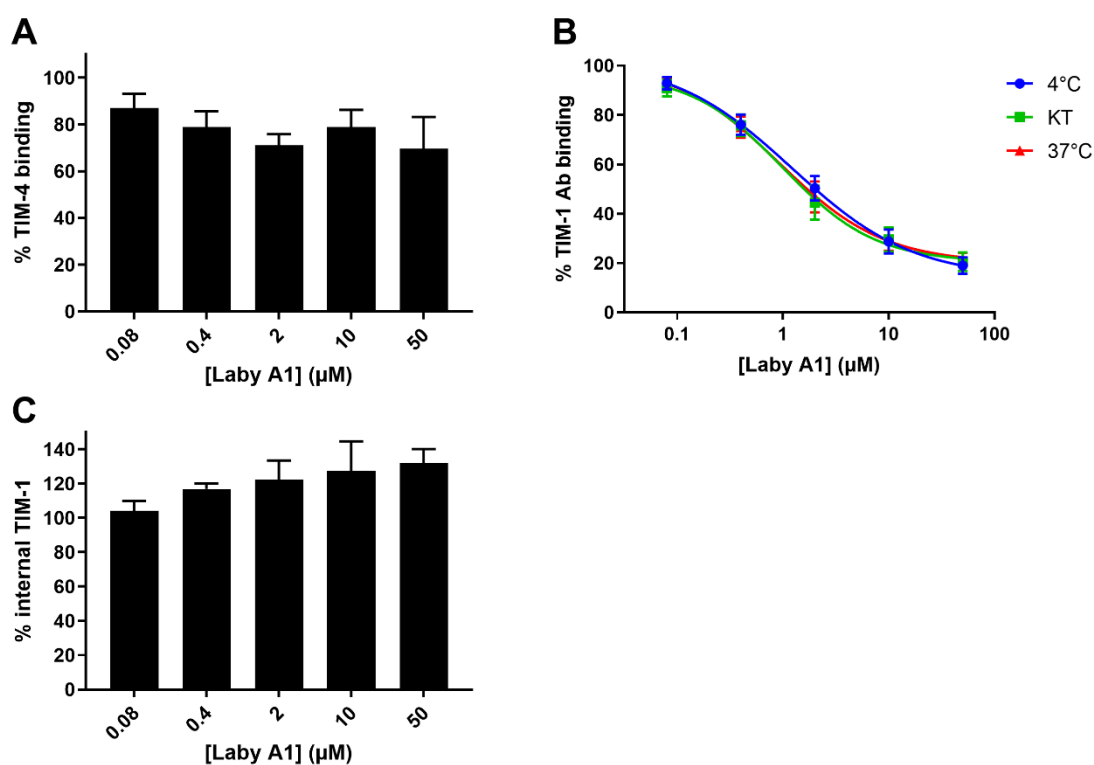


Figure 6.8 Potential interaction of Laby A1 with TIM-1. (A) A549 cells were incubated with various concentrations of Laby A1 for 4 hours. Afterwards recombinant human TIM-4 protein, fused with His tag, was added and incubated for 4 hours. TIM-4 binding to A549 cells was determined using flow cytometry with an anti-His Ab. Mean \pm SEM of 3 independent experiments is shown. (B) A549 cells were incubated with Laby A1 (10 μ M) for 30 min at 4°C, RT or 37°C, after which TIM-1 expression was determined using flow cytometry. Mean \pm SEM of 3 independent experiments is shown. (C) A549 cells were incubated with various

concentrations of Laby A1 for 4 hours at 37°C, followed by intracellular TIM-1 staining. TIM-1 Ab binding was compared at pH 7 and pH 2 to determine the amount of internalized TIM-1. Mean \pm SEM of 3 independent experiments is shown.

Finally, we used electrical impedance to determine if Laby A1 influences cell morphology of HEK293 and HEK293 TIM-1 cells differently. As shown in Figure 6.9, HEK293 TIM-1 had a more pronounced impedance profile after Laby A1 treatment than wild type cells. This is most clear in the first 2 hours after Laby A1 addition and disappears after 4 hours. Although this enforces the observations made in Figure 6.7 and confirms that this observation is due to TIM-1 expression, it does not give insight into the mechanism of TIM-1 – Laby A1 interaction. Therefore, we will look at the consequences of Laby A1 incubation on TIM-1 function.

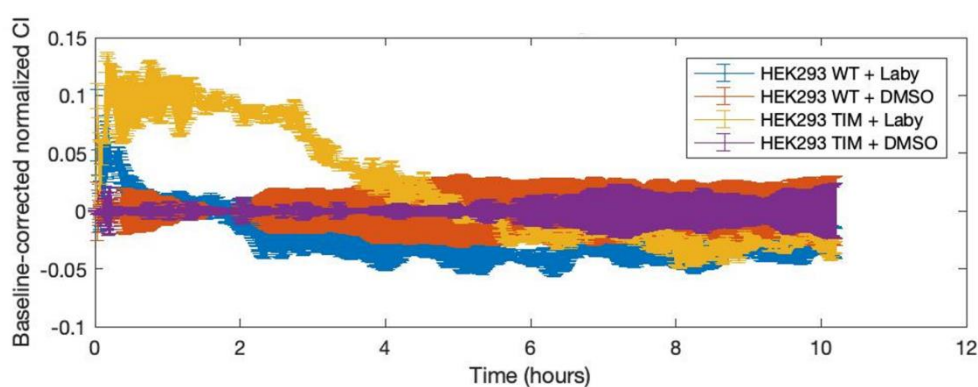


Figure 6.9 Laby A1 has a more pronounced effect on the electrical impedance profile of HEK293 TIM-1 than compared to HEK293 cells. HEK293 and HEK293 TIM-1 cell number and morphology changes after Laby A1 incubation (10 μ M) were observed over time using electrical impedance. The cell index was monitored using the xCELLigence system. Data are normalized compared to untreated cell controls. Data from one experiment are shown.

6.2.3.2 Optimization of a phagocytosis assay to study TIM-1 function and Laby A1 interaction

To determine if Laby A1 interferes with TIM-1 function, we optimized a phagocytosis assay. TIM-1 binds to phospholipids exposed on the cell membrane of apoptotic cells. This induces their engulfment and subsequent phagocytosis.¹⁶⁸ Jurkat cells were treated for 24 hours with camptothecin, a topoisomerase inhibitor that induces apoptosis. Various cell types were seeded. The next day, these cells were incubated with Laby A1 or another test compound for one hour. Meanwhile,

the apoptotic Jurkat cells were incubated with pHrodo Red succinimidyl ester. This pH-dependent dye binds to the cells and only emits fluorescent signal when localized in the acidic environment of the phagolysosome. Then, these stained cells were added to the phagocytic cells and incubated for selected time periods to allow phagocytosis. The fluorescent signal, which is proportional to the number of engulfed Jurkat cells, was determined with flow cytometry.

First, we determined to what extent the number of apoptotic cells influenced phagocytosis, using different camptothecin concentrations. To this end, Jurkat cells were treated with 0.5 μM – 1 mM camptothecin. The proportion of apoptotic/dead Jurkat cells was determined using annexin V staining while also the amount of phagocytosis by A549 cells was determined. Upon increasing camptothecin concentration, the percentage of apoptotic cells increases from 60 to 90 % while the phagocytosis rose from 25 to 40 as indicated in Figure 6.10A and 6.10B, respectively. Because 50 μM camptothecin causes clear apoptosis, allows sufficient phagocytosis detection, and does not unnecessarily exhaust the camptothecin stock, we have chosen to treat Jurkat cells with this concentration in future experiments.

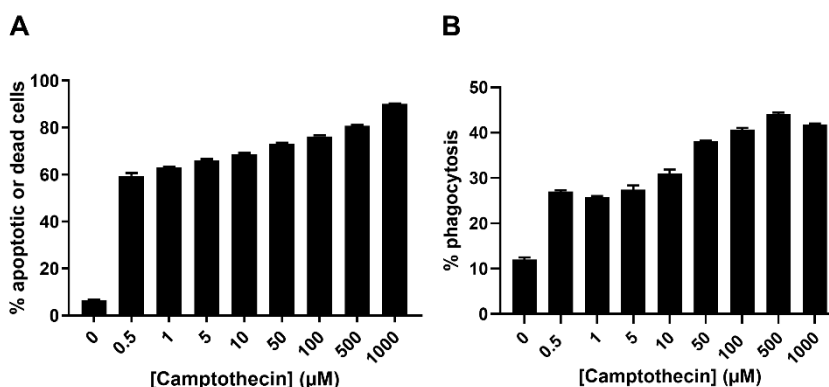


Figure 6.10 Determination of optimal camptothecin concentration. Jurkat cells were treated for 24 hours with various concentrations of camptothecin. (A) Jurkat cells were stained with annexin V-PE (BD Biosciences) to determine the proportion of apoptotic or dead cells. (B) Jurkat cells were stained with pHrodo Red, and phagocytosis by A549 cells was determined. Percentage phagocytosis was determined as the relative number of A549 cells that emitted pHrodo Red fluorescence. Mean \pm SEM of 3 replicates of one experiment is shown.

Then we evaluated the possible role of TIM-1 in the phagocytosis of apoptotic Jurkat cells. Therefore, we compared phagocytosis of untreated and apoptotic

Jurkat cells in TIM-1⁺ (A549 and Jeg-3) and TIM-1⁻ (CHO.k1 and U87) cells after different time points. Apoptotic cells (treated with camptothecin) were more engulfed than untreated cells. In addition, phagocytosis of apoptotic cells was more pronounced in TIM-1⁺ compared to TIM-1⁻ cells (Figure 6.11). Although we cannot confirm this is due to TIM-1 expression, it is a possible explanation. Apoptotic Jurkat cells are demonstrated to expose 240 attomol PS on their outer phospholipid leaflet, compared to about 0.9 attomol/cell on healthy Jurkat cells.³⁰⁸ This increases interaction with PS receptor TIM-1 and explains the observed differences between untreated and apoptotic Jurkat cells, and between cells with and without TIM-1 expression. CHO cells are nonprofessional phagocytes that interact with particles via electrostatic interactions, which explains the low degree of phagocytosis of Jurkat cells.³⁰⁹ In U87 cells, phagocytosis also remains at a negligible level. To our knowledge, U87 cells are no phagocytes, but it has been shown that they internalize particles through micropinocytosis.³¹⁰ Another possible explanation for our observations is that the presence of additional surface receptors contributes to increased phagocytosis in A549 and Jeg-3 cells. In our subsequent experiments we continued with A549 cells, since TIM-1 expression is more pronounced in these cells compared to Jeg-3 cells (Figure 6.1). Because phagocytosis was most pronounced after 3 hours incubation, we used this incubation time.

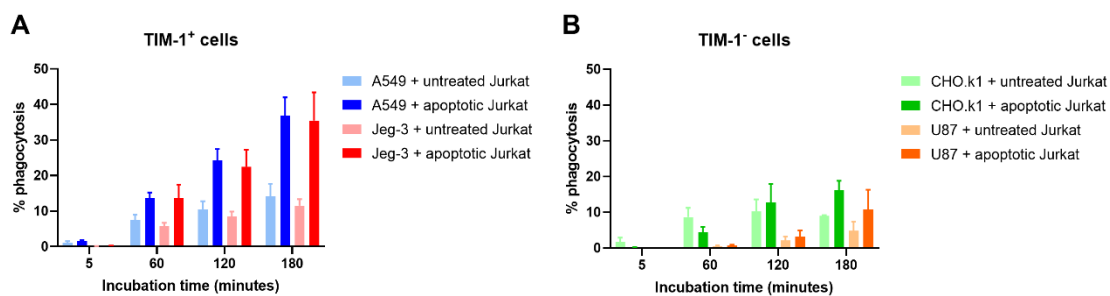


Figure 6.11 Phagocytosis is more pronounced in TIM-1⁺ cells. Confluent monolayers of (A) TIM-1⁺ A549 or Jeg-3 cells or (B) TIM-1⁻ CHO.k1 or U87 cells were incubated with pHrodo Red-stained untreated or camptothecin-treated Jurkat cells for various time points to allow phagocytosis. Percentage phagocytosis was determined as the relative number of A549 cells that emitted pHrodo Red fluorescence. Mean \pm SEM of 3 independent experiments is shown.

To further resolve whether phagocytosis of apoptotic cells is TIM-1-dependent, we compared phagocytosis in WT HEK293T cells and TIM-1-transfected HEK293T cells. To allow more accurate comparison with the previous work of Carnec *et al.*,

we performed the assay at 4°C and 37°C.¹⁰² The samples kept at 4°C were used to determine background fluorescence. As shown in Figure 6.12, TIM-1 did indeed increase phagocytosis, supporting the idea that TIM-1 is involved. Also in WT HEK293T cells there is a basal level of phagocytosis, which can be related to the very low level of TIM-1 expression in these cells, according to our flow cytometry results (Figure 6.1), or to the presence of other surface receptors involved in phagocytosis. According to Carnec *et al.*, phagocytosis of apoptotic cells is negligible in the wild type HEK293T cell line.¹⁰²

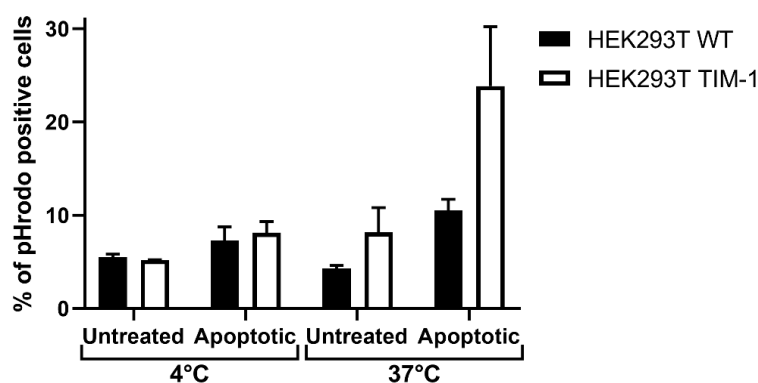


Figure 6.12 Phagocytosis of apoptotic cells is increased in TIM-1-transfected HEK293T cells. (A) Confluent monolayers of HEK293T cells were incubated for 3 hours at 4°C or at 37°C with pHrodo Red-stained untreated or apoptotic Jurkat cells and phagocytosis was compared between wt and TIM-1 transfected HEK293T cells using flow cytometry by determining the HEK293T population that emitted pHrodo Red fluorescence. HEK293T TIM-1 cells were co-stained with anti-TIM-1 Ab and the phagocytosis percentage in the TIM-1⁺ population was determined. Mean \pm SEM of 2 independent experiments is shown.

Finally, we determined the effect of Laby A1s on TIM-1-mediated phagocytosis (Figure 6.13). Cytochalasin D, an actin polymerization inhibitor, was included as a positive control in our experiments.¹⁸² It dose-dependently inhibited phagocytosis ($IC_{50} \pm SEM$: $1.7 \pm 0.3 \mu M$), which validates our assay. Laby A1 dose-dependently inhibited phagocytosis, however it only reached 50% inhibition at the highest concentration tested (50 μM). We also evaluated the lantibiotics from which the antiviral activity was determined in Chapter 5. The inhibitory effect of Laby A2 on phagocytosis is minimal, reaching only 26% at the highest concentration tested (50 μM). Duramycin inhibited phagocytosis with 24% its highest non-toxic dose (1 μM). Nisin did not interfere with phagocytosis.

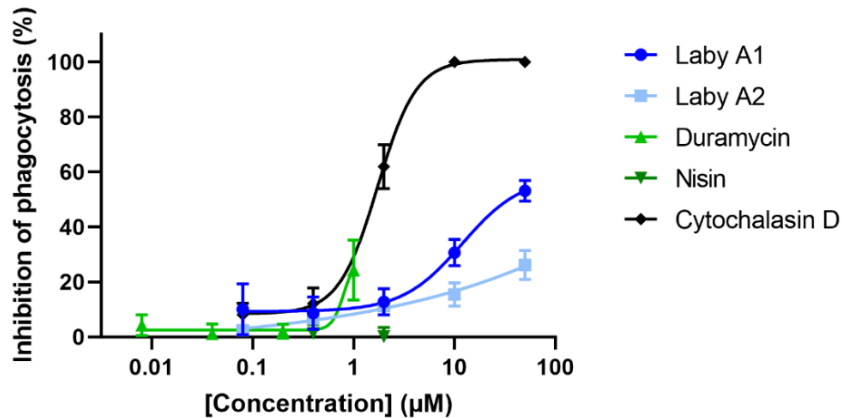


Figure 6.13 Inhibition of phagocytosis by lantibiotics. A549 cells were incubated with compounds for 1h, washed, and incubated with pHrodo Red-stained apoptotic Jurkat cells for 3h. Fluorescence was quantified. Data are represented as % inhibition of phagocytosis relative to the controls. Negative control: fluorescence of untreated A549 cells incubated for 5 min with apoptotic Jurkat cells. Positive control: fluorescence emitted by untreated A549 cells incubated for 3h with apoptotic Jurkat cells. Mean \pm SEM of 4 independent experiments is shown.

6.3 Conclusion

In this chapter, we studied the PSR TIM-1, an essential viral entry receptor. First, we studied the effect of TIM-1 surface expression on ZIKV infection and vice versa. We confirmed that TIM-1 expression enhances ZIKV-induced CPE and increases ZIKV and DENV replication and that a TIM-1-specific Ab blocks this infection (Figures 6.2-6.5). Finally, we showed that ZIKV decreases TIM-1 surface expression and that this is probably due to the CPE of the virus (Figure 6.6).

Secondly, we tried to unravel the possible interaction between TIM-1 and Laby A1, a potent antiviral peptide (Chapter 5). Laby A1 decreased TIM-1 surface expression in a dose-dependent and cell type-independent way (Figure 6.7). Ligand binding and internalization experiments could not clarify if this was observed because of Laby A1 binding to the receptor or because of decreased surface expression due to receptor internalization (Figure 6.8). Therefore, we determined if Laby A1 affects TIM-1 functioning by optimizing a phagocytosis assay (Figures 6.10-6.12). Laby A1 inhibited phagocytosis by TIM-1⁺ cells to some extent but did not completely block the receptor (Figure 6.13).

These experiments confirm the important role of TIM-1 in ZIKV infection and underline the need for the optimization of novel functional assays to study the potential of TIM-1 as antiviral target.

Chapter 7

CD300a: an entry receptor for ZIKV?

This chapter contains unpublished results.

7.1 Introduction

The second PSR of interest in this thesis is CD300a. This phospholipid receptor belongs to the CD300 receptor family. It has been shown that CD300a binds to DENV and promotes its infection.¹⁰² More specifically, CD300a appears to bind to the phospholipids PE and PS associated with the viral envelope. Furthermore, CD300a also increases WNV, YFV and CHIKV infection. However, its role in ZIKV infection remains unexplored, as well as its potential as antiviral target.

In this chapter, we evaluate the effect of CD300a surface expression on ZIKV infection. We compare ZIKV replication in WT compared to cells stably transfected with CD300a. Furthermore, we determine the consequences of blocking CD300a with receptor-specific antibody in dendritic cells that endogenously express this receptor.

7.2 Results and discussion

7.2.1 CD300a expression in cell lines

We used flow cytometry to determine the cell surface expression of CD300a on all cell lines that were used throughout this thesis. The tested epithelial cell lines did not express CD300a (Figure 7.1). To our knowledge, this is according to the literature. Among the evaluated suspension cell lines, CD300a was endogenously expressed on the T cell line SupT1. The other tested T cell line, *i.e.* Jurkat cells, did not express CD300a. It is known that some T and B cell subsets express CD300a.²¹⁰ Furthermore, CD300a was also expressed on the surface of cell lines stably transfected with the receptor, allowing to study the consequences of CD300a expression on ZIKV infection.

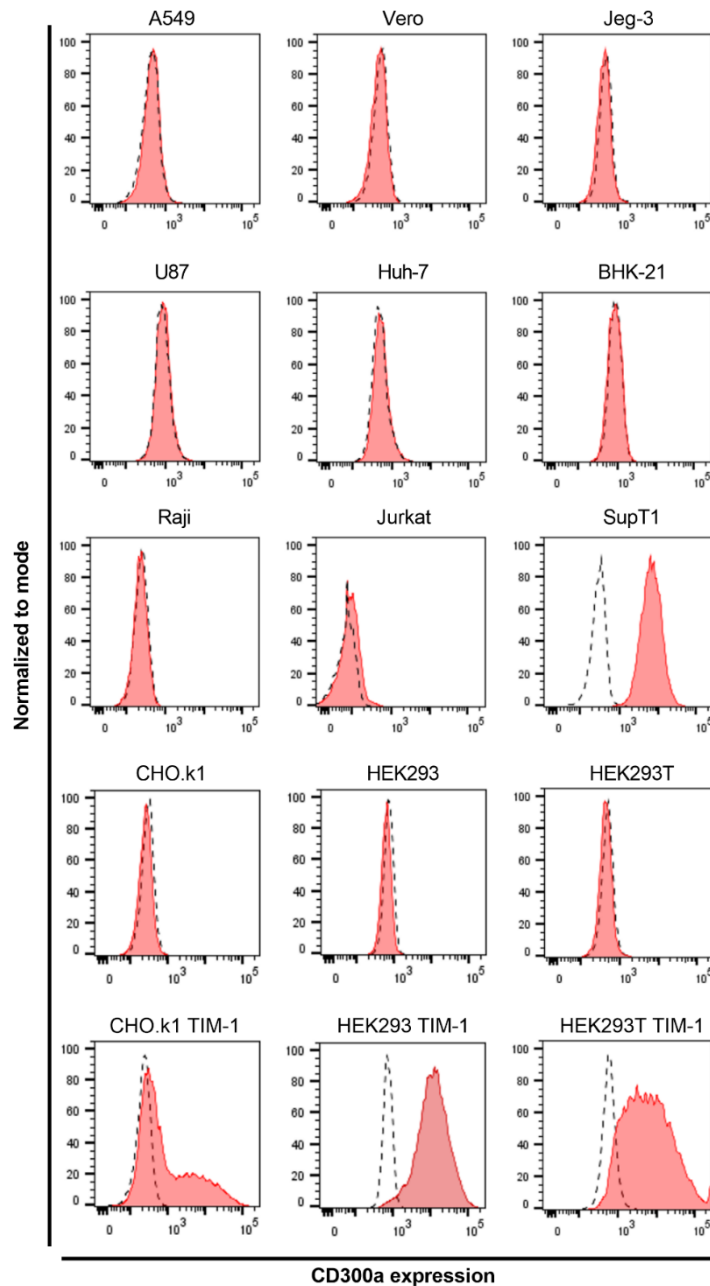


Figure 7.1 CD300a surface expression in various cell lines. Cells were stained with IgG1-PE isotype control or CD300a-PE. Dashed black and filled red histograms represent isotype control and CD300a staining, respectively. Data from one representative staining experiment are shown.

7.2.2 CD300a increases production of infectious ZIKV

To study the role of the CD300a receptor in ZIKV infection, we stably transfected this receptor in HEK293, HEK293T and CHO.k1 cells. Receptor expression was validated using flow cytometry (Figure 7.1). After overnight incubation, WT and CD300a-transfected cells were infected with ZIKV MR766 at MOI 1. After 24 hours viral titer in the supernatant was determined using a plaque assay.

Except for the CHO.k1 cell line, all cells were susceptible to infection. Even though previous research suggests that HEK293T cells are unsusceptible, our results contradict these observations.⁶⁷ Hence, we evaluated HEK293 cells, from which the HEK293T cells originated, but also in this cell line we could observe ZIKV production. However, as shown in Figure 7.2, the production of viral progeny in HEK293(T) cells is rather low and therefore we considered them as a good model for entry receptor studies. After CD300a transfection, production of infectious ZIKV increased significantly in these cell lines (Figure 7.2). This is the first time that the effect of CD300a as a viral entry factor has been demonstrated for ZIKV infection.

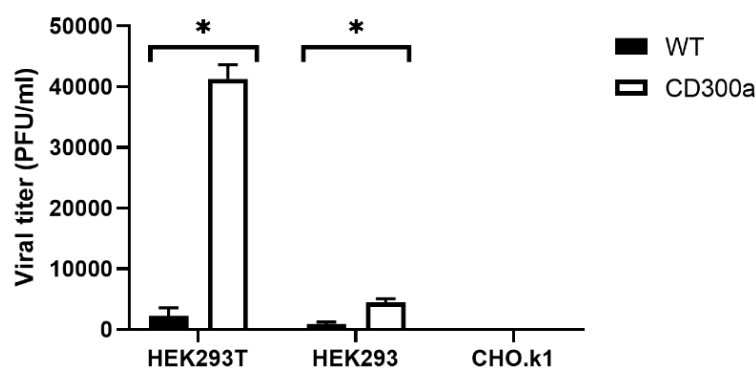


Figure 7.2 CD300a strongly increases ZIKV infection in various stably transfected cell lines. (B) WT and CD300a-transfected HEK293, HEK293T or CHO.k1 cells were infected after overnight growth with ZIKV MR766 (MOI 1) for one hour. Unbound virus was replaced by assay medium and 24 hpi viral titer in supernatant was determined by plaque assay in BHK-21 cells. Significance was calculated by using a two-sample t test, with * indicating a significance level of $p < 0.05$. Data from 2-3 experiments performed in triplicate are shown (Mean \pm SEM).

As shown in Figure 7.2, CHO.k1 cells remain unsusceptible to infection in our plaque assay even though CD300a is expressed. In accordance, when we used RT-qPCR as a more precise readout to quantify viral infection, almost no viral load was detected in WT or CD300a-transfected CHO.k1 cells (Figure 7.3). This suggests that CD300a alone is not sufficient for ZIKV infection and that other host factors are required for productive infection as well. As a control, we stably transfected CHO.k1 cells with TIM-1. These transfected cells were also unsusceptible to infection (results not shown), further confirming the need for other host factors. These observations in CHO.k1 cells are in line with previous results.²⁹⁵ Although it is a hamster cell line, other rodent-derived cell lines such as

BHK-21 are highly susceptible to ZIKV infection.⁸⁰ It has also been shown that CHO cells are capable of clathrin-mediated endocytosis, the mechanism by which ZIKV enters the cell.³¹¹

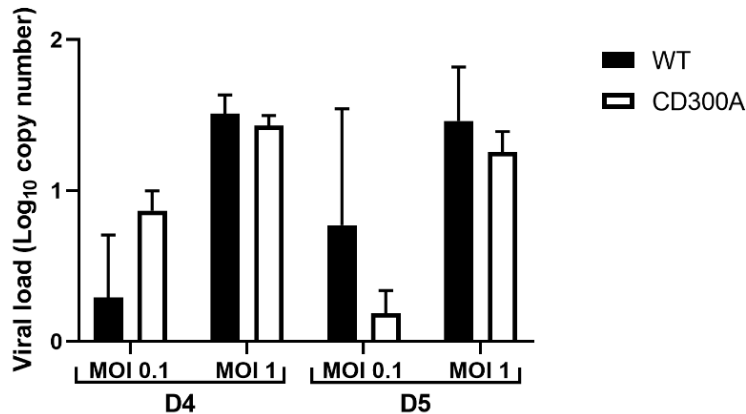


Figure 7.3 ZIKV does not replicate in CHO.k1 cells. WT and CD300a-transfected CHO.k1 cells were infected after overnight growth with ZIKV MR766 at MOI 0.1 or 1. Four (D4) or 5 (D5) days pi viral titer in supernatant was determined using RT-qPCR. Mean \pm SEM of 1 experiment performed in duplicate is shown.

7.2.3 CD300a expression increases ZIKV-induced CPE

ZIKV is known to cause severe CPE in human cell lines such as A549, Jeg-3, and Huh-7.^{80,295} We investigated the effect of CD300a receptor expression on ZIKV-induced CPE in HEK293 cells. In general, virus-induced CPE in CD300a-transfected cells appears faster and is more pronounced compared to WT cells. Three days pi, there is a heavily disturbed cell monolayer at MOI 1 in HEK293 CD300a cells, with only rather small CPE ‘spots’ in WT cells (Figure 7.4 upper panel). Four days pi, CPE is also observed at MOI 0.1 in CD300a-transfected cells, while in WT cells it is only observed at MOI 1 (Figure 7.4 middle panel). After 5 days pi CPE is observed in all conditions: WT cell monolayers are heavily disturbed but CD300a⁺ cells are completely detached from the bottom of the plate (Figure 7.4 lower panel). We made comparable observations in HEK293T cells but, because our HEK293 cells grow more confluent, these results are shown.

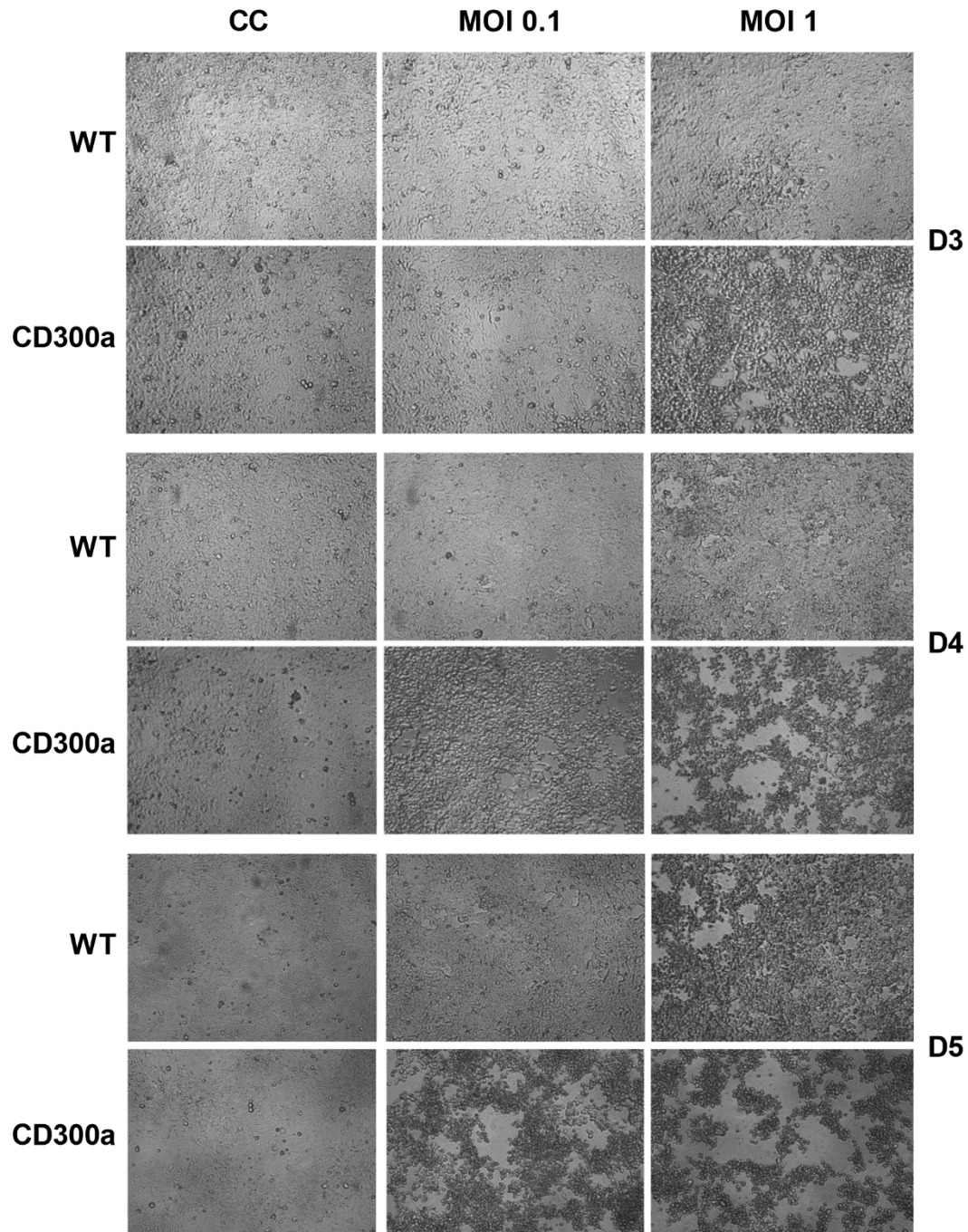


Figure 7.4 ZIKV induces more CPE in CD300a-transfected compared to WT HEK293 cells. Seeded WT and CD300a-transfected HEK293 cells were infected with ZIKV MR766 at MOI 0.1 or 1 for one hour. Unbound virus was replaced by assay medium and 3 (D3), 4 (D4) and 5 (D5) days pi CPE was determined. Results from one representative experiment are shown.

Importantly, when we compare ZIKV-induced CPE in CD300a-transfected cells with TIM-1-transfected HEK293 cells (respectively Figure 7.4 and Figure 6.2), it is clear that TIM-1 is responsible for a faster induction of cell death than CD300a.

Three days after infection at MOI 0.1, TIM-1 transfected cells are completely detached from the well bottom, while the monolayer is barely disturbed in ZIKV-infected CD300a-transfected cells. It takes until 5 days pi before the monolayer of CD300a-transfected cells has detached completely at MOI 0.1. This difference can be explained by the more abundant expression of TIM-1 on the cell membrane compared to CD300a, leading to attachment and entry of more virions. However, flow cytometry results suggests the opposite (Figure 6.1 and Figure 7.1). Another possible explanation is that TIM-1 enhances virus-induced CPE since it induces internalization of ZIKV particles, which directly leads to ZIKV entry and replication. On the other hand, CD300a might merely act as an attachment receptor, concentrating more virions on the cell surface without internalizing them.^{53,102}

7.2.4 CD300a expression increases ZIKV replication

We used RT-qPCR to study ZIKV replication in WT and CD300a-transfected HEK293T cells. Cells were infected with ZIKV MR766 at different MOIs and 3 days pi the amount of viral RNA in the supernatant was quantified. As shown in Figure 7.5A, surface expression of CD300a significantly increases ZIKV replication. When viral replication in HEK293T cells is compared with CD300a-transfected HEK293T cells, there is an increase in viral load of log 2 at MOI 0.01 and MOI 0.1 and log 1.5 at MOI 1. To confirm that this increase is CD300a-dependent, we pre-incubated the cells with a specific antibody recognizing CD300a. Although viral replication was not completely blocked, this Ab reduced viral load with \sim log 1.5 at MOI 0.01 and 0.1 and with log 1 at MOI 1, demonstrating the role of CD300a (Figure 7.5A).

To assess if there is a general enhancement of ZIKV infection by CD300a, we infected HEK293T CD300a cells with various ZIKV strains: two ancestral (MR766 and IbH 30656) and two contemporal (PRVABC59 and FLR). As shown in Figure 7.5B, all strains infected the cells, and replication increased at higher MOI. Replication was somewhat higher by the contemporal strains MR766 and IBH 30656. This was also reflected by observing virus-induced CPE: MR766 and IBH 30656 had more disruptive effects on the cells (results not shown).

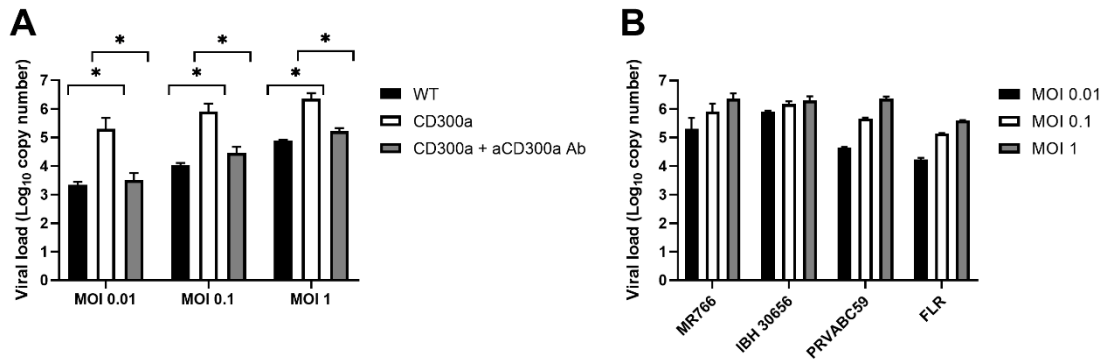


Figure 7.5 CD300a expression increases viral load in ZIKV-infected HEK293T cells and is inhibited by aCD300a Ab. Cells were seeded and incubated overnight. They were infected with ZIKV (MOI 0.01, 0.1 and 1) for 1 hour. Unbound virus was replaced by assay medium and cells were incubated for 3 days. Viral RNA in supernatant was quantified using RT-qPCR. Mean \pm SEM of (A) 3 or (B) 1 independent experiment(s), each performed in duplicate, is shown. (A) HEK293T or HEK293T CD300a cells were infected with ZIKV MR766 in the absence or presence of aCD300a (10 μ g/ml). Significance was calculated by comparing the means of two groups using a two-sample t-test; * $p < 0.05$. (B) HEK293T CD300a cells were infected with ZIKV strain MR766, IBH 30656, PRVABC59 or FLR at various MOI.

7.2.5 aCD300a Ab inhibits ZIKV and DENV infection

To determine if CD300a surface expression increases production of infectious virus, we used the plaque assay. HEK293T and HEK293T CD300a cells were infected with ZIKV or DENV-2 for 24 hours, followed by determination of viral titer in BHK-21 cells. As shown in Figure 7.6, CD300a transfection increases ZIKV titer by 11-fold (Figure 7.6A). When cells are pre-incubated with aCD300a Ab, this increase in infectivity is inhibited by 82%. This CD300a-effect is less pronounced in DENV infection, with 3-fold increased titer after transfection (Figure 7.6B). This could possibly be attributed to a DENV stock of low quality. After aCD300a Ab pre-treatment, infection is inhibited completely.

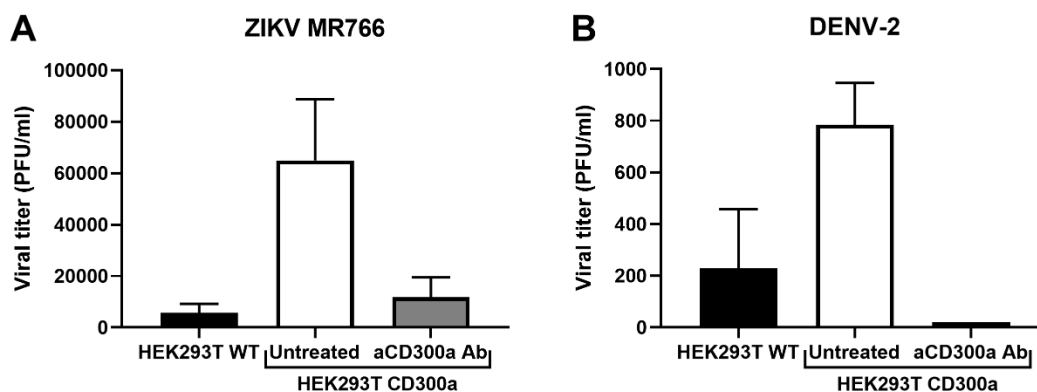


Figure 7.6 aCD300a Ab inhibits ZIKV and DENV infection in CD300a-transfected HEK293T cells. HEK293T and HEK293T CD300a cells were infected after overnight growth with ZIKV MR766 (A) or DENV-2 (B) at MOI 1 for one hour. Unbound virus was then replaced by assay medium and 24 hpi viral titer in supernatant was determined using the plaque assay in BHK-21 cells. HEK293T CD300a cells were also pre-treated for 30 min with 10 μ g/ml aCD300a Ab (grey graphs). In (A), viral titer was calculated using the 10^{-3} dilution, while in (B) this was the 10^{-2} dilution. Data from 3 independent experiments performed in triplicate are shown (mean \pm SEM). Significance was calculated by comparing the means of two groups using a two-sample t-test; * $p < 0.05$.

7.2.5 Anti-CD300a decreases ZIKV infection in MDDC

To evaluate the relevance of CD300a as a ZIKV entry factor in a more physiological context, we studied MDDCs isolated from primary human cells. Dendritic cells are known to express CD300a, and this was confirmed by flow cytometry (Figure 7.7A).²⁰⁸ They also express DC-SIGN, another Flavivirus entry factor.¹²⁴ We used antibodies against these receptors to determine their contribution to ZIKV infection. When cells were incubated with anti-CD300a Ab, viral load decreased by 45%. When cells were treated with both Abs, infection was inhibited by 87%. Anti-DC-SIGN alone also inhibited infection with 80% (Figure 7.7B). To our knowledge, this is the first time that the effect of blocking CD300a on Flavivirus infection is evaluated in primary dendritic cells.

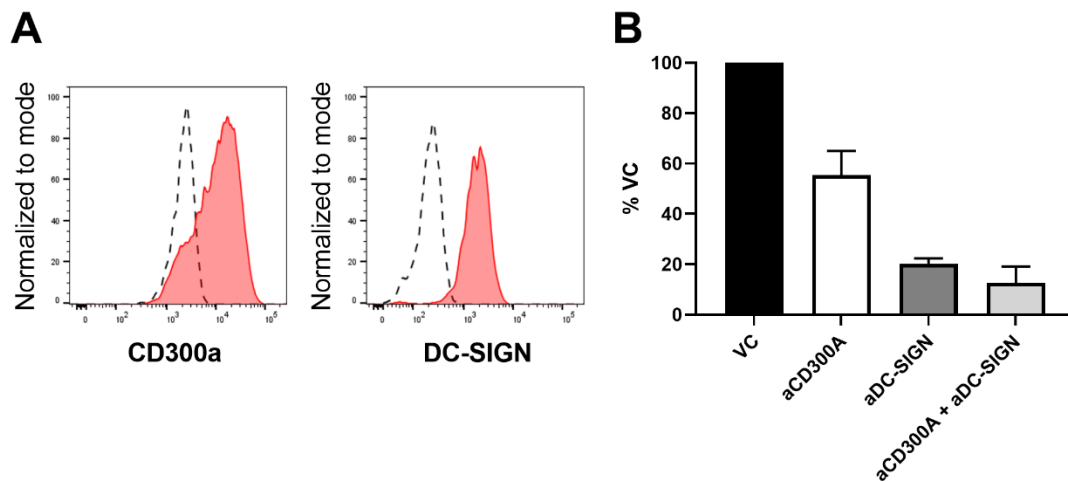


Figure 7.7 aCD300a inhibits ZIKV infection. (A) Surface expression of CD300a and DC-SIGN on MDDC. Dashed black and filled red histograms represent isotype control and receptor stainings, respectively. Data from one representative experiment are shown. (B) Immature MDDC were pre-incubated with either aCD300a, aDC-SIGN, or both antibodies (10 μ g/ml) for 30 min. They were infected with ZIKV MR766 (MOI 0.1) for 48 hours and the viral titer of lysed cells was determined with RT-qPCR. Data are represented as % viral load compared to virus control (VC). Mean \pm SEM from 1 experiment performed in duplicate of 2 donors is shown.

7.3 Conclusion

In this study, we demonstrated for the first time the importance of the PSR CD300a in ZIKV infection. Stable transfection of CD300a on HEK293(T) cells increased susceptibility to ZIKV infection, as measured by increased virus-induced CPE, viral replication and viral titer (Figures 7.2-7.4). This increased infection could be inhibited by pre-incubating cells with specific aCD300a Ab, also in dendritic cells, which endogenously express CD300a (Figures 7.5-7.7).

The precise role of the receptor in ZIKV entry, *i.e.* virus attachment or attachment and subsequent internalization, still has to be determined.

Chapter 8

General discussion

The occurrence of many outbreaks of viral epidemics in the last decades (*e.g.* HIV, ZIKV, EBOV, SARS-CoV-2,...) highlight the need of novel antiviral drugs and strategies. Because certain cellular receptors function as gates that allow entry of the virus, a promising antiviral strategy is to find viral entry inhibitors that behave as gatekeepers and help block viral infection at a very early stage, thereby preventing subsequent disease. In this thesis, we focused on the development of broad-spectrum antivirals that target viral entry in susceptible human cells. These antivirals can either interact with viral or cellular factors involved in the complex entry processes.

In this final discussion, we will address the main findings of our research and discuss them in a broader context, while also we will provide future prospects and will point out limitations related to this antiviral strategy in general and this research in specific.

8.1 Evaluation of entry inhibitors against enveloped viruses

In the first two research chapters, we have determined the antiviral activity and mechanism of action of two distinct groups of molecules that inhibit entry of enveloped viruses, *i.e.* lignosulfonate derivatives (**Chapter 4**) and labyrinthopeptins (**Chapter 5**).

8.1.1 Lignosulfonates display broad anti-HIV activity by interacting with the viral envelope

In Chapter 4, we have examined the antiviral activity of sulfonated lignin derivatives. It was previously shown by our research group that LA^{low}, a commercially available lignosulfonate, inhibits entry of HIV and HSV into their target cells.²³⁰ This makes the compound an interesting candidate for the development of microbicides, which prevent sexual transmission of HIV. In the search for more potent candidates and their mechanism of action, we have evaluated the anti-HIV and anti-HSV activity of 24 sulfonated lignin derivatives. We

demonstrated that the antiviral activity of the lignosulfonates correlated with their molecular weight. In addition, these compounds exert their antiviral activity by inhibiting gp120 glycoprotein adsorption to susceptible target cells. We suggest that electrostatic interactions between the gp120 glycoprotein and the negatively loaded lignosulfonates are critical in this process.

Apart from having identified compounds with higher antiviral activity, our results are in line with those obtained previously for LA^{low}.^{230,312} In Gordts *et al.*, we additionally showed that LA^{low} does not harm the vaginal microbiota.²³⁰ Together with its low cost, non-toxicity, and inhibition of dual HIV/HSV infection, these are all good properties for the application of lignosulfonates as microbicide.

During the ongoing search for effective microbicides that protect women by preventing sexual HIV transmission, various candidates have been under investigation. Currently, three sulfated polyanionic compounds have been evaluated as topical microbicides in phase III clinical trials. The first one, carrageenan, was considered as safe and it suggested efficacy, but it failed the trial because of absence of statistical significance.^{313,314} The second one, cellulose sulfate, was also safe, but the trial was aborted prematurely because the first results suggested even an increased risk of HIV transmission. However, these results turned out to be non-significant.³¹⁵ Because of this early closure, a parallel phase III trial was stopped as well, although in this study results suggested efficacy, albeit non-significant.³¹⁶ Finally, a 0.5% and 2% PRO 2000 (naphthalene sulfonate) gel was evaluated in phase III clinical trials. Despite safe and accepted use, efficacy as microbicide could not be demonstrated.³¹⁷ It turns out that in all three cases there is a clear discrepancy between promising results in preclinical and early clinical testing, and absence of efficacy in phase III clinical trials. Several reasons for these negative results were proposed: influence of vaginal pH by the product, decrease of activity in the presence of seminal fluid, product loss due to dilution or leakage, or disruption of vaginal epithelial integrity.²⁷⁸ These potential problems should be investigated during preclinical testing. The most important issue was the low drug adherence during the trial period which profoundly influenced the reported outcome.³¹⁴ Special efforts need to be made to increase drug adherence, for example by making application methods more user-friendly, e.g. through microbicide-containing intravaginal rings.³¹⁸ Also, the way that

adherence can be measured and reported should be improved, since self-reporting of drug adherence has been shown to be incongruent with actual adherence.^{314,319}

Although none of these polyanionic compounds has made it to the market, it has never been demonstrated that they are unsafe or even could increase the risk of HIV transmission. Their antiviral activity profile and potential applications remain interesting. The findings in our study aid to develop specific nanotechnology-based polyanionic microbicide candidates, such as polyanionic dendrimers. Recently, more attention is going to this class of compounds.³²⁰ They are highly branched, star-shaped, and nano-sized molecules with a central core, several layers, and functional groups at the outer surface. Lignosulfonates resemble dendrimers somewhat, both structurally (being branched polymers) and behaviorally (exposing their sulfonate groups when in solution).³²¹ The implementation of several end-groups in dendrimers allows multivalent interactions with the virus envelope proteins. Polyanionic dendrimers possess several benefits such as structural uniformity and monodispersity, stability, and a high targeting-efficiency.^{249,322}

This study reveals that the conversion of wood pulp into paper produces a variation of lignin-derived byproducts with broad antiviral activity by interfering with the viral entry process, that is dependent on their molecular weight. The results obtained here suggest that lignosulfonates might be useful as potential microbicides against HIV and HSV sexual transmission. However, thorough preclinical development needs to be done, *e.g.* by studying the interaction with biological entities (epithelia, semen,...) and especially the application method. Currently, drug-releasing vaginal rings are at the forefront of ongoing efforts to develop microbicide-based strategies for prevention of heterosexual HIV transmission.^{254,323}

8.1.2 Labyrinthopeptin A1 inhibits DENV and ZIKV infection by interfering with the viral phospholipid membrane

In Chapter 5, we have evaluated the antiviral activity of the lantibiotic Labyrinthopeptin A1 (Laby A1) against ZIKV and DENV, and have determined its mechanism of action. In line with other recent reports of Laby A1, our study demonstrates the potential of this peptide as an antiviral drug for the treatment of ZIKV and DENV. We have demonstrated that Laby A1 interacts with the phospholipids PE and PS, which are located in the viral membrane. This interaction

leads to lysis of the virus and as such prevents further interaction with cellular receptors and subsequent entry.^{125, this thesis}

Our results are confirmed by the study of Prochnow *et al.*¹²⁵ Next to DENV and ZIKV, Laby A1 also inhibits replication of other enveloped viruses. In Férrir *et al.*, the broad anti-HIV and anti-HSV activity of Laby A1 was demonstrated.¹²⁷ Blockus *et al.*, demonstrated that Laby A1 inhibits RSV.¹²⁶ Furthermore, the peptide inhibits other pathogenic viruses as well, such as CHIKV, HCV, YFV and WNV.^{125, this thesis} Altogether, this demonstrates that Laby A1 is an entry inhibitor exerting broad-spectrum antiviral activity against a wide range of enveloped viruses.

Laby A1 does, however, not inhibit every enveloped virus included in the experiments (Table 5.2). We did not observe inhibition of parainfluenza virus 3, Sindbis virus, and the evaluated influenza and coronaviruses by Laby A1. Prochnow *et al.* hypothesize that virus sensitivity to Laby A1 depends on the PE fraction and on the presence of lipid rafts in the viral envelope, both being positively correlated with sensitivity. Further experiments will have to unravel the virus specificity of Laby A1.

We wondered if sensitivity to Laby A1 also depends on the budding site of the virus, *i.e.* from which cellular membrane the virus receives its lipid bilayer. The composition of virus envelopes acquired from the plasma membrane (*i.e.* HIV, influenza viruses) differs from those obtained at the ER or Golgi complex (*i.e.* flavi- and coronaviruses). The latter have for example a higher PE content.³²⁴ However, as shown in Table 5.2, we demonstrate that Laby A1 activity does not correlate with the budding site.

Furthermore, we were interested in determining if entry receptor preference of the virus is related to Laby A1 sensitivity. Entry of (para)influenza viruses depends on sialic acid-containing receptors, while coronaviruses interact with angiotensin-converting enzyme 2. These viruses do not interact with TIM-1, a viral entry receptor that interacts with envelope PS and PE. They are also insensitive to Laby A1 treatment. Since both TIM-1 and Laby A1 interact with PS and PE, this suggests that interaction with Laby A1 and TIM-1 requires that these phospholipids must be exposed to some extent. To test this hypothesis, it would be interesting to evaluate the activity of Laby A1 against other viruses interacting with TIM-1, *e.g.* EBOV, and to determine if HSV interacts with TIM-1.

Compounds targeting the viral lipid envelope have also been called Lipid Envelope Antiviral Disruption (LEAD) molecules, with various examples in preclinical development.³²⁵ A first example is the small molecule CLR01. It binds to lipid raft-rich regions in the viral envelope of e.g. HIV, EBOV and ZIKV, causing disruption of the lipid bilayer.³²⁶ Another example is the brain-penetrating peptide AH-D, which induces pore formation of the viral membrane. AH-D inhibits ZIKV infection *in vitro* and in a mouse model of congenital ZIKV infection.^{327,328} Interestingly, this compound shows high selectivity by only binding to the highly curved membranes of the viral envelope, while not interacting with larger cellular membranes. A last example is the secreted phospholipase PLA₂, which selectively binds to lipid membranes acquired from the ER, thus inhibiting viruses such as DENV, HCV and JEV.³²⁹

Laby A1 is not the only lantibiotic exerting antiviral activity by binding to viral envelope phospholipids. Duramycin, a 19 aa tetracyclic lantibiotic, inhibits several viruses such as DENV, WNV and EBOV by binding to PE, but it shows a lower selectivity and thus possesses a less favorable safety window than Laby A1.^{171,306} Cinnamycin, a lantibiotic closely related to duramycin, also binds to PE, but also exerts pronounced cytotoxic effects.^{125,306} Spectroscopy experiments by lawamoto *et al.* determined that duramycin and cinnamycin induce curvature changes in PE-containing membranes.³⁰⁶ We did not determine this for Laby A1 but these findings further explain the virucidal activity of Laby A1, disturbing the viral envelope. Altogether, these examples highlight the attractive approach of targeting the viral envelope lipids and the importance of further investigating this strategy in the future.

Remaining open questions concern resistance and bioavailability. Resistance development to these compounds is less likely to occur, since this would require composition changes in the cellular and viral lipid bilayer. This is also exemplified by the lack of resistance development when HIV-1 or DENV-2 was continuously passaged in the presence of Laby A1.^{302 unpublished results}

The peptide nature of Laby A1 is important to keep in mind during its further development as antiviral drug. Peptide drugs are associated with short half-lives, low bioavailability, immunogenicity, and high production and application costs. However, these issues might be tackled in several ways. The acute nature of

emerging viruses generally demands only short-term use of antiviral therapy. No accumulation in the body is necessary. Furthermore, this also implicates lower production costs. Laby A1 is a peptide with virucidal activity, which implies that it can inactivate circulating virions in the blood, without the need to penetrate the cell. This reduces the chance of interaction with intracellular proteins and signaling pathways. Also, researchers are developing methods to upscale the synthetic production of labyrinthopeptins, which also reduces production costs.³³⁰ These and other technical innovations allow the investigation of several peptide inhibitors active against a range of enveloped viruses.³³¹

A valuable next step in the Laby A1 development is its thorough pharmacokinetic evaluation. Prochnow *et al.* already performed a first pharmacokinetic study in mice and demonstrated the favorable stability parameters of Laby A1.¹²⁵ Together with the lack of resistance development, these are promising properties for further preclinical development of Laby A1, starting with evaluating its efficacy in animal models and determining its immunogenicity.

8.2 Involvement of phosphatidylserine receptors in ZIKV entry

In the last two research chapters, we have studied the roles of the entry receptors TIM-1 and CD300a in ZIKV infection. More specifically, in **Chapter 6** we have examined TIM-1 as a potential antiviral target. We have also evaluated whether the antiviral activity of Laby A1 is (partially) dependent on the interaction with TIM-1. In addition, the role of CD300a as an entry receptor in ZIKV infection was evaluated in **Chapter 7**.

8.2.1 TIM-1 enhances entry of ZIKV and possibly interacts with Labyrinthopeptin A1

In Chapter 6, we have studied the role of the PSR TIM-1 in ZIKV infection, as this receptor enhances entry of the virus into target cells.⁶⁷ This was our starting point to study if the antiviral activity of Laby A1 depends on interaction with TIM-1. Overall, we confirmed the observation that TIM-1 expression increases ZIKV (and DENV) replication.^{67,101} Infection was blocked by pre-incubating the cells with a specific TIM-1 Ab.

In Chapters 6 and 7, the majority of the experiments was performed with receptor-transfected cell lines that are not endogenously expressing the receptor of interest. This was obviously useful to determine the consequences of receptor expression on virus infection, but also has a major drawback for subsequent studies: the pathways induced upon virus-receptor interaction might deviate from those in cells naturally expressing this receptor.

Therefore, we also studied ZIKV and DENV infection in A549 cells, because they endogenously express this receptor. A549 cells originate from lung carcinoma tissue and although they are no natural target for ZIKV or DENV-2 infections, these cells can be easily infected with both viruses.^{59,295} A remarkable observation in ZIKV-infected A549 cells was the decrease of TIM-1 expression, which was more pronounced than in DENV-infected cells. According to our experimental results, this is principally due to the higher CPE induced by ZIKV compared to DENV, which disturbs the integrity of the cell membrane and changes receptor expression.

In the future, we want to evaluate the effect of various pathway inhibitors on ZIKV and DENV infection in cell lines using CEI, an interesting technique to study pathway modulation in real-time.²⁴³ This can help us to unravel the observed divergent CPE induction by ZIKV and DENV in A549 cells. Flaviviruses control cell growth and survival by regulating several mechanisms such as apoptosis, necrosis, autophagy and oxidative stress.^{332–335} Interestingly, research has shown that the use of PI3K inhibitors accelerates DENV-induced CPE in A549 cells.³³⁶ DENV infection induces the PI3K/Akt pathway in order to delay apoptosis in the early stages of the viral life cycle, thereby enhancing viral replication. Recently, this delay in apoptosis induction has also been observed for ZIKV infection.³³⁷

More research is needed to further unravel the role of TIM-1 in ZIKV and DENV infection as well. We wonder if the above mentioned virus-induced CPE is related to the virus interacting with TIM-1, and with subsequent TIM-1 intracellular signaling, e.g. via the PI3K/Akt pathway (Section 1.3.2.3). These and other questions could be studied using cell types endogenously expressing TIM-1, followed by specific silencing of the receptor. For example, it has been proposed that DENV-induced autophagy induction is the result of TIM-1 signaling following virus binding.³³⁸

After having evaluated the role of TIM-1 in ZIKV infection, we were interested in the potential interaction between TIM-1 and the antiviral peptide Laby A1. In an initial experiment, we observed that Laby A1 was capable to decrease TIM-1 expression, which triggered us to perform some additional assays to study this observation in more detail. Unfortunately, these experiments did not result in satisfactory findings and led to contradictory observations. More research is needed to determine the interaction with Laby A1 and TIM-1. A possible follow-up experiment could be tracing internalization of the receptor after Laby A1 incubation. For example, a TIM-1 construct fused to a fluorescent protein can allow us to track receptor internalization using microscopy. In addition, SPR experiments could also be useful to evaluate the binding of Laby A1 to TIM-1.

So, further studies are necessary in order to determine if Laby A1 exerts an additional mechanism of action, besides the phospholipid-binding properties of the peptide. This would raise additional implications related to further development. For example, an additional mechanism of action might further increase the barrier for resistance development. Furthermore, TIM-1 interaction could induce undesirable side effects. These points are further addressed in Section 8.3.2.

Because our findings further confirmed that TIM-1 is an interesting target for pharmacological modulation, we started to optimize a functional assay, *i.e.* the phagocytosis assay. However, the assay should be further optimized in order to ascertain that it is specific to monitor TIM-1-mediated phagocytosis.

In the future, it would be interesting to develop additional TIM-1 functional assays to evaluate potential TIM-1 inhibitors. For example, it is described in literature that TIM-1 expression is associated with T cell activation after stimulation.^{175,178} It would be an interesting path to study the effect of inhibitors on this upregulation.

8.2.2 CD300a enhances entry of ZIKV

In Chapter 7, we have demonstrated for the first time that expression of the PSR CD300a enhances entry and replication of various ZIKV strains, which has previously also been confirmed for DENV, WNV, YFV and CHIKV.¹⁰²

The subsequent step in this research project will be mainly directed at determining if CD300a and/or ZIKV are internalized after virus binding using microscopic and quantitative techniques. As proposed by Carnec *et al.*, we expect no receptor internalization due to the inhibitory properties of CD300a and the dispensability of

its cytoplasmic tail.¹⁰² Another remaining open question is the physiological relevance of this receptor in Flavivirus infection, as not every cell type expressing the receptor is susceptible to infection.¹⁰²

Besides TIM-1 and CD300a as possible entry receptors, it would also be interesting to study the roles of other PSR in DENV and ZIKV infection, such as TIM-3 and the TAM receptor Mer. Meertens *et al.* have shown that TIM-3 slightly promotes DENV infection, but to a lesser extent than TIM-1 or TIM-4.¹⁰¹ The role of TIM-3 in ZIKV infection has not yet been studied. The limited role of TIM-3 might be explained by the absence of a long mucin domain compared to TIM-1 and TIM-4 (Figure 1.8). It has been demonstrated that a mucin domain of sufficient length is crucial for the receptor to function as entry receptor.¹⁹⁴ This also suggests that CD300a, which lacks a long mucin domain as well, merely functions as a viral attachment receptor rather than an entry receptor.

To our knowledge, the role of Mer in DENV or ZIKV entry has never been studied. However, this receptor tyrosine kinase is also involved in phagocytosis of apoptotic cells and is broadly expressed on many cell types of different tissues and thus might also function as entry receptor of flaviviruses.¹⁶⁵

These are all pressing questions to answer. TIM-1 is the only receptor for which it is demonstrated that it enhances internalization of DENV. However, it is also known that the presence of this receptor is not indispensable for infection to occur. Hence, it is likely that other entry receptors are involved as well that others still have to be identified.

8.3 Considerations and limitations related to...

8.3.1 ... broad-spectrum antivirals

As mentioned in Section 1.2.1, one of the major benefits of BSA includes that they are immediately available when a novel epidemic emerges. However, there are also some drawbacks associated with the development of BSA. The main objections are resistance development, more associated with virus-acting agents, and toxicity, rather concerning host-directed agents. In terms of resistance development, it should be considered if a combination of various drugs targeting different factors or stages in the viral life cycle could prevent resistance development. Of course, the short treatment period for acute viral infections

reduces the chance of resistance development as well. The lack of specificity of BSA might induce toxicity and also make it less efficacious to clear the virus than species-specific drugs. However, studies have shown that any reduction in viral load already improves the patient's disease severity.^{339,340} In fact, BSA have an important role in the beginning of viral epidemics, until more specific measures, such as a preventive vaccine, are available.

The potential of BSA is demonstrated by the promising results obtained with the repurposing of both virus-acting (*e.g.* remdesivir) and host-directed agents (*e.g.* dexamethasone) during the SARS-CoV 2 crisis.^{139,141,142,341,342}

Next to the high need for antiviral drug development, we also want to stress the crucial role of vaccines, and the fact that these strategies go hand in hand. Vaccines have the great benefit that they provide long-term protection against infection, and prevention is better than cure. However, vaccine development also requires thorough knowledge of the immunological properties of the infection, which is often highly complex. For example, a DENV vaccine must prevent infection with all four serotypes and ideally also of other closely related flaviviruses, to prevent ADE.³⁵ While vaccines are of less use when people are already sick, administering an antiviral is the preferred choice of combatting the infection. In short, both vaccines and antivirals are required for an effective strategy during viral outbreaks.³⁴³ The current SARS-CoV-2 pandemic illustrates this: research efforts are focused on the search for both vaccines and antivirals.

8.3.2 ... entry inhibitors

Besides important benefits (Section 1.2.2), the use of entry inhibitors as antiviral agents also has its limitations, which is exemplified by the clinically used antiretroviral drugs. Enfuvirtide is a peptide that inhibits the final steps of the membrane fusion process between HIV and target cells. It has to be administered twice daily by subcutaneous injection, which can cause unpleasant side effects. Because of the chronic nature of antiretroviral therapy, this drug is also associated with high costs and therefore only prescribed when other treatments have failed. The second example is maraviroc, a small molecule that inhibits entry of R5 HIV strains by antagonizing the CCR5 receptor. Because of this narrow target spectrum, its use is limited to people infected with R5 HIV isolates.

Not every viral or cellular factor is a favorable target for entry inhibitor development. For example, viral envelope proteins tend to be highly variable between species, so to assure broad activity it is important that conserved regions in the protein are targeted. Of course, there are other valuable targets for BSA development, such as the viral replication process and the cellular defense system.^{10,344} As demonstrated for HIV treatment regimens, the combination of drugs targeting various steps in the viral life cycle has significant benefits.³⁴

Although TIM-1 is an attractive target for entry inhibitor development, it is also possible that inhibiting this protein is associated with undesirable cellular toxicity. Indeed, besides viruses, other cellular processes depend on TIM-1-mediated binding to PS and PE, and these processes could also be affected by TIM-1 inhibitors. Therefore, the safety profile of candidate TIM-1 inhibitors should be thoroughly evaluated in animal models.

Interestingly, TIM-1 KO mice are viable and undergo normal development, which suggests that TIM-1 is not involved in tissue homeostasis, and inhibition has no extremely toxic consequences.^{197,345} However, we cannot completely extrapolate these findings to humans, since mice possess additional TIM receptors such as TIM-2, which are not expressed in humans. TIM-2 shows a high degree of sequence homology to TIM-1 and might thus take over TIM-1 functions in TIM-1 deficient mice.¹⁶⁶ This might be an important drawback when evaluating the safety profile of TIM-1 inhibitors in a mouse model. A double KO model might solve this issue.

Recently, a monoclonal TIM-1 Ab conjugated to a cytotoxic small molecule was evaluated in humans to treat various cancers in which TIM-1 is upregulated.^{190,205} The TIM-1 antibody is used to direct the chemotherapeutic to specific tumor cells, an innovative approach in cancer therapy. The compound exhibited signs of antitumoral activity and a tolerable toxicity profile, but was discontinued due to commercial reasons. Despite this unfortunate decision, it is clear that TIM-1 is worth investigating. Hence, we are encouraged to further evaluate TIM-1 as an antiviral target.

A final general comment is that this PhD project is based on *in vitro* cellular experiments, which is associated with many choices of the exploited models and methods, all having their benefits and limitations. A significant example is this:

because flaviviruses are transmitted by mosquitoes, we decided to culture ZIKV and DENV stocks in the mosquito cell line C6/36. Research has shown that the choice of the cellular system used to serially propagate DENV stocks determines its susceptibility to antiviral entry inhibitors because the virus adapts its entry route to the used cell line.³⁴⁶ This is an important note to keep in mind when evaluating novel entry inhibitors.

List of references

1. Fields, B. N., Knipe, D. M., Howley, P. M. & Griffin, D. E. *Fields Virology*. (2001).
2. Johnson, N. P. A. S. & Mueller, J. Updating the accounts: global mortality of the 1918-1920 'Spanish' influenza pandemic. *Bull. Hist. Med.* **76**, 105–115 (2002).
3. Theiler, M. & Smith, H. H. The use of yellow fever virus modified by in vitro cultivation for human immunization. *J. Exp. Med.* **65**, 787–800 (1937).
4. Barberis, I., Myles, P., Ault, S. K., Bragazzi, N. L. & Martini, M. History and evolution of influenza control through vaccination: From the first monovalent vaccine to universal vaccines. *J. Prev. Med. Hyg.* **57**, E115–E120 (2016).
5. Musso, D., Ko, A. & Baud, D. Zika virus infection — after the pandemic. *N. Engl. J. Med.* **381**, 1444–1457 (2019).
6. Jacob, S. T., Crozier, I., Fischer, W. A., Hewlett, A., Kraft, C. S., Vega, M.-A. de La, Soka, M. J., Wahl, V., Griffiths, A., Bollinger, L. & Kuhn, J. H. Ebola virus disease. *Nat. Rev. Dis. Prim.* **6**, 13 (2020).
7. WHO disease outbreak news. <https://www.who.int/csr/don/archive/year/2020/en/>.
8. Guzman, M. G., Gubler, D. J., Izquierdo, A., Martinez, E. & Halstead, S. B. Dengue infection. *Nat. Rev. Dis. Prim.* **2**, 16055 (2016).
9. Economische impact van het coronavirus. <https://economie.fgov.be/nl/themas/ondernemingen/coronavirus/economische-impact-van-het>.
10. Boldescu, V., Behnam, M. A. M., Vasilakis, N. & Klein, C. D. Broad-spectrum agents for flaviviral infections: dengue, Zika and beyond. *Nat. Publ. Gr.* (2017) doi:10.1038/nrd.2017.33.
11. Cavicchioli, R., Ripple, W. J., Timmis, K. N., Azam, F., Bakken, L. R., Baylis, M., Behrenfeld, M. J., Boetius, A., Boyd, P. W., Classen, A. T., Crowther, T. W., Danovaro, R., Foreman, C. M., Huisman, J., Hutchins, D. A., Jansson, J. K., Karl, D. M., ... Webster, N. S. Scientists' warning to humanity: microorganisms and climate change. *Nat. Rev. Microbiol.* **17**, 569–586 (2019).
12. Rohr, J. R., Barrett, C. B., Civitello, D. J., Craft, M. E., Delius, B., Deleo, G. A., Hudson, P. J., Jouanard, N., Nguyen, K. H., Ostfeld, R. S., Remais, J. V., Riveau, G., Sokolow, S. H. & Tilman, D. Emerging human infectious diseases and the links to global food production. *Nat. Sustain.* **2**, 445–456 (2019).
13. Ksiazek, T. G., Erdman, D., Goldsmith, C., Zaki, S. R., Peret, T., Emery, S., Tong, S., Urbani, C., Comer, J. A., Lim, W., Rollin, P. E., Ha Nghiem, K., Dowell, S., Ling, A.-E., Humphrey, C., Shieh, W.-J., Guarner, J., ... Anderson, L. J. A novel coronavirus associated with severe acute respiratory syndrome. *N. Engl. J. Med.* (2003) doi:10.1056/NEJMoa030781.
14. Zaki, A. M., van Boheemen, S., Bestebroer, T. M., Osterhaus, A. D. M. E. & Fouchier, R. A. M. Isolation of a novel Coronavirus from a man with pneumonia in Saudi Arabia. *N. Engl. J. Med.* **367**, 1814–1820 (2012).
15. Zhu, N., Zhang, D., Wang, W., Li, X., Yang, B., Song, J., Zhao, X., Huang, B., Shi, W., Lu, R., Niu, P., Zhan, F., Ma, X., Wang, D., Xu, W., Wu, G., Gao, G. F. & Tan, W. A novel Coronavirus from patients with pneumonia in China, 2019. *N. Engl. J. Med.* **382**, 727–733 (2020).
16. Global HIV & AIDS statistics — 2019 fact sheet. <https://www.unaids.org/en/resources/fact-sheet>.
17. Deeks, S. G., Overbaugh, J., Phillips, A. & Buchbinder, S. HIV infection. *Nat.*

- Rev. Dis. Prim.* **1**, 15035 (2015).
18. Lucas, W. Viral capsids and envelopes: structure and function. *eLS* (2010) doi:doi:10.1002/9780470015902.a0001091.pub2.
 19. Watts, J. M., Dang, K. K., Gorelick, R. J., Leonard, C. W., Bess, J. W., Swanstrom, R., Burch, C. L. & Weeks, K. M. Architecture and secondary structure of an entire HIV-1 RNA genome. *Nature* **460**, 711–716 (2009).
 20. Pancera, M., Zhou, T., Druz, A., Georgiev, I. S., Soto, C., Gorman, J., Huang, J., Acharya, P., Chuang, G. Y., Ofek, G., Stewart-Jones, G. B. E., Stuckey, J., Bailer, R. T., Joyce, M. G., Louder, M. K., Tumba, N., Yang, Y., ... Kwong, P. D. Structure and immune recognition of trimeric pre-fusion HIV-1 Env. *Nature* **514**, 455–461 (2014).
 21. Leonard, C. K., Spellman, M. W., Riddle, L., Harris, R. J., Thomas, J. N. & Gregory, T. J. Assignment of intrachain disulfide bonds and characterization of potential glycosylation sites of the type 1 recombinant human immunodeficiency virus envelope glycoprotein (gp120) expressed in chinese hamster ovary cells. *J. Biol. Chem.* **265**, 10373–10382 (1990).
 22. Chan, D. C., Fass, D., Berger, J. M. & Kim, P. S. Core structure of gp41 from the HIV envelope glycoprotein. *Cell* **89**, 263–273 (1997).
 23. Frankel, A. D. & Young, J. A. T. HIV-1: Fifteen Proteins and an RNA. *Annu. Rev. Biochem.* **67**, 1–25 (1998).
 24. Ugolini, S., Mondor, I. & Sattentau, Q. J. HIV-1 attachment: another look. 144–149 (1999).
 25. Geijtenbeek, T. B. H., Kwon, D. S., Torensma, R., Van Vliet, S. J., Van Duijnhoven, G. C. F., Middel, J., Cornelissen, I. L. M. H. A., Nottet, H. S. L. M., KewalRamani, V. N., Littman, D. R., Figdor, C. G. & Van Kooyk, Y. DC-SIGN, a dendritic cell-specific HIV-1-binding protein that enhances trans-infection of T cells. *Cell* **100**, 587–597 (2000).
 26. Owen, J. A., Punt, J., Stranford, S. A., Jones, P. P. & Kuby, J. *Kuby Immunology*. (2013).
 27. Kwong, P. D., Wyatt, R., Robinson, J., Sweet, R. W., Sodroski, J. & Hendrickson, W. A. Structure of an HIV gp120 envelope glycoprotein in complex with the CD4 receptor and a neutralizing human antibody. *Nature* **393**, 648–659 (1998).
 28. D'huys, T., Claes, S., Van Loy, T. & Schols, D. CXCR7/ACKR3-targeting ligands interfere with X7 HIV-1 and HIV-2 entry and replication in human host cells. *Heliyon* **4**, e00557 (2018).
 29. Wilen, C. B., Tilton, J. C. & Doms, R. W. HIV: Cell Binding and Entry. *Cold Spring Harb. Perspect. Med.* **2**, 1–14 (2012).
 30. Engelman, A. & Cherepanov, P. The structural biology of HIV-1: mechanistic and therapeutic insights. *Nat. Rev. Microbiol.* **10**, 279–290 (2012).
 31. Freed, E. O. HIV - 1 assembly, release and maturation. *Nat. Rev. Microbiol.* **13**, 484–496 (2015).
 32. Overbaugh, J. & Bangham, C. R. M. Selection forces and constraints on retroviral sequence variation. *Science (80-)*. **292**, 1106–1109 (2001).
 33. Murray, A. J., Kwon, K. J., Farber, D. L. & Siliciano, R. F. The latent reservoir for HIV-1: how immunologic memory and clonal expansion contribute to HIV-1 persistence. *J. Immunol.* **197**, 407–417 (2016).
 34. Arts, E. J. & Hazuda, D. J. HIV-1 antiretroviral drug therapy. *Cold Spring Harb. Perspect. Med.* **2**, 1–23 (2012).
 35. St. John, A. L. & Rathore, A. P. S. Adaptive immune responses to primary and secondary dengue virus infections. *Nat. Rev. Immunol.* **19**, 218–230 (2019).

36. Cao-Lormeau, V. M., Blake, A., Mons, S., Lastère, S., Roche, C., Vanhomwegen, J., Dub, T., Baudouin, L., Teissier, A., Larre, P., Vial, A.-L., Decam, C., Choumet, V., Halstead, S. K., Willison, H. J., Musset, L., Manuguerra, J.-C., ... Ghawché, F. Guillain-Barré Syndrome outbreak associated with Zika virus infection in French Polynesia: a case-control study. *Lancet* **387**, 1531–1539 (2016).
37. Mlakar, J., Korva, M., Tul, N., Popović, M., Poljšak-Prijatelj, M., Mraz, J., Kolenc, M., Resman Rus, K., Vesnaver Vipotnik, T., Fabjan Vodusek, V., Vizjak, A., Pižem, J., Petrovec, M. & Avšič Županc, T. Zika virus associated with microcephaly. *N. Engl. J. Med.* **374**, 951–958 (2016).
38. Pierson, T. C. & Diamond, M. S. The emergence of Zika virus and its new clinical syndromes. *Nature* **560**, 573–581 (2018).
39. Kuno, G., Chang, G.-J. J., Tsuchiya, K. R., Karabatsos, N. & Cropp, C. B. Phylogeny of the Genus Flavivirus. *J. Virol.* **72**, 73–83 (1998).
40. Neufeldt, C. J., Cortese, M., Acosta, E. G. & Bartenschlager, R. Rewiring cellular networks by members of the Flaviviridae family. *Nat. Rev. Immunol.* **16**, 125–142 (2018).
41. Zhang, X., Jia, R., Shen, H., Wang, M., Yin, Z. & Cheng, A. Structures and functions of the envelope glycoprotein in flavivirus infections. *Viruses* **9**, 1–14 (2017).
42. Zhang, Y., Zhang, W., Ogata, S., Clements, D., Strauss, J. H., Baker, T. S., Kuhn, R. J. & Rossman, M. G. Conformational changes of the flavivirus E glycoprotein. *Structure* **12**, 1607–1618 (2004).
43. Hasan, S. S., Sevvana, M., Kuhn, R. J. & Rossmann, M. G. Structural biology of Zika virus and other flaviviruses. *Nat. Struct. Mol. Biol.* **25**, 13–20 (2018).
44. Mead, P. S., Hills, S. L. & Brooks, J. T. Zika virus as a sexually transmitted pathogen. *Curr. Opin. Infect. Dis.* **31**, 39–44 (2018).
45. European Centre for Disease Prevention and Control. Sexual transmission of dengue in Spain - 18 November 2019. ECDC: Stockholm; 2019.
46. Perera-Lecoin, M., Meertens, L., Carnec, X. & Amara, A. Flavivirus entry receptors: an update. *Viruses* **6**, 69–88 (2013).
47. Elong Ngono, A. & Shresta, S. Immune response to dengue and Zika. *Annu. Rev. Immunol.* **36**, 279–308 (2018).
48. Laureti, M., Narayanan, D., Rodriguez-andres, J., Fazakerley, J. K. & Kedzierski, L. Flavivirus receptors: diversity, identity, and cell entry. *Front. Immunol.* **9**, 1–11 (2018).
49. Acosta, E. G., Castilla, V. & Damonte, E. B. Alternative infectious entry pathways for dengue virus serotypes into mammalian cells. *Cell. Microbiol.* **11**, 1533–1549 (2009).
50. Cruz-Oliveira, C., Freire, J. M., Conceição, T. M., Higa, L. M., Castanho, M. A. R. B. & Da Poian, A. T. Receptors and routes of dengue virus entry into the host cells. *FEMS Microbiol. Rev.* **39**, 155–170 (2015).
51. Stiasny, K. & Heinz, F. X. Flavivirus membrane fusion. *J. Gen. Virol.* **87**, 2755–2766 (2006).
52. Smit, J. M., Moesker, B., Rodenhuis-Zybert, I. & Wilschut, J. Flavivirus cell entry and membrane fusion. *Viruses* **3**, 160–171 (2011).
53. Dejarnac, O., Hafirassou, M. L., Chazal, M., Versapuech, M., Gaillard, J., Perera-Lecoin, M., Umana-Diaz, C., Bonnet-Madin, L., Carnec, X., Tinevez, J. Y., Delaugerre, C., Schwartz, O., Roingeard, P., Jouvenet, N., Berlioz-Torrent, C., Meertens, L. & Amara, A. TIM-1 ubiquitination mediates dengue virus entry. *Cell*

- Rep.* **23**, 1779–1793 (2018).
54. Agrelli, A., de Moura, R., Crovella, S. & Brandão, L. A. C. Zika virus entry mechanisms in human cells. *Infect. Genet. Evol.* **69**, 22–29 (2019).
 55. Campos, J. L. S., Mongkolsapaya, J. & Screaton, G. R. The immune response against flaviviruses. *Nat. Immunol.* **19**, 1189–1198 (2018).
 56. Wu, S. J. L., Grouard-Vogel, G., Sun, W., Mascola, J. R., Brachtel, E., Putvatana, R., Louder, M. K., Filgueira, L., Marovich, M. A., Wong, H. K., Blauvelt, A., Murphy, G. S., Robb, M. L., Innes, B. L., Birx, D. L., Hayes, C. G., Frankel, S. S., ... Wong, K. T. Phenotyping of peripheral blood mononuclear cells during acute dengue illness demonstrates infection and increased activation of monocytes in severe cases compared to classic dengue fever. *Am. J. Trop. Med. Hyg.* **6**, 1411–1418 (2000).
 57. Blackley, S., Kou, Z., Chen, H., Quinn, M., Rose, R. C., Schlesinger, J. J., Coppage, M. & Jin, X. Primary human splenic macrophages, but not T or B cells, are the principal target cells for dengue virus infection in vitro. *J. Virol.* **81**, 13325–13334 (2007).
 58. Durbin, A. P., Vargas, M. J., Wanionek, K., Hammond, S. N., Gordon, A., Rocha, C., Balmaseda, A. & Harris, E. Phenotyping of peripheral blood mononuclear cells during acute dengue illness demonstrates infection and increased activation of monocytes in severe cases compared to classic dengue fever. *Virology* **376**, 429–435 (2008).
 59. Lee, Y. R., Su, C. Y., Chow, N. H., Lai, W. W., Lei, H. Y., Chang, C. L., Chang, T. Y., Chen, S. H., Lin, Y. S., Yeh, T. M. & Liu, H. S. Dengue viruses can infect human primary lung epithelia as well as lung carcinoma cells, and can also induce the secretion of IL-6 and RANTES. *Virus Res.* **126**, 216–225 (2007).
 60. Wei, H. Y., Jiang, L. F., Fang, D. Y. & Guo, H. Y. Dengue virus type 2 infects human endothelial cells through binding of the viral envelope glycoprotein to cell surface polypeptides. *J. Gen. Virol.* **84**, 3095–3098 (2003).
 61. Couvelard, A., Marianneau, P., Bedel, C., Drouet, M. T., Vachon, F., Hénin, D. & Deubel, V. Report of a fatal case of dengue infection with hepatitis: Demonstration of dengue antigens in hepatocytes and liver apoptosis. *Hum. Pathol.* **30**, 1106–1110 (1999).
 62. Huerre, M. R., Trong Lan, N., Marianneau, P., Bac Hue, N., Khun, H., Thanh Hung, N., Thi Khen, N., Drouet, M. T., Que Huong, V. T., Quang Ha, D., Buisson, Y. & Deubel, V. Liver histopathology and biological correlates in five cases of fatal dengue fever in Vietnamese children. *Virchows Arch.* **438**, 107–115 (2001).
 63. Jessie, K., Fong, M. Y., Devi, S., Lam, S. K. & Wong, K. T. Localization of dengue virus in naturally infected human tissues, by immunohistochemistry and in situ hybridization. *J. Infect. Dis.* **189**, 1411–1418 (2004).
 64. Balsitis, S. J., Coloma, J., Castro, G., Alava, A., Flores, D., McKerrow, J. H., Robert Beatty, P. & Harris, E. Tropism of dengue virus in mice and humans defined by viral nonstructural protein 3-specific immunostaining. *Am. J. Trop. Med. Hyg.* **80**, 416–424 (2009).
 65. Miner, J. J. & Diamond, M. S. Zika virus pathogenesis and tissue tropism. *Cell Host Microbe* **21**, 134–142 (2017).
 66. Bowen, J. R., Quicke, K. M., Maddur, M. S., O'Neal, J. T., McDonald, C. E., Fedorova, N. B., Puri, V., Shabman, R. S., Pulendran, B. & Suthar, M. S. Zika virus antagonizes Type I Interferon responses during infection of human dendritic cells. *PLoS Pathog.* **13**, 1–30 (2017).
 67. Hamel, R., Dejarnac, O., Wichit, S., Ekchariyawat, P., Neyret, A., Luplertlop, N.,

- Perera-Lecoin, M., Surasombatpattana, P., Talignani, L., Thomas, F., Cao-Lormeau, V.-M., Choumet, V., Briant, L., Desprès, P., Amara, A., Yssel, H. & Missé, D. Biology of Zika virus infection in human skin cells. *J. Virol.* **89**, 8880–8896 (2015).
68. Garcez, P. P., Loiola, E. C., Da Costa, R. M., Higa, L. M., Trindade, P., Delvecchio, R., Nascimento, J. M., Brindeiro, R., Tanuri, A. & Rehen, S. K. Zika virus: Zika virus impairs growth in human neurospheres and brain organoids. *Science (80-.)*. **352**, 816–818 (2016).
 69. Retallack, H., Di Lullo, E., Arias, C., Knopp, K. A., Laurie, M. T., Sandoval-Espinosa, C., Leon, W. R. M., Krencik, R., Ullian, E. M., Spatazza, J., Pollen, A. A., Mandel-Brehm, C., Nowakowski, T. J., Kriegstein, A. R. & De Risi, J. L. Zika virus cell tropism in the developing human brain and inhibition by azithromycin. *Proc. Natl. Acad. Sci. U. S. A.* **113**, 14408–14413 (2016).
 70. Lin, M. Y., Wang, Y. L., Wu, W. L., Wolseley, V., Tsai, M. T., Radic, V., Thornton, M. E., Grubbs, B. H., Chow, R. H. & Huang, I. C. Zika virus infects intermediate progenitor cells and post-mitotic committed neurons in human fetal brain tissues. *Sci. Rep.* **7**, 1–8 (2017).
 71. Tabata, T., Petitt, M., Puerta-Guardo, H., Michlmayr, D., Wang, C., Fang-Hoover, J., Harris, E. & Pereira, L. Zika virus targets different primary human placental cells, suggesting two routes for vertical transmission. *Cell Host Microbe* **20**, 155–166 (2016).
 72. Quicke, K. M., Bowen, J. R., Johnson, E. L., McDonald, C. E., Ma, H., O’Neal, J. T., Rajakumar, A., Wrammert, J., Rimawi, B. H., Pulendran, B., Schinazi, R. F., Chakraborty, R. & Suthar, M. S. Zika virus infects human placental macrophages. *Cell Host Microbe* **20**, 83–90 (2016).
 73. Aagaard, K. M., Lahon, A., Suter, M. A., Arya, R. P., Seferovic, M. D., Vogt, M. B., Hu, M., Stossi, F., Mancini, M. A., Harris, R. A., Kahr, M., Eppes, C., Rac, M., Belfort, M. A., Park, C. S., Lacorazza, D. & Rico-Hesse, R. Primary human placental trophoblasts are permissive for Zika virus (ZIKV) replication. *Sci. Rep.* **7**, 1–14 (2017).
 74. Spencer, J. L., Lahon, A., Tran, L. L., Arya, R. P., Kneubehl, A. R., Vogt, M. B., Xavier, D., Rowley, D. R., Kimata, J. T. & Rico-Hesse, R. R. Replication of Zika virus in human prostate cells: A potential source of sexually transmitted virus. *J. Infect. Dis.* **217**, 538–547 (2018).
 75. Kumar, A., Jovel, J., Lopez-Orozco, J., Limonta, D., Airo, A. M., Hou, S., Stryapunina, I., Fibke, C., Moore, R. B. & Hobman, T. C. Human sertoli cells support high levels of zika virus replication and persistence. *Sci. Rep.* **8**, 1–11 (2018).
 76. Adams Waldorf, K. M., Stencel-Baerenwald, J. E., Kapur, R. P., Studholme, C., Boldenow, E., Vornhagen, J., Baldessari, A., Dighe, M. K., Thiel, J., Merillat, S., Armistead, B., Tisoncik-Go, J., Green, R. R., Davis, M. A., Dewey, E. C., Fairgrieve, M. R., Gatenby, J. C., ... Rajagopal, L. Fetal brain lesions after subcutaneous inoculation of Zika virus in a pregnant nonhuman primate. *Nat. Med.* **22**, 1256–1259 (2016).
 77. Hirsch, A. J., Smith, J. L., Haese, N. N., Broeckel, R. M., Parkins, C. J., Kreklywich, C., DeFilippis, V. R., Denton, M., Smith, P. P., Messer, W. B., Colgin, L. M. A., Ducore, R. M., Grigsby, P. L., Hennebold, J. D., Swanson, T., Legasse, A. W., Axthelm, M. K., ... Streblow, D. N. Zika Virus infection of rhesus macaques leads to viral persistence in multiple tissues. *PLoS Pathog.* **13**, 1–23 (2017).
 78. Mansuy, J. M., Suberbielle, E., Chapuy-Regaud, S., Mengelle, C., Bujan, L.,

- Marchou, B., Delobel, P., Gonzalez-Dunia, D., Malnou, C. E., Izopet, J. & Martin-Blondel, G. Zika virus in semen and spermatozoa. *Lancet Infect. Dis.* **16**, 1106–1107 (2016).
79. Dhiman, G., Abraham, R. & Griffin, D. E. Human Schwann cells are susceptible to infection with Zika and yellow fever viruses, but not dengue virus. *Sci. Rep.* **9**, 1–11 (2019).
 80. Chan, J. F. W., Yip, C. C. Y., Tsang, J. O. L., Tee, K. M., Cai, J. P., Chik, K. K. H., Zhu, Z., Chan, C. C. S., Choi, G. K. Y., Sridhar, S., Zhang, A. J., Lu, G., Chiu, K., Lo, A. C. Y., Tsao, S. W., Kok, K. H., Jin, D. Y., ... Yuen, K. Y. Differential cell line susceptibility to the emerging Zika virus: implications for disease pathogenesis, non-vector-borne human transmission and animal reservoirs. *Emerg. Microbes Infect.* **5**, e93 (2016).
 81. Oliveira, L. G. & Peron, J. P. S. Viral receptors for flaviviruses: Not only gatekeepers. *J. Leukoc. Biol.* **106**, 695–701 (2019).
 82. Kostyuchenko, V. A., Lim, E. X. Y., Zhang, S., Fibriansah, G., Ng, T., Ooi, J. S. G., Shi, J. & Lok, S. Structure of the thermally stable Zika virus. *Nature* **533**, 425–428 (2016).
 83. Pindi, C., Chirasani, V. R., Rahman, M. H., Ahsan, M., Revanasiddappa, P. D. & Senapati, S. Molecular basis of differential stability and temperature sensitivity of Zika versus dengue virus protein shells. *Sci. Rep.* **10**, 8411 (2020).
 84. Geijtenbeek, T. B. H. & Gringhuis, S. I. Signalling through C-type lectin receptors: Shaping immune responses. *Nature Reviews Immunology* vol. 9 465–479 (2009).
 85. Pokidysheva, E., Zhang, Y., Battisti, A. J., Bator-Kelly, C. M., Chipman, P. R., Xiao, C., Gregorio, G. G., Hendrickson, W. A., Kuhn, R. J. & Rossmann, M. G. Cryo-EM reconstruction of dengue virus in complex with the carbohydrate recognition domain of DC-SIGN. *Cell* **124**, 485–493 (2006).
 86. Liu, P., Ridilla, M., Patel, P., Betts, L., Gallichotte, E., Shahidi, L., Thompson, N. L. & Jacobson, K. Beyond attachment: Roles of DC-SIGN in dengue virus infection. *Traffic* **18**, 218–231 (2017).
 87. Chen, Y., Maguire, T., Hileman, R. E., Fromm, J. R., Esko, J. D., Linhardt, R. J. & Marks, R. M. Dengue virus infectivity depends on envelope protein binding to target cell heparan sulfate. *Nat. Med.* **3**, 3–8 (1997).
 88. Hilgard, P. & Stockert, R. Heparan sulfate proteoglycans initiate dengue virus infection of hepatocytes. *Hepatology* **32**, 1069–1077 (2000).
 89. Kim, S. Y., Zhao, J., Liu, X., Fraser, K., Lin, L., Zhang, X., Zhang, F., Dordick, J. S. & Linhardt, R. J. Interaction of Zika Virus Envelope Protein with Glycosaminoglycans. *Biochemistry* **56**, 1151–1162 (2017).
 90. Tan, C. W., Sam, I. C., Chong, W. L., Lee, V. S. & Chan, Y. F. Polysulfonate suramin inhibits Zika virus infection. *Antiviral Res.* **143**, 186–194 (2017).
 91. Aoki, C., Hidari, K. I. P. J., Itonori, S., Yamada, A., Takahashi, N., Kasama, T., Hasebe, F., Islam, M. A., Hatano, K., Matsuoka, K., Taki, T., Guo, C. T., Takahashi, T., Sakano, Y., Suzuki, T., Miyamoto, D., Sugita, M., ... Suzuki, Y. Identification and characterization of carbohydrate molecules in mammalian cells recognized by dengue virus type 2. *J. Biochem.* **139**, 607–614 (2006).
 92. Wichit, S., Jitmittraphap, A., Hidari, K. I. P. J., Thaisomboonsuk, B., Petmitr, S., Ubol, S., Aoki, C., Itonori, S., Morita, K., Suzuki, T., Suzuki, Y. & Jampangern, W. Dengue virus type 2 recognizes the carbohydrate moiety of neutral glycosphingolipids in mammalian and mosquito cells. *Microbiol. Immunol.* **55**, 135–140 (2011).

93. Lozach, P. Y., Burleigh, L., Staropoli, I., Navarro-Sanchez, E., Harriague, J., Virelizier, J. L., Rey, F. A., Desprès, P., Arenzana-Seisdedos, F. & Amara, A. Dendritic cell-specific intercellular adhesion molecule 3-grabbing non-integrin (DC-SIGN)-mediated enhancement of dengue virus infection is independent of DC-SIGN internalization signals. *J. Biol. Chem.* **280**, 23698–23708 (2005).
94. Tassaneetrithep, B., Burgess, T. H., Granelli-Piperno, A., Trumpfheller, C., Finke, J., Sun, W., Eller, M. A., Pattanapanyasat, K., Sarasombath, S., Birx, D. L., Steinman, R. M., Schlesinger, S. & Marovich, M. A. DC-SIGN (CD209) mediates dengue virus infection of human dendritic cells. *J. Exp. Med.* **197**, 823–829 (2003).
95. Navarro-Sanchez, E., Altmeyer, R., Amara, A., Schwartz, O., Fieschi, F., Virelizier, J. L., Arenzana-Seisdedos, F. & Desprès, P. Dendritic-cell-specific ICAM3-grabbing non-integrin is essential for the productive infection of human dendritic cells by mosquito-cell-derived dengue viruses. *EMBO Rep.* **4**, 723–728 (2003).
96. Carbaugh, D. L., Baric, R. S. & Lazear, H. M. Envelope Protein Glycosylation Mediates Zika Virus Pathogenesis. *J. Virol.* **93**, 1–16 (2019).
97. Routhu, N. K., Lehoux, S. D., Rouse, E. A., Bidokhti, M. R. M., Giron, L. B., Anzurez, A., Reid, S. P., Abdel-Mohsen, M., Cummings, R. D. & Byraredy, S. N. Glycosylation of zika virus is important in host–virus interaction and pathogenic potential. *Int. J. Mol. Sci.* **20**, (2019).
98. Miller, J. L., DeWet, B. J. M., Martinez-Pomares, L., Radcliffe, C. M., Dwek, R. A., Rudd, P. M. & Gordon, S. The mannose receptor mediates dengue virus infection of macrophages. *PLoS Pathog.* **4**, (2008).
99. Chen, S. T., Lin, Y. L., Huang, M. T., Wu, M. F., Cheng, S. C., Lei, H. Y., Lee, C. K., Chiou, T. W., Wong, C. H. & Hsieh, S. L. CLEC5A is critical for dengue-virus-induced lethal disease. *Nature* **453**, 672–676 (2008).
100. Yoshikawa, F. S. Y., Pietrobon, A. J., Branco, A. C. C. C., Pereira, N. Z., Oliveira, L. M. D. S., Machado, C. M., Duarte, A. J. D. S. & Sato, M. N. Zika Virus Infects Newborn Monocytes without Triggering a Substantial Cytokine Response. *J. Infect. Dis.* **220**, 32–40 (2019).
101. Meertens, L., Carnec, X., Lecoïn, M. P., Ramdasi, R., Guivel-Benhassine, F., Lew, E., Lemke, G., Schwartz, O. & Amara, A. The TIM and TAM families of phosphatidylserine receptors mediate dengue virus entry. *Cell Host Microbe* **12**, 544–557 (2012).
102. Carnec, X., Meertens, L., Dejarnac, O., Perera-Lecoïn, M., Hafirassou, M. L., Kitaura, J., Ramdasi, R., Schwartz, O. & Amara, A. The phosphatidylserine and phosphatidylethanolamine receptor CD300a binds dengue virus and enhances infection. *J. Virol.* **90**, 92–102 (2016).
103. Chu, J. J. H. & Ng, M. L. Interaction of West Nile virus with $\alpha\beta 3$ integrin mediates virus entry into cells. *J. Biol. Chem.* **279**, 54533–54541 (2004).
104. Zhu, Z., Mesci, P., Bernatchez, J. A., Gimple, R. C., Wang, X., Schafer, S. T., Wettersten, H. I., Beck, S., Clark, A. E., Wu, Q., Prager, B. C., Kim, L. J. Y., Dhanwani, R., Sharma, S., Garancher, A., Weis, S. M., Mack, S. C., ... Rich, J. N. Zika Virus Targets Glioblastoma Stem Cells through a SOX2-Integrin $\alpha\beta 5$ Axis. *Cell Stem Cell* **26**, 187–204.e10 (2020).
105. Thepparit, C. & Smith, D. R. Serotype-Specific Entry of Dengue Virus into Liver Cells: Identification of the 37-Kilodalton/67-Kilodalton High-Affinity Laminin Receptor as a Dengue Virus Serotype 1 Receptor. *J. Virol.* **78**, 12647–12656 (2004).

106. Phaik, H. T., Wan, W. J. & Cardoso, M. J. Two dimensional VOPBA reveals laminin receptor (LAMR1) interaction with dengue virus serotypes 1, 2 and 3. *Viol. J.* **2**, 1–11 (2005).
107. Upanan, S., Kuadkitkan, A. & Smith, D. R. Identification of dengue virus binding proteins using affinity chromatography. *J. Virol. Methods* **151**, 325–328 (2008).
108. Reyes-del Valle, J., Chávez-Salinas, S., Medina, F. & del Angel, R. M. Heat Shock Protein 90 and Heat Shock Protein 70 Are Components of Dengue Virus Receptor Complex in Human Cells. *J. Virol.* **79**, 4557–4567 (2005).
109. Pujhari, S., Brustolin, M., Macias, V. M., Nissly, R. H., Nomura, M., Kuchipudi, S. V. & Rasgon, J. L. Heat shock protein 70 (Hsp70) mediates Zika virus entry, replication, and egress from host cells. *Emerg. Microbes Infect.* **8**, 8–16 (2019).
110. Gao, F., Duan, X., Lu, X., Liu, Y., Zheng, L., Ding, Z. & Li, J. Novel binding between pre-membrane protein and claudin-1 is required for efficient dengue virus entry. *Biochem. Biophys. Res. Commun.* **391**, 952–957 (2010).
111. Li, Y., Kakinami, C., Li, Q., Yang, B. & Li, H. Human Apolipoprotein A-I Is Associated with Dengue Virus and Enhances Virus Infection through SR-BI. *PLoS One* **8**, (2013).
112. Alcalá, A. C., Maravillas, J. L., Meza, D., Ramirez, O. T., Ludert, J. E. & Palomares, L. A. The dengue virus non-structural protein 1 (NS1) use the scavenger receptor B1 as cell receptor in human hepatic and mosquito cells. *bioRxiv* 871988 (2019) doi:10.1101/871988.
113. Hershkovitz, O., Rosental, B., Rosenberg, L. A., Navarro-Sanchez, M. E., Jivov, S., Zilka, A., Gershoni-Yahalom, O., Brient-Litzler, E., Bedouelle, H., Ho, J. W., Campbell, K. S., Rager-Zisman, B., Despres, P. & Porgador, A. NKp44 Receptor Mediates Interaction of the Envelope Glycoproteins from the West Nile and Dengue Viruses with NK Cells. *J. Immunol.* **183**, 2610–2621 (2009).
114. Chen, Y.-C., Wang, S.-Y. & King, C.-C. Bacterial Lipopolysaccharide Inhibits Dengue Virus Infection of Primary Human Monocytes/Macrophages by Blockade of Virus Entry via a CD14-Dependent Mechanism. *J. Virol.* **73**, 2650–2657 (1999).
115. Murphy, B. R. & Whitehead, S. S. Immune response to dengue virus and prospects for a vaccine. *Annu. Rev. Immunol.* **29**, 587–619 (2011).
116. Guzman, M. G., Alvarez, M. & Halstead, S. B. Secondary infection as a risk factor for dengue hemorrhagic fever/dengue shock syndrome: An historical perspective and role of antibody-dependent enhancement of infection. *Arch. Virol.* **158**, 1445–1459 (2013).
117. Terzian, A. C. B., Schanoski, A. S., De Oliveira Mota, M. T., Da Silva, R. A., Estofolete, C. F., Colombo, T. E., Rahal, P., Hanley, K. A., Vasilakis, N., Kalil, J. & Nogueira, M. L. Viral load and cytokine response profile does not support antibody-dependent enhancement in dengue-primed Zika virus-infected patients. *Clin. Infect. Dis.* **65**, 1260–1265 (2017).
118. Moller-Tank, S. & Maury, W. Phosphatidylserine receptors: enhancers of enveloped virus entry and infection. *Virology* 565–580 (2014) doi:10.1016/j.virol.2014.09.009.Phosphatidylserine.
119. Hadinegoro, S. R., Arredondo-García, J. L., Capeding, M. R., Deseda, C., Chotpitayasunondh, T., Dietze, R., Hj Muhammad Ismail, H. I., Reynales, H., Limkittikul, K., Rivera-Medina, D. M., Tran, H. N., Bouckenoghe, A., Chansinghakul, D., Cortés, M., Fanouillere, K., Forrat, R., Frago, C., ... Saville, M. Efficacy and long-term safety of a dengue vaccine in regions of endemic disease. *N. Engl. J. Med.* **373**, 1195–1206 (2015).

120. Halstead, S. B. & Russell, P. K. Protective and immunological behavior of chimeric yellow fever dengue vaccine. *Vaccine* **34**, 1643–1647 (2016).
121. De La Guardia, C. & Leonart, R. Progress in the identification of dengue Virus entry/fusion inhibitors. *Biomed Res. Int.* **2014**, 1–13 (2014).
122. Mounce, B. C., Cesaro, T., Carrau, L., Vallet, T. & Vignuzzi, M. Curcumin inhibits Zika and chikungunya virus infection by inhibiting cell binding. *Antiviral Res.* **142**, 148–157 (2017).
123. Sharma, N., Murali, A., Singh, S. K. & Giri, R. Epigallocatechin gallate, an active green tea compound inhibits the Zika virus entry into host cells via binding the envelope protein. *Int. J. Biol. Macromol.* **104**, 1046–1054 (2017).
124. Alen, M. M. F., de Burghgraeve, T., Kaptein, S. J. F., Balzarini, J., Neyts, J. & Schols, D. Broad Antiviral activity of Carbohydrate-binding agents against the four serotypes of dengue virus in monocyte-derived dendritic cells. *PLoS One* **6**, (2011).
125. Prochnow, H., Rox, K., Birudukota, S., Weichert, L., Hotop, S.-K., Klahn, P., Mohr, K., Franz, S., Banda, D. H., Blockus, S., Schreiber, J., Haid, S., Oeyen, M., Martinez, J. P., Süßmuth, R. D., Wink, J., Meyerhans, A., ... Brönstrup, M. Labyrinthopeptins exert broad-spectrum antiviral activity through lipid-binding-mediated virolysis. *J. Virol.* **94**, 1–24 (2020).
126. Blockus, S., Sake, S. M., Wetzke, M., Grethe, C., Graalman, T., Pils, M., Le Goffic, R., Galloux, M., Prochnow, H., Rox, K., Hüttel, S., Rupcic, Z., Wiegmann, B., Dijkman, R., Rameix-Welti, M. A., Eléouët, J. F., Duprex, W. P., ... Pietschmann, T. Labyrinthopeptins as virolytic inhibitors of respiratory syncytial virus cell entry. *Antiviral Res.* **177**, 104774 (2020).
127. Férir, G., Petrova, M. I., Andrei, G., Huskens, D., Hoorelbeke, B., Snoeck, R., Vanderleyden, J., Balzarini, J., Bartoschek, S., Brönstrup, M., Süßmuth, R. D. & Schols, D. The lantibiotic peptide labyrinthopeptin A1 demonstrates broad anti-HIV and anti-HSV activity with potential for microbicidal applications. *PLoS One* **8**, (2013).
128. de Wispelaere, M., Lian, W., Potisopon, S., Li, P., Jang, J., Ficarro, S., Clark, M. J., Zhu, X., Kaplan, J. B., Pitts, J. D., Wales, T. E., Wang, J., Engen, J. R., Marto, J., Gray, N. S. & Yang, P. L. Inhibition of flaviviruses by targeting a conserved pocket on the viral envelope protein. *Cell Chem. Biol.* **25**, 1006–1016 (2018).
129. Taguwa, S., Yeh, M. Te, Rainbolt, T. K., Nayak, A., Shao, H., Gestwicki, J. E., Andino, R. & Frydman, J. Zika Virus Dependence on Host Hsp70 Provides a Protective Strategy against Infection and Disease. *Cell Rep.* **26**, 906–920.e3 (2019).
130. Taguwa, S., Maringer, K., Li, X., Bernal-Rubio, D., Rauch, J. N., Gestwicki, J. E., Andino, R., Fernandez-Sesma, A. & Frydman, J. Defining Hsp70 subnetworks in dengue virus replication reveals key vulnerability in Flavivirus infection. *Cell* **163**, 1108–1123 (2015).
131. Cagno, V., Tseligka, E. D., Jones, S. T. & Tapparel, C. Heparan sulfate proteoglycans and viral attachment: True receptors or adaptation bias? *Viruses* **11**, 1–24 (2019).
132. Rausch, K., Hackett, B. A., Weinbren, N. L., Reeder, S. M., Sadovsky, Y., Hunter, C. A., Schultz, D. C., Coyne, C. B. & Cherry, S. Screening bioactives reveals Nanchangmycin as a broad spectrum antiviral active against Zika virus. *Cell Rep.* **18**, 804–815 (2017).
133. Merits, A., Varghese, F. S., Saul, S., Rausalu, K., Susi, P., Hakanen, M., Kümmerer, B. M. & Ahola, T. Obatoclax Inhibits Alphavirus Membrane Fusion

- by Neutralizing the Acidic Environment of Endocytic Compartments. *Antimicrob. Agents Chemother.* **61**, 1–17 (2016).
134. Li, F., Lang, Y., Ji, Z., Xia, Z., Han, Y., Cheng, Y., Liu, G., Sun, F., Zhao, Y., Gao, M., Chen, Z., Wu, Y., Li, W. & Cao, Z. A scorpion venom peptide Ev37 restricts viral late entry by alkalizing acidic organelles. *J. Biol. Chem.* **294**, 182–194 (2019).
 135. Jung, E., Nam, S., Oh, H., Jun, S., Ro, H. J., Kim, B., Kim, M. & Go, Y. Y. Neutralization of Acidic Intracellular Vesicles by Niclosamide Inhibits Multiple Steps of the Dengue Virus Life Cycle In Vitro. *Sci. Rep.* **9**, 1–12 (2019).
 136. De Clercq, E. & Li, G. Approved antiviral drugs over the past 50 years. *Clin. Microbiol. Rev.* **29**, 695–747 (2016).
 137. Sidwell, R. W., Huffman, J. H., Khare G. P., L., Allen, B., Witkowski J. T., R. & Robins, K. Broad-spectrum antiviral activity of Virazole: 1-f8- D-Ribofuranosyl-1,2,4-triazole- 3-carboxamide. *Science (80-)*. **177**, 705 LP-706 (1972).
 138. Krueger, R. F. & Mayer, G. D. Tilorone hydrochloride: an orally active antiviral agent. *Science (80-)*. **169**, 1213 LP-1214 (1970).
 139. Andersen, P. I., Ianevski, A., Lysvand, H., Vitkauskiene, A., Oksenysh, V., Bjørås, M., Telling, K., Lutsar, I., Dumpis, U., Irie, Y., Tensen, T., Kantele, A. & Kainov, D. E. Discovery and development of safe-in-man broad-spectrum antiviral agents. *Int. J. Infect. Dis.* **93**, 268–276 (2020).
 140. Bekerman, B. E. & Einav, S. Combating emerging viral threats. *Science (80-)*. **348**, 282–283 (2015).
 141. Wang, Y., Zhang, D., Du, G., Du, R., Zhao, J., Jin, Y., Fu, S., Gao, L., Cheng, Z., Lu, Q., Hu, Y., Luo, G., Wang, K., Lu, Y., Li, H., Wang, S., Ruan, S., ... Wang, C. Remdesivir in adults with severe COVID-19: a randomised, double-blind, placebo-controlled, multicentre trial. *Lancet* **395**, 1569–1578 (2020).
 142. Goldman, J. D., Lye, D. C. B., Hui, D. S., Marks, K. M., Bruno, R., Montejano, R., Spinner, C. D., Galli, M., Ahn, M.-Y., Nahass, R. G., Chen, Y.-S., SenGupta, D., Hyland, R. H., Osinusi, A. O., Cao, H., Blair, C., Wei, X., ... Subramanian, A. Remdesivir for 5 or 10 days in patients with severe covid-19. *N. Engl. J. Med.* 1–11 (2020) doi:10.1056/nejmoa2015301.
 143. DiMasi, J. A., Grabowski, H. G. & Hansen, R. W. Innovation in the pharmaceutical industry: new estimates of R&D costs. *J. Health Econ.* **47**, 20–33 (2016).
 144. Mazzon, M. & Marsh, M. Targeting viral entry as a strategy for broad-spectrum antivirals. *F1000 Res.* **8**, 1–10 (2019).
 145. Wang, Q. Y. & Shi, P.-Y. Flavivirus entry inhibitors. *ACS Infect. Dis.* **1**, 428–434 (2015).
 146. Martin, S. J., Reutelingsperger, C. P., McGahon, a J., Rader, J. a, van Schie, R. C., LaFace, D. M. & Green, D. R. Early redistribution of plasma membrane phosphatidylserine is a general feature of apoptosis regardless of the initiating stimulus: inhibition by overexpression of Bcl-2 and Abl. *J. Exp. Med.* **182**, 1545–1556 (1995).
 147. Voll, R. E., Herrmann, M., Roth, E. A., Stach, C., Kalden, J. R. & Girkontaite, I. Immunosuppressive effects of apoptotic cells. *Nature* **390**, 350–351 (1997).
 148. Amara, A. & Mercer, J. Viral apoptotic mimicry. *Nat. Rev. Microbiol.* **13**, 461–469 (2015).
 149. Morizono, K. & Chen, I. S. Y. Role of phosphatidylserine receptors in enveloped virus infection. *J. Virol.* **88**, 4275–4290 (2014).
 150. Liu, S., Delalio, L. J., Isakson, B. E. & Wang, T. T. AXL-mediated productive

- infection of human endothelial cells by Zika virus. *Circ. Res.* **119**, 1183–1189 (2016).
151. Richard, A. S., Shim, B. S., Kwon, Y. C., Zhang, R., Otsuka, Y., Schmitt, K., Berri, F., Diamond, M. S. & Choe, H. AXL-dependent infection of human fetal endothelial cells distinguishes Zika virus from other pathogenic flaviviruses. *Proc. Natl. Acad. Sci. U. S. A.* **114**, 2024–2029 (2017).
 152. Nowakowski, T. J., Pollen, A. A., Di Lullo, E., Sandoval-Espinosa, C., Bershteyn, M. & Kriegstein, A. R. Expression analysis highlights AXL as a candidate Zika virus entry receptor in neural stem cells. *Cell Stem Cell* **18**, 591–596 (2016).
 153. Meertens, L., Labeau, A., Dejarnac, O., Cipriani, S., Sinigaglia, L., Bonnet-Madin, L., Le Charpentier, T., Hafirassou, M. L., Zamborlini, A., Cao-Lormeau, V. M., Couplier, M., Missé, D., Jouvenet, N., Tabibiazar, R., Gressens, P., Schwartz, O. & Amara, A. Axl mediates Zika virus entry in human glial cells and modulates innate immune responses. *Cell Rep.* **18**, 324–333 (2017).
 154. Wells, M. F., Salick, M. R., Wiskow, O., Ho, D. J., Worringer, K. A., Ihry, R. J., Kommineni, S., Bilican, B., Klim, J. R., Hill, E. J., Kane, L. T., Ye, C., Kaykas, A. & Eggan, K. Genetic ablation of AXL does not protect human neural progenitor cells and cerebral organoids from Zika virus infection. *Cell Stem Cell* **19**, 703–708 (2016).
 155. Govero, J., Esakky, P., Scheaffer, S. M., Fernandez, E., Drury, A., Platt, D. J., Gorman, M. J., Richner, J. M., Caine, E. A., Salazar, V., Moley, K. H. & Diamond, M. S. Zika virus infection damages the testes in mice. *Nature* **540**, 438–442 (2016).
 156. Hastings, A. K., Yockey, L. J., Jagger, B. W., Hwang, J., Uraki, R., Gaitsch, H. F., Parnell, L. A., Cao, B., Mysorekar, I. U., Rothlin, C. V., Fikrig, E., Diamond, M. S. & Iwasaki, A. TAM receptors are not required for Zika virus infection in mice. *Cell Rep.* **19**, 558–568 (2017).
 157. Jemielity, S., Wang, J. J., Chan, Y. K., Ahmed, A. A., Li, W., Monahan, S., Bu, X., Farzan, M., Freeman, G. J., Umetsu, D. T., DeKruyff, R. H. & Choe, H. TIM-family proteins promote infection of multiple enveloped viruses through virion-associated phosphatidylserine. *PLoS Pathog.* **9**, (2013).
 158. Moller-Tank, S., Kondratowicz, A. S., Davey, R. A., Rennert, P. D. & Maury, W. Role of the phosphatidylserine receptor TIM-1 in enveloped-virus entry. *J. Virol.* **87**, 8327–8341 (2013).
 159. Marsh, D. G., Neely, J. D., Breazeale, D. R., Ghosh, B., Freidhoff, L. R., Ehrlich-Kautzy, E., Schou, C., Krishnaswamy, G. & Beaty, T. H. Linkage analysis of IL4 and other chromosome 5q31.1 markers and total serum immunoglobulin E concentrations. *Science (80-.)*. **264**, 1152–1156 (1994).
 160. Postma, D. S., Bleecker, E. R., Amelung, P. J., Holroyd, K. J., Xu, J., Panhuysen, C. I. M., Meyers, D. A. & Levitt, R. C. Genetic susceptibility to asthma — bronchial hyperresponsiveness. *N. Engl. J. Med.* **333**, 894–900 (1995).
 161. McIntire, J. J., Umetsu, S. E., Akbari, O., Potter, M., Kuchroo, V. K., Barsh, G. S., Freeman, G. J., Umetsu, D. T. & DeKruyff, R. H. Identification of Tapr (an airway hyperreactivity regulatory locus) and the linked Tim gene family. *Nat. Immunol.* **2**, 1109–1116 (2001).
 162. Kaplan, G., Totsuka, A., Thompson, P., Akatsuka, T., Moritsugu, Y. & Feinstone, S. M. Identification of a surface glycoprotein on African green monkey kidney cells as a receptor for hepatitis A virus. *EMBO J.* **15**, 4282–4296 (1996).
 163. Feigelstock, D., Thompson, P., Mattoo, P., Zhang, Y. & Kaplan, G. G. The Human Homolog of HAVcr-1 Codes for a Hepatitis A Virus Cellular Receptor. *J.*

- Viol.* **72**, 6621–6628 (1998).
164. Ichimura, T., Bonventre, J. V., Bailly, V., Wei, H., Hession, C. A., Cate, R. L. & Sanicola, M. Kidney injury molecule-1 (KIM-1), a putative epithelial cell adhesion molecule containing a novel immunoglobulin domain, is up-regulated in renal cells after injury. *J. Biol. Chem.* **273**, 4135–4142 (1998).
 165. Lemke, G. Biology of the TAM receptors. *Cold Spring Harb. Perspect. Biol.* **5**, 1–17 (2013).
 166. Freeman, G. J., Casasnovas, J. M., Umetsu, D. T. & Dekruyff, R. H. TIM genes: A family of cell surface phosphatidylserine receptors that regulate innate and adaptive immunity. *Immunol. Rev.* **235**, 172–189 (2010).
 167. Santiago, C., A, B., Martinez-Munoz, L., M, M., Kaplan, G. G., Freeman, G. J. & Casasnovas, J. M. TIM-4 structures identify a metal ion-dependent ligand binding site where phosphatidylserine binds. *Immunity* **27**, 941–951 (2007).
 168. Kobayashi, N., Karisola, P., Peña-Cruz, V., Dorfman, D. M., Jinushi, M., Umetsu, S. E., Butte, M. J., Nagumo, H., Chernova, I., Zhu, B., Sharpe, A. H., Ito, S., Dranoff, G., Kaplan, G. G., Casasnovas, J. M., Umetsu, D. T., DeKruyff, R. H. & Freeman, G. J. TIM-1 and TIM-4 glycoproteins bind phosphatidylserine and mediate uptake of apoptotic cells. *Immunity* **27**, 927–940 (2007).
 169. Balasubramanian, S., Kota, S. K., Kuchroo, V. K., Humphreys, B. D. & Strom, T. B. TIM family proteins promote the lysosomal degradation of the nuclear receptor NUR77. *Sci. Signal.* **5**, 1–7 (2013).
 170. Echbarthi, M., Zonca, M., Mellwig, R., Schwab, Y., Kaplan, G., Dekruyff, R. H., Roda-Navarro, P. & Casasnovas, J. M. Distinct trafficking of cell surface and endosomal TIM-1 to the immune synapse. *Traffic* **16**, 1193–1207 (2015).
 171. Richard, A. S., Zhang, A., Park, S.-J., Farzan, M., Zong, M. & Choe, H. Virion-associated phosphatidylethanolamine promotes TIM1-mediated infection by Ebola, dengue, and West Nile viruses. *Proc. Natl. Acad. Sci.* **112**, 14682–14687 (2015).
 172. Meyers, J. H., Chakravarti, S., Schlesinger, D., Illes, Z., Waldner, H., Umetsu, S. E., Kenny, J., Zheng, X. X., Umetsu, D. T., DeKruyff, R. H., Strom, T. B. & Kuchroo, V. K. TIM-4 is the ligand for TIM-1, and the TIM-1-TIM-4 interaction regulates T cell proliferation. *Nat. Immunol.* **6**, 455–464 (2005).
 173. Angiari, S., Donnarumma, T., Rossi, B., Dusi, S., Pietronigro, E., Zenaro, E., DellaBianca, V., Toffali, L., Piacentino, G., Budui, S., Rennert, P., Xiao, S., Laudanna, C., Casasnovas, J. M., Kuchroo, V. K. & Constantin, G. TIM-1 glycoprotein binds the adhesion receptor P-selectin and mediates T cell trafficking during inflammation and autoimmunity. *Immunity* **40**, 542–553 (2014).
 174. Umetsu, S. E., Lee, W. L., McIntire, J. J., Downey, L., Sanjanwala, B., Akbari, O., Berry, G. J., Nagumo, H., Freeman, G. J., Umetsu, D. T. & DeKruyff, R. H. TIM-1 induces T cell activation and inhibits the development of peripheral tolerance. *Nat. Immunol.* **6**, 447–454 (2005).
 175. De Souza, A. J., Oriss, T. B., O'Malley, K. J., Ray, A. & Kane, L. P. T cell Ig and mucin 1 (TIM-1) is expressed on in vivo-activated T cells and provides a costimulatory signal for T cell activation. *Proc. Natl. Acad. Sci. U. S. A.* **102**, 17113–17118 (2005).
 176. de Souza, A. J., Oak, J. S., Jordanhazy, R., DeKruyff, R. H., Fruman, D. A. & Kane, L. P. T cell Ig and mucin domain-1-mediated T cell activation requires recruitment and activation of phosphoinositide 3-kinase. *J. Immunol.* **180**, 6518–6526 (2008).
 177. Mariat, C., Degauque, N., Balasubramanian, S., Kenny, J., DeKruyff, R. H.,

- Umetsu, D. T., Kuchroo, V., Zheng, X. X. & Strom, T. B. Tim-1 signaling substitutes for conventional signal 1 and requires costimulation to induce T cell proliferation. *J. Immunol.* **182**, 1379–1385 (2009).
178. Binné, L. L., Scott, M. L. & Rennert, P. D. Human TIM-1 Associates with the TCR Complex and Up-Regulates T Cell Activation Signals. *J. Immunol.* **178**, 4342–4350 (2007).
 179. Xiao, S., Najafian, N., Reddy, J., Albin, M., Zhu, C., Jensen, E., Imitola, J., Korn, T., Anderson, A. C., Zhang, Z., Gutierrez, C., Moll, T., Sobel, R. A., Umetsu, D. T., Yagita, H., Akiba, H., Strom, T., ... Kuchroo, V. K. Differential engagement of Tim-1 during activation can positively or negatively costimulate T cell expansion and effector function. *J. Exp. Med.* **204**, 1691–1702 (2007).
 180. Sonar, S. S., Hsu, Y. M., Conrad, M. L., Majeau, G. R., Kilic, A., Garber, E., Gao, Y., Nwankwo, C., Willer, G., Dudda, J. C., Kim, H., Bailly, V., Pagenstecher, A., Rennert, P. D. & Renz, H. Antagonism of TIM-1 blocks the development of disease in a humanized mouse model of allergic asthma. *J. Clin. Invest.* **120**, 2767–2781 (2010).
 181. Rodriguez-Manzanet, R., Hartt-Meyers, J., Balasubramanian, S., Slavik, J., Dardalhon, V., Kassam, N., Greenfield, E. A., Sobel, R. A., Strom, T. B., Hafler, D. A. & Kuchroo, V. K. Tim-4 expressed on antigen-presenting cells induces T cell expansion and survival. *Clin. Immunol.* **123**, 4706–4713 (2008).
 182. Ichimura, T., Asseldonk, E. J. P. V., Humphreys, B. D., Gunaratnam, L., Duffield, J. S. & Bonventre, J. V. Kidney injury molecule-1 is a phosphatidylserine receptor that confers a phagocytic phenotype on epithelial cells. *J. Clin. Invest.* **118**, 1657–1668 (2008).
 183. Angiari, S. & Constantin, G. Regulation of T cell trafficking by the T cell immunoglobulin and mucin domain 1 glycoprotein. *Trends Mol. Med.* **20**, 675–684 (2014).
 184. McIntire, J. J., Umetsu, D. T. & DeKruyff, R. H. TIM-1, a novel allergy and asthma susceptibility gene. *Springer Semin. Immunopathol.* **25**, 335–348 (2004).
 185. Xie, X., Shi, X., Chen, P. & Rao, L. Associations of TIM-1 genetic polymorphisms with asthma: a meta-analysis. *Lung* **195**, 353–360 (2017).
 186. McIntire, J. J., Umetsu, S. E., Macaubas, C., Hoyte, E. G., Cinnioglu, C., Cavalli-Sforza, L. L., Barsh, G. S., Hallmayer, J. F., Underhill, P. A., Risch, N. J., Freeman, G. J., DeKruyff, R. H. & Umetsu, D. T. Hepatitis A virus link to atopic disease. *Nature* **425**, 576 (2003).
 187. Chae, S. C., Song, J. H., Shim, S. C., Yoon, K. S. & Chung, H. T. The exon 4 variations of Tim-1 gene are associated with rheumatoid arthritis in a Korean population. *Biochem. Biophys. Res. Commun.* **315**, 971–975 (2004).
 188. Yu, Y., Zhu, C., Zhou, S. & Chi, S. Association between C1q, TRAIL, and Tim-1 Gene Polymorphisms and Systemic Lupus Erythematosus. *Genet. Test. Mol. Biomarkers* **22**, 546–553 (2018).
 189. Song, J., Yu, J., Prayogo, G. W., Cao, W., Wu, Y., Jia, Z. & Zhang, A. Understanding kidney injury molecule 1: A novel immune factor in kidney pathophysiology. *Am. J. Transl. Res.* **11**, 1219–1229 (2019).
 190. Thomas, L. J., Vitale, L., O'Neill, T., Dolnick, R. Y., Wallace, P. K., Minderman, H., Gergel, L. E., Forsberg, E. M., Boyer, J. M., Storey, J. R., Pilsmaier, C. D., Hammond, R. A., Widger, J., Sundarapandian, K., Crocker, A., Marsh, H. C. & Keler, T. Development of a novel antibody-drug conjugate for the potential treatment of ovarian, lung, and renal cell carcinoma expressing TIM-1. *Mol. Cancer Ther.* **15**, 2946–2954 (2016).

191. Niu, J., Jiang, Y., Xu, H., Zhao, C., Zhou, G., Chen, P. & Cao, R. TIM-1 promotes Japanese encephalitis virus entry and infection. *Viruses* **10**, 1–17 (2018).
192. Wang, J., Qiao, L., Hou, Z. & Luo, G. TIM-1 promotes hepatitis C virus cell attachment and infection. *J. Virol.* **91**, 1–13 (2017).
193. Kondratowicz, A. S., Lennemann, N. J., Sinn, P. L., Davey, R. A., Hunt, C. L., Moller-Tank, S., Meyerholz, D. K., Rennert, P., Mullins, R. F., Brindley, M., Sandersfeld, L. M., Quinn, K., Weller, M., McCray, P. B., Chiorini, J. & Maury, W. T-cell immunoglobulin and mucin domain 1 (TIM-1) is a receptor for Zaire ebolavirus and Lake Victoria marburgvirus. *Proc. Natl. Acad. Sci. U. S. A.* **108**, 8426–8431 (2011).
194. Moller-Tank, S., Albritton, L. M., Rennert, P. D. & Maury, W. Characterizing Functional Domains for TIM-Mediated Enveloped Virus Entry. *J. Virol.* **88**, 6702–6713 (2014).
195. Brouillette, R. B., Phillips, E. K., Patel, R., Mahauad-Fernandez, W., Moller-Tank, S., Rogers, K. J., Dillard, J. A., Cooney, A. L., Martinez-Sobrido, L., Okeoma, C. & Maury, W. TIM-1 mediates dystroglycan-independent entry of Lassa virus. *J. Virol.* **92**, 1–15 (2018).
196. Younan, P., Iampietro, M., Nishida, A., Ramanathan, P., Santos, R. I., Dutta, M., Lubaki, N. M., Koup, R. A., Katze, M. G. & Bukreyev, A. Ebola virus binding to Tim-1 on T lymphocytes induces a cytokine storm. *MBio* **8**, 1–20 (2017).
197. Brunton, B., Rogers, K., Phillips, E. K., Brouillette, R. B., Bouls, R., Butler, N. S. & Maury, W. TIM-1 serves as a receptor for ebola virus in vivo, enhancing viremia and pathogenesis. *PLoS Negl. Trop. Dis.* **13**, 1–20 (2019).
198. Li, M., Ablan, S. D., Miao, C., Zheng, Y. M., Fuller, M. S., Rennert, P. D., Maury, W., Johnson, M. C., Freed, E. O. & Liu, S. L. TIM-family proteins inhibit HIV-1 release. *Proc. Natl. Acad. Sci. U. S. A.* **111**, (2014).
199. Li, M., Waheed, A. A., Yu, J., Zeng, C., Chen, H. Y., Zheng, Y. M., Feizpour, A., Reinhard, B. M., Gummuluru, S., Lin, S., Freed, E. O. & Liu, S. L. TIM-mediated inhibition of HIV-1 release is antagonized by Nef but potentiated by SERINC proteins. *Proc. Natl. Acad. Sci. U. S. A.* **116**, 5705–5714 (2019).
200. Chua, B. A., Ngo, J. A., Situ, K. & Morizono, K. Roles of phosphatidylserine exposed on the viral envelope and cell membrane in HIV-1 replication. *Cell Commun. Signal.* **17**, 1–9 (2019).
201. Sizing, I. D., Bailly, V., McCoon, P., Chang, W., Rao, S., Pablo, L., Rennard, R., Walsh, M., Li, Z., Zafari, M., Dobles, M., Tarilonte, L., Miklasz, S., Majeau, G., Godbout, K., Scott, M. L. & Rennert, P. D. Epitope-dependent effect of anti-murine TIM-1 monoclonal antibodies on T cell activity and lung immune responses. *J. Immunol.* **178**, 2249–2261 (2007).
202. Vega-Carrascal, I., Reeves, E. P. & McElvaney, N. G. The role of TIM-containing molecules in airway disease and their potential as therapeutic targets. *J. Inflamm. Res.* **5**, 77–87 (2012).
203. Hosseini, H., Yi, L., Kanellakis, P., Cao, A., Tay, C., Peter, K., Bobik, A., Toh, B. H. & Kyaw, T. Anti-TIM-1 monoclonal antibody (RMT1-10) attenuates atherosclerosis by expanding IgM-producing B1a cells. *J. Am. Heart Assoc.* **7**, 1–16 (2018).
204. Du, P., Xiong, R., Li, X. & Jiang, J. Immune regulation and antitumor effect of TIM-1. *J. Immunol. Res.* **2016**, (2016).
205. McGregor, B. A., Gordon, M., Flippot, R., Agarwal, N., George, S., Quinn, D. I., Rogalski, M., Hawthorne, T., Keler, T. & Choueiri, T. K. Safety and efficacy of CDX-014, an antibody-drug conjugate directed against T cell immunoglobulin

- mucin-1 in advanced renal cell carcinoma. *Invest. New Drugs* (2020) doi:10.1007/s10637-020-00945-y.
206. Yang, L., Kuchroo, V., Bonventre, J. V., Yang, L., Brooks, C. R., Xiao, S., Sabbisetti, V., Yeung, M. Y., Hsiao, L., Ichimura, T., Kuchroo, V. & Bonventre, J. V. KIM-1 – mediated phagocytosis reduces acute injury to the kidney Find the latest version: KIM-1 – mediated phagocytosis reduces acute injury to the kidney. **125**, 1620–1636 (2015).
 207. Clark, G. J., Ju, X., Tate, C. & Hart, D. N. J. The CD300 family of molecules are evolutionarily significant regulators of leukocyte functions. *Trends Immunol.* **30**, 209–217 (2009).
 208. Borrego, F. The CD300 molecules: An emerging family of regulators of the immune system. *Blood* **121**, 1951–1960 (2013).
 209. Vitallé, J., Terrén, I., Orrantia, A., Zenarruzabeitia, O. & Borrego, F. CD300 receptor family in viral infections. *Eur. J. Immunol.* **49**, 364–374 (2019).
 210. Zenarruzabeitia, O., Vitallé, J., Eguizabal, C., Simhadri, V. R. & Borrego, F. The Biology and Disease Relevance of CD300a, an Inhibitory Receptor for Phosphatidylserine and Phosphatidylethanolamine. *J. Immunol.* **194**, 5053–5060 (2015).
 211. Alvarez, Y., Tang, X., Coligan, J. E. & Borrego, F. The CD300a (IRp60) inhibitory receptor is rapidly up-regulated on human neutrophils in response to inflammatory stimuli and modulates CD32a (FcγRIIa) mediated signaling. *Mol. Immunol.* **45**, 253–258 (2008).
 212. Simhadri, V. R., Andersen, J. F., Calvo, E., Choi, S. C., Coligan, J. E. & Borrego, F. Human CD300a binds to phosphatidylethanolamine and phosphatidylserine, and modulates the phagocytosis of dead cells. *Blood* **119**, 2799–2809 (2012).
 213. Nielsen, R., Bustamante, C., Clark, A. G., Glanowski, S., Sackton, T. B., Hubisz, M. J., Fledel-Alon, A., Tanenbaum, D. M., Civello, D., White, T. J., Sninsky, J. J., Adams, M. D. & Cargill, M. A scan for positively selected genes in the genomes of humans and chimpanzees. *PLoS Biol.* **3**, 0976–0985 (2005).
 214. Rozenberg, P., Reichman, H., Moshkovits, I. & Munitz, A. CD300 family receptors regulate eosinophil survival, chemotaxis, and effector functions. *J. Leukoc. Biol.* **104**, 21–29 (2018).
 215. Kang, X., Kim, J., Deng, M., John, S., Chen, H., Wu, G., Phan, H. & Zhang, C. C. Inhibitory leukocyte immunoglobulin-like receptors: Immune checkpoint proteins and tumor sustaining factors. *Cell Cycle* **15**, 25–40 (2016).
 216. Speckman, R. A., Wright Daw, J. A., Helms, C., Duan, S., Cao, L., Taillon-Miller, P., Kwok, P. Y., Menter, A. & Bowcock, A. M. Novel immunoglobulin superfamily gene cluster, mapping to a region of human chromosome 17q25, linked to psoriasis susceptibility. *Hum. Genet.* **112**, 34–41 (2003).
 217. Coustan-Smith, E., Song, G., Clark, C., Key, L., Liu, P., Mehrpooya, M., Stow, P., Su, X., Shurtleff, S., Pui, C. H., Downing, J. R. & Campana, D. New markers for minimal residual disease detection in acute lymphoblastic leukemia. *Blood* **117**, 6267–6276 (2011).
 218. Burakoff, R., Chao, S., Perencevich, M., Ying, J., Friedman, S., Makrauer, F., Odze, R., Khurana, H. & Liew, C. C. Blood-based biomarkers can differentiate ulcerative colitis from Crohn's disease and noninflammatory diarrhea. *Inflamm. Bowel Dis.* **17**, 1719–1725 (2011).
 219. Silva, R., Moir, S., Kardava, L., Debell, K., Simhadri, V. R., Ferrando-Martínez, S., Leal, M., Peña, J., Coligan, J. E. & Borrego, F. CD300a is expressed on human B cells, modulates BCR-mediated signaling, and its expression is down-

- regulated in HIV infection. *Blood* **117**, 5870–5880 (2011).
220. Vitallé, J., Tarancón-Díez, L., Jiménez-Leon, M. R., Terrén, I., Orrantia, A., Roca-Oporto, C., López-Cortés, L., Ruiz-Mateos, E., Zenarruzabeitia, O. & Borrego, F. CD300a identifies a CD4⁺ memory T cell subset with a higher susceptibility to HIV-1 infection. *AIDS Publish Ah*, (2020).
 221. Bachelet, I., Munitz, A. & Levi-Schaffer, F. Abrogation of allergic reactions by a bispecific antibody fragment linking IgE to CD300a. *J. Allergy Clin. Immunol.* **117**, 1314–1320 (2006).
 222. Alen, M. M. F., Kaptein, S. J. F., De Burghgraeve, T., Balzarini, J., Neyts, J. & Schols, D. Antiviral activity of carbohydrate-binding agents and the role of DC-SIGN in dengue virus infection. *Virology* **387**, 67–75 (2009).
 223. Pannecouque, C., Daelemans, D. & De Clercq, E. Tetrazolium-based colorimetric assay for the detection of HIV replication inhibitors: Revisited 20 years later. *Nat. Protoc.* **3**, 427–434 (2008).
 224. Lambeth, C. R., White, L. J., Johnston, R. E. & Silva, a M. De. Flow cytometry-based assay for titrating dengue virus. *J. Clin. Microbiol.* **43**, 3267–3272 (2005).
 225. Pauwels, R., Balzarini, J., Baba, M., Snoeck, R., Schols, D., Herdewijn, P., Desmyter, J. & De Clercq, E. Rapid and automated tetrazolium-based colorimetric assay for the detection of anti-HIV compounds. *J. Virol. Methods* **20**, 309–321 (1988).
 226. Van Hout, A., D’Huys, T., Oeyen, M., Schols, D. & Van Loy, T. Comparison of cell-based assays for the identification and evaluation of competitive CXCR4 inhibitors. *PLoS One* **12**, 1–18 (2017).
 227. Montefiori, D. C. HIV Protocols. **485**, (2009).
 228. Schols, D., Struyf, S., Van Damme, J., Esté, J. A., Henson, G. & De Clercq, E. Inhibition of T-tropic HIV strains by selective antagonization of the chemokine receptor CXCR4. *J. Exp. Med* **186**, 2–7 (1997).
 229. Daelemans, D., Pauwels, R., De Clercq, E. & Pannecouque, C. A time-of-drug addition approach to target identification of antiviral compounds. *Nat. Protoc.* **6**, 925–933 (2011).
 230. Gordts, S. C., Férir, G., D’huys, T., Petrova, M. I., Lebeer, S., Snoeck, R., Andrei, G. & Schols, D. The low-cost compound lignosulfonic acid (LA) exhibits broad-spectrum anti-HIV and anti-HSV activity and has potential for microbicidal applications. *PLoS One* **10**, e0131219 (2015).
 231. Férir, G., Hänchen, A., François, K. O., Hoorelbeke, B., Huskens, D., Dettner, F., Süßsmuth, R. D. & Schols, D. Feglymycin, a unique natural bacterial antibiotic peptide, inhibits HIV entry by targeting the viral envelope protein gp120. *Virology* **433**, 308–319 (2012).
 232. Balzarini, J., Van Herrewege, Y., Vermeire, K., Vanham, G. & Schols, D. Carbohydrate-binding agents efficiently prevent Dendritic Cell-Specific Intercellular adhesion molecule-3 – Grabbing Nonintegrin (DC-SIGN)-directed HIV-1 transmission to T lymphocytes. *Mol. Pharmacol.* **71**, 3–11 (2007).
 233. Esté, J. A., Schols, D., De Vreese, K., Van Laethem, K., Vandamme, A.-M., Desmyter, J. & De Clercq, E. Development of resistance of human immunodeficiency virus type 1 to dextran sulfate associated with the emergence of specific mutations in the envelope gp120 glycoprotein. *Mol. Pharmacol.* **52**, 98–104 (1997).
 234. de Vreese, K., Kofler-Mongold, V., Leutgeb, C., Weber, V., Vermeire, K., Schacht, S., Anné, J., de Clercq, E., Datema, R. & Werner, G. The molecular target of bicyclams, potent inhibitors of human immunodeficiency virus

- replication. *J. Virol.* **70**, 689–96 (1996).
235. Huskens, D., Van Laethem, K., Vermeire, K., Balzarini, J. & Schols, D. Resistance of HIV-1 to the broadly HIV-1-neutralizing, anti-carbohydrate antibody 2G12. *Virology* **360**, 294–304 (2007).
 236. Drosten, C., Götting, S., Schilling, S., Asper, M., Panning, M., Schmitz, H. & Günther, S. Rapid detection and quantification of RNA of Ebola and Marburg viruses, Lassa virus, Crimean-Congo hemorrhagic fever virus, Rift Valley fever virus, dengue virus, and yellow fever virus by real-time reverse transcription-PCR. *J. Clin. Microbiol.* **40**, 2323–2330 (2002).
 237. De Burghgraeve, T., Selisko, B., Kaptein, S., Chatelain, G., Leyssen, P., Debing, Y., Jacobs, M., Van Aerschot, A., Canard, B. & Neyts, J. 3',5' Di-o-trityluridine inhibits in vitro flavivirus replication. *Antiviral Res.* **98**, 242–247 (2013).
 238. Lanciotti, R. S., Kosoy, O. L., Laven, J. J., Velez, J. O., Lambert, A. J., Johnson, A. J., Stanfield, S. M. & Duffy, M. R. Genetic and serologic properties of Zika virus associated with an epidemic, Yap State, Micronesia, 2007. *Emerg. Infect. Dis.* **14**, 1232–1239 (2008).
 239. Jacobs, S., Delang, L., Verbeken, E., Neyts, J. & Kaptein, S. J. F. A viral polymerase inhibitor reduces zika virus replication in the reproductive organs of male mice. *Int. J. Mol. Sci.* **20**, (2019).
 240. Krutzik, P. O. & Nolan, G. P. Intracellular phospho-protein staining techniques for flow cytometry: Monitoring single cell signaling events. *Cytometry* **55A**, 61–70 (2003).
 241. Miksa, M., Komura, H., Wu, R., Shah, K. G. & Wang, P. A novel method to determine the engulfment of apoptotic cells by macrophages using pHrodo succinimidyl ester. *J. Immunol. Methods* **342**, 71–77 (2009).
 242. Hoorelbeke, B., Huskens, D., Férrir, G., François, K. O., Takahashi, A., Van Laethem, K., Schols, D., Tanaka, H. & Balzarini, J. Actinohivin, a broadly neutralizing prokaryotic lectin, inhibits HIV-1 infection by specifically targeting high-mannose-type glycans on the gp120 envelope. *Antimicrob. Agents Chemother.* **54**, 3287–3301 (2010).
 243. Doijen, J., Van Loy, T., De Haes, W., Landuyt, B., Luyten, W., Schoofs, L. & Schols, D. Signaling properties of the human chemokine receptors CXCR4 and CXCR7 by cellular electric impedance measurements. *PLoS One* **12**, 1–21 (2017).
 244. Morgenstern, J. & Land, H. Advanced mammalian gene transfer: high titre retroviral vectors with multiple drug selection markers and a complementary helper-free packaging cell line. doi:10.1093/nar/18.12.3587. *Nucleic Acids Res.* **18**, 3587–3596 (1990).
 245. Global health estimates 2016: deaths by cause, age, sex, by country and by region, 2000–2016. Geneva: World Health Organization; 2018. https://www.unaids.org/sites/default/files/media_asset/2020_women-adolescent-girls-and-hiv_en.pdf.
 246. Antimisiaris, S. G. & Mourtas, S. Recent advances on anti-HIV vaginal delivery systems development. *Adv. Drug Deliv. Rev.* **92**, 123–145 (2015).
 247. Dellar RC, Dlamini S & Karim QA. Adolescent girls and young women: key populations for HIV epidemic control. *J. Int. AIDS Soc.* **18**, 19408 (2015).
 248. Shattock, R. J. & Rosenberg, Z. Microbicides: topical prevention against HIV. *Cold Spring Harb. Perspect. Med.* **2**, 1–18 (2012).
 249. Sepulveda-Crespo, D., Cena-Diez, R., Jimenez, J. L. & Munoz-Fernandez, M. A. Mechanistic studies of viral entry: an overview of dendrimer-based

- microbicides as entry inhibitors against both HIV and HSV-2 overlapped infections. *Med. Res. Rev.* **00**, 1–31 (2016).
250. Machado, A., Cunha-Reis, C., Araújo, F., Nunes, R., Seabra, V., Ferreira, D., das Neves, J. & Sarmiento, B. Development and in vivo safety assessment of tenofovir-loaded nanoparticles-in-film as a novel vaginal microbicide delivery system. *Acta Biomater.* **44**, 332–340 (2016).
 251. Malcolm, R. K., Boyd, P. J., McCoy, C. F. & Murphy, D. J. Microbicide vaginal rings: technological challenges and clinical development. *Adv. Drug Deliv. Rev.* **103**, 33–56 (2016).
 252. Benítez-Gutiérrez, L., Soriano, V., Requena, S., Arias, A., Barreiro, P. & de Mendoza, C. Treatment and prevention of HIV infection with long-acting antiretrovirals. *Expert Rev. Clin. Pharmacol.* **11**, 507–517 (2018).
 253. Hoesley, C. J., Chen, B. A., Anderson, P. L., Dezzutti, C. S., Strizki, J., Sprinkle, C., Heard, F., Bauermeister, J., Hall, W., Jacobson, C., Berthiaume, J., Mayo, A., Gundacker, H., Richardson-Harman, N. & Piper, J. Phase 1 safety and pharmacokinetics study of MK-2048/Vicriviroc (MK-4176)/MK-2048A intravaginal rings. *Clin. Infect. Dis.* 1–8 (2018) doi:10.1093/cid/ciy653.
 254. McBride, J. W., Boyd, P., Dias, N., Cameron, D., Offord, R. E., Hartley, O., Kett, V. L. & Malcolm, R. K. Vaginal rings with exposed cores for sustained delivery of the HIV CCR5 inhibitor 5P12-RANTES. *J. Control. Release* **298**, 1–11 (2019).
 255. Linnakoski, R., Reshamwala, D., Veteli, P., Cortina-Escribano, M., Vanhanen, H. & Marjomäki, V. Antiviral agents from fungi: diversity, mechanisms and potential applications. *Front. Microbiol.* **9**, (2018).
 256. Grice, I. D. & Mariottini, G. L. *Glycans with antiviral activity from marine organisms. Results and Problems in Cell Differentiation* vol. 65 (2018).
 257. Hassan, S. T. S., Masarčíková, R. & Berchová, K. Bioactive natural products with anti-herpes simplex virus properties. *J. Pharm. Pharmacol.* **67**, 1325–1336 (2015).
 258. Boerjan, W., Ralph, J. & Baucher, M. Lignin biosynthesis. *Annu. Rev. Plant Biol.* **54**, 519–546 (2003).
 259. Upton, B. M. & Kasko, A. M. Strategies for the conversion of lignin to high-value polymeric materials: Review and perspective. *Chem. Rev.* **116**, 2275–2306 (2016).
 260. Chatterjee, S. & Saito, T. Lignin-derived advanced carbon materials. *ChemSusChem* **8**, 3941–3958 (2015).
 261. Bugg, T. D. H. & Rahmanpour, R. Enzymatic conversion of lignin into renewable chemicals. *Curr. Opin. Chem. Biol.* **29**, 10–17 (2015).
 262. Wang, C., Kelley, S. S. & Venditti, R. A. Lignin-based thermoplastic materials. *ChemSusChem* **9**, 770–783 (2016).
 263. Vishtal, A. & Kraslawski, A. Challenges in industrial applications of technical lignins. *BioResources* **6**, 3547–3568 (2011).
 264. May, C. Foreign Patents: Extraction of fat. *J. Am. Chem. Soc.* **1**, 176 (1879).
 265. Windschitl, P. M. & Stern, M. D. Evaluation of calcium lignosulfonate-treated soybean meal as a source of rumen protected protein for dairy cattle. *J. Dairy Sci.* **71**, 3310–3322 (1988).
 266. Mansfield, H. R. & Stern, M. D. Effects of soybean hulls and lignosulfonate-treated soybean meal, on ruminal fermentation in lactating dairy cows. *J. Dairy Sci.* **77**, 1070–1083 (1994).
 267. Acar, N., Moran, E. T., Revington, W. H. & Bilgili, S. F. Effect of improved pellet quality from using a calcium lignosulfonate binder on performance and carcass

- yield of broilers reared under different marketing schemes. *Poult. Sci.* **70**, 1339–1334 (1990).
268. Alonso, M. V., Oliet, M., Rodríguez, F., García, J., Gilarranz, M. A. & Rodríguez, J. J. Modification of ammonium lignosulfonate by phenolation for use in phenolic resins. *Bioresour. Technol.* **96**, 1013–1018 (2005).
 269. Grierson, L. H., Knight, J. C. & Maharaj, R. The role of calcium ions and lignosulphonate plasticiser in the hydration of cement. *Cem. Concr. Res.* **35**, 631–636 (2005).
 270. Ghosh, T., Chattopadhyay, K., Marschall, M., Karmakar, P., Mandal, P. & Ray, B. Focus on antivirally active sulfated polysaccharides: From structure-activity analysis to clinical evaluation. *Glycobiology* **19**, 2–15 (2009).
 271. Ciejka, J., Wytrwal, M., Nowakowska, M., Ochman, M., Milewska, A., Golda, A., Szczubialka, K., Wojarski, J. & Pyrc, K. Novel polyanions inhibiting replication of influenza viruses. *Antimicrob. Agents Chemother.* **60**, 1955–1966 (2016).
 272. Hwu, J. R., Lin, S.-Y., Tsay, S.-C., Singha, R., Pal, B. K., Leyssen, P. & Neyts, J. Development of new sulfur-containing conjugated compounds as anti-HCV agents. *Phosphorus. Sulfur. Silicon Relat. Elem.* **186**, 1144–1152 (2011).
 273. Witvrouw, M. & De Clercq, E. Sulfated polysaccharides extracted from sea algae as potential antiviral drugs. *Gen. Pharmacol.* **29**, 497–511 (1997).
 274. Monteil-Rivera, F. Green processes for lignin conversion through chemurgy and green chemistry. in *Quality Living Through Chemurgy and Green Chemistry* 263–300 (Springer Berlin Heidelberg, 2016). doi:10.1007/978-3-662-53704-6_10.
 275. García-Gallego, S., Díaz, L., Jiménez, J. L., Gómez, R., De La Mata, F. J. & Muñoz-Fernández, M. Á. HIV-1 antiviral behavior of anionic PPI metallo-dendrimers with EDA core. *Eur. J. Med. Chem.* **98**, 139–148 (2015).
 276. Suazo, P. A., Tognarelli, E. I., Kalergis, A. M. & González, P. A. Herpes simplex virus 2 infection: molecular association with HIV and novel microbicides to prevent disease. *Med. Microbiol. Immunol.* **204**, 161–176 (2015).
 277. Thurman, A. R. & Doncel, G. F. Herpes simplex virus and HIV: genital infection synergy and novel approaches to dual prevention. *Int. J. STD AIDS* **23**, 613–619 (2012).
 278. Pirrone, V., Wigdahl, B. & Krebs, F. C. The rise and fall of polyanionic inhibitors of the human immunodeficiency virus type 1. *Antiviral Res.* **90**, 168–182 (2011).
 279. Zolla-Pazner, S. Identifying epitopes of HIV-1 that induce protective antibodies. *Nat. Rev. Immunol.* **4**, 199–210 (2004).
 280. Gallaher, W. R., Ball, J. M., Garry, R. F., Griffin, M. C. & Montelaro, R. C. A general model for the transmembrane proteins of HIV and other retroviruses. *AIDS Res. Hum. Retroviruses* **5**, 431–440 (1989).
 281. Sanders, R. W., Vesanen, M., Schuelke, N., Master, A., Schiffner, L., Kalyanaraman, R., Paluch, M., Berkhout, B., Maddon, P. J., Olson, W. C., Lu, M. & Moore, J. P. Stabilization of the soluble, cleaved, trimeric form of the envelope glycoprotein complex of human immunodeficiency virus type 1. *J. Virol.* **76**, 8875–8889 (2002).
 282. Huang, J., Zhang, L. & Chen, F. Effects of lignin as a filler on properties of soy protein plastics. I. Lignosulfonate. *J. Appl. Polym. Sci.* **88**, 3284–3290 (2003).
 283. Carneiro, F. A., Bianconi, M. L., Weissmüller, G., Stauffer, F. & Poian, A. T. Da. Membrane recognition by vesicular stomatitis virus involves enthalpy-driven protein-lipid interactions. *J. Virol.* **76**, 3756–3764 (2002).
 284. Sepúlveda-crespo, D., Mata, F. J. De, Gómez, R. & Muñoz-fernández, M. A.

- Sulfonate-ended carbosilane dendrimers with a flexible scaffold cause inactivation of HIV-1 virions and gp120 shedding. *Nanoscale* **10**, 8998–9011 (2018).
285. Prokofjeva, M. M., Imbs, T. I., Shevchenko, N. M., Spirin, P. V, Horn, S., Fehse, B., Zvyagintseva, T. N. & Prassolov, V. S. Fucoidans as Potential Inhibitors of HIV-1. *Mar. Drugs* **11**, 3000–3014 (2013).
 286. Chatterjee, C., Paul, M., Xie, L. & van der Donk, W. A. Biosynthesis and mode of action of Lantibiotics. *Chem. Rev.* **105**, 633–684 (2005).
 287. Cotter, P. D., Hill, C. & Ross, R. P. Bacteriocins: developing innate immunity for food. *Nat. Rev. Microbiol.* **3**, 777–788 (2005).
 288. Dischinger, J., Basi Chipalu, S. & Bierbaum, G. Lantibiotics: Promising candidates for future applications in health care. *Int. J. Med. Microbiol.* **304**, 51–62 (2014).
 289. Meindl, K., Schmiederer, T., Schneider, K., Reicke, A., Butz, D., Keller, S., Gühring, H., Vértesy, L., Wink, J., Hoffmann, H., Brönstrup, M., Sheldrick, G. M. & Süßmuth, R. D. Labyrinthopeptins: A new class of carbacyclic lantibiotics. *Angew. Chemie Int. Ed.* **49**, 1151–1154 (2010).
 290. Müller, W. M., Schmiederer, T., Ensle, P. & Süßmuth, R. D. In vitro biosynthesis of the prepeptide of type-III lantibiotic labyrinthopeptin A2 including formation of a C-C bond as a post-translational modification. *Angew. Chemie - Int. Ed.* **49**, 2436–2440 (2010).
 291. Gharsallaoui, A., Oulahal, N., Joly, C. & Degraeve, P. Nisin as a Food Preservative: Part 1: Physicochemical Properties, Antimicrobial Activity, and Main Uses. *Crit. Rev. Food Sci. Nutr.* **56**, 1262–1274 (2016).
 292. Wink, J., Kroppenstedt, R. M., Seibert, G. & Stackebrandt, E. *Actinomadura namibiensis* sp. nov. *Int. J. Syst. Evol. Microbiol.* **53**, 721–724 (2003).
 293. Krawczyk, J. M., Völler, G. H., Krawczyk, B., Kretz, J., Brönstrup, M. & Süßmuth, R. D. Heterologous expression and engineering studies of labyrinthopeptins, class III lantibiotics from *actinomadura namibiensis*. *Chem. Biol.* **20**, 111–122 (2013).
 294. Vicenti, I., Boccuto, A., Giannini, A., Dragoni, F., Saladini, F. & Zazzi, M. Comparative analysis of different cell systems for Zika virus (ZIKV) propagation and evaluation of anti-ZIKV compounds in vitro. *Virus Res.* **244**, 64–70 (2018).
 295. Himmelsbach, K. & Hildt, E. Identification of various cell culture models for the study of Zika virus. *World J. Virol.* **7**, 10–20 (2018).
 296. Lin, Y. L., Lei, H. Y., Lin, Y. S., Yeh, T. M., Chen, S. H. & Liu, H. S. Infection of five human liver cell lines by dengue-2 virus. *J. Med. Virol.* **60**, 425–431 (2000).
 297. Tricarico, P. M., Caracciolo, I., Crovella, S. & D'Agaro, P. Zika virus induces inflammasome activation in the glial cell line U87-MG. *Biochem. Biophys. Res. Commun.* **492**, 597–602 (2017).
 298. Bayer, A., Lennemann, N. J., Ouyang, Y., Bramley, J. C., Morosky, S., Marques, E. T. D. A., Cherry, S., Sadovsky, Y. & Coyne, C. B. Type III Interferons produced by human placental trophoblasts confer protection against Zika virus infection. *Cell Host Microbe* **19**, 705–712 (2016).
 299. Sallusto, F. & Lanzavecchi, A. Efficient presentation of soluble antigen by cultured human dendritic cells is maintained by granulocyte/macrophage colony-stimulating factor plus interleukin 4 and downregulated by tumor necrosis factor α . *J. Exp. Med.* **179**, 1109–1118 (1994).
 300. García-Nicolás, O., Lewandowska, M., Ricklin, M. E. & Summerfield, A. Monocyte-derived dendritic cells as model to evaluate species tropism of

- mosquito-borne flaviviruses. *Front. Cell. Infect. Microbiol.* **9**, 1–13 (2019).
301. Sreaton, G., Mongkolsapaya, J., Yacoub, S. & Roberts, C. New insights into the immunopathology and control of dengue virus infection. *Nat. Rev. Immunol.* **15**, 745–759 (2015).
 302. Alen, M. The role of DC-SIGN and the mode of action of entry inhibitors in dengue virus infection. *PhD Thesis, KU Leuven* (2012).
 303. Österlund, P., Jiang, M., Westenius, V., Kuivanen, S., Järvi, R., Kakkola, L., Lundberg, R., Melén, K., Korva, M., Avšič – Županc, T., Vapalahti, O. & Julkunen, I. Asian and African lineage Zika viruses show differential replication and innate immune responses in human dendritic cells and macrophages. *Sci. Rep.* **9**, 1–15 (2019).
 304. Foo, S. S., Chen, W., Chan, Y., Lee, W. S., Lee, S. A., Cheng, G., Nielsen-Saines, K., Brasil, P. & Jung, J. U. Biomarkers and immunoprofiles associated with fetal abnormalities of ZIKV-positive pregnancies. *JCI insight* **3**, 1–11 (2018).
 305. Naveca, F. G., Pontes, G. S., Chang, A. Y. H., da Silva, G. A. V., do Nascimento, V. A., Monteiro, D. C. da S., da Silva, M. S., Abdalla, L. F., Santos, J. H. A., de Almeida, T. A. P., Mejía, M. del C. C., de Mesquita, T. G. R., Encarnação, H. V. de S., Gomes, M. de S., Amaral, L. R., Campi-Azevedo, A. C., Coelho-Dos-Reis, J. G., ... Ramasawmy, R. Analysis of the immunological biomarker profile during acute zika virus infection reveals the overexpression of CXCL10, a chemokine linked to neuronal damage. *Mem. Inst. Oswaldo Cruz* **113**, 1–13 (2018).
 306. Iwamoto, K., Hayakawa, T., Murate, M., Makino, A., Ito, K., Fujisawa, T. & Kobayashi, T. Curvature-dependent recognition of ethanolamine phospholipids by duramycin and cinnamycin. *Biophys. J.* **93**, 1608–1619 (2007).
 307. Das, A., Hirai-Yuki, A., González-López, O., Rhein, B., Moller-Tank, S., Brouillette, R., Hensley, L., Misumi, I., Lovell, W., Cullen, J. M., Whitmire, J. K., Maury, W. & Lemon, S. M. TIM1 (HAVCR1) is not essential for cellular entry of either quasi-enveloped or naked hepatitis a virions. *MBio* **8**, 1–14 (2017).
 308. Borisenko, G. G., Matsura, T., Liu, S. X., Tyurin, V. A., Jianfei, J., Serinkan, F. B. & Kagan, V. E. Macrophage recognition of externalized phosphatidylserine and phagocytosis of apoptotic Jurkat cells - Existence of a threshold. *Arch. Biochem. Biophys.* **413**, 41–52 (2003).
 309. Fukasawa, M., Sekine, F., Miura, M., Nishijima, M. & Hanada, K. Involvement of heparan sulfate proteoglycans in the binding step for phagocytosis of latex beads by Chinese hamster ovary cells. *Exp. Cell Res.* **230**, 154–162 (1997).
 310. Li, Y., Cheng, D., Cheng, R., Zhu, X., Wan, T., Liu, J. & Zhang, R. Mechanisms of U87 astrocytoma cell uptake and trafficking of monomeric versus protofibril Alzheimer's disease amyloid- β proteins. *PLoS One* **9**, 1–12 (2014).
 311. Peng, M., Yin, N. & Zhang, W. Endocytosis of Fc α R is clathrin and dynamin dependent, but its cytoplasmic domain is not required. *Cell Res.* **20**, 223–237 (2010).
 312. Qiu, M., Wang, Q., Chu, Y., Yuan, Z., Song, H., Chen, Z. & Wu, Z. Lignosulfonic acid exhibits broadly anti-HIV-1 activity - potential as a microbicide candidate for the prevention of HIV-1 sexual transmission. *PLoS One* **7**, 1–12 (2012).
 313. Altini, L., Blanchard, K., Coetzee, N., De Kock, A., Elias, C., Ellertson, C., Friedland, B., Hoosen, A., Jones, H. E., Kilmarx, P. H., Marumo, M., McGrory, E., Monedi, C., Ndlovu, G., Nkompala, B., Pistorius, A., Ramjee, G., ... Winikoff, B. Expanded safety and acceptability of the candidate vaginal microbicide Carraguard[®] in South Africa. *Contraception* **82**, 563–571 (2010).
 314. Skoler-Karpoff, S., Ramjee, G., Ahmed, K., Altini, L., Plagianos, M. G., Friedland,

- B., Govender, S., De Kock, A., Cassim, N., Palanee, T., Dozier, G., Maguire, R. & Lahteenmaki, P. Efficacy of Carraguard for prevention of HIV infection in women in South Africa: a randomised, double-blind, placebo-controlled trial. *Lancet* **372**, 1977–1987 (2008).
315. Van Damme, L., Govinden, R., Mirembe, F. M., Guédou, F., Solomon, S., Becker, M. L., Pradeep, B. S., Krishnan, A. K., Alary, M., Pande, B., Ramjee, G., Deese, J., Crucitti, T. & Taylor, D. Lack of effectiveness of cellulose sulfate gel for the prevention of vaginal HIV transmission. *N. Engl. J. Med.* **359**, 463–472 (2008).
316. McNeil, L., Otusanya, S., Oduyebo, O., Wang, C.-H., Umo-Otong, J., Ogunsola, F., Crucitti, T., Abdellati, S., Halpern, V., Mehta, N., Obunge, O., Onyejebu, N. & Taylor, D. Effectiveness of Cellulose Sulfate Vaginal Gel for the Prevention of HIV Infection: Results of a Phase III Trial in Nigeria. *PLoS One* **3**, e3784 (2008).
317. McCormack, S., Ramjee, G., Kamali, A., Rees, H., Crook, A. M., Gafos, M., Jentsch, U., Pool, R., Chisembele, M., Kapiga, S., Mutemwa, R., Vallely, A., Palanee, T., Sookrajh, Y., Lacey, C. J., Darbyshire, J., Grosskurth, H., ... Weber, J. PRO2000 vaginal gel for prevention of HIV-1 infection (Microbicides Development Programme 301): A phase 3, randomised, double-blind, parallel-group trial. *Lancet* **376**, 1329–1337 (2010).
318. Ugaonkar, S. R., Wesenberg, A., Wilk, J., Seidor, S., Mizenina, O., Kizima, L., Rodriguez, A., Zhang, S., Levendosky, K., Kenney, J., Aravantinou, M., Derby, N., Grasperge, B., Gettie, A., Kumar, N., Roberts, K., Robbiani, M., ... Zydowsky, T. M. A novel intravaginal ring to prevent HIV-1, HSV-2, HPV, and unintended pregnancy. *J Control Release* **213**, 57–68 (2015).
319. Ramjee, G., Kamali, A. & McCormack, S. The last decade of microbicide clinical trials in Africa: From hypothesis to facts. *Aids* **24**, 40–49 (2010).
320. García-Gallego, S., Franci, G., Falanga, A., Gómez, R., Folliero, V., Galdiero, S., De La Mata, F. J. & Galdiero, M. Function oriented molecular design: Dendrimers as novel antimicrobials. *Molecules* **22**, 1–29 (2017).
321. Myrvold, B. O. A new model for the structure of lignosulphonates. Part 1. Behaviour in dilute solutions. *Ind. Crops Prod.* **27**, 214–219 (2008).
322. Ceña-Diez, R., García-Broncano, P., de la Mata, F. J., Gómez, R. & Muñoz-Fernández, M. Á. Efficacy of HIV antiviral polyanionic carbosilane dendrimer G2-S16 in the presence of semen. *Int. J. Nanomedicine* **11**, 2443–2450 (2016).
323. Nel, A., Van Niekerk, N., Kapiga, S., Bekker, L. G., Gama, C., Gill, K., Kamali, A., Kotze, P., Louw, C., Mabude, Z., Miti, N., Kusemererwa, S., Tempelman, H., Carstens, H., Devlin, B., Isaacs, M., Malherbe, M., ... Rosenberg, Z. Safety and efficacy of a dapivirine vaginal ring for HIV prevention in women. *N. Engl. J. Med.* **375**, 2133–2143 (2016).
324. Casares, D., Escribá, P. V. & Rosselló, C. A. Membrane lipid composition: Effect on membrane and organelle structure, function and compartmentalization and therapeutic avenues. *Int. J. Mol. Sci.* **20**, (2019).
325. Jackman, J. A., Shi, P. Y. & Cho, N. J. Targeting the Achilles Heel of Mosquito-Borne Viruses for Antiviral Therapy. *ACS Infect. Dis.* **5**, 4–8 (2019).
326. Röcker, A. E., Müller, J. A., Dietzel, E., Harms, M., Krüger, F., Heid, C., Sowislok, A., Riber, C. F., Kupke, A., Lippold, S., von Einem, J., Beer, J., Knöll, B., Becker, S., Schmidt-Chanasit, J., Otto, M., Vapalahti, O., ... Münch, J. The molecular tweezer CLR01 inhibits Ebola and Zika virus infection. *Antiviral Res.* **152**, 26–35 (2018).
327. Camargos, V. N., Foureaux, G., Medeiros, D. C., da Silveira, V. T., Queiroz-

- Junior, C. M., Matosinhos, A. L. B., Figueiredo, A. F. A., Sousa, C. D. F., Moreira, T. P., Queiroz, V. F., Dias, A. C. F., Santana, K. T. O., Passos, I., Real, A. L. C. V., Silva, L. C., Mourão, F. A. G., Wnuk, N. T., ... Souza, D. G. In-depth characterization of congenital Zika syndrome in immunocompetent mice: Antibody-dependent enhancement and an antiviral peptide therapy. *EBioMedicine* **44**, 516–529 (2019).
328. Jackman, J. A., Costa, V. V., Park, S., Real, A. L. C. V., Park, J. H., Cardozo, P. L., Ferhan, A. R., Olmo, I. G., Moreira, T. P., Bambirra, J. L., Queiroz, V. F., Queiroz-Junior, C. M., Foureaux, G., Souza, D. G., Ribeiro, F. M., Yoon, B. K., Wynendaele, E., ... Cho, N. J. Therapeutic treatment of Zika virus infection using a brain-penetrating antiviral peptide. *Nat. Mater.* **17**, 971–977 (2018).
329. Chen, M., Aoki-Utsubo, C., Kameoka, M., Deng, L., Terada, Y., Kamitani, W., Sato, K., Koyanagi, Y., Hijikata, M., Shindo, K., Noda, T., Kohara, M. & Hotta, H. Broad-spectrum antiviral agents: secreted phospholipase A2 targets viral envelope lipid bilayers derived from the endoplasmic reticulum membrane. *Sci. Rep.* **7**, 1–8 (2017).
330. Rupcic, Z., Hüttel, S., Kanaki, S., Bernecker, S. & Stadler, M. Large scale production and downstream processing of labyrinthopeptins from the actinobacterium *Actinomadura namibiensis*. *Bioengineering* **5**, 42 (2018).
331. Su, X., Wang, Q., Wen, Y., Jiang, S. & Lu, L. Protein- and peptide-based virus inactivators: inactivating viruses before their entry into cells. *Front. Microbiol.* **11**, 1–19 (2020).
332. Okamoto, T., Suzuki, T., Kusakabe, S., Tokunaga, M., Hirano, J., Miyata, Y. & Matsuura, Y. Regulation of apoptosis during flavivirus infection. *Viruses* **9**, 1–12 (2017).
333. Jain, B., Chaturvedi, U. C. & Jain, A. Role of intracellular events in the pathogenesis of dengue; An overview. *Microb. Pathog.* **69–70**, 45–52 (2014).
334. Chiramel, A. I. & Best, S. M. Role of autophagy in Zika virus infection and pathogenesis. *Virus Res.* **254**, 34–40 (2018).
335. Jorge Rodrigues de Sousa, Do Socorro da Silva Azevedo, R., Quaresma, J. A. S. & Da Costa Vasconcelos, P. F. Cell death and zika virus: An integrated network of the mechanisms of cell injury. *Infect. Drug Resist.* **12**, 2917–2921 (2019).
336. Lee, C.-J., Liao, C.-L. & Lin, Y.-L. Flavivirus activates phosphatidylinositol 3-kinase signaling to block caspase-dependent apoptotic cell death at the early stage of virus infection. *J. Virol.* **79**, 8388–8399 (2005).
337. Turpin, J., Frumence, E., Desprès, P., Viranaicken, W. & Krejbich-Trotot, P. The Zika virus delays cell death through the anti-apoptotic Bcl-2 family proteins. *Cells* **8**, 1338 (2019).
338. Chu, L. W., Yang, C. J., Peng, K. J., Chen, P. L., Wang, S. J. & Ping, Y. H. TIM-1 as a signal receptor triggers dengue virus-induced autophagy. *Int. J. Mol. Sci.* **20**, (2019).
339. Vaughn, D. W., Green, S., Kalayanarooj, S., Innis, B. L., Nimmannitya, S., Suntayakorn, S., Endy, T. P., Raengsakulrach, B., Rothman, A. L., Ennis, F. A. & Nisalak, A. Dengue Viremia Titer, Antibody Response Pattern, and Virus Serotype Correlate with Disease Severity. *J. Infect. Dis.* **181**, 2–9 (2000).
340. De La Vega, M. A., Caleo, G., Audet, J., Qiu, X., Kozak, R. A., Brooks, J. I., Kern, S., Wolz, A., Sprecher, A., Greig, J., Lokuge, K., Kargbo, D. K., Kargbo, B., Di Caro, A., Grolla, A., Kobasa, D., Strong, J. E., ... Kobinger, G. P. Ebola viral load at diagnosis associates with patient outcome and outbreak evolution. *J. Clin.*

- Invest.* **125**, 4421–4428 (2015).
341. Ledford, H. Coronavirus breakthrough: dexamethasone is first drug shown to save lives. *Nature* **582**, (2020).
 342. Li, G. & De Clercq, E. Therapeutic options for the 2019 novel coronavirus (2019-nCov). *Nat. Rev. Drug Discov.* **19**, 149–150 (2020).
 343. Monto, A. S. Vaccines and antiviral drugs in pandemic preparedness. *Emerg. Infect. Dis.* **12**, 55–60 (2006).
 344. Zhu, J. Da, Meng, W., Wang, X. J. & Wang, H. C. R. Broad-spectrum antiviral agents. *Front. Microbiol.* **6**, 1–15 (2015).
 345. Curtiss, M. L., Gorman, J. V., Businga, T. R., Traver, G., Singh, M., Meyerholz, D. K., Kline, J. N., Murphy, A. J., Valenzuela, D. M., Colgan, J. D., Rothman, P. B. & Cassel, S. L. Tim-1 regulates Th2 responses in an airway hypersensitivity model. *Eur. J. Immunol.* **42**, 651–661 (2012).
 346. Acosta, E. G., Piccini, L. E., Talarico, L. B., Castilla, V. & Damonte, E. B. Changes in antiviral susceptibility to entry inhibitors and endocytic uptake of dengue-2 virus serially passaged in Vero or C6/36 cells. *Virus Res.* **184**, 39–43 (2014).

Acknowledgements, personal contribution and conflict of interest

Merel Oeyen designed the studies under guidance of Prof. Dominique Schols and Prof. Kurt Vermeire. Merel Oeyen prepared and executed most of the experiments and performed the data analysis.

Contributions to this work are listed below:

Cell culturing was performed by Merel Oeyen, Eef Meyen and Eric Fonteyn. Isolation of PBMCs was done by Eric Fonteyn and MDDC preparation was done by Merel Oeyen and Eric Fonteyn. HIV and HSV experiments were performed by Merel Oeyen whereas Flavivirus, TIM-1 and CD300a experiments were prepared and analyzed by Merel Oeyen and performed by Merel Oeyen and Eef Meyen. Antiviral screening experiments with other viruses were performed by Leentje Persoons, Bianca Stals, and Anita Camps. HIV p24 ELISA was performed by Daisy Ceusters and Evelyne Van Kerckhove. VSVG-HIV-1 pseudovirus assay was performed by Emiel Vanhulle. Flow cytometry was conducted by Merel Oeyen and Eef Meyen whereas FACS sorting was conducted by Geert Schoofs. Molecular biology experiments were performed by Merel Oeyen with essential inputs for the experimental design from Dr. Thomas D'huys and Dr. Anneleen Van Hout. Liposomes were synthesized by Merel Oeyen with help from Dr. Belén Martínez Gualda, or by Prof. Kristina Sepčič. SPR experiments were performed and analyzed by Sam Noppen. Bio-plex experiments were performed by Sandra Claes and analyzed by Merel Oeyen. CEI experiments were performed by Eef Meyen and analyzed by Dr. Jordi Doijen. Chemical analysis of lignosulfonates was done by S. Iversby and A.-H. Gaaseud Oerseng from Borregaard LignoTech.

Merel Oeyen wrote this thesis manuscript with essential inputs from Prof. Dominique Schols, Prof. Kurt Vermeire, Dr. Anneleen Van Hout, Dr. Jordi Doijen, Eva Pauwels, Dr. Wout Frederickx and Ella Sartini.

Illustrations were designed by Merel Oeyen with Adobe Illustrator 24.1 (Adobe, San José, CA, USA).

The author declares that she has no conflicts of interest with the content of this thesis.

Curriculum vitae

Personalia

Name Merel Oeyen
Date of birth 4th of January 1990
Place of birth Leuven, Belgium
Phone number +32 (0)478 67 65 05
Email address merel.oeyen@kuleuven.be
oeyenmerel@gmail.com

Education

- 2015-2020 PhD in Biomedical Sciences**
Laboratory of Virology and Chemotherapy
Rega Institute for Medical Research, KU Leuven, Leuven, Belgium
- 2013-2015 Master of Biomedical Sciences: Infectious and Tropical Diseases (Magna cum laude)**
UAntwerpen, Antwerpen, Belgium
Thesis: Evaluation of potential HIV inhibitors that act through specific interaction with the chemokine receptor CXCR4
Laboratory of Virology and Chemotherapy, Rega Institute for Medical Research
Promoter: Prof. Dominique Schols
- 2011-2013 Master of Science in Biology (cum laude)**
KU Leuven, Leuven, Belgium
Thesis: Co-phylogeographic study of the flatworm *Gyrodactylus gondae* and its goby host *Pomatoschistus minutus*
Laboratory of Biodiversity and Evolutionary Genomics
Promoter: Prof. Filip Volckaert
- 2008-2011 Bachelor of Science in Biology**
KU Leuven, Leuven, Belgium
- 2002-2008 Latin-Sciences education**
Paridaens Instituut, Leuven, Belgium

Publications in peer-reviewed journals

Prochnow H, Rox K, Birudukota S, Weichert L, Hotop S-K, Klahn P, Mohr K, Franz S, Banda DH, Blockus S, Schreiber J, Haid S, **Oeyen M**, Martinez JP, Süßmuth RD, Wink J, Meyerhans A, Goffinet C, Messerle M, Schulz TH, Kröger A, Schols D, Pietschmann T, Brönstrup M. (2020) Labyrinthopeptins exert broad-spectrum antiviral activity through lipid-binding-mediated virolysis. *Journal of Virology* 94 (2): 1-24.

Oeyen M, Noppen S, Vanhulle E, Claes S, Myrvold BO, Vermeire K, Schols D. (2019) A unique class of lignin derivatives displays broad anti-HIV activity by interacting with the viral envelope. *Virus Research* 274: 197760.

Huyse T, **Oeyen M**, Larmuseau MHD, Volckaert FAM. (2017) Co-phylogeographic study of the flatworm *Gyrodactylus gondae* and its goby host *Pomatoschistus minutus*. *Parasitology International* 66: 119-125.

Van Hout A, D'huys T, **Oeyen M**, Schols D, Van Loy T. (2017) Comparison of cell-based assays for the identification and evaluation of competitive CXCR4 inhibitors. *PLOS One* 12(4): 1-18.

Presentations and posters at (inter)national meetings and symposia

Oeyen M, Noppen S, Myrvold BO, Schols D. (2019) Lignin derivatives displaying broad anti-HIV and anti-HSV activity. Presented at the Belgian Society for Microbiology annual meeting, Brussels, Belgium. Poster presentation.

Oeyen M (2019) Labyrinthopeptin A1 exerts broad-spectrum antiviral activity against dengue and Zika virus. Presented at the UFMG – KU Leuven – QMUL meeting on Infection and Immunity, Rega Institute, Leuven, Belgium. Oral presentation.

Oeyen M, Meyen E, Claes S, Süssmuth RD, Schols D (2018) Labyrinthopeptin A1 exerts broad spectrum antiviral activity against dengue and Zika virus. Presented at the International Conference on Antiviral Research (ICAR), Porto, Portugal. Oral and poster presentation.

Claes S, **Oeyen M**, Schols D (2017) Immune responses in viral infections and effects of antiviral drug candidates measured by multiplex biomarker analysis. Presented at the Belgian Immunological Society annual meeting, Leuven, Belgium. Poster presentation.

Oeyen M, Claes S, Süssmuth RD, Schols D (2017) Labyrinthopeptin A1 exerts broad-spectrum antiviral activity against Zika virus. Presented at the Belgian Society for Microbiology annual meeting, Brussels, Belgium. Poster presentation.

Van Hout A, D'huys T, **Oeyen M**, Van Loy T, Schols D (2016) Evaluation of the anti-CXCR4 activity profile of published GPCR inhibitors. Presented at the Belgian Society for Microbiology Annual meeting, Brussels, Belgium. Poster presentation.